



Universidad de Valladolid



**PROGRAMA DE DOCTORADO EN INGENIERÍA QUÍMICA Y
AMBIENTAL**

TESIS DOCTORAL:

**From biogas to biomethane. Biological
conversion of H₂ and CO₂ to CH₄**

Presentada por **Natalia Alfaro Borjabad**
para optar al grado de
Doctora por la Universidad de Valladolid

Dirigida por:
Fernando Fdz-Polanco Fdz de Moreda
María Fdz-Polanco Íñiguez de la Torre
Israel Díaz Villalobos



Universidad de Valladolid



**PROGRAMA DE DOCTORADO EN INGENIERÍA QUÍMICA Y
AMBIENTAL**

TESIS DOCTORAL:

**Del biogás al biometano. Conversión
biológica de H₂ y CO₂ a CH₄**

**Presentada por Natalia Alfaro Borjabad
para optar al grado de
Doctora por la Universidad de Valladolid**

**Dirigida por:
Fernando Fdz-Polanco Fdz de Moreda
María Fdz-Polanco Íñiguez de la Torre
Israel Díaz Villalobos**



Universidad de Valladolid



**Memoria para optar al grado de Doctor,
con Mención Doctor Internacional,
presentada por la Ingeniera Química:
Natalia Alfaro Borjabad**

Siendo tutores en la Universidad de Valladolid:

Fernando Fdz-Polanco Fdz de Moreda
María Fdz-Polanco Íñiguez de la Torre
Israel Díaz Villalobos

**Y en Technical University of Denmark, Department of
Environmental Engineering (Denmark):**

Irini Angelidaki
Panagiotis Kougias

Valladolid, Octubre de 2018



Universidad de Valladolid



UNIVERSIDAD DE VALLADOLID
ESCUELA DE INGENIERÍAS INDUSTRIALES

Secretaría

La presente tesis doctoral queda registrada en el folio número _____ del correspondiente libro de registro número _____

Valladolid, a _____ de _____ de 2018

Fdo. El encargado del registro



Universidad de Valladolid

Fernando Fdz-Polanco Fdz de Moreda

Profesor Emérito

**Departamento de Ingeniería Química y Tecnología del Medio Ambiente
Universidad de Valladolid**

María Fdz-Polanco Íñiguez de la Torre

Profesora Titular de Universidad

**Departamento de Ingeniería Química y Tecnología del Medio Ambiente
Universidad de Valladolid**

Israel Díaz Villalobos

Investigador Postdoctoral

**Departamento de Ingeniería Química y Tecnología del Medio Ambiente
Universidad de Valladolid**

Certifican que:

NATALIA ALFARO BORJABAD ha realizado bajo su dirección el trabajo “From biogas to biomethane. Biological conversion of H₂ and CO₂ to CH₄”, en el Departamento de Ingeniería Química y Tecnología del Medio Ambiente de la Escuela de Ingenierías Industriales de la Universidad de Valladolid. Considerando que dicho trabajo reúne los requisitos para ser presentado como Tesis Doctoral expresan su conformidad con dicha presentación.

Valladolid, a _____ de _____ de 2018

**Fdo. Fernando Fdz-
Polanco Fdz de
Moreda**

**Fdo. María Fdz-
Polanco Íñiguez de la
Torre**

**Fdo: Israel Díaz
Villalobos**



Universidad de Valladolid

Reunido el tribunal que ha juzgado la Tesis Doctoral titulada “From biogas to biomethane. Biological conversion of H₂ and CO₂ to CH₄” presentada por Natalia Alfaro Borjabad y en cumplimiento con lo establecido por el Real Decreto 99/2011 de 28 de enero de 2011 acuerda conceder por _____ la calificación de _____.

Valladolid, a _____ de _____ de

PRESIDENTE

SECRETARIO

VOCAL

Acronyms	1
Abstract	5
Resumen	9
Chapter 1. Introduction	15
1.1 ANAEROBIC DIGESTION AND BIOGAS	17
1.2 BIOGAS UPGRADING	19
1.2.1 Physical and chemical technologies	20
1.2.2 Biological technologies	23
1.3 HYDROGEN ASSISTED BIOLOGICAL BIOGAS UPGRADING	24
1.3.1 Power-to-Gas (P2G) technology	25
1.3.2 Chemoautotrophic biogas upgrading configurations	30
1.3.2.1 Ex-situ biogas upgrading	30
1.3.2.2 In-situ biogas upgrading	38
1.3.2.3 Hybrid biogas upgrading	42
1.3.2.4 Comparison of ex-situ, in-situ and hybrid biomethanation systems	44
1.3.3 H ₂ intermittency	45
1.3.4 Microbial communities in biological biogas upgrading systems	46
Chapter 2. Aims and scope	49
2.1 RESEARCH MOTIVATION	51
2.2 OBJECTIVES OF THE THESIS	52
2.3 THESIS OUTLINE	52
Chapter 3. Experimental materials and methods	55
3.1 EXPERIMENTAL SETUPS	57
3.1.1 Pilot Plants	57
3.1.1.1 Hollow-fiber membrane bioreactors	57
3.1.1.2 Ceramic membrane bioreactor	61
3.1.2 Lab-scale reactors	63
3.1.2.1 Trickle biofilter reactors	63
3.1.2.2 Up-flow reactors	66
3.2 RAW MATERIALS	68
3.3 ANALYTICAL METHODS	72
3.4 MICROBIAL ANALYSIS	75
3.4.1 DNA extraction	75
3.4.2 Denaturing Gradient Gel Electrophoresis (DGGE)	76

3.4.3	Fluorescence In Situ Hybridization (FISH)	77
3.4.4	16S rRNA gene sequencing	78
3.5	CALCULATIONS	79
3.5.1	Efficiency of hydrogen utilization, η_{H_2}	79
3.5.2	Carbon dioxide conversion efficiency, η_{CO_2}	80
3.5.3	Methane yield, Y_{CH_4}	80
3.5.4	Methane production rate	81
3.5.5	Gas transfer coefficient, $k_L a$	82
3.5.6	Gas transfer rate (r_i) and biological kinetics parameters (r_{utH_2} , U , f_x)	83

Chapter 4. A feasibility study on the bioconversion of CO₂ and H₂ to biomethane by gas sparging through polymeric membranes **85**

4.1	INTRODUCTION	87
4.2	MATERIALS AND METHODS	88
4.2.1	Pilot Plant	88
4.2.2	Operating conditions	88
4.2.3	Monitoring and experimental analysis	89
4.2.4	Calculations	89
4.2.5	Microbial analysis	90
4.3	RESULTS AND DISCUSSION	90
4.3.1	Performance of the conversion of H ₂ and CO ₂ to CH ₄	90
4.3.2	Mass transfer capacity in the MBR	93
4.3.3	Biological activity	95
4.3.4	Microbial community	98
4.3.5	Application of the MBR for biogas upgrading	104
4.4	CONCLUSIONS	105

Chapter 5. Evaluation of process performance, energy consumption and microbiota characterization in a ceramic membrane bioreactor for ex-situ biomethanation of H₂ and CO₂ **107**

5.1	INTRODUCTION	109
5.2	MATERIALS AND METHODS	109
5.2.1	Pilot Plant	109
5.2.2	Operating conditions	110
5.2.3	Monitoring and experimental analysis	111
5.2.4	Calculations	111
5.2.5	Microbial analysis	113
5.3	RESULTS AND DISCUSSION	113

5.3.1	Conversion of H ₂ and CO ₂ to CH ₄	113
5.3.2	MBR mass transfer capacity.....	116
5.3.3	Biological activity.....	117
5.3.4	Consumption of energy.....	119
5.3.5	Microbial community.....	121
5.4	CONCLUSIONS.....	131

Chapter 6. Process performance and microbial community structure in thermophilic trickling biofilter reactors for ex-situ biogas upgrading..... 133

6.1	INTRODUCTION.....	135
6.2	MATERIALS AND METHODS.....	136
6.2.1	Reactors.....	136
6.2.2	Operating conditions.....	136
6.2.3	Monitoring and experimental analysis.....	137
6.2.4	Calculations.....	138
6.2.5	Microbial community analysis.....	138
6.3	RESULTS AND DISCUSSION.....	139
6.3.1	Process performance of trickling biofilter reactors.....	139
6.3.2	Microbial community profiles in the liquid media and biofilm.....	142
6.3.3	Practical considerations derived from the current study.....	150
6.4	CONCLUSIONS.....	152

Chapter 7. H₂ addition through a submerged membrane for in-situ biogas upgrading in the anaerobic digestion of sewage sludge 153

7.1	INTRODUCTION.....	155
7.2	MATERIALS AND METHODS.....	155
7.2.1	Pilot Plants.....	155
7.2.2	Operating conditions.....	156
7.2.3	Monitoring and experimental analysis.....	157
7.2.4	Calculations.....	157
7.2.5	Microbial analysis.....	158
7.3	RESULTS AND DISCUSSION.....	158
7.3.1	Performance of the conversion of H ₂ and CO ₂ to CH ₄	158
7.3.2	Mass transfer capacity in the MBR.....	164
7.3.3	Anaerobic digestion performance.....	165
7.3.3.1	VFA evolution.....	165

7.3.3.2	OLR	166
7.3.3.3	pH, NH ₄ ⁺ and solids removal	167
7.3.4	Dewaterability of digested sludge.....	168
7.3.5	Microbial community	169
7.4	CONCLUSIONS	184

Chapter 8. Intermittent provision of H₂ in up-flow reactors for ex-situ biogas upgrading..... 187

8.1	INTRODUCTION	189
8.2	MATERIALS AND METHODS	190
8.2.1	Reactors.....	190
8.2.2	Operating conditions.....	190
8.2.3	Monitoring and experimental analysis.....	193
8.2.4	Calculations	193
8.2.5	Microbial community analysis.....	194
8.3	RESULTS AND DISCUSSION.....	194
8.3.1	Performance of reactor 1	195
8.3.2	Performance of reactor 2	199
8.3.3	Performance of reactor 3	203
8.3.4	Comparison of reactors' performance and H ₂ intermittency	206
8.3.5	Microbial community	209
8.4	CONCLUSIONS	219

Chapter 9. Conclusions and future perspectives 221

9.1	CONCLUSIONS	223
9.2	FUTURE PERSPECTIVES.....	225

Chapter 10. References..... 229

Annexes 243

About the author..... 263

Acknowledgements 275

Acronyms



AD	Anaerobic Digestion
CAPEX	Capital Expenditure
COD	Chemical Oxygen Demand
CSTR	Continuous Stirred Tank Reactors
DAPI	4',6-DiAmidino-2-PhenylIndole
DGGE	Denaturing Gradient Gel Electrophoresis
DNA	DeoxyriboNucleic Acid
EU	European Union
FID	Flame Ionization Detector
FISH	Fluorescence In Situ Hybridization
GC	Gas Chromatography
HPLC	High Performance Liquid Chromatography
HRT	Hydraulic Retention Time
ICP	Inductively Coupled Plasma
LCV	Lower Calorific Value
MBR	Membrane Bioreactor
MER	Methane Evolution Rate
NCBI	National Centre for Biotechnology Information
OES	Optical Emission Spectrophotometer
OLR	Organic Loading Rate
OTU	Operational Taxonomic Unit
PBS	Phosphate-Buffered Saline
PCR	Polymerase Chain Reaction
PSA	Pressure Swing Adsorption
PVDF	PolyVinylidene DiFluoride
P2G	Power-to-Gas
rRNA	Ribosomal RiboNucleic Acid
SAO	Syntrophic Acetate Oxidizer
SRA	Sequence Read Archive
TBF	Trickling BioFilter
TCD	Thermal Conductivity Detector
TKN	Total Kjeldahl Nitrogen
TS	Total Solids
TSS	Total Suspended Solids
UASB	Upflow Anaerobic Sludge Blanket
VFA	Volatile Fatty Acid
VS	Volatile Solids
VSS	Volatile Suspended Solids
WWTP	Waste Water Treatment Plant

Abstract



ABSTRACT

Anaerobic digestion of biomass produces biogas with 70-60% CH₄ and 30-40% CO₂. However, biogas with more than 90% CH₄ has higher heating value, can be injected into the natural gas grid or can be used as alternative vehicle fuel. Biogas upgrading aims to increase the CH₄ concentration in biogas.

In this context, hydrogen assisted biological biogas upgrading has emerged as an attractive method for biogas upgrading. In this process, H₂ produced by water electrolysis using off-peak electricity surplus from wind power is coupled with the CO₂ contained in the biogas to convert them to CH₄ via hydrogenotrophic methanogenesis (Power-to-Gas). Currently, it can be defined in two concepts namely ex-situ and in-situ depending on where the H₂ is provided with respect to the anaerobic digestion. In both cases, the H₂ gas-liquid mass transfer and the H₂ intermittency are the challenges of the process.

The aim of the present thesis is to study, develop and optimize the biological biogas upgrading process.

To reach the objective, five series of experiments were performed for ex-situ and in-situ processes at thermophilic and mesophilic conditions, employing different reactor configurations (MBRs, TBFs and up-flow reactors) and feedings (H₂ + CO₂, H₂ + biogas and H₂ + sewage sludge) at lab and pilot scale. In order to improve the H₂ gas-liquid mass transfer, different H₂ diffusion systems (hollow-fiber and ceramic membranes, 3-phase system of TBFs and 2 stainless steel diffusers combined with 2 inert alumina ceramic sponges) were evaluated. The effects of gas recirculation (in MBRs) and directional and counter-directional H₂ injection to the trickling media (in TBFs) on biomethanation efficiency were studied. Different H₂ stop-feeding periods of 1, 2 and 3 weeks and the subsequent H₂ reinjection were experienced in order to evaluate the dynamicity of the ex-situ process under H₂ intermittent provision. Concerning about the effect of H₂ on biogas microbiome, microbial community analysis were carried out.

The results obtained in the present thesis demonstrated the feasibility of H₂-mediated biological biogas upgrading in both ex-situ and in-situ processes.

The results verified that membrane modules can be employed to transfer H₂ efficiently, allowing the biological conversion to take place satisfactorily. The ex-situ systems transformed 95% of H₂ fed at the maximum loading rates of 40.2 L_{H2}/L_R·d (hollow-fiber MBR) and 30.0 L_{H2}/L_R·d (ceramic MBR) reaching CH₄ production rates of 8.84 L_{CH4}/L_R·d and 6.60 L_{CH4}/L_R·d, CH₄ contents of 76% and 81% and $k_L a_{H_2}$ values of 430 h⁻¹ and 268 h⁻¹, respectively. Ceramic membranes were proposed to address and solve the long-term bioconversion stability challenge of hollow-fiber membranes at 55 °C.

TBF reactors resulted in attractive configurations with promising results for the biomethanation process. The investigated systems, by means of a single-pass gas flow, upgraded biogas with 97% H₂ utilization efficiency at H₂ loading rate of 7.2 L_{H2}/L_R·d, reaching a CH₄ production rate of 1.74 L_{CH4}/L_R·d and CH₄ content of 95%, fulfilling the specifications to be used as substitute to natural gas. The results demonstrated that the injection of the influent gas mixture in counter-flow to the trickling media greatly reduced acetate production compared to the injection with the directional flow of the liquid media.

In the in-situ experiment, H₂ injection resulted in a 42% increase in CH₄ production in comparison with the conventional anaerobic digestion of sewage sludge and 73% CH₄ content was achieved while the biodegradation potential was not compromised.

Gas recirculation was shown to improve the H₂ gas-liquid mass transfer significantly improving the performance of the reactors. Moreover, gas recirculation seemed to have a positive effect on the in-situ biomethanation when the OLR increased.

The feasibility of the system recovery to reach the initial conditions of CH₄ (production, content and yield) during the intermittent provision of H₂ was demonstrated, regardless of the length of the H₂ lack. The repetition of the H₂ intermittent provision was shown to have a positive effect on the system recovery time, since the reactors recovered faster as more H₂ stop/start periods were applied.

The selection-effect of H₂ on community composition was revealed by microbial analysis. *Methanothermobacter*, *Methanoculleus*, *Methanospirillum*, *Methanolinea* and *Methanobacterium* were the hydrogenotrophic *archaea* genus present.

Resumen



RESUMEN

La digestión anaerobia de biomasa produce biogás con un 70-60% de CH_4 y un 30-40% de CO_2 . Sin embargo, un biogás con más del 90% de CH_4 tiene mayor valor calorífico, se puede inyectar en la red de gas natural o se puede usar como combustible alternativo de vehículos. El enriquecimiento de biogás tiene como objetivo aumentar la concentración de CH_4 en el biogás.

En este contexto, el enriquecimiento biológico de biogás asistido por hidrógeno ha surgido como un método atractivo para el enriquecimiento de biogás. En este proceso, el H_2 generado a través de la electrólisis del agua utilizando el excedente de electricidad producida a partir de la energía eólica, reacciona con el CO_2 contenido en el biogás para ser ambos convertidos a CH_4 a través de la metanogénesis hidrogenotrófica (Energía-a-Gas). El enriquecimiento biológico de biogás se puede realizar en un proceso ex-situ o in-situ dependiendo de donde se proporcione el H_2 respecto a la digestión anaerobia. En ambos casos, la transferencia de materia gas-líquido del H_2 y la intermitencia de dicho gas son los retos del proceso.

El objetivo de la presente tesis es estudiar, desarrollar y optimizar el proceso de enriquecimiento biológico de biogás.

Para alcanzar dicho objetivo, se realizaron cinco experimentos de procesos ex-situ e in-situ en condiciones termófilas y mesófilas, empleando diferentes configuraciones de reactores (biorreactores de membrana, biofiltros percoladores y reactores de flujo ascendente) y diferentes alimentaciones ($\text{H}_2 + \text{CO}_2$, $\text{H}_2 + \text{biogás}$ y $\text{H}_2 + \text{fango de depuradora}$) a escala de laboratorio y piloto. Se evaluaron diferentes sistemas de difusión de H_2 (membranas de fibra hueca y cerámica, sistema de 3 fases de biofiltros percoladores y 2 difusores de acero inoxidable combinados con 2 esponjas cerámicas de alúmina interte) con el objetivo de mejorar la transferencia de materia gas-líquido del H_2 . Además, se estudió el efecto de la recirculación de gas (en los biorreactores de membrana) y el efecto de la inyección direccional y contradireccional del H_2 respecto del flujo del medio de goteo (en biofiltros percoladores) en la eficiencia de biometanización. Se experimentaron distintos periodos de parada de H_2 de 1, 2 y 3 semanas y posterior reinyección del mismo con el objetivo de evaluar la dinamicidad

del proceso ex-situ durante el suministro intermitente de H₂. Se llevaron a cabo análisis de la comunidad microbiana para estudiar el efecto del H₂ en la población.

Los resultados obtenidos en la presente tesis demostraron la viabilidad del enriquecimiento biológico de biogás asistido por H₂ tanto para los procesos ex-situ como para los in-situ.

Los resultados verificaron que los módulos de membrana pueden ser empleados para transferir H₂ de forma eficiente, permitiendo que la conversión biológica tenga lugar satisfactoriamente.

Los sistemas ex-situ transformaron el 95% del H₂ alimentado a las cargas máximas de 40.2 L_{H₂}/L_R·d (biorreactor de membrana de fibra hueca) y 30.0 L_{H₂}/L_R·d (biorreactor de membrana cerámica) alcanzando producciones de CH₄ de 8.84 L_{CH₄}/L_R·d y 6.60 L_{CH₄}/L_R·d, contenidos de CH₄ de 76% y 81% y valores de $k_L a_{H_2}$ de 430 h⁻¹ y 268 h⁻¹, respectivamente. Se propusieron las membranas cerámicas para abordar y resolver el reto de la estabilidad de la bioconversión a largo plazo de las membranas de fibra hueca a 55 °C.

Los biofiltros percoladores resultaron ser configuraciones atractivas con resultados prometedores para el proceso de biometanización. Los sistemas investigados, a través de un solo paso del flujo de gas, enriquecieron el biogás con una eficiencia de utilización del H₂ del 97% a una carga de H₂ de 7.2 L_{H₂}/L_R·d, alcanzando una producción de CH₄ de 1.74 L_{CH₄}/L_R·d y un contenido de CH₄ del 95%, cumpliendo con las especificaciones para que pueda ser utilizado como sustituto del gas natural. Los resultados demostraron que la inyección de la mezcla de gas de entrada a contracorriente con el flujo del líquido de goteo redujo en gran medida la producción de acetato en comparación con la inyección en corriente.

En el experimento in-situ, la inyección de H₂ dio como resultado un aumento del 42% en la producción de CH₄ en comparación con la digestión anaerobia convencional de fango de depuradora, logrando un contenido de CH₄ del 73%, mientras que el potencial de biodegradación no se vio comprometido.

La recirculación de gas mejoró significativamente la transferencia de materia gas-líquido del H₂ mejorando así el rendimiento de los reactores. Además, la recirculación de gas pareció tener un efecto positivo en la biometanización in-situ cuando la carga orgánica aumentó.

Se demostró la viabilidad de la recuperación del sistema para alcanzar las condiciones iniciales de CH₄ (producción, contenido y rendimiento) durante el suministro intermitente de H₂, independientemente de la duración de la parada de H₂. La repetición del suministro intermitente de H₂ mostró un efecto positivo en el tiempo de recuperación del sistema, ya que los reactores se recuperaron cada vez más rápido a medida que se aplicaron más periodos de parada/inicio de H₂.

Los análisis microbianos desvelaron el efecto de la selección del H₂ sobre la composición de la comunidad. Los géneros de *archaea* hidrogenotróficas presentes fueron *Methanothermobacter*, *Methanoculleus*, *Methanospirillum*, *Methanolinea* y *Methanobacterium*.

Chapter 1

Introduction



1.1 ANAEROBIC DIGESTION AND BIOGAS

Anaerobic digestion (AD) of biomass, organic wastes and by-products is an effective and well-established renewable energy technology for bioenergy production in the EU (EuroObservER, 2013) and a promising way for world sustainable energy production (Weiland, 2010).

AD is a microbial-mediated process in which organic carbon is converted, by subsequent oxidations and reductions, to its most oxidized state (CO_2) and to its most reduced form (CH_4) (Kougiás and Angelidaki, 2018).

It is well known that AD is responsible for carbon recycling in different environments, including wetlands, rice fields, intestine of animals, aquatic sediments and manures. This process is also extensively applied in industrial scale for valorization of organic wastes as sludge, manure, agricultural wastes, industrial organic wastes, etc.

In many cases, the treatment of biowastes by AD processes is the optimal way to convert organic waste into useful products such as energy and soil conditioner (fertilizer).

The main advantages of the industrial AD process rely on the production of a versatile energy carrier and the high degree of organic matter reduction with small increase - in comparison to the aerobic process - of the bacterial biomass.

AD produces biogas via biological processes by means of different groups of microorganisms acting synergistically, which use several pathways to digest at anaerobic conditions the organic substrates (Kougiás et al., 2017) (Figure 1).

Although biogas is composed by some minor components as N_2 (0-3%), vapour water (5-10%), O_2 (0-1%), H_2S (0-10,000 ppmv), NH_3 , hydrocarbons (0-200 mg/m^3) and siloxanes (0-41 mg/m^3) (Muñoz et al., 2015; Petersson and Wellinger, 2009), its main composition is typically 70-60% methane (CH_4) and 30-40% carbon dioxide (CO_2). The relative content of CH_4 and CO_2 in biogas is mainly dependent on the nature of the substrate and pH of the reactor where biogas is produced (Angelidaki et al., 2018).

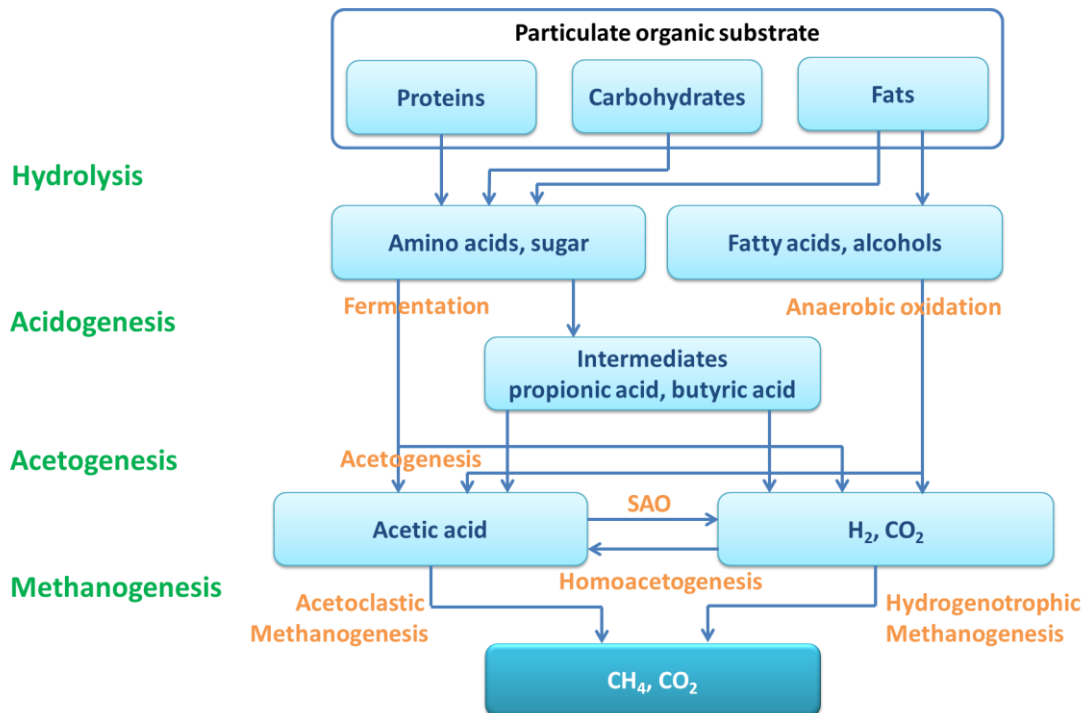


Figure 1. Schematic description of the AD process.

As biogas is commonly burned to produce electricity and heat, apart from CH₄, all the other gasses contained in biogas are unwanted and are considered as biogas pollutants. On the one hand, H₂S, NH₃ and siloxanes are toxic and extremely corrosive, damaging the combined heat and power unit and metal parts via emission of SO₂ from combustion. On the other hand, the higher the CO₂ or N₂ content is, the lower the calorific value in biogas. The energy content of CH₄ described by the Lower Calorific Value (LCV) is 50.4 MJ/kg CH₄ or 36 MJ/m³ CH₄ at STP conditions and for biogas with CH₄ content in the range of 60–65%, the LCV is approximately 20–25 MJ/m³ biogas (Angelidaki et al., 2018). Therefore, it is well understood the target of the highest CH₄ as possible in the biogas regarding the energetic interest.

Nowadays, there are different treatments targeting at removing the undesired compounds from the biogas expanding its range of applications. The first treatment is related to biogas cleaning and includes removal of harmful and/or toxic compounds such as H₂S, volatile organic compounds, siloxanes, CO and NH₃. The second treatment is called biogas upgrading and aims to increase the low calorific value of the biogas, and thus, to convert it to higher fuel standard (Sun et al., 2015).

1.2 BIOGAS UPGRADING

Currently, there is an increasing interest in exploiting biogas as a substitute of natural gas (Kougias et al., 2017). The aim of biogas upgrading is to increase CH₄ content in biogas raising its calorific value and thus its potential applications as alternative to natural gas (Deng and Hägg, 2010). Through this process, the CH₄ content in the biogas is increased by removing or transforming the contained CO₂. Thereafter, the upgraded biogas can be injected and distributed through the existing natural gas grids or it can be used as vehicle fuel (Deublein and Steinhauser, 2011; Deng and Hägg, 2010). In case the upgraded biogas is purified to specifications similar to natural gas, the final product is called biomethane (Kougias et al., 2017).

Nowadays, the specifications of the natural gas composition are depending on national regulations and in some countries more than 95% CH₄ content is required; however, European Commission has recently issued a mandate for determining harmonized standards for gas quality (Angelidaki et al., 2018).

Biomethane can show a substantial impact in future energy systems in Europe because of EU policies to increase the share of renewable and low carbon fuels and contribute to the decarbonization of heat and transport (Wall et al., 2018; European Commission 0382, 2017). In addition, biomethane production allows to reduce reliance on natural gas imports (EurObserver, 2014) and permits its transport and utilization far from the place where is obtained.

Upgrading biogas to biomethane is one of the technologies that attract great interest in the bioenergy industry. An increasing number of biogas plants with biogas upgrading units are emerging in Europe in the recent years (Figure 2a). As shown in Figure 2a, most of the biomethanation plants are in Germany, while other European countries such Sweden, UK and Switzerland have also constructed biomethanation facilities (Figure 2b).

The technical features of upgrading technologies, i.e. physical/chemical and biological methods are below discussed.

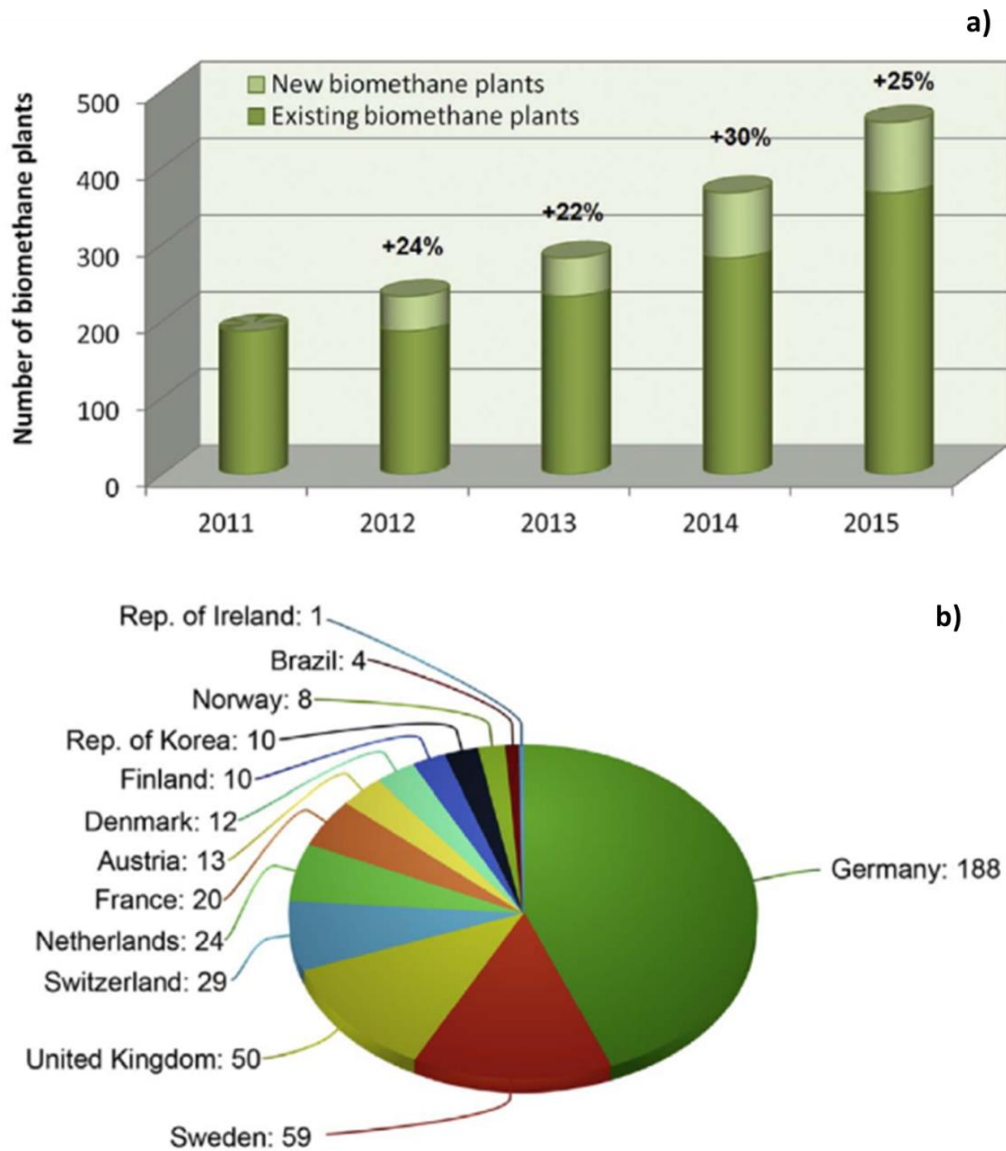


Figure 2. Development of biogas upgrading technologies distributed according to countries and years; **a)** number of operating biomethane plants, **b)** location of existing biomethane plants (Angelidaki et al., 2018).

1.2.1 Physical and chemical technologies

Currently, commercial technologies for biogas upgrading are mainly based on physical or chemical methods involving processes of physical absorption (using water scrubbing, organic solvents or amine solutions), pressure swing adsorption (PSA) and membrane separation (Muñoz et al., 2015; Wu et al., 2015). In addition, cryogenic

separation and chemical hydrogenation processes are other technologies which are still under development (Angelidaki et al., 2018).

The distribution of applied commercial technologies is represented in Figure 3 and Table 1 shows the comparison of the biomethanation efficiencies in different pilot and commercial biogas upgrading technologies.

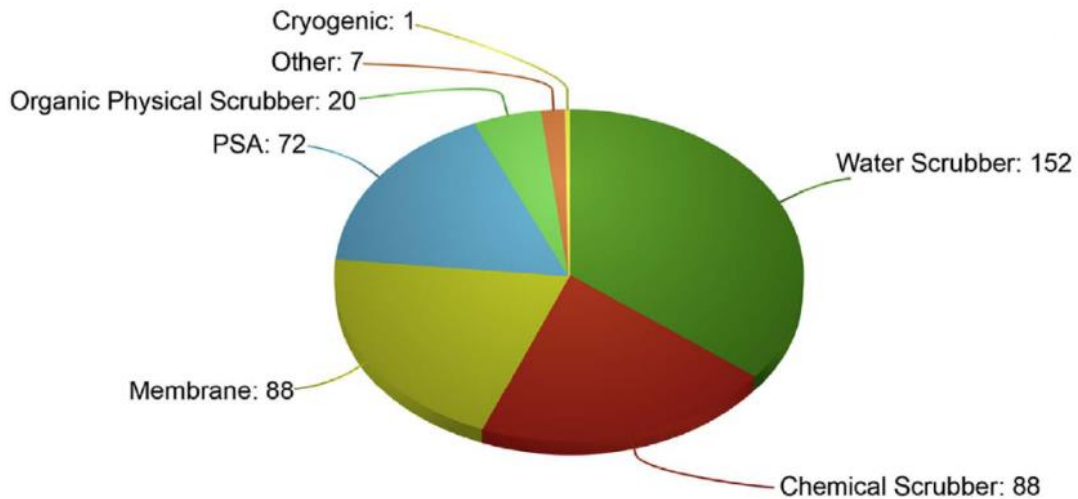


Figure 3. Distribution of applied commercial biogas upgrading technologies (Angelidaki et al., 2018).

Although the methane recovery from physicochemical processes can reach more than 96% (Table 1), these technologies only separate CH_4 from CO_2 thus requiring further steps to avoid CO_2 emissions (Bauer et al., 2013; Muñoz et al., 2015). In general, the use of chemical substances, high pressures and high temperatures are required to ensure an efficient biomethanation facing significant challenges in terms of energy consumption thus increasing process costs (Angelidaki et al., 2018; Sun et al., 2015). Therefore, apart from the addition of substantial cost to the upgraded biogas, possible environmental disadvantages take place. Moreover, these technologies involve high investment costs due to their technical complexity and methane losses to the atmosphere are produced. For all these reasons, other biogas upgrading technologies are desirable as an alternative to physical and chemical methods.

Table 1. Comparison of different pilot and commercial biogas upgrading technologies (Angelidaki et al., 2018; Andriani et al., 2014; Bauer et al., 2013; Bekkering et al., 2010; Jürgensen et al., 2014; MeGa-stoRE, 2016; Muñoz et al., 2015; Ryckebosch et al., 2011; Serejo et al., 2015; Toledo-Cervantes et al., 2017). nf: not found.

	Water scrubbing	Physical scrubbing	Sabatier process	PSA	Membrane separation	Cryogenic	Chemical absorption
Consumption for raw biogas (kWh/Nm³)	0.25-0.30	0.2-0.3	nf	0.23-0.30	0.18-0.20	0.76	0.05-0.15
Consumption for clean biogas (kWh/Nm³)	0.3-0.9	0.4	nf	0.29-1.00	0.14-0.26	nf	0.05-0.25
Heat consumption (kWh/Nm³)	None	<0.2	nf	None	None	nf	0.5-0.75
Heat demand (°C)		55-80	270			-196	100-180
Operation pressure (bar)	4-10	4-8	8-10	3-10	5-8	80	Atmospheric
Pressure at outlet (bar)	7-10	1.3-7.5		4-5	4-6	8-10	4-5
Cost	Medium	Medium	Medium	Medium	High	High	High
CH₄ losses (%)	<2	2-4	nf	<4	<0.6	2	<0.1
CH₄ recovery (%)	96-98	96-98	97-99	96-98	96-98	97-98	96-99
Pre-purification	Recommended	Recommended	Recommended	Yes	Recommended	Yes	Yes
H₂S co-removal	Yes	Possible	No	Possible	Possible	Yes	Contaminant
N₂ and O₂ co-removal	No	No	No	Possible	Partial	Yes	No

1.2.2 Biological technologies

An alternative to the commercial methods for biogas upgrading are the biological biogas upgrading technologies, constituting a cheaper and environmentally friendly alternative moving towards sustainable energy production.

The main advantage of biological biogas upgrading technologies compared to physicochemical methods is related to the fact that the CO_2 is converted into other energy containing or high value added products at mild operational conditions (atmospheric pressure and moderate temperature levels) contributing significantly to a sustainable bio-based and circular economy (Angelidaki et al., 2018). Moreover, biological methanation has shown higher tolerance to the impurities usually present in biogas in comparison to the catalytic pathway.

In general, the biological biogas upgrading technologies can be classified into chemoautotrophic and photosynthetic. Most of these configurations have been experimentally proven and are at an early stage of pilot or full scale implementation. In addition, biological biogas upgrading can be performed through other fermentation processes or through microbial electrochemical methods.

The chemoautotrophic biogas upgrading methods are based on the action of hydrogenotrophic methanogens that can utilize H_2 to convert CO_2 to CH_4 , namely hydrogen assisted biological biogas upgrading.

Similarly to these chemoautotrophic methods, photosynthetic biogas upgrading is an alternative method to sequester CO_2 in order to obtain an enriched CH_4 gas by means of phototrophic organisms like microalgae in enclosed or open bioreactors (Muñoz et al., 2015).

Although CO_2 in biogas can be biologically converted to CH_4 by these two methods, the production of valuable liquid products (acetate, butyrate, caproate, caprylate, ethanol, butanol, etc.) from CO_2 in biogas through fermentation processes is attractive as well because of their fuel value (Agler et al., 2011). However, not only the effects of biogas impurities on fermentation but also the methods to enhance the selectivity of the liquid products need to be investigated.

CO₂ removal in biogas to produce CH₄ by electrochemical systems has been presented as a potential sustainable and cost-effective way to upgrade biogas (Lovley and Nevin, 2013; Van Eerten-Jansen et al., 2012). In a microbial electrolysis cell, electrons released by bacteria from the oxidation of organics in anode can combine with protons to generate hydrogen in the cathode chamber which be used for biogas upgrading (Zhang and Angelidaki, 2014). However, most of the current investigations are based on lab-scale experiments thus the technical and economic limitations for scaling up remain unexplored.

1.3 HYDROGEN ASSISTED BIOLOGICAL BIOGAS UPGRADING

An attractive chemoautotrophic method for biogas upgrading is the biological conversion of H₂ and CO₂ to CH₄ via hydrogenotrophic methanogenesis (which is in the last stage of the AD process as it is shown in Figure 1) based on the reaction (Eq. 1):



The bioconversion is performed by hydrogenotrophic *archaea*, a group of microorganisms that utilize CO₂ as carbon source and H₂ as an electron donor in order to produce biomethane (Muñoz et al., 2015). Additionally, some of the H₂ and CO₂ are used as elemental sources for cell growth (Bryant, 1979). Following the stoichiometric equation, the addition of H₂ to the system should be four times the CO₂ volume.

This technology fixes CO₂ by means of its conversion with H₂ to biomethane, decreasing the CO₂ emissions to the atmosphere and then the greenhouse gases, reducing by this way its impact in the global warming which can be translated into an effective CO₂ mitigation technology and providing enhanced environmental benefits of biogas technologies.

Moreover, hydrogenotrophic methanogenesis can operate exploiting mixed culture and can be applied in mild operating conditions, without using chemical substances, markedly reducing operation costs (Götz et al., 2015).

1.3.1 Power-to-Gas (P2G) technology

In order to make the biological upgrading method renewable maintaining a sustainable energy process, the H₂ required in the reaction (Eq. 1) should derive from renewable source and needs to be generated by an external source. H₂ gas can be produced from biomass gasification, reforming of biomethane, biological H₂ production, or through electrolysis of water (Turner et al., 2008).

Nowadays, water electrolysis using renewable energy sources such as wind and solar power is considered the only environmentally friendly technology in large scale application to obtain H₂ for bioconversion of CO₂ to CH₄ (Muñoz et al., 2015). Water electrolysis is a clean power source free of CO₂ emissions, splitting the water to O₂ and H₂ with direct electric current passing through two electrodes and a membrane, according to Eq. 2:



EU countries with high implementation of renewable energies, suffer of seasonal surpluses where production exceeds demand and an appreciable portion of electricity production is lost in most cases. H₂ generation from water electrolysis using off-peak electricity surplus from wind and solar power can solve the limitations of variable wind and solar power production, site-specificity of these sources and electricity storage (Levene et al., 2007; Ni et al., 2006) thus allowing long-term energy storage avoiding energy squandering (Cruz, 2008), which is an important and remarkable point nowadays in the idea of environmental conservation and responsible use of energy.

However, H₂ limitations and drawbacks are linked to its transportation and management (Granovskii et al., 2006) because of its low density which requires high storage volumes and the technology for direct utilization is not developed yet.

Then, the direct transformation of H₂ into biomethane by coupling it with CO₂ permits renewable energy in the form of biomethane to be stored, injected and distributed through the natural gas grid or employed as fuel for vehicles (Deublein and Steinhauser, 2011; Deng and Hägg, 2010).

Therefore, the coupling of biogas/CO₂ production from the anaerobic digestion of organic matter with the exploitation of H₂ that is generated due to excess renewable energies is an effective and attractive method for bioenergy production creating a unique synergy of renewable energy sources called Power-to-Gas (P2G) (Power to Gas Strategy, 2011; Kougias et al., 2017; Götz et al., 2015) (Figure 4).

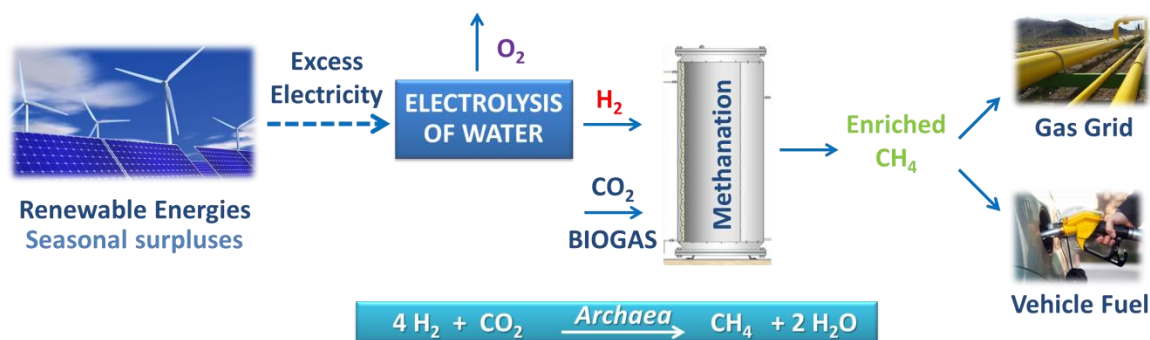


Figure 4. Power-to-Gas concept.

Consequently, integration of P2G technology for conversion of H₂ to CH₄ is a promising means to convert electricity to a chemical energy carrier, which can easily be stored in the existing natural gas infrastructure (Angelidaki et al., 2018). Apart from CH₄ energy content (36 MJ/m³) is remarkably higher compared to H₂ one (10.88 MJ/m³) (Luo et al., 2012), the upgrading process exploits the existing facilities of the biogas plants and therefore reduces the initial investment cost. Moreover, several opportunities have been identified for the integration of P2G in wastewater treatment plants (WWTP) (Patterson et al., 2017).

Nowadays, commercial water electrolyzers are able to cold start within a few minutes (Bhandari et al., 2014; Persson et al., 2015), enabling the system to offer grid-balancing services, assisting the power grid to meet the supply of electricity to the demand (Guinot et al., 2015). Therefore, this P2G technology provides large-scale energy storage, as the end-use of biomethane is not limited in the gas grid and also avoids safety management issues associated with H₂ production and handling (Collet et al., 2017).

Furthermore, as stated above for chemoautotrophic biogas upgrading methods, the CO_2 is not separated or absorbed but converted to CH_4 leading to a significant increment of the final energy value of the output “windgas” (i.e. CH_4 produced using the surplus energy from wind turbines) or “solargas” (i.e. CH_4 produced using the surplus energy from photovoltaic panels) (Kougias et al., 2017).

Finally, P2G technology serves as a precondition for the sustainability of the ambitious biogas implementation plan of decoupling the biogas production from the biomass availability (Angelidaki et al., 2018).

Figure 5 shows a timeline which clearly represent the evolution and concatenation of worldwide P2G projects with years (Bailera et al., 2017). As shown in Figure 5, Tohoku University and Hitachi Zosen initiated their research in P2G systems in 1996 appearing as pioneers in this field.

As shown in Figure 5, most of the projects were launched from 2009 onwards when the international community massively discovered the great potential of P2G in excess electricity storage. General information of P2G projects is summarized in Table 2.

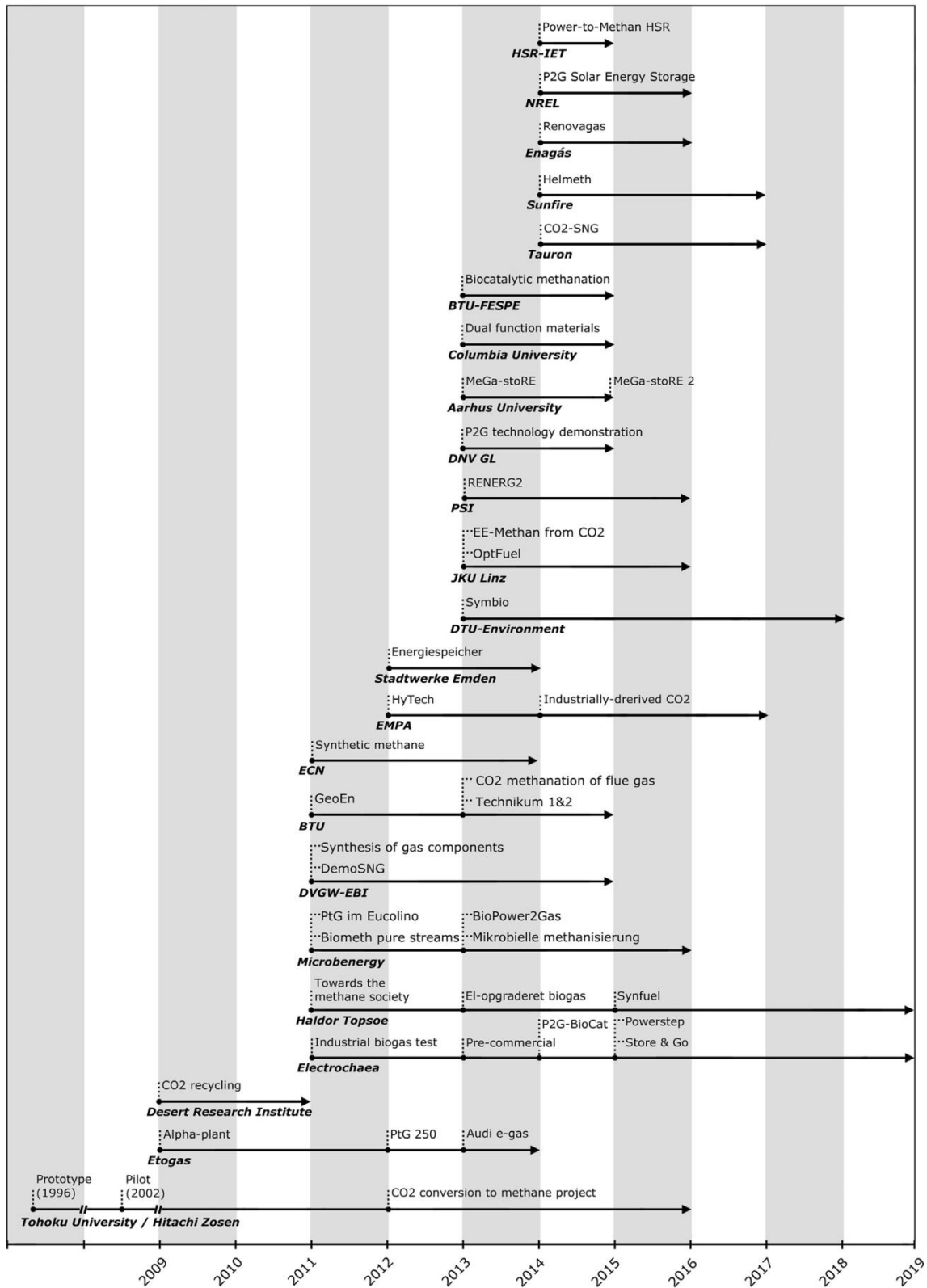


Figure 5. Timeline of worldwide existing P2G projects with pilot and demo plants (Bailera et al., 2017).

Table 2. Worldwide P2G projects with pilot and demo plants (Bailera et al., 2017).

Process type	Project Name	Location	Period	Institutions
CO ₂ methanation	Audi e-gas	Werlte, Germany	2013	ETOGAS, ZSW, Fraunhofer IWES, EWE Biogas, Audi
CO ₂ methanation Biogas upgrading	Power to Gas 250 Alpha-plant	Stuttgart, Germany Bad Hersfeld, Germany	2012–2014 2012	ETOGAS, ZSW, Fraunhofer IWES ETOGAS, ZSW, Fraunhofer IWES, HBFZ
Biogas upgrading	Alpha-plant	Morbach, Germany	2011	ETOGAS, ZSW, Fraunhofer IWES, Juwi
CO ₂ methanation	Alpha-plant	Werlte, Germany	2010–2011	ETOGAS, ZSW, EWE Biogas
CO ₂ methanation	Alpha-plant	Stuttgart, Germany	2009	ETOGAS, ZSW
n/a	STORE & GO	Switzerland, Germany, Italy	2015–2019	Electrochaea, DVGW, E.ON, Regio Energie, EII Spa, HSR, PoliTo, JKU Linz-EI, RUG, Atmosat, CEA, Climeworks, DBI-GUT, BFP, EDI, EMPA, EPFL-IPESSE, EPFL-MER, EPFL-CEN, Energy Valley
Biogas upgrading	POWERSTEP – Full scale demonstration of energy positive sewage treatment plant concepts towards market penetration	n/a	2015–2018	Electrochaea, KWB, TU Wien, Eawag, Fraunhofer IPM, Veolia, Veolia-WT, NEAS, Biofos, BWB, UBA, APS, Sustec, Artemis, Arctic
Biogas upgrading	P2G-BioCat project	Avedøre, Denmark	2014–2016	Electrochaea, Hydrogenics, Audi, NEAS, HMN Gashandel, Biofos, Insero
Biogas upgrading	Pre-commercial	Foulum, Denmark	2013	Electrochaea, E.ON, Energie 360°, EWZ, NEAS, AU
Biogas upgrading	Industrial Biogas Test	Chicago, United States	2011	Electrochaea, UChicago, AB InBev
Biogas upgrading	BioPower2Gas	Allendorf, Germany	2013–2016	Microbenergy, Schmack, Carbotech, EnergieNetz, EAM EnergiePlus, CUBE, DBFZ, Ide
Biogas upgrading	Mikrobielle Methanisierung	Schwandorf, Germany	2013	Microbenergy, Schmack, FENES, ZVKS
Biogas upgrading	Power-to-Gas im Eucolino	Schwandorf, Germany	2011	Microbenergy, Schmack
CO ₂ methanation	Biological methanation of pure streams	Schwandorf, Germany	2011	Microbenergy, Schmack
CO ₂ methanation	HELMETH	n/a	2014–2017	Sunfire, KIT, PoliTo, ERIC, TS-Torino, NTUA, DVGW
Syngas upgrading	SYNFUEL	n/a	2015–2019	Haldor Topsoe, DTU, AAU, Chalmers, DONG, Energinet.dk, INSA, TU Berlin, NU, CAS, MIT, AVL
Biogas upgrading	El-opgraderet biogas	Foulum, Denmark	2013–2016	Haldor Topsoe, Ea, AU, PlanEnergi, HMN Naturgas, NGF, EnergiMidt, DGC, Cemtec, Xergi
Biogas upgrading	På Vej Mod Metansamfundet /Towards the methane society	Midtjylland, Denmark	2011–2012	Haldor Topsoe, AU, AgroPark, HIRC, Planenergi, GreenHydrogen, HMN Naturgas, Lemvig Biogas, DTU, INBIOM
Biogas upgrading	MeGa-stoRE 2 – Optimising and Upscaling	n/a	2015–n/a	AU, NGF, DTU, Elplatek, GreenHydrogen
Biogas upgrading	MeGa-stoRE – Methane Gas storage of Renewable Energy	Lemvig, Denmark	2013–2015	AU, Elplatek, GreenHydrogen, Lemvig Biogas, DTU-Mekanik, AU Herning
Biogas upgrading	SYMBIO	Denmark	2013–2018	DTU-Environment, SDU, UM, Energinet.dk, Maabjerg BioEnergy
Biogas upgrading	RENOVAGAS	Spain	2014–2016	Enagas, ICP-CSIC, CNH2, FCC-Aqualia, Gas Natural Fenosa, Tecnalia, Abengoa
CO ₂ methanation	Technical assumptions, technology demonstration and results P2G project	Rozenburg, Netherlands	2013–2015	DNV GL, TKI Gas, Stedin, Rotterdam Council, Ressort Wonen
Syngas upgrading	Synthetic methane: a medium for storage and transportation of excess renewable energy	Netherlands	2011–2014	ECN, TU-Delft, Hanze UAS
Syngas upgrading	DemoSNG	Köping, Sweden	2011–2015	DVGW-EBI, KIT, KTH, Cortus, Gas Natural Fenosa
CO ₂ methanation	Storage of electric energy from renewable sources in the natural gas grid – water electrolysis and synthesis of gas components	Baden-Wurtemberg, Germany	2011–2014	DVGW-EBI, EnBW, Fraunhofer ISE, H-Tec, IoLiTec, Outotec
CO ₂ methanation	CO ₂ -SNG	Poland	2014–2017	Tauron, CEA, Atmosat, AGH-UST, IchPW, Rafako, WT & T Polska
CO ₂ methanation	CO ₂ recycling via reaction with hydrogen	Reno, United States	2009	DRI, RCO ₂ AS
CO ₂ methanation	Pilot- und Demonstrationsanlage Power-to-Methane HSR	Rapperswil, Switzerland	2014–2015	HSR-IET, HSR, Audi, Climeworks, Erdgas Obersee, Erdgas Regio
Biogas upgrading	Kommunale Kläranlagen als Energiespeicher	Emden, Germany	2012–2014	Stadtwerke Emden, BEE, Thalen Consult, ibis Umwelttechnik, GA-Group
CO ₂ methanation	CO ₂ Conversion to Methane Project	Rayong, Thailand	2012–2016	Hitachi Zosen, DAE, PTTEP
CO ₂ methanation	Pilot plant – Tohoku Institute of Technology	Tohoku, Japan	2002–2005	Tohoku University, TohTech, Hokudai, DAE, NRI, MES, Ryoka
CO ₂ methanation	Prototype plant – Tohoku University	Tohoku, Japan	1996	Tohoku University, IMR, TohTech, Hokudai, DAE, NRI, MES, Ryoka
CO ₂ methanation	EE-Methan from CO ₂	Leoben, Austria	2013–2016	JKU Linz, MU Leoben, TU Wien, Christof Group, Profactor, ÖVGW, FGW
Biogas upgrading	OptFuel	Leoben, Austria	2013–2016	JKU Linz, MU Leoben, TU Wien, Christof Group, Profactor, ÖVGW, FGW
CO ₂ methanation	P2G Solar Energy Storage RD & D	Golden, United States	2014–2016	NREL, SoCalGas
CO ₂ methanation / Biogas upgrading	RENERG ²	Villigen, Switzerland	2013–2016	PSI, EMPA, ETH Zurich, ZHAW, EPFL
CO ₂ methanation	Catalytic methanation of industrially-derived CO ₂	Dübendorf, Switzerland	2014–2017	EMPA, ZHAW
Biogas upgrading	SmartCat	Dübendorf, Switzerland	n/a	EMPA, ZHAW, Zeochem, VSG
CO ₂ methanation	HyTech	Dübendorf, Switzerland	2012–2015	EMPA, ZHAW, EPFL, PSI
CO ₂ methanation	CO ₂ -Methanation of flue gas	Brandenburg, Germany	2013–2015	BTU, Panta Rhei, Vattenfall
CO ₂ methanation	CO ₂ catalysis, pilot plant - Technikum 1 & 2	Cottbus, Germany	2013–2014	BTU
CO ₂ methanation	GeoEn	Cottbus, Germany	2011–2013	BTU, GFZ, Uni-Postdam
CO ₂ methanation	Dual function materials for CO ₂ capture and conversion using renewable H ₂	New York, United States	2013–2015	Columbia University, BASF
CO ₂ methanation	Biocatalytic methanation in an anaerobic three-phase system	Cottbus, Germany	2013–2015	BTU-FESPE

1.3.2 Chemoautotrophic biogas upgrading configurations

The chemoautotrophic biological biogas upgrading process can be defined in three concepts namely ex-situ, in-situ and hybrid designs (Kougias et al., 2017) depending on where the H_2 is provided with respect to the anaerobic digestion process. Till now, the ex-situ and in-situ processes are experimentally studied and proven and several research works are available in literature. However, the hybrid design is currently under development and the first results related to that technology have been published recently.

1.3.2.1 Ex-situ biogas upgrading

The ex-situ biogas upgrading concept relies to the supply of H_2 and CO_2 (or biogas) to an exclusively methanogenic bioreactor that contains (pure or enriched) hydrogenotrophic *archaea*, resulting in their subsequent conversion to CH_4 (Figure 6).

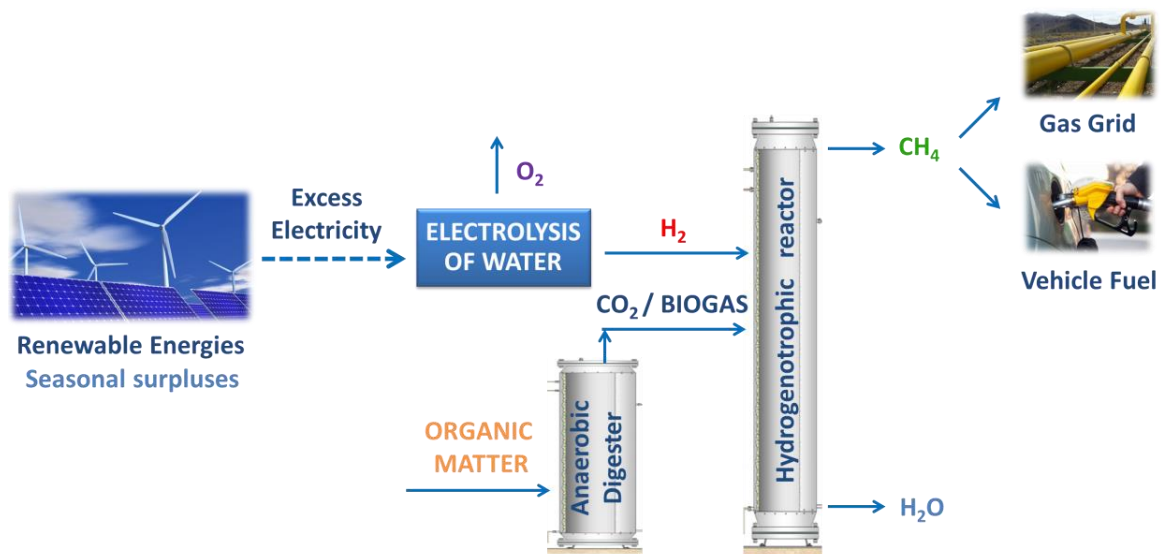


Figure 6. Ex-situ biogas upgrading concept.

Till now, several studies investigated the ex-situ biogas upgrading process in different temperature conditions and it was demonstrated that the operating temperature was important for the biomethanation efficiency. It was found that the performance of the reactors and efficiency of the system is improved at thermophilic conditions (Bassani

et al., 2015; Yun et al., 2017; Luo and Angelidaki, 2012). Another study concluded that an increment of the operating temperature from 55 °C to 65 °C leads to more efficient biomethanation operation (Guneratnam et al., 2017).

The limiting factor in ex-situ systems is the efficient diffusion of H₂ in the liquid phase, which will make it available for the microorganisms (Bassani et al., 2016; Martin et al., 2013). Dimensionless Henry's constant of H₂ is 50 and 55 g/L_G/g/L_{H₂O} at 35 and 55 °C respectively (Ju et al., 2008) so the H₂ gas-liquid mass transfer was found to be the main constraint to the successful development of the technology. H₂ gas-liquid mass transfer rate is described by the following equation (Bassani et al., 2016) (Eq. 3):

$$r_t = 22.4 \cdot K_L a_{H_2} \cdot (H_{2g} - H_{2l}) \quad (\text{Eq. 3})$$

where r_t (L/L_R·d) is the H₂ gas-liquid mass transfer rate, 22.4 (L/mol) is the gas volume to mol ratio (1 mol of gas corresponds to 22.4 L at 273.15 K and 1 atm), $k_L a_{H_2}$ is the specific gas transfer coefficient (h⁻¹), H_{2g} (mol/L) represents the H₂ concentration in the gas phase while H_{2l} (mol/L) is the H₂ dissolved in the liquid phase. Therefore, it is obvious that the H₂ gas-liquid mass transfer rate is proportionally correlated with the $k_L a_{H_2}$ value.

To address this technical challenge, different reactor configurations have been investigated at lab or pilot scale aiming at maximizing the H₂ gas-liquid mass transfer. Reactors based on different diffusion devices, high-speed stirring or gas recirculation flow have been tested to enhance the H₂ mass transfer into the liquid phase.

Continuous Stirred Tank Reactors

Regarding Continuous Stirred Tank Reactors (CSTR), a stirring speed range between 70 and 800 rpm was investigated in several studies (Table 3) at thermophilic and mesophilic conditions. Excepting the 100 L CSTR used in Kim et al. (2013), the rest of experiments were performed at lab-scale with small reactor working volumes (0.6 - 3.5 L) and small H₂ loading rates (Table 3).

Table 3. Comparison of ex-situ biological upgrading processes in CSTR configurations (na= not available).

Reactor Working Volume (L)	Stirring speed (rpm)	Gas Diffusion system	Liquid media	Temperature (°C)	Gas recirculation (L/L _R ·d)	H ₂ loading rate (L/L _R ·d)	H ₂ efficiency (%)	CH ₄ content (%)	CH ₄ production rate (L/L _R ·d)	pH	VFA accumulation	Reference
1.2	300	Two stainless steel diffusers (2 µm)	Anaerobic digestate	55	80	1.9	60	54	na	8.2	Yes	Kougias et al., 2017
					240	1.9	60	79	na	8.4	Yes	
2.0	na	Diffuser	Anaerobic digestate	55	No	0.51	92	85	0.36	8.5	Stable	Bassani et al., 2015
2.0	na	Diffuser	Anaerobic digestate	37	No	0.19	93	89	0.10	8.2	Stable	Bassani et al., 2015
100.0	70	Gas dissolution device	Anaerobic sludge from municipal WWTP	35	No	18.0	na	92	4.1	7.2	na	Kim et al., 2013
3.5	700	na	Pure Culture <i>Methanothermobacter thermautotrophicus</i>	60	No	82.0	89	na	21	7.4	na	Martin et al., 2013
0.6	500	Ceramic diffusers	Enriched hydrogenotrophic culture	55	No	1.8	98	94	0.9		Yes	Luo and Angelidaki, 2012
	500				No	3.6	97	95	1.5	Yes		
	500				No	7.2	95	90	2.6	7.8	Yes	
	800				No	7.2	97	94	2.7	Yes		
	800				No	14.4	95	91	5.3	Yes		

Although most of the experiments were performed using anaerobic digestate as inoculum (Kougias et al., 2017; Bassani et al., 2015; Kim et al., 2013), an enriched hydrogenotrophic culture (Luo and Angelidaki, 2012) and a pure culture of *Methanothermobacter thermautotrophicus* (Martin et al., 2013) have been investigated as well. Stainless steel diffusers were the most common gas diffusion systems in the ex-situ experiments (Table 3).

The biogas upgrading efficiency in CSTRs resulted in final CH₄ content between 54 and 95% with H₂ efficiencies ranging from 60 to 98% (Table 3).

However, considering the implementation of these CSRT systems at industrial scale, high energy needs and operational costs would be required for the biological methanation.

Bubble column reactors

Bubble column configurations showed the big positive influence of the gas diffusion device and pore size on upgrading performance regarding H₂ gas-liquid mass transfer (Table 4). Moreover, some of these studies confirmed the positive effect of gas recirculation on upgrading performance previously described (Guiot et al., 2011) improving the contact between gases and the liquid media of the reactor thus increasing $k_L a_{H_2}$ value markedly.

Bubble column configurations have been studied at thermophilic conditions in small reactor working volumes (0.85 - 2.8 L) at lab-scale (Bassani et al., 2017; Kougias et al., 2017). Stainless steel diffusers (2 µm pore size), stainless steel diffusers (0.5 µm and 2 µm pore size) combined with alumina ceramic sponge and Al₂O₃ ceramic membrane (0.4 µm and 1.2 µm) were employed as gas diffusion systems.

The biogas upgrading efficiency in bubble columns resulted in final CH₄ content between 66 and 98% with H₂ efficiencies ranging from 78 to 100% (Table 4).

Table 4. Comparison of ex-situ biological upgrading processes in bubble column reactor configurations (na= not available).

Reactor Type	Reactor Working Volume (L)	Gas Diffusion system	Liquid media	Temperature (°C)	Gas recirculation (L/L _R ·d)	H ₂ loading rate (L/L _R ·d)	H ₂ efficiency (%)	CH ₄ content (%)	CH ₄ production rate (L/L _R ·d)	pH	VFA accumulation	Reference
Up-flow	0.85	3 stainless steel diffusers (0.5 µm) combined with alumina ceramic sponge	Enriched hydrogenotrophic inoculum	55	3, 6, 10 and 20	1, 2 and 4	100	90 - 95	0.08, 0.11, 0.33, 0.35, 0.72 and 0.79	8.1-8.8	Decreasing	Bassani et al., 2017
	0.85	3 stainless steel diffusers (2 µm) combined with alumina ceramic sponge	Enriched hydrogenotrophic inoculum		3, 6, 10 and 20	1, 2 and 4	99-100	92 - 96	0.09, 0.10, 0.38, 0.39, 0.69 and 0.82	8.0-8.8	Decreasing	
	0.85	Al ₂ O ₃ ceramic membrane (0.4 µm)	Enriched hydrogenotrophic inoculum		3, 6, 10 and 20	1, 2 and 4	99 – 100	88 – 95	0.09, 0.12, 0.35, 0.40, 0.70 and 0.70	8.1-8.8	Decreasing	
	0.85	Al ₂ O ₃ ceramic membrane (1.2 µm)	Enriched hydrogenotrophic inoculum		3, 6, 10 and 20	1, 2 and 4	99 - 100	92 - 96	0.17, 0.21, 0.37, 0.37, 0.73 and 0.71	8.1-8.9	Decreasing	
Bubble column	1.20	Two stainless steel diffusers (2 µm)	Anaerobic digestate	55	80	1.9	84	73	na	8.2	Yes	Kougias et al., 2017
					240		>95	98	na	8.5	Yes	
Up-flow in series	1.40+1.40	Two stainless steel diffusers (2 µm)	Anaerobic digestate	55	34	0.8	78	66	na	8.3	Yes	Kougias et al., 2017
	1.40+1.40				103	0.8	99	98	na	8.5	Yes	

Membrane bioreactors (MBR) were also evaluated at lab-scale for the transfer of H₂ by gas diffusion through the hollow-fiber membrane material, reaching a final concentration of biomethane in upgraded biogas of more than 95% (Strevett et al., 1995), as well as high methanogenic activity even at low pH values or high concentrations of reaction intermediates (Ju et al., 2008) at mesophilic conditions.

Therefore, considering the implementation of bubble column systems at industrial scale for the biological biomethanation, further studies are needed to assess the feasibility of the bioconversion at higher scales (pilot-scale), operating with higher H₂ loading rates and higher reactor volumes.

Trickling biofilter (TBF) reactors

More recently, a different approach has been proposed for supporting the biomethanation using trickling biofilter (TBF) reactors. TBF reactors consist of a column that is packed with material of high specific surface area, on which biofilm is developed. The formation of biofilm of mixed anaerobic consortia serves as a good biocatalyst for the completion of the process.

Compared to systems where the microorganisms are suspended in liquid media, biofilms present certain advantages, such as immobilization of the microbial community (avoiding discharge from the system) and increased resistance to inhibitory or toxic compounds (Hori and Matsumoto, 2010). This technology not only avoids the need for traditional biogas upgrading, but also paves the way for the development of advance renewable energy systems.

Although most of the TBF reactors have been studied at mesophilic conditions (Dupnock and Deshusses, 2017; Rachbauer et al., 2016; Burkhardt et al., 2015; Burkhardt and Busch, 2013; Lee et al., 2010), literature shows two studies at thermophilic conditions (Strübing et al., 2017; Alitalo et al., 2015). Only in the study performed by Burkhardt and Busch (2013) gas recirculation rate was applied.

Lab and pilot-scale reactors have been investigated with different packing materials and final CH₄ content ranged from 71 to 98% (Table 5).

Table 5. Comparison of ex-situ biological upgrading processes in TBF reactor configurations (na= not available).

Reactor Type	Reactor Working Volume (L)	Support/Packed Material	Trickling liquid	Inoculum	Temperature (°C)	H ₂ loading rate (L/L _R ·d)	H ₂ efficiency (%)	CH ₄ content (%)	CH ₄ production rate (L/L _R ·d)	pH	VFA accumulation	Reference
Trickle-bed reactor	58.1	RFK and Hel-X bio carrier HXF12KLL	10 L/h Counter-flow	Anaerobic sludge from WWTP	55	1.7 – 62.1	na	71 - 98	1.7 – 15.4	Controlled	na	Strübing et al., 2017
Trickle-bed reactor	na	Polyuretane foam	na With the flow	Enriched hydrogenotrophic culture	35	na	na	20 - 30	11.0 – 30.0	6.7 – 8.0	na	Dupnock and Deshusses, 2017
Trickle-bed reactor	5.8	Polypropylene packing rings	15 L/h Counter-flow	Enriched hydrogenotrophic culture	37	5.0 - 11.0	na	95 - 98	1.2 - 2.5	7.4 – 7.7	No	Rachbauer et al., 2016
Fixed bed reactor in series	4.0	Vermiculite shales and granular perlite	1L/72h With the flow	Methanogenic culture	55	25.2	100	>90	6.4	6.9	na	Alitalo et al., 2015
Trickle-bed reactor	61.0	Bioflow 40	6 L/h Counter-flow	Anaerobic sludge from WWTP	37	0.4 – 6.0	100	95 - 98	0.2 – 1.5	7.2 – 7.4	na	Burkhardt et al., 2015
Trickle-bed reactor	26.8	Bioflow 40	0.5 L/h Counter-flow	Digested sludge from sewage treatment plant	35	2.5 – 4.5	94 - 100	93 - 98	0.7 – 1.2	na	na	Burkhardt and Busch, 2013
Fixed bed reactor	7.8	Reticulated polyester urethane sponge	na	Anaerobic culture from sewage treatment plant	35	0.9 – 6.3	na	na	1.0 – 3.2	na	No	Lee et al., 2012

Although the feeding gas mixture was injected in the reactors either with the flow or counter-flow to the liquid media (Table 5), the possible influence of the injection direction on the biogas upgrading process is still unexplored.

Moreover, the study of the microbial community involved in ex-situ biogas upgrading process in TBF reactors has been scarcely studied only at mesophilic conditions in one work (Dupnock and Deshusses, 2017), remaining uncharacterized at thermophilic conditions.

Biofilm plug-flow reactor

The performance of a novel biofilm plug flow reactor containing a mixed anaerobic microbial culture was investigated by Savvas et al. (2017) for the conversion of H₂ and CO₂ to CH₄. The reactor comprised a 7 m length of a single walled flexible PVC tube with a 13 mm internal diameter which was filled with polyethylene wheels (Kaldnes k1) that served as the biofilm attachment media. The total working volume was approximately 0.75 L and the reactor worked at mesophilic conditions (37 °C).

Unlike conventional gas-liquid contactors that depend on agitation, gas diffusion was decoupled from power consumption for mixing by increasing the gas phase inside the reaction space whilst increasing the gas residence time.

The study showed that it is possible to obtain high biomethanation conversion rates and efficiencies by changing the way a mixed microbial culture is utilized, with the specific aim of reducing the liquid volume in the reactor while increasing the gas residence time.

The novelty of the present design (in horizontal mode, Figure 7) relied on the adhesive properties of water which allowed the minimization of the liquid media volume used for nutrient replenishment of the biofilm as opposed to trickling bed reactor designs.

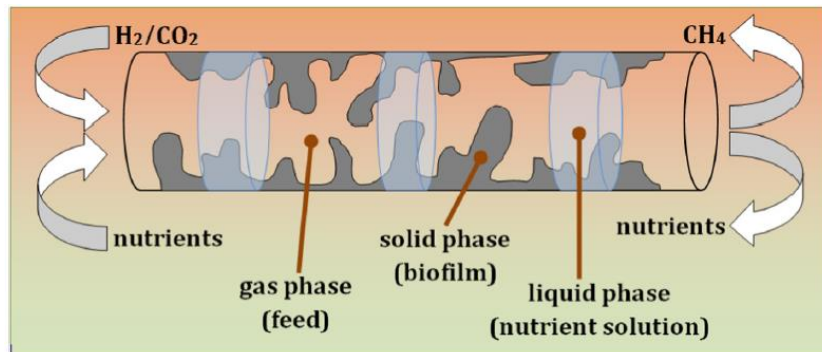


Figure 7. Novel biofilm plug-flow reactor studied by Savvas et al. (2017).

The mixed mesophilic culture exhibited good biofilm formation and metabolic activity. With minimal energy input for liquid media transfer, 99% and 90% CH_4 conversion efficiencies were achieved at total gas throughputs of 100 and 150 $\text{L/L}_R\cdot\text{d}$, respectively. At a gas input rate of 230 $\text{L/L}_R\cdot\text{d}$, methane rates reached 40 $\text{L/L}_R\cdot\text{d}$, which are the highest to date achieved by fixed film biomethanation systems. Additionally, significant gas transfer related parasitic energy savings could be achieved and demonstrated when using the novel plug flow design as compared to a CSTR.

1.3.2.2 In-situ biogas upgrading

The addition of H_2 to conventional anaerobic digesters of organic matter with the aim of removing CO_2 from biogas while increasing the production of biomethane is called in-situ biogas upgrading technology (Figure 8). As H_2 is supplied directly to the anaerobic digester so that hydrogenotrophic *archaea* can consume H_2 and CO_2 , additional units for upgrading may be avoided (Zabranska and Pokorna, 2018; Rittmann, 2015).

In-situ upgrading has been only studied (Table 6) in a few lab-scale bioreactors (0.3 – 3.5 L): completely mixed anaerobic digesters of manure (Luo and Angelidaki, 2013a, Luo and Angelidaki, 2013b; Luo et al., 2012) or of sewage sludge (Agneessens et al., 2018; Agneessens et al., 2017; Wang et al., 2013) and in UASB reactors treating potato-starch wastewater (Bassani et al., 2016). In these studies, H_2 gas was bubbled through gas diffusers or diffused within across the biofilm found on hollow-fiber membrane modules (Table 6).

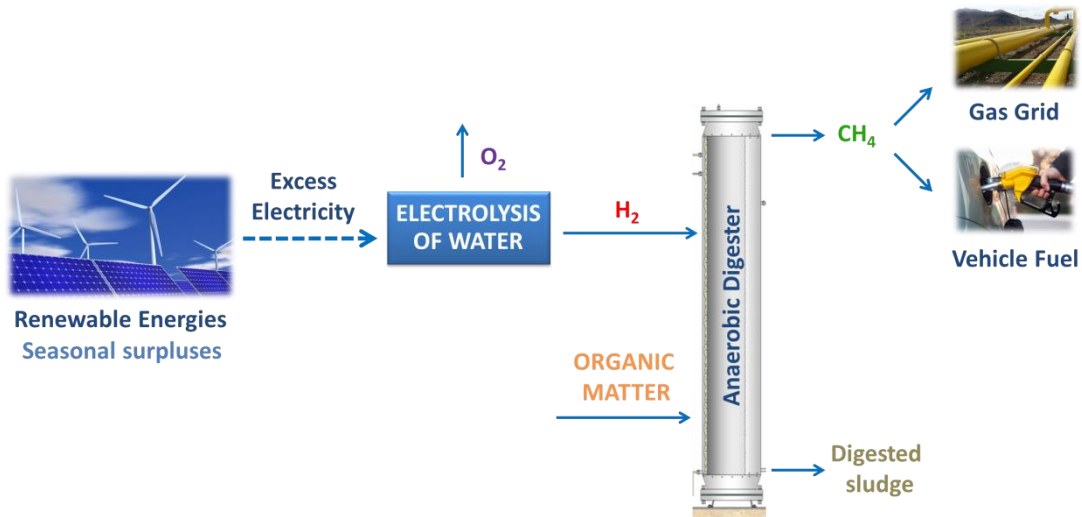


Figure 8. In-situ biogas upgrading concept.

Therefore, there is a need to advance on in-situ upgrading with external H_2 supply, where only a few small lab-scale bioreactors and configurations have been tested.

Mechanical stirring at rates between 65 and 1000 rpm has been applied in those completely mixed reactors to ease organic matter removal and H_2 conversion. However, an increase in mixing may also significantly increase the operation cost, though it could increase the hydrogen consumption rate. Therefore, efficient H_2 distribution systems would be a better choice compared to increasing mixing intensity.

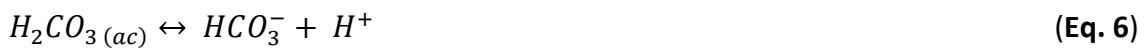
The methane evolution rate (MER), which expresses the increase in the specific CH_4 production rate ($L/L_R \cdot d$) under H_2 supply with respect to the lack thereof, reported in in-situ studies ranged from 0.08 to 0.39 ($L/L_R \cdot d$) (Table 6; Lecker et al., 2017), while the concentration of CH_4 in upgraded biogas was between 40 and 99%.

However, feasibility of in-situ upgrading not only requires efficient H_2 and CO_2 conversion into CH_4 but also preserved organic matter removal and convenient integration in the available facilities (Agneessens et al., 2017).

Table 6. Comparison of in-situ biological upgrading processes (na= not available).

Reactor Type	Reactor Working Volume (L)	Gas Diffusion system	Organic Substrate	OLR (g VS/L·d)	HRT (d)	Temperature (°C)	Gas recirculation (L/L _R ·d)	H ₂ loading rate (L/L _R ·d)	H ₂ efficiency (%)	CH ₄ content (%)	MER (L/L _R ·d)	pH	VFA accumulation	Reference
CSTR	0.3	Stirring: 450 rpm	Sludge and straw	0.5, 1.5, 2	21	38	-	1.3	na	83 - 94	0.09 – 0.20	7.92 – 8.33	Yes	Agneessens et al., 2018
CSTR	0.3	Stirring: 1000 rpm	Sludge and straw	0.77	20	38	-	0.3 – 1.7	58 - 99	77 - 100	0.08 – 0.21	7.89 – 8.43	Stable	Agneessens et al., 2017
UASB	1.4	Metallic diffuser + Rashing rings	Potato starch wastewater	3.73	7	55	0, 4.1, 6.2	2.6, 3.5	51	40 - 45	0.18 – 0.27	7.6 - 7.9	Yes	Bassani et al., 2016
		Alumina ceramic sponge						1.8, 2.1, 2.6	67, 87, 85	52, 87, 85	0.35, 0.20, 0.00	7.9, 7.8, 8.2	Yes	
		Two chambers in series Single long chamber						6.2	1.8	87	68	0.28	8.2	
CSTR	2.0	Hollow-fiber membrane + stirring 200 rpm	Sewage sludge	1.08	10	37	-	0.41, 0.92	96	90, 99	0.32, 0.75	7.5, 8	No	Wang et al., 2013
CSTR	0.6	Hollow-fiber membrane	Cattle manure and whey	1.67	15	55	-	0.93, 1.44, 1.76	na	78, 90, 96	0.22, 0.35, 0.38	7.6, 7.9, 8.3	Yes	Luo and Angelidaki 2013a
CSTR	0.6	Column diffuser (0.5-1 mm) + 150, 300 rpm	Cattle manure and whey	1.7	15	55	-	1.7	71, 83	53, 68	0.28, 0.34	7.7, 7.8	No	Luo and Angelidaki 2013b
		Ceramic diffuser (14-40 μm) + 150 rpm							-	87	75	0.39	7.9	
CSTR	3.5	Two ceramic diffusers + 65 rmp stirring	Cattle manure	1.9	14	55	-	0.69	80	65	0.08	8.3	Yes	Luo et al., 2012

One of the main technical challenges that this technology faces is related with the increment of pH level resulting from CO₂ removal to values above 8.5, leading to inhibition of methanogenesis (Angelidaki et al., 2018; Weiland, 2010). The elevation of pH is attributed to the removal of bicarbonate which is the key buffer in the biogas process. As shown in Eq. 6 and Eq. 7, CO₂ dissolved in the liquid phase of the reactor is dissociated to H⁺ and HCO₃⁻. The utilization of CO₂ will lead to a decrease of H⁺ causing a concomitant increase in the pH.



Previous experiments in in-situ biogas upgrading reactors showed a slight inhibition of methanogenesis due to bicarbonate consumption (Agneessens et al., 2018; Agneessens et al., 2017; Luo et al., 2012) verifying the argument that in conventional biogas production systems, a pH of 8.3 - 8.5 is the threshold for optimum biomethanation process both for mesophilic and thermophilic conditions (Bassani et al., 2015). pH values higher than 8 have been reported with uneven effects on organic matter removal efficiency (Luo et al., 2012; Bassani et al., 2016).

In order to alleviate this technical challenge, co-digestion with acidic waste was proposed to arrest increase of pH (Luo and Angelidaki, 2013b). More specifically, it was demonstrated that the co-digestion of manure with cheese whey wastewater maintained the pH in an optimal range during the whole biogas upgrading process. An alternative approach to circumvent this challenge was the application of pH control permitting successful upgrading to almost pure biomethane (Luo et al., 2014).

Another important issue that has to be considered during the in-situ biogas upgrading process is related with the oxidation of Volatile Fatty Acids (VFA) and alcohols which is only thermodynamically feasible in cases that H₂ concentration is very low (Bastone et

al., 2002). On contrary, high H_2 levels (> 10 Pa) inhibit the anaerobic digestion and promote the accumulation of electron sinks (Liu and Whitman, 2008).

It has been consistently informed inhibition of butyrate and propionate degradation under high H_2 partial pressure (Speece, 2008; Rittmann, 2001), as well as the accumulation lactate and ethanol (Liu and Whitman, 2008), breaking the balance of the system with the possibility of acidification caused by VFA accumulation.

Similarly to the ex-situ biogas upgrading processes, an additional key parameter is the solubilization of H_2 to the liquid phase as it must cross the interface between the gas and the liquid phase in order to be available for the microorganisms. Thus, the above mentioned poor mass transfer of H_2 into the liquid phase could be a limiting factor that would hamper the performance of the reactor. Despite everything, in-situ upgrading digesters with high HRT do not require specific mass transfer coefficients as high as the ex-situ process because of the lower specific CO_2 rates to convert.

For all the above reasons, the reactor designs, the device that is used to inject H_2 and the application of gas recirculation flows are considered as fundamental elements for the implementation of sufficient in-situ biogas upgrading (Bassani et al., 2016).

1.3.2.3 Hybrid biogas upgrading

Ex-situ and in-situ biogas upgrading can be implemented together forming an integrated system known as hybrid biogas upgrade (Kougias et al., 2017). In the hybrid technology, usually initially in-situ technology captures a part of the CO_2 , upgrading the biogas to higher grade (80–90% CH_4), followed by ex-situ process, where the enriched biogas is polished to a CH_4 content higher than 98% (Figure 9).

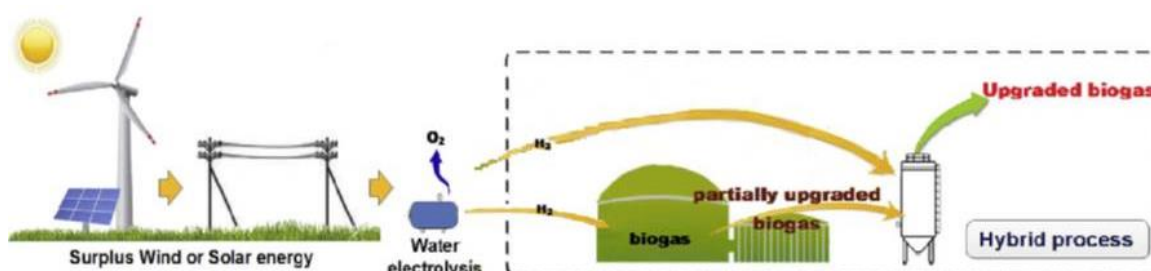


Figure 9. Hybrid biogas upgrading concept (from Corbellini et al., 2018).

The advantage of the hybrid technology is that it addresses the problem of pH enhancement during the in-situ process, while a considerably smaller separate reactor is needed for the ex-situ.

Currently, only one hybrid biogas upgrading study has been performed and published (Corbellini et al., 2018). In this work, a hybrid biogas upgrading configuration composed of two-stage thermophilic reactors was proposed. Hydrogen was directly injected in the first CSTR reactor for the in-situ stage and its output gas was subsequently transferred to a second up-flow reactor for the ex-situ stage, in which enriched hydrogenotrophic culture was responsible for the hydrogenation of CO₂ to CH₄.

The CSTR, which had a working volume of 3 L and was operated at HRT of 15 days, was initially inoculated with thermophilic digestate from a biogas plant. During the whole experiment, this first reactor was co-digesting cattle manure and potato-starch. The up-flow reactor (0.85 L working volume) was inoculated with 0.6 L of undiluted degassed digestate and 0.25 L of active enriched hydrogenotrophic inoculum obtained from a biogas upgrading reactor. Degassed digestate (HRT of 28 days) was provided to this second reactor in order to supply the microbial community with all the necessary nutrients. H₂ was injected into the first reactor (0.55 L/L_R·d) using three stainless steel diffusers (2 µm pore size) while it was dispersed into the second reactor through a ceramic membrane.

The overall objective of the work was to perform an initial CH₄ enrichment in the in-situ reactor, avoiding deterioration of the process due to elevated pH levels, and subsequently, to complete the biogas upgrading process in the ex-situ chamber. The CH₄ content in the first stage reactor reached on average 87% and the corresponding value in the second stage was 91%, with a maximum of 95%. CH₄ production rate was 0.36 - 0.43 L/L_R·d. The CO₂ was decreased by 57% and 98% of the H₂ injected was utilized.

The effect of H₂ injection on the microbial community in both reactors was analyzed by 16s rRNA gene amplicon sequencing. The results demonstrated an increment in relative abundance of hydrogenotrophic methanogens and homoacetogens in the in-

situ reactor, while the microbial community in the ex-situ reactor was simpler and dominated by hydrogenotrophic methanogens.

1.3.2.4 Comparison of ex-situ, in-situ and hybrid biomethanation systems

Ex-situ method has several advantages compared to the in-situ process as (Angelidaki et al., 2018; Ahern et al., 2015):

- It secures the stability of the conventional biogas process because the upgrading is occurring in a separate unit.
- It can handle high volumes of influent gases decreasing the gas retention time even to 1 h, which minimize the dimensions of the biogas upgrading chamber.
- The biochemical process is simpler since there is no degradation of organic substrate, and initial steps of anaerobic digestion such as hydrolysis and acidogenesis are not performed, avoiding many biological and mechanical challenges present in the anaerobic digestion.
- It is a biomass independent process.
- Other external source of waste CO₂ (biogas, syngas) can be used making the process more flexible.
- By this process it is feasible to supply power to remote from the centralized grid rural areas.
- The possible MER of ex-situ systems is very high compared to the CH₄ streams in in-situ systems.

However, the extension of a biogas reactor to perform methanation of CO₂ in-situ relies to its simplicity and requires less additional investment costs in existing biogas plants (as it mainly utilizes the existing infrastructure of them) than ex-situ upgrading (Ahern et al., 2015).

Real biogas represents a new challenge for the methanation due to the additional CH₄, which is inert for the reaction and just increases the velocity of the gas flow through

the reactor (Rachbauer et al., 2016). The reduction of the partial pressure of H₂ and CO₂ due to the presence of non-reactive gases also has an adverse influence on the gas–liquid mass transfer (Seifert et al., 2013).

Although the feasibility of the hybrid biogas upgrading concept was demonstrated by one study (Corbellini et al. 2018), further studies should be conducted to address the specific issues identified for further process performance in order to develop strategies targeting the optimization of the technology.

1.3.3 H₂ intermittency

Electricity from renewable sources like photovoltaic and wind energy plants could play an important role in a future European electricity system (Sensfuss and Pfluger, 2014). Due to their fluctuating electricity generation profile, a high share of these renewable energies lead to a strong demand for new electricity storage solutions (Heide et al., 2010).

As discussed previously, biological hydrogen methanation is a highly promising approach to move the type of energy from electricity to natural gas via water electrolysis and the subsequent step of bioconversion of H₂ and CO₂ into CH₄.

However, a question that needs to be addressed is related with the robustness of the process. Due to the fact that H₂ assisted biogas upgrading technology is based on the surplus of renewable electricity generated by wind or solar power, the system should be resilient to variable weather conditions and thus to different input H₂ flow rates.

Some studies affirm that dormant cultures can be quickly reactivated in large-scale AD systems and that methanogens can be fed intermittently (Lettinga, 1995; Martin et al., 2013). However, it is mandatory to elucidate the biomethanation efficiency during intermittent provision of H₂.

Some preliminary tests have been conducted in which the gas feed was interrupted in ex-situ biogas upgrading systems with TBF reactor configurations. The achievement potential recovery was obtained after three days of H₂ suspension at mesophilic

conditions (Burkhardt et al., 2015) and after one day (Strübing et al., 2017) of H₂ lack at thermophilic conditions.

Nevertheless, further research related to longer and repeated H₂ intermittent periods and the microbial tolerance towards periodical H₂ provision should be undertaken in order to draw conclusions on the dynamic operation of the biogas upgrading systems, as the feasibility of the H₂ intermittency is a challenge of the biogas upgrading technology not studied yet.

1.3.4 Microbial communities in biological biogas upgrading systems

In the context of anaerobic digestion process, biological biogas upgrading can be obtained via two different processes (Figure 10). The first one, hydrogenotrophic methanogenesis pathway, is mediated by hydrogenotrophic methanogenic *archaea* performing the direct conversion of CO₂ to CH₄ with the use of external H₂ according to Eq. 1, highly energetically favorable at pH 7. The second metabolism is indirect and is based on the conversion of CO₂ to acetate by homoacetogenic bacteria via the Wood-Ljungdahl pathway, which is also an exergonic process (Eq. 8). Then, acetoclastic methanogenic *archaea* convert the acetate into CH₄ (Eq. 9).

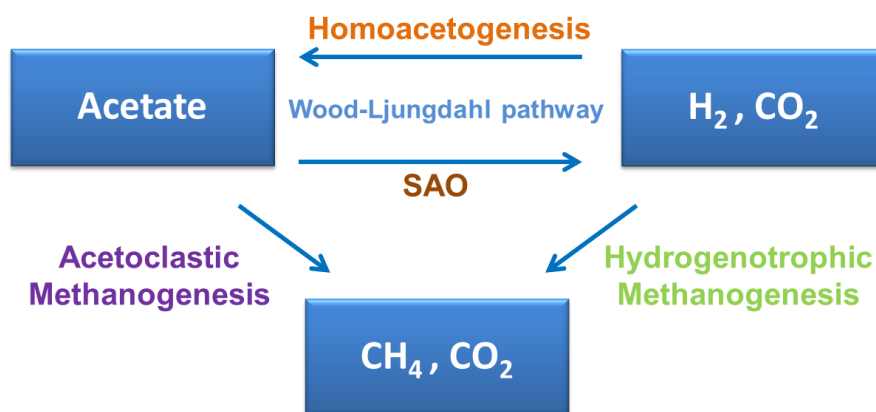


Figure 10. Metabolic pathways for hydrogen assisted biological biogas upgrading.

Under standard methanogenic conditions, H₂ derives from acetate oxidation or syntrophic acetate oxidation via an endergonic reaction and the energy loss is compensated when H₂ partial pressure is kept low by hydrogenotrophic methanogens. In this case, the low H₂ partial pressure is fundamental to enable proton reduction and energy conservation (Stams and Plugge, 2009).

Due to the crucial role of H₂ concentration on equilibrium of biochemical reactions, the addition of external H₂ has a strong selective pressure on the microbial community, shaping its composition with a massive increase of both hydrogenotrophic methanogens and homoacetogenic species (Schuchmann and Müller, 2014). In contrast, exogenous addition of H₂ is responsible for inhibiting syntrophic acetogens involved in propionate and butyrate degradation and syntrophic acetate oxidizers (SAO) (Demirel and Scherer, 2008).

Hydrogenotrophic methanogens are the key players for efficient biogas upgrading process. Pure cultures, such as *Methanobacterium thermoautotrophicum* and *Methanococcus thermolithotrophicus*, have been studied showing high H₂ and CO₂ conversion rates (Peillex et al., 1990, Peillex et al., 1988; Jee et al., 1988). However, cost acquisition of such cultures for large scale biomethane production may avoid the process profitability.

Therefore, the adaptation of biomass from a conventional (mesophilic or thermophilic) anaerobic digester to high rates of H₂ and CO₂ presents an interesting and economic advantage from the industrial point of view as an unspecific anaerobic sludge could be employed as inoculum with an acclimated population for the biomethane production. Moreover, adapted microbial communities are more robust and do not require sterile conditions, which would add extra costs to the process.

Microbial analysis performed during biogas upgrading experiments revealed that the most frequently found hydrogenotrophic methanogenic genera were *Methanobacterium*, *Methanoculleus*, *Methanomicrobium* and *Methanothermobacter* (Agneessens et al., 2017; Bassani et al., 2017; Luo and Angelidaki, 2013b; Mulat et al., 2017; Kougias et al., 2017), whereas *Methanosarcina* and, more generally, acetoclastic methanogens are usually present at lower abundance (Agneessens et al., 2017; Bassani

et al., 2015; Mulat et al., 2017). Parameters affecting the stimulation and dominant presence of homoacetogens have been studied (Agneessens et al., 2017; Agneessens et al., 2018).

Chapter 2

Aims and scope



2.1 RESEARCH MOTIVATION

The worldwide increasing demand for energy and the new directives set by the “Green Energy Agreement” create an intensive interest towards exploitation of renewable energy sources. Wind and biomass are promoted worldwide as sustainable forms of energy and, currently, there is an increasing interest in exploiting biogas as a substitute of natural gas via biogas upgrading process.

In this context, hydrogen assisted biological biogas upgrading has emerged as an attractive method for biogas upgrading. However, the H₂ gas-liquid mass transfer and the H₂ intermittency are the challenges of the process.

Different reactor configurations and diffusion devices have been previously investigated mainly at lab-scale for ex-situ upgrading aiming at maximizing the H₂ gas-liquid mass transfer. Despite the fact that membrane bioreactors at lab-scale resulted in an attractive alternative in order to H₂ transfer by gas diffusion through the membrane material, further studies are needed to assess the feasibility of the H₂ and CO₂ bioconversion at higher scales operating with higher H₂ loading rates regarding the implementation of these systems at industrial scale.

Most of the trickling biofilter reactors have been studied at mesophilic conditions although it was found that the efficiency of biogas upgrading reactors is improved at thermophilic conditions. Therefore, trickling biofilters performance at thermophilic conditions should be further evaluated. Likewise, the possible influence of H₂ down-flow or up-flow operation to the liquid media on biomethanation efficiency is still unexplored. Moreover, microbial community involved in ex-situ processes in trickling biofilters at thermophilic conditions remains uncharacterized.

Although some preliminary tests have been conducted in which the H₂ gas feed was interrupted for 1 and 3 days in ex-situ systems, further research related to longer and repeated H₂ intermittent periods and the microbial tolerance towards periodical H₂ provision should be undertaken in order to draw conclusions on the dynamic operation of the biogas upgrading systems and to evaluate the feasibility of this process for an industrial application.

Finally, there is a need to advance on in-situ upgrading, where only a few small lab-scale configurations have been tested. Moreover, several opportunities have been identified for the integration of Power-to-Gas in wastewater treatment plants.

Therefore, more research focus on the study and optimization of the biogas upgrading biotechnology should be carried out in order to overcome the above mentioned challenges or research gaps and move hydrogen assisted biological biogas upgrading process from a promising lab-scale process to a sustainable full scale technology.

2.2 OBJECTIVES OF THE THESIS

This thesis proposes an innovative process in which H_2 generated by water electrolysis using off-peak electricity surplus from wind power is biologically converted by binding CO_2 to CH_4 . The overall objective of the present thesis was to study, develop and optimize the biological biogas upgrading process.

More specifically, the individual goals to achieve the overall objective of the thesis were:

1. Assessment of the feasibility of the bioconversion of H_2 and CO_2 /biogas to CH_4 for ex-situ and in-situ biogas upgrading processes.
2. Improvement of H_2 gas-liquid mass transfer.
3. Study of the effect of gas recirculation.
4. Application of membrane technology for ex-situ biogas upgrading at pilot-scale.
5. Effect of the H_2 down-flow and up-flow operation in trickling biofilter reactors.
6. Evaluation of the intermittent provision of H_2 .
7. Analysis of microbial community.

2.3 THESIS OUTLINE

In the present thesis, all experimental and literature review work was focused on the achievement of the main objective and the individual goals above described, as shown in Figure 11.

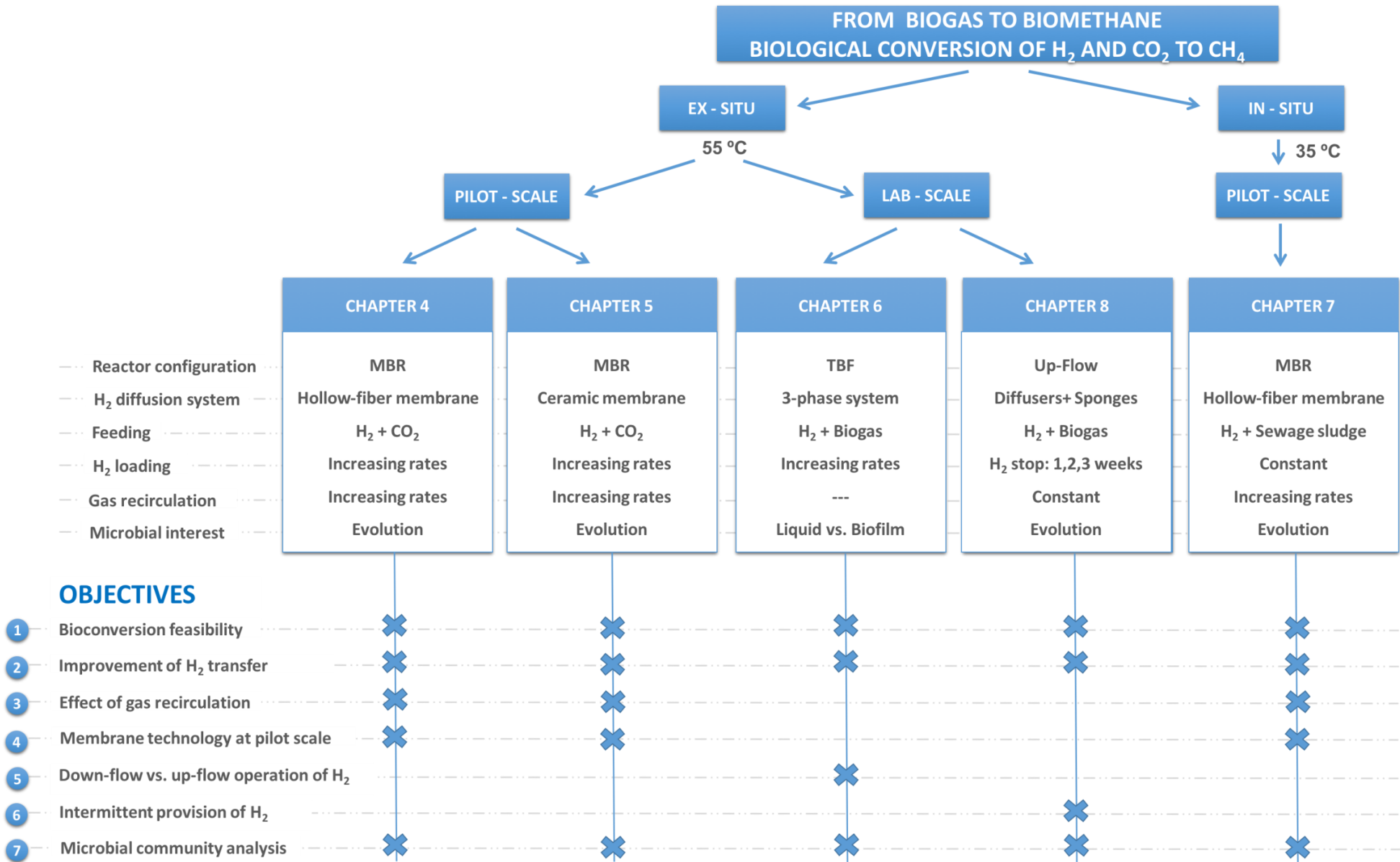


Figure 11. Thesis outline.

Chapter 3

Experimental materials and methods



3.1 EXPERIMENTAL SETUPS

3.1.1 Pilot Plants

3.1.1.1 Hollow-fiber membrane bioreactors

a) Ex-situ biogas upgrading experiment (Chapter 4)

One 40 L cylindrical reactor (0.18 m x 1.20 m) with a working volume of 31 L was taken. The reactor was insulated and the walls were heated with electric resistance.

Feed gas (H_2 and CO_2) was obtained from two gas cylinders, and the rate was regulated with rotameters (Aalborg, USA). Feed line was preheated in a thermostatic bath (55 ± 1 °C), mixed with the recirculation, filtered by $0.45 \mu m$ (Millex, Millipore) and connected to the upper part of the membrane module as shown in Figure 12 a.

The hollow-fiber membrane module (Porous fibers, Spain) (Figure 12 b) was placed in the bioreactor to generate gas bubbles. The module consisted of 232 polymeric fibers (PVDF) with a pore size of $0.4 \mu m$ and fiber length of 0.55 m. The total membrane surface was $0.93 m^2$ and the module occupied 2.6 L.

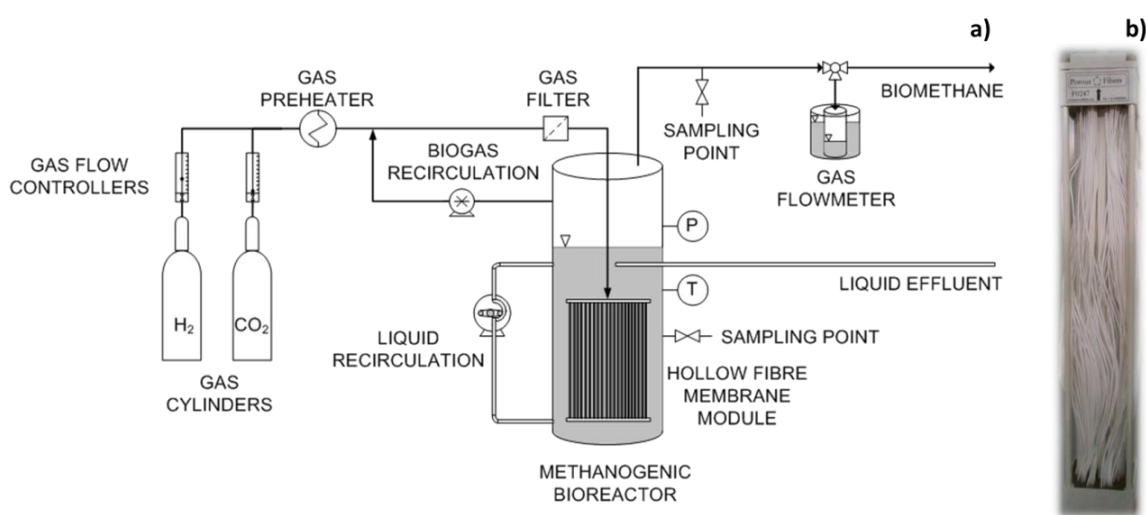


Figure 12. a) Pilot plant diagram; **b)** Hollow-fiber membrane module

The bioreactor was equipped with a gas pump to recirculate biogas from the headspace through the membrane module, and one peristaltic pump (Watson-Marlow) to mix the liquid at a constant rate of $32 L/L_R \cdot d$.

b) In-situ biogas upgrading experiment (Chapter 7)

The experiment was performed using two insulated cylindrical bioreactors with total and working volumes of 28 L and 20 L, respectively. An electric resistance was used to maintain the temperature of the reactor to a desired value (35 ± 1 °C).

One reactor (R1) was used as upgrading reactor, while the other (R2) was utilized as control reactor (Figure 13).

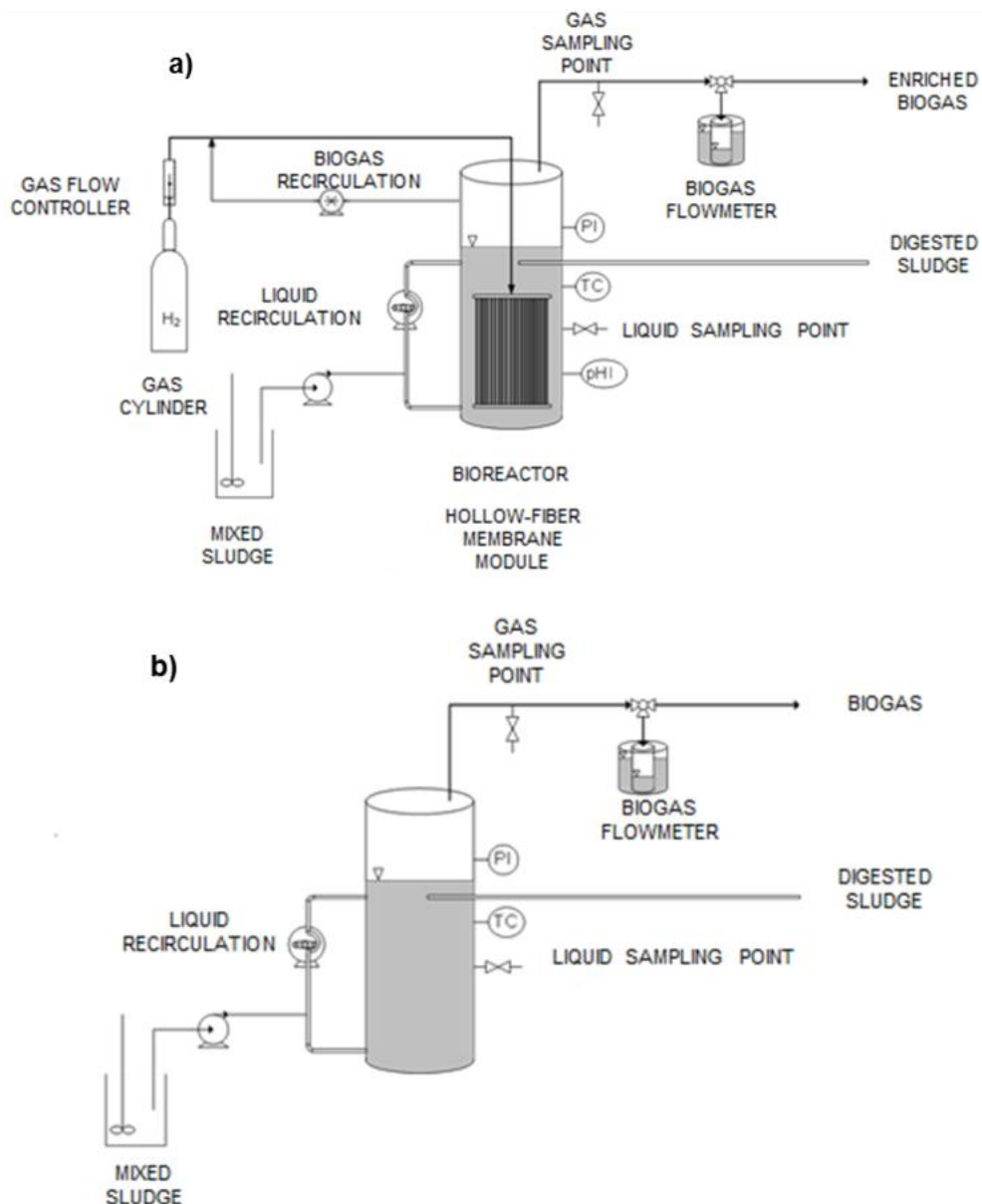


Figure 13. Diagram of the pilot plants.

a) Upgrading reactor (R1); **b)** Control reactor (R2).

R1 was equipped with a hollow-fiber membrane module (ZeeWeed[®]-1, General Electric, Spain) (Figure 14a), consisted of polymeric fibers (PVDF) with 0.4 μm pore size and an area of 0.093 m^2 , which was used in order to generate small bubbles. Figure 14 b) shows the dimensions of the polymeric module employed in the experiment while length of the fibers is shown in Figure 14 c).

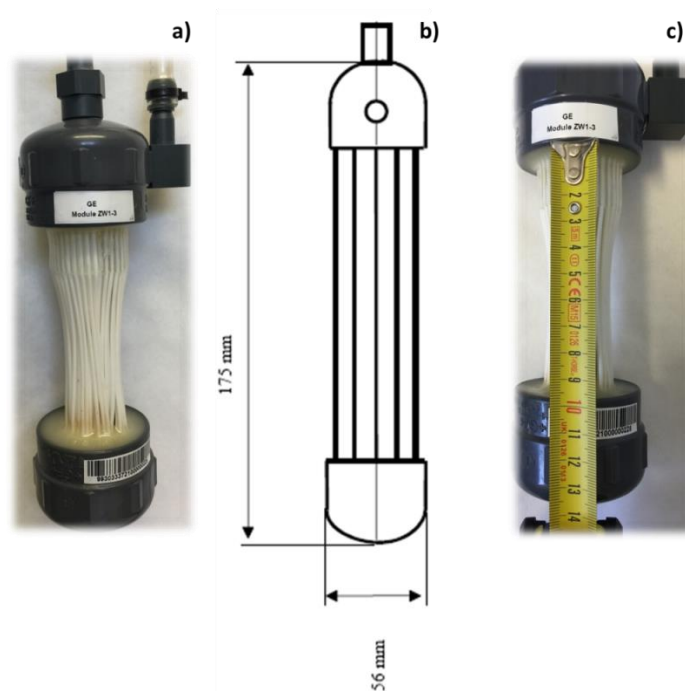


Figure 14. Hollow-fiber membrane module ZeeWeed[®]-1 employed in the experiment in R1. **a)** Module; **b)** Dimensions; **c)** Fiber length.

Peristaltic pumps (Watson-Marlow) were used for feeding and mixing of R1 and R2. Peristaltic pumps for feeding and sludge recirculation were operated at a rate of 0.05 and 72 L/L_R·d, respectively. A feeding tank, equipped with a magnetic stirrer, with thickened mixed sludge, was installed for both reactors.

H₂ was fed from a gas cylinder using a mass-flow controller (Aalborg, USA). The gas mixture composed by H₂ feeding and biogas recirculation lines was injected in R1 with a peristaltic pump (Watson-Marlow) through the upper part of the membrane module as shown in Figure 13 a). A pH probe (Crison Instruments, pH probe 53 35, Spain), was installed in R1 for continuously monitoring of pH.

R2 was fed only with thickened mixed sludge without biogas recirculation and H₂ supply (Figure 13 b).

Pilot plants employed in the in-situ biogas upgrading experiment are shown in Figure 15.

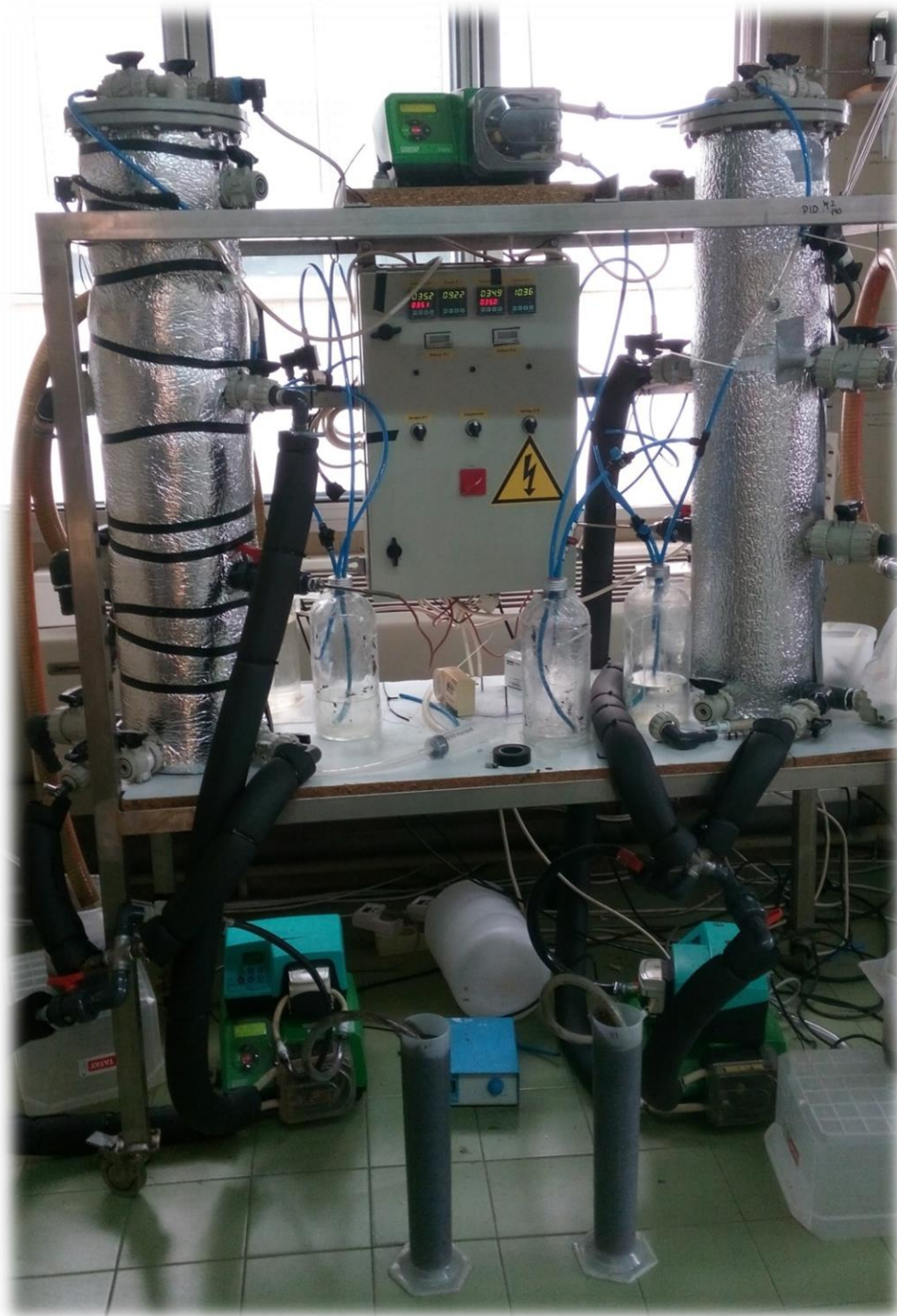


Figure 15. Pilot plants employed in the in-situ biogas upgrading experiment.

Left: Control reactor (R2); **Right:** Upgrading reactor (R1).

3.1.1.2 Ceramic membrane bioreactor

Ex-situ biogas upgrading experiment (Chapter 5)

The experiment was performed using one insulated cylindrical membrane bioreactor with a working volume of 60 L in which an electric resistance was used to heat reactor walls (55 ± 1 °C).

Reactor was equipped with a ceramic tubular membrane module (ATECH, Germany) consisted of 28 tubes of Al_2O_3 with $0.8 \mu\text{m}$ pore size, fiber length of 1.19 m (total length of 1.33 m), 5.1 L volume and an area of approximately 1 m^2 which was used as gas sparging surface in order to generate fine small bubbles (Figure 16).



Figure 16. Ceramic membrane module employed in the experiment.

a) Dimensions; **b)** Ceramic Tubes.

Hydrogenotrophic reactor was fed continuously with H_2 and CO_2 from gas cylinders and two mass-flow controllers (Aalborg, USA) were used to regulate the rate of both gases. Feed and recirculation lines were mixed and then preheated in a thermostatic bath at 55 ± 1 °C. The gas mixture was injected in the reactor through upper part of ceramic membrane as given in schematic representation of the reactor in Figure 17.

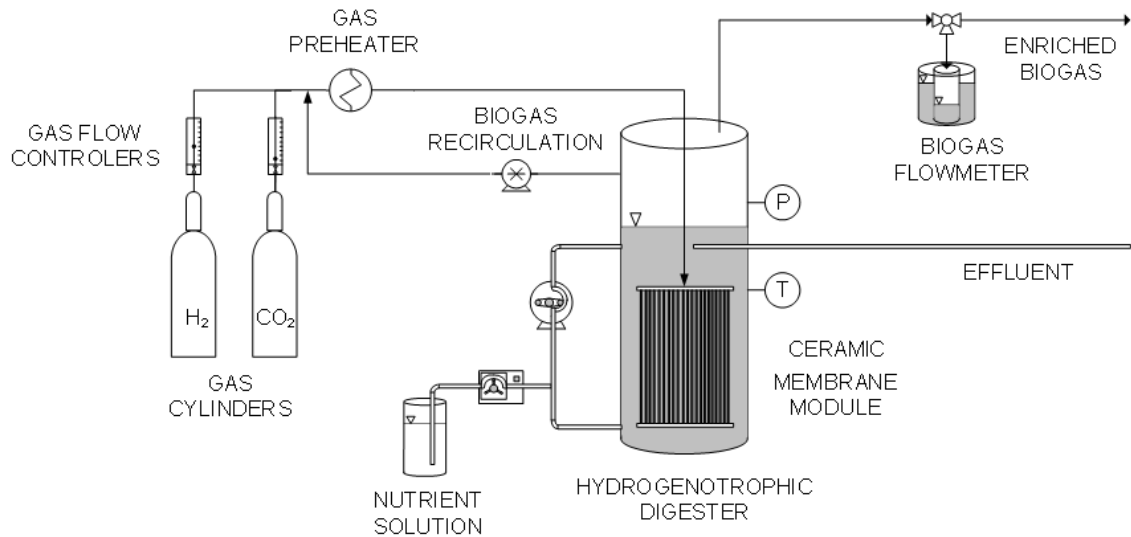


Figure 17. Diagram of the ceramic MBR.

The reactor counted with a compressor to recirculate biogas from the headspace of the reactor through the membrane module. A peristaltic pump was employed to avoid solids deposition at a rate of 24 L/L_R-d.

The pilot plant employed in the ex-situ biogas upgrading experiment is shown in Figure 18.



Figure 18. Ceramic MBR pilot plant employed in the ex-situ biogas upgrading experiment.

3.1.2 Lab-scale reactors

3.1.2.1 Trickling biofilter reactors

Ex-situ biogas upgrading experiment (Chapter 6)

Two TBF reactors made of poly(methyl methacrylate) with 1 L working volume (packed bed) and dimension ratio length:diameter of 9:1 were used for the experiments.

Glass rings (5x6 mm each with specific surface area of 0.002 m²/g) were used as packing material (Figure 19).

A water recirculation system was used to heat the reactors by means of D10 mm silicon tubes wrapping their entire cylindrical surface (Figure 19).

Polyethylene foam was used to cover the wrapped reactors for insulation.

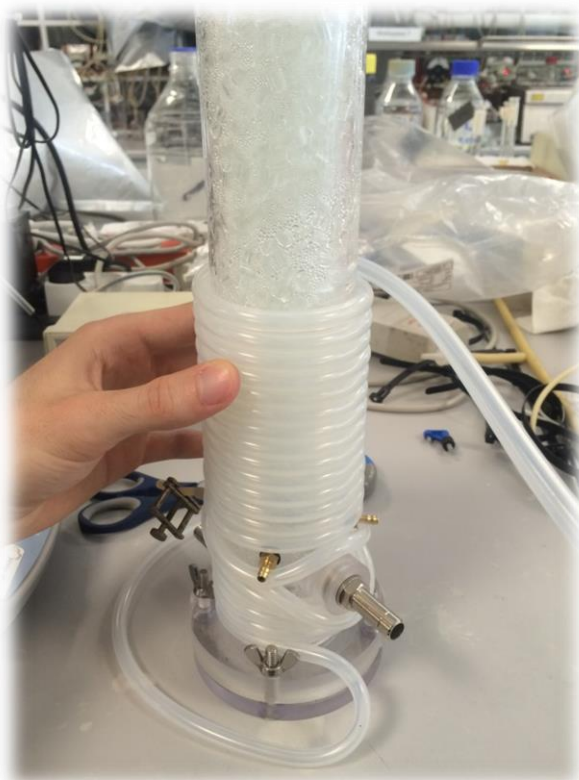


Figure 19. Glass rings used as packing material and water recirculation system to heat the reactors.

The difference between the two reactor configurations was the direction of the injected gas flow and the outlet gas port.

The gas mixture in the first reactor, denoted as R1, was injected in a counter-flow to the trickling media, while the outlet gas port (i.e. port that allow gases to exit the reactor) was placed at the top of the reactor (Figure 20 a).

On the contrary, the influent gas in the second reactor, denoted as R2, was directed with the flow of the recirculating liquid. Therefore, an outlet port was placed in the bottom of the reactor so as the liquid, which would be saturated with gas, to be removed from the reactor and subsequently be recirculated (Figure 20 b).

Each reactor configuration was connected with a glass vessel (1 L working volume), which contained the recirculation liquid media. The vessel was equipped with a thermal jacket so as to operate at stable thermophilic temperature (54 ± 1 °C).

The liquid was pumped out from the vessel and trickled over the packed bed through seven ports (each port had a diameter of 2 mm) that were distributed at the upper lid of the reactors.

The liquid recirculation took place for 30 seconds every half an hour using of a peristaltic pump set at a flow rate of 2.8 L/L_R·d.

The gas feed (H₂, CO₂ and CH₄) was continuously introduced to the reactors using peristaltic pumps (Watson-Marlow).

No gas recirculation was applied, resulting in a single-pass plug flow operation.

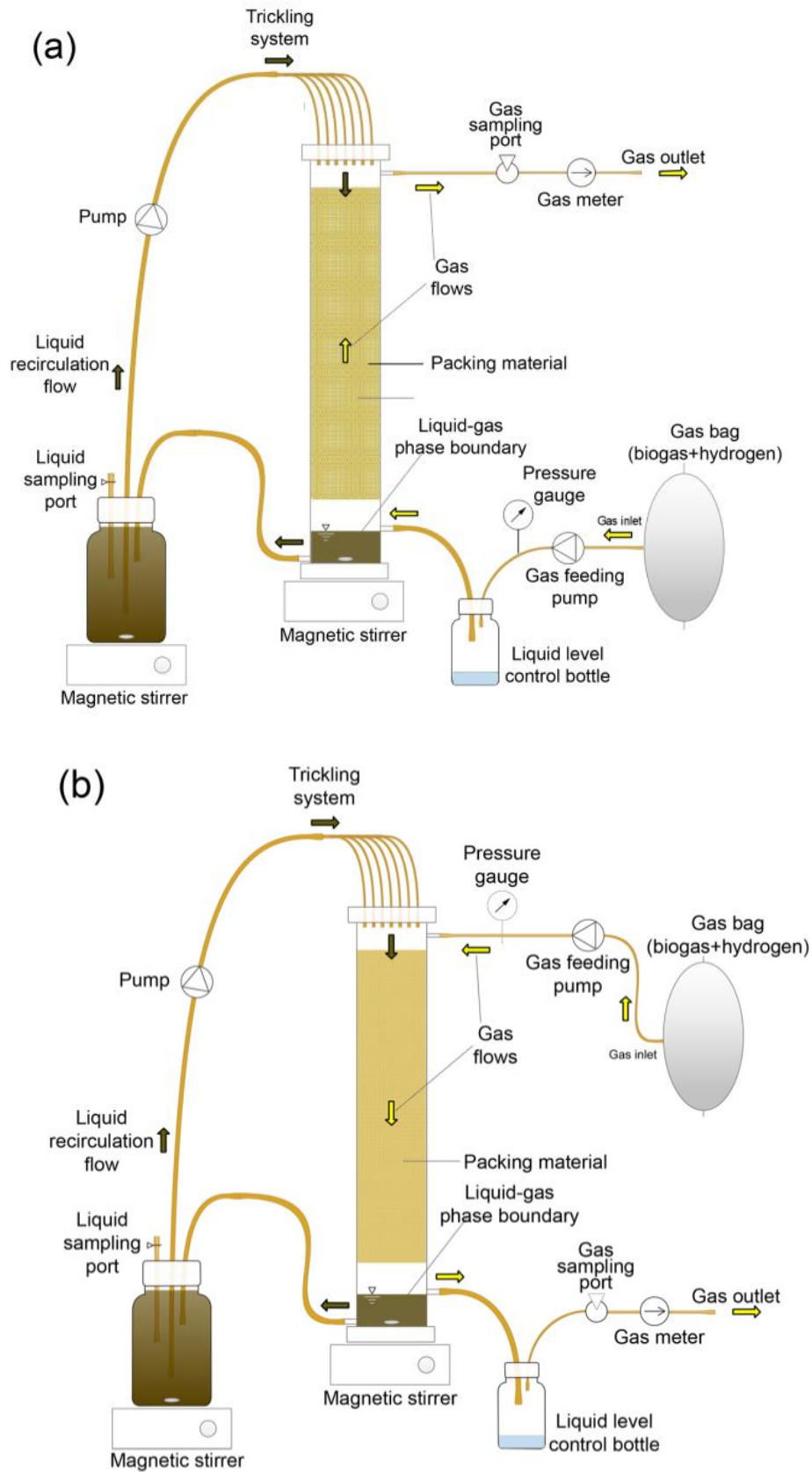


Figure 20. Schematic representation of the trickling biofilter reactors.

a) R1 (counter-flow); **b)** R2 (with the flow).

Reactors employed in the ex-situ biogas upgrading experiment are shown in Figure 21.

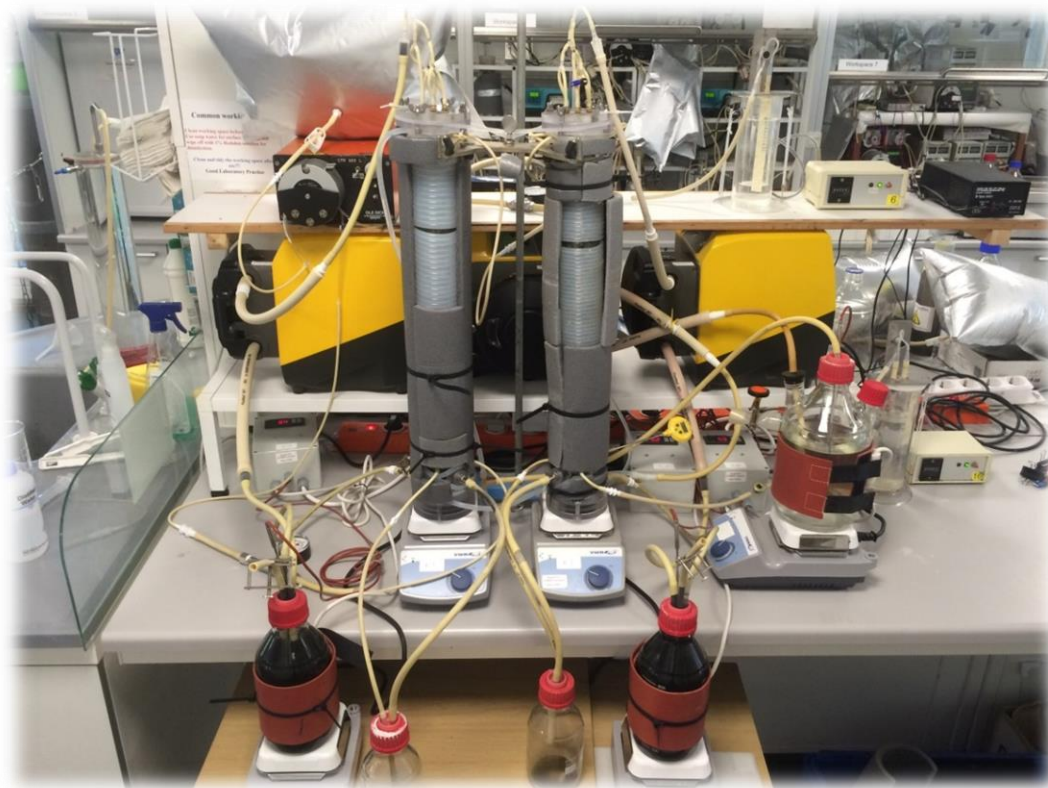


Figure 21. Reactors employed in the ex-situ biogas upgrading experiment.

Left: R1 (counter-flow); **Right:** R2 (with the flow).

3.1.2.2 Up-flow reactors

Ex-situ biogas upgrading experiment (Chapter 8)

The experiment was performed using the same up-flow reactor configuration for three reactors (R1, R2 and R3) with total and working volumes of 1.4 L and 1.0 L for each setup, respectively. A schematic representation of the reactor configuration is given in Figure 22.

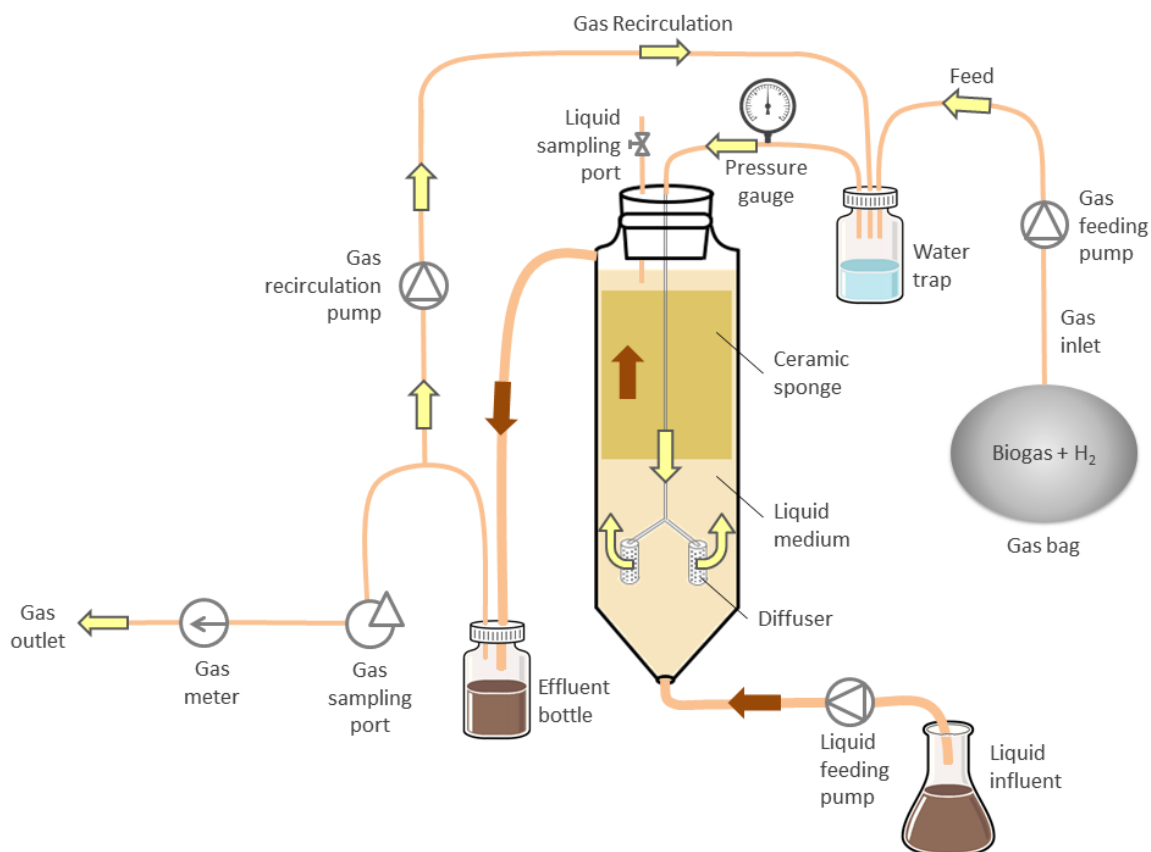


Figure 22. Diagram of the up-flow reactors.

Reactors were maintained at temperature working conditions ($55^{\circ}\text{C} \pm 1^{\circ}\text{C}$) by circulating hot water through a water jacket around the glass walls of the reactors.

Each reactor was equipped with two stainless steel diffusers (located at the bottom of the reactors, each having 26 mm length and 13 mm diameter with $0.5\ \mu\text{m}$ pore size) and two inert alumina ceramic sponges (Cerapor, Drache) (Figure 22) used as gas sparging surface in order to generate fine small bubbles improving the gas-liquid mass transfer by increasing the contact area and time between the injected gases and the liquid.

Feeding gas mixture (H_2 , CO_2 and CH_4) was continuously injected in the reactors through the diffusion system being previously mixed with the gas recirculation line (Figure 22). The gas mixture was stored inside gas tight aluminium bags and was provided to the diffusers using peristaltic pumps (Watson-Marlow). The bags were filled with fresh gas mixture every day.

The reactors counted with a peristaltic pump (Watson-Marlow) to recirculate gas from the headspace of the reactor through the diffusion system ensuring good reactor mixing.

On a daily basis, digestate serving as nutrient source was provided to the reactors using peristaltic pumps (Watson-Marlow) at a rate of 0.02 L/L_R·d.

Up-flow reactor setups employed in the experiment are shown in Figure 23.



Figure 23. Up-flow reactors employed in the experiment (R1, R2 and R3).

3.2 RAW MATERIALS

Table 7 summarizes the raw materials used in all the experiments. A more detailed description of the raw materials is provided in the corresponding chapter of each experiment.

Table 7. Raw materials employed in the experiments.

	Raw material	Origin/Brand	Experiment in Chapter
Gas Substrates	H ₂ (100%)	Linde®, Spain	4, 5 and 7
	CO ₂ (100%)	Linde®, Spain	4 and 5
	H ₂ /CO ₂ /CH ₄ (62%/15%/23%)	AGA A/S, Denmark	6 and 8
Flushing Gases	He (100%)	Linde®, Spain	4
	N ₂ (100%)	Linde®, Spain	7
		AGA A/S, Denmark	6
Inoculum	Thermophilic anaerobic sludge	Thermophilic anaerobic digester in our laboratory Valladolid, Spain	4 and 5
	Enriched hydrogenotrophic culture	Previous laboratory biogas upgrading column reactors (Bassani et al., 2017)	6 and 8
	Mesophilic anaerobic sludge (sewage sludge)	Mesophilic anaerobic digester in the WWTP of Valladolid, Spain	7
Nutrient Solution	Synthetic compounds	Macro and micro nutrient solutions according to Angelidaki and Sanders (2004)	4 and 5
	Centrate wastewater	Centrifugation of anaerobically digested mixed sludge of the WWTP of Valladolid, Spain	5
	Digestate	Digestate from Snertinge biogas plant, Denmark	6 and 8
Organic substrate	Thickened mixed sludge	Mixed primary and secondary sludge from WWTP of Valladolid	7

The gas cylinders of CO₂, He and N₂ were placed indoors of the laboratory for the experiments while the gas cylinders of H₂ and H₂/CO₂/CH₄ were located outdoors for safety reasons.

Figure 24 a and Figure 24 b show the central system of H₂ gas supply (Linde HiQ®) which was used to perform the efficient and safe distribution of H₂ gas from a central storage installation to the consumption point in the laboratory (Figure 24 c).

Figure 25 show the location of H₂/CO₂/CH₄ gas cylinder staying outdoors of the laboratory.

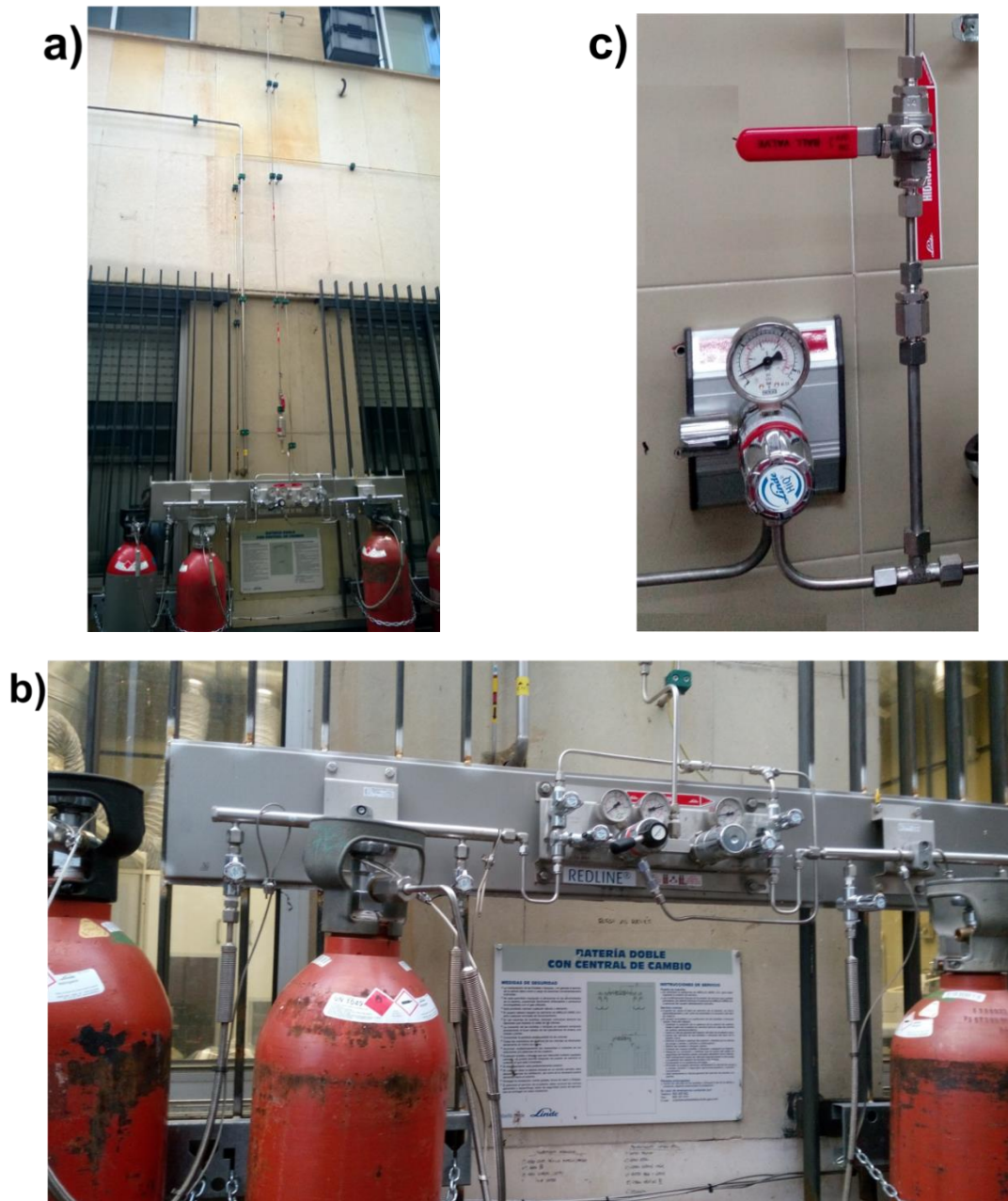


Figure 24. H₂ distribution system. **a)** Central system of H₂ gas supply outdoors; **b)** Panel of central system of H₂ gas supply; **c)** H₂ consumption point.



Figure 25. Gas cylinder staying outdoors.

After the collection of the inoculums, they were introduced directly in the reactors in order to perform the inoculation as soon as possible avoiding any possible undesirable conditions to affect the microbial community present in the inoculum.

The digestate used as nutrient solution was placed in an incubator at thermophilic conditions after its collection to be used during the whole experimental work.

Centrate wastewater was collected once every two weeks from the WWTP and maintained at 4 °C before its use.

The thickened mixed sludge was stored at 4°C for a maximum period of two weeks prior to be fed to the reactors since it was collected once every two weeks from the WWTP.

3.3 ANALYTICAL METHODS

Table 8 shows the physicochemical parameters measured in all the experiments and the methods employed in order to perform the different analysis. Other parameters measured were the dissolved H₂ concentration, the dewaterability of sludge, elemental analysis and trace elements.

Table 8. Physicochemical parameters measured in all the experiments.

Parameter	Method	Model, Brand, Country	Experiment in Chapter
Temperature	Controlled with a PID and measured with a temperature probe	PT100 probe	4, 5 and 7
	Closed water recirculation system with a boiler and a temperature probe	-	6 and 8
Headspace pressure	Monitored with a pressure probe	Endress Hauser Cerabar PMC131 probe	4, 5 and 7
	Pressure gauge	WIKA, Denmark	6 and 8
Gas production rate	Water displacement gas-metering systems	Handmade gas flow-meters	4, 5, 6, 7 and 9
Gas composition	GC-TCD, dry basis	Varian CP-3800, Agilent, Spain	4, 5 and 7
		Mikrolab Aarhus A/S, Denmark	6
		TRACE 1310, Thermo Scientific, Italy	8
pH	pH meter	PH BASIC 20-pH probe 53 37, Crison, Spain	4, 5 and 7
	pH meter	PHM210-pHC3105-8, Radiometer analytical, Denmark	6 and 8
TS/VS/TSS/VSS	Standard Methods (APHA, 2005)	-	4, 5, 6, 7 and 9
NH ₄ ⁺	Standard Methods (APHA, 2005)	-	4, 5, 6, 7 and 9
TKN	Standard Methods (APHA, 2005)	-	6 and 8
VFA	GC-FID as described by Díaz et al. (2010)	GC-7820A, Agilent, Spain	4, 5 and 7
	GC-FID as described by Kougias et al. (2015)	GC-2010, Shimadzu, Japan	6 and 8
PO ₄ ³⁻	HPLC	HPLC-717, Waters, Spain	4 and 5

Dissolved H₂ concentration

Dissolved H₂ concentration was measured periodically in the experiment of Chapter 4 by gas–liquid partition with a modified version of the method described in Yu et al. (2006).

8 mL of liquid were sampled from the reactor and subsequently injected into a 10 mL gas-tight serological bottle. The bottles contained 200 µL of concentrated H₂SO₄ in order to prevent any biological activity in the sample. They were closed with butyl septa, sealed with aluminum caps and degassed with helium prior to the sample injection.

H₂ in the headspace of the bottles was measured 8 h after sample injection by GC–TCD (as shown in Table 9) and liquid concentration was estimated through mass balances. A higher variability between replicates is expected in this modified version since analysis were only performed in duplicate in comparison to the original method where triplicate aqueous samples were withdrawn. Due to the nature of the GC detection limit for H₂ (1% in volume), the minimum dissolved H₂ concentration that can be measured is 0.022 mg/L.

In view of the obtained results of dissolved H₂ concentration in the experiment of Chapter 4, H₂ concentration in the liquid phase was considered negligible for the rest of the experiments (Chapters 5-8) as a result of H₂ complete consumption by methanogens in this phase.

Dewaterability

The dewaterability of sewage sludge from the experiment of Chapter 7 was assessed by determining centrifugability (% solids recovery) and filterability (filtration constant). These two parameters were analyzed in triplicate according to Standard Methods (APHA, 2005) and Kopp and Dichtl (2001).

Elemental analysis

The elemental analysis of the inoculum and the digestate used as nutrient solution from the experiment of Chapter 8 was performed using an elemental analyzer, model CHNS vario Marco Cube.

First of all, liquid samples were dried in a freeze dryer over a weekend and then, the elemental analysis was performed.

Sulfanilamide was used as calibration standard with nominated weight of 20 mg. 10 mg of dried sample in triplicate were used for the analysis. Sludge A from VKI was employed as reference sample in triplicate.

The temperatures of the combustion and reduction tubes were 1050 °C and 950 °C, respectively.

Analysis of trace elements

Similarly to elemental analysis, liquid samples of the inoculum and the digestate used as nutrient solution from the experiment of Chapter 8 were dried in a freeze dryer over a weekend and then, the analysis of trace elements was performed.

Firstly, the digestion of the trace elements was done and then, ICP_OES (Inductively Coupled Plasma_ Optical Emission Spectrophotometer) was employed to determine the concentrations.

Samples were digested in a microwave (Anton Paar, model 3000) using method USEPA 3051A. 0.1 g of dried samples in duplicate, 9 mL HNO₃ suprapur 68%, 3 mL HCl suprapur 30% and 0.50 mL suprapur H₂O₂ were used.

Temperature of 170 °C, power of 1400 W and pressure of 40 bars were the microwave conditions for the digestion. After the process, a final volume of 50 mL was obtained. Sludge A from VKI used as reference sample.

For the determination of trace elements, ICP_OES model Avio 200 (Perkin_Elmer) was used. The calibration range for Al, Ca, Fe, K, Mg, Na, P and S was 0-1.0-5.0-10-20 mg/L

making by dilution from stock solution DTU-3 (Inorganic Ventures, USA). The calibration range for Ba, Co, Cu, Mn, Ni, Sr and Zn was 0-0.05-0.10-0.50-1.0-5.0 mg/L making by dilution from stock solution DTU-3 (Inorganic Ventures, USA).

Quality Control 1 (low level) and 2 (high level) were Environmat Drinking water (Canada) and mixing stock solution (Sigma_Aldrich) with sludge A from VKI used as reference sample. Yttrium was used as internal standard with a concentration of 1 mg Y/L and 2% Cs (as CsCl) in online injection. All calibrations and quality solutions were acidified to 12% HNO₃ and 1,8 % HCl.

3.4 MICROBIAL ANALYSIS

Several microbiological techniques were employed in order to have deeper understanding about the microbial community in each experiment. For that purpose, first of all, samples were collected in sterile tubes and immediately stored at -20 °C. After that, microbiota characterization was performed.

3.4.1 DNA extraction

On the one hand, regarding the samples from experiments of Chapter 4, Chapter 5 and Chapter 7, the protocol described in the Fast[®] DNA Spin Kit for Soil (MP Biomedicals, LLC) handbook was used to extract DNA. The integrity of the extracted DNA was checked by electrophoresis on a 1.2% (w/v) agarose gel. DNA purity was tested using a NanoDrop spectrophotometer (NanoDrop Technologies, Wilmington, USA).

On the other hand, regarding the samples from experiments of Chapter 6 and Chapter 8, genomic DNA was extracted from samples in triplicates using the PowerSoil[®] DNA Isolation Kit (MO BIO laboratories Inc., Carlsbad, CA USA) following the instructions of the manufacturer, except from the addition of an initial purification step using 2 mL of Phenol:Chloroform:Isoamyl Alcohol pH 8 (Sigma-Aldrich, DK). The quantity and quality assessment of the extracted DNA were performed using NanoDrop (ThermoFisher Scientific, Waltham, MA) and Qubit Fluorometer (ThermoFisher Scientific, Waltham, MA), respectively.

3.4.2 Denaturing Gradient Gel Electrophoresis (DGGE)

After the extraction of genomic DNA, polymerase chain reaction (PCR) amplification and denaturing gradient gel electrophoresis (DGGE) analysis were performed in samples from experiments of Chapter 4, Chapter 5 and Chapter 7.

The V6–V8 region of the bacterial 16S rRNA genes was amplified by PCR using the universal bacterial primers 968-F-GC and 1401-R (Sigma-Aldrich, St. Louis, MO, USA). The DGGE analysis of the amplicons was performed with a D-Code Universal Mutation Detection System (Bio-Rad Laboratories) using 8% (w/v) polyacrylamide gels with a urea/formamide denaturing gradient of 45 to 65%. DGGE running conditions were applied according to Roest et al. (2005).

The gels were stained with GelRed Nucleic Acid Gel Stain (biotium) and the most relevant, dominant and intense bands were excised from the DGGE gel in order to identify the microorganisms present in the samples. Using the GelCompar IITM software (Applied Maths BVBA, Sint-Martens-Latem, Belgium) DGGE profiles were compared. After image normalization, bands were defined for each sample using the bands search algorithm within the program.

Similarity indices were calculated from the densitometric curves of the scanned DGGE profiles by using the Pearson product–moment correlation coefficient (Häne et al., 1993). The peak heights in these densitometric curves were also used to determine the Shannon–Wiener diversity index (H). This index reflects the relative number of DGGE bands (sample richness) and relative intensity of every band (evenness). It ranges from 1.5 to 3.5 (low and high species evenness and richness, respectively) according to McDonald (2003).

The taxonomic position of the sequenced DGGE bands was obtained using the RDP classifier tool (50% confidence level) (Wang et al., 2007). The closest cultured and uncultured relatives to each band were obtained using the BLAST search tool at the NCBI (National Centre for Biotechnology Information) (McGinnis and Madden, 2004). Sequences were deposited in GenBank Data Library (www.ncbi.nlm.nih.gov/genbank).

3.4.3 Fluorescence In Situ Hybridization (FISH)

Fluorescence In Situ Hybridization (FISH) analysis were performed in samples from experiments of Chapter 5 and Chapter 7.

First of all, samples were centrifuged during 5 minutes and 10000 rpm at 4°C removing the supernatant. Paraformaldehyde (4% w/v) was used to fix biomass samples (250 µL) during 3 h. Then, they were washed three times with phosphate-buffered saline (PBS). Aliquots of 10 µL of samples were deposited on the wells of gelatin-coated, acid-washed, glass microscope slides and dehydrated by passing through a 50%, 80% and 100% (v) ethanol series.

Hybridization with formamide (30% v) and the oligonucleotide probes was at 46 °C for 2 h. The following probes were used: EUB338 I (for most of bacteria, 5'-GCTGCCTCCCGTAGGAGT-3'), EUB338 plus (for Planctomycetales and Verrucomicrobiales, 5'-GCWGCCACCCGTAGGTGT-3') and ARCH915 (for most of *archaea*, 5'-GTGCTCCCCGCAATTCCT-3') (Daims et al., 1999).

After hybridization step, and once the slides were washed and dried, the specimens were counter-stained for 5 min at room temperature with the DNA stain DAPI to quantify the total number of cells.

28 images were randomly acquired from inside each well on the slides using a Leica DM4000B microscope (Leica Microsystems, Wetzlar, Germany) for quantitative FISH analysis. *Archaea* appear red due to hybridization with the ARCH915 probe (red) while bacteria appear green due to hybridization with the EUB338 I and EUB338 plus probes (green) and DAPI (cyan).

DAIME software was used to calculate the relative biovolumes of total *archaea* and total bacteria from the total DAPI-stained biomass. They were split into individual color channels before image segmentation (Daims et al. 2006).

3.4.4 16S rRNA gene sequencing

16S rRNA gene sequencing analysis was performed in samples from Chapter 6 and Chapter 8 after genomic DNA extraction.

Microbial community profiles were determined using 16S rRNA gene V4 hypervariable region with universal primers (515F/806R).

Sequencing was performed using Illumina MiSeq platform. The raw sequenced data were processed using CLC Workbench software (V.8.0.2) with Microbial genomics module plug in (QIAGEN Bioinformatics, Germany). The detailed procedure followed was previously described by Treu et al. (2018).

BLASTn against 16S ribosomal RNA (bacteria and *archaea*) database was used to assist and/or verify the taxonomical assignment obtained by CLC (Greengenes v13_5 database). Heat maps showing relative abundance and fold change of most relevant operational taxonomic units (OTUs) were done using Multiexperiment Viewer software (MeV 4.9.0) (Saeed et al., 2003).

Statistical analysis and corresponding graphs were performed using STAMP software (Parks and Beiko, 2010) and RStudio to assess the dissimilarity among the samples identifying the significance of changes in relative abundance.

The current studies will focus on the high abundant OTUs, i.e. relative abundance higher than 0.5% (Chapter 6) or 1% (Chapter 8) with respect to the total number of sequences, which were present in at least one sample.

Raw reads were deposited in Sequence Read Archive (SRA) database of NCBI (<https://www.ncbi.nlm.nih.gov/sra>).

3.5 CALCULATIONS

The general calculations which are common to some of the experiments are described below while the specific calculations for each experiment are detailed in their corresponding chapter.

3.5.1 Efficiency of hydrogen utilization, η_{H_2}

The efficiency of H_2 utilization, denoted as η_{H_2} (%), was determined according to the following equations, depending on the influent gas mixture employed.

For experiments with H_2 and CO_2 (80% and 20% v) or H_2 (100% v) as gas substrates, η_{H_2} was calculated directly as follows (Eq. 10):

$$\eta_{H_2} = \frac{H_2 \text{ loading rate} - H_2 \text{ rate in output gas}}{H_2 \text{ loading rate}} \cdot 100 \quad (\text{Eq. 10})$$

where H_2 loading rate is the rate of H_2 fed ($L_{H_2}/L_R \cdot d$) and H_2 rate in output gas is the rate of H_2 in the effluent gas ($L_{H_2}/L_R \cdot d$) which were calculated with Eq. 11 and Eq. 12:

$$H_2 \text{ loading rate} = \text{Input gas rate} \cdot x_{H_2,IN} \quad (\text{Eq. 11})$$

$$H_2 \text{ rate in output gas} = \text{Output gas rate} \cdot x_{H_2,OUT} \quad (\text{Eq. 12})$$

where Input gas rate is the influent gas mixture rate ($L/L_R \cdot d$), $x_{H_2,IN}$ is the molar fraction of H_2 (dry basis) in the influent gas mixture, Output gas rate is the total rate of effluent gas ($L/L_R \cdot d$) and $x_{H_2,OUT}$ is the molar fraction of H_2 (dry basis) in the effluent gas.

For experiments with H_2 , CO_2 and CH_4 (62%, 15% and 23% v, respectively) as influent gas mixture, η_{H_2} was determined by subtracting the extra H_2 fed that was contained in the influent gas mixture (as it remains unutilized according to the stoichiometry of hydrogenotrophic methanogenesis of Eq. 1) as follows (Eq. 13):

$$\eta_{H_2} = \frac{H_2 \text{ loading rate} - H_2 \text{ rate in output gas} - \text{extra } H_2 \text{ fed}}{H_2 \text{ loading rate} - \text{extra } H_2 \text{ fed}} \cdot 100 \quad (\text{Eq. 13})$$

where *extra H₂ fed* (L_{H₂}/L_R·d) was calculated with Eq. 14 taking into account the 2% extra H₂ present in the influent gas mixture:

$$\text{extra } H_2 \text{ fed} = \text{Input gas rate} \cdot 0.02 \quad (\text{Eq. 14})$$

3.5.2 Carbon dioxide conversion efficiency, η_{CO_2}

CO₂ conversion efficiency (η_{CO_2} , %) was calculated based on the CO₂ fraction contained in the gas phase, as described by Eq.15:

$$\eta_{CO_2} = \frac{CO_2 \text{ used}}{CO_2 \text{ loading rate}} \cdot 100 \quad (\text{Eq. 15})$$

where *CO₂ loading rate* represents the rate of CO₂ fed (L_{CO₂}/L_R·d) and *CO₂ used* is the CO₂ utilization rate (L_{CO₂}/L_R·d) which were calculated as follows (Eq. 16 and Eq. 17):

$$CO_2 \text{ loading rate} = \text{Input gas rate} \cdot x_{CO_2,IN} \quad (\text{Eq. 16})$$

where $x_{CO_2,IN}$ is the molar fraction of CO₂ (dry basis) in the influent gas mixture.

$$CO_2 \text{ used} = CO_2 \text{ loading rate} - CO_2 \text{ rate in output gas} \quad (\text{Eq. 17})$$

where *CO₂ rate in output gas* is the rate of CO₂ in the effluent gas (L_{CO₂}/L_R·d) calculated with Eq. 18:

$$CO_2 \text{ rate in output gas} = \text{Output gas rate} \cdot x_{CO_2,OUT} \quad (\text{Eq. 18})$$

where $x_{CO_2,OUT}$ is the molar fraction of CO₂ (dry basis) in the effluent gas.

3.5.3 Methane yield, Y_{CH_4}

Methane yield (Y_{CH_4} , L_{CH₄}/L_{H₂}) was defined as the volume of CH₄ generated per volume of H₂ fed to the bioreactor (Eq. 19):

$$Y_{CH_4} = \frac{CH_4 \text{ production rate}}{H_2 \text{ loading rate}} \quad (\text{Eq. 19})$$

where CH_4 production rate is the rate of CH_4 produced in the biogas upgrading system ($L_{CH_4}/L_R \cdot d$).

For experiments with H_2 and CO_2 (80% and 20% v) as gas substrates, Y_{CH_4} was calculated with Eq. 20:

$$Y_{CH_4} = \frac{(\text{Output gas rate} - H_2O \text{ rate in output gas}) \cdot x_{CH_4,OUT}}{H_2 \text{ loading rate}} \quad (\text{Eq. 20})$$

where H_2O rate in output gas is the rate of water in the effluent gas (calculated with vapor pressure given by Antoine equation, $L_{H_2O}/L_R \cdot d$) and $x_{CH_4,OUT}$ is the molar fraction of CH_4 (dry basis) in the effluent gas.

For experiments with H_2 , CO_2 and CH_4 (62%, 15% and 23% v, respectively) as influent gas mixture, Y_{CH_4} was determined by considering negligible the H_2O rate in the output gas and subtracting the extra H_2 fed that was contained in the influent gas mixture (as it remains unutilized according to the stoichiometry of hydrogenotrophic methanogenesis of Eq. 1) as follows (Eq. 21):

$$Y_{CH_4} = \frac{CH_4 \text{ production rate}}{H_2 \text{ loading rate} - \text{extra } H_2 \text{ fed}} \quad (\text{Eq. 21})$$

where CH_4 production rate ($L_{CH_4}/L_R \cdot d$), H_2 loading rate ($L_{H_2}/L_R \cdot d$) and extra H_2 fed ($L_{H_2}/L_R \cdot d$) were calculated according to Eq. 23 (below described), Eq. 11 and Eq. 14, respectively.

CH_4 in the liquid effluent can be neglected due to the low solubility of CH_4 in water (dimensionless Henry's constant of 33 and 45 at 35 and 55 °C, respectively) and the low liquid effluent rate.

3.5.4 Methane production rate

The methane production rate ($L_{CH_4}/L_R \cdot d$) was determined according to the following equations, depending on the influent gas mixture employed.

For experiments with H_2 and CO_2 (80% and 20% v) or H_2 (100% v) as gas substrates, CH_4 production rate was calculated directly as follows (Eq. 22):

$$CH_4 \text{ production rate} = \text{Output gas rate} \cdot x_{CH_4,OUT} \quad (\text{Eq. 22})$$

For experiments with H₂, CO₂ and CH₄ (62%, 15% and 23% v, respectively) as influent gas mixture, CH₄ production rate was determined by subtracting the CH₄ volume that was contained in the influent gas mixture from the output gas as follows (Eq. 23):

$$CH_4 \text{ production rate} = CH_{4,OUT} \text{ rate} - CH_{4,IN} \text{ rate} \quad (\text{Eq. 23})$$

where $CH_{4,OUT} \text{ rate}$ is the outflow CH₄ rate ($L_{CH_4}/L_R \cdot d$) calculated with Eq. 22 and $CH_{4,IN} \text{ rate}$ is the CH₄ that was injected in the reactor due to the gas mixture ($L_{CH_4}/L_R \cdot d$) and determined based on the Eq. 24:

$$CH_{4,IN} = \text{Input gas rate} \cdot x_{CH_4,IN} \quad (\text{Eq. 24})$$

where $x_{CH_4,IN}$ is the molar fraction of CH₄ (dry basis) in the influent gas mixture (0.23).

3.5.5 Gas transfer coefficient, $k_L a$

A mass balance to the gas phase in the bioreactor (Eq. 25) was performed to calculate the mass transfer coefficient for H₂, $k_L a_{H_2}$ (h⁻¹):

$$\dot{m}_{H_2,IN} = \dot{m}_{H_2,OUT} + \dot{m}_{H_2,G \rightarrow L} \quad (\text{Eq. 25})$$

where $\dot{m}_{H_2,IN}$ is the mass flow rate of H₂ fed (g/d), $\dot{m}_{H_2,OUT}$ is the mass flow rate of H₂ in the effluent gas (g/d) and $\dot{m}_{H_2,G \rightarrow L}$ is the mass flow rate of H₂ transferred from the gas to the liquid phase in the bioreactor (g/d).

Under steady-state conditions, $\dot{m}_{H_2,G \rightarrow L}$ is given by Eq. 26 assuming that all the resistance to mass transfer is in the gas-liquid interphase:

$$\dot{m}_{H_2,G \rightarrow L} = V_R \cdot k_L a_{H_2} \cdot \left(\frac{c_{H_2,G,membrane}}{H_{H_2}} - c_{H_2,L} \right) \quad (\text{Eq. 26})$$

where V_R is the working volume of the bioreactor (L), $c_{H_2,G,membrane}$ is the concentration of H₂ in the stream supplied to the membrane (g/m³), H_{H_2} is the dimensionless Henry's constant for H₂ (50 and 55 at 35 and 55 °C, respectively) and $c_{H_2,L}$ is the concentration of H₂ in the liquid phase (g/m³). $c_{H_2,L} \approx 0$ when the high

turbulence provoked by gas sparging rate prevents a concentration gradient in the liquid phase and dissolved H₂ is consumed completely by methanogens as mentioned above.

Then, combining Eq. 25 and Eq. 26, $k_L a_{H_2}$ can be obtained (Eq. 27):

$$k_L a_{H_2} = \frac{\dot{m}_{H_2,IN} - \dot{m}_{H_2,OUT}}{V_R \cdot \left(\frac{c_{H_2,G,membrane}}{H_{H_2}} \right)} \quad (\text{Eq. 27})$$

$c_{H_2,G,membrane}$ is given by Eq. 28:

$$c_{H_2,G,membrane} = \frac{c_{H_2,IN} \cdot Q_{IN} + c_{H_2,OUT} \cdot Q_R}{Q_{IN} + Q_R} \quad (\text{Eq. 28})$$

where $c_{H_2,IN}$ and $c_{H_2,OUT}$ are the H₂ concentrations in feed and effluent gas respectively (g/m³), Q_{IN} is the volumetric gas feed rate (m³/d) and Q_R the volumetric gas recirculation rate (m³/d).

Yu et al. (2006) demonstrated that the mass transfer coefficient for a given gaseous substrate can be estimated when the coefficient for a reference gas is known in the same reactor and under the same operating conditions (Eq. 29); thus, the mass transfer coefficient for CO₂ ($k_L a_{CO_2}$, h⁻¹) was estimated.

$$k_L a_{CO_2} / k_L a_{H_2} = \frac{(1/V_{mCO_2})^{0.4}}{(1/V_{mH_2})^{0.4}} \quad (\text{Eq. 29})$$

where V_{mH_2} and V_{mCO_2} are the molecular volume of H₂ and CO₂ (14.3 and 34 mL/mol, respectively) (Wilke and Chang, 1955).

3.5.6 Gas transfer rate (r_t) and biological kinetics parameters (r_{utH_2} , U , f_x)

H₂ gas-liquid mass transfer rate (r_t , L_{H₂}/L_R·d) was calculated according to Eq. 30:

$$r_t = H_2 \text{ loading rate} - H_2 \text{ rate in output gas} \quad (\text{Eq. 30})$$

From $\dot{m}_{H_2,G \rightarrow L}$, some parameters of the biological kinetics and stoichiometry were calculated performing a mass balance to H_2 in the liquid phase of the bioreactor (Eq. 31):

$$\dot{m}_{H_2,G \rightarrow L} = \dot{m}_{H_2,OUT,L} + r_{ut_{H_2}} \quad (\text{Eq. 31})$$

where $\dot{m}_{H_2,OUT,L}$ is the effluent mass flow rate of dissolved H_2 (g/d) and $r_{ut_{H_2}}$ is the H_2 utilization rate (g/d).

H_2 in the liquid effluent can be neglected as well as it is several orders of magnitude lower than the mass flow rates of H_2 in gaseous streams. H_2 concentration in the liquid phase is negligible as a result of the H_2 complete consumption by methanogens in this phase.

From $r_{ut_{H_2}}$, the specific substrate utilization rate (U , $g_{COD}/g_{VSS} \cdot d$) was obtained with Eq. 32 including the conversion factors $8 g_{COD}/g_{H_2}$ and $24 h/d$:

$$U = \frac{0.33 \cdot r_{ut_{H_2}}}{X \cdot V_R} \quad (\text{Eq. 32})$$

where X is the microorganisms concentration (g_{VSS}/L).

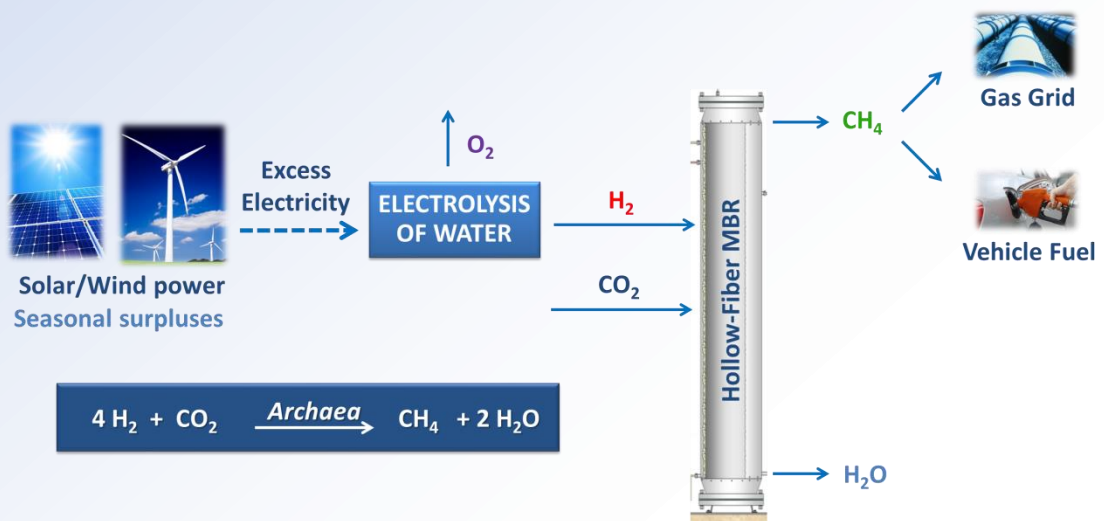
Finally, the fraction of H_2 employed for microorganisms growth (f_X , anabolism) was estimated (Eq. 33) given the fact that the mass flow rate of H_2 consumed to produce energy (catabolism) can be obtained from the methane production rate according to Eq. 1:

$$f_X = \frac{r_{ut_{H_2}} - (\dot{m}_{CH_4,OUT}/2)}{r_{ut_{H_2}}} \quad (\text{Eq. 33})$$

where the term $\dot{m}_{CH_4,OUT}/2$ is defined as the effluent mass flow rate of CH_4 as equivalent H_2 $(\dot{m}_{CH_4,OUT})_{H_2eq}$ according to Eq. 1.

Chapter 4

A feasibility study on the bioconversion of CO_2 and H_2 to biomethane by gas sparging through polymeric membranes



4.1 INTRODUCTION

The main barrier to the successful development of the biogas upgrading technology on an industrial scale is the H₂ gas-liquid mass transfer. To address this technical challenge, different reactor configurations have been investigated with the aim of maximizing the H₂ gas-liquid mass transfer. As previously described in the Chapter 1, reactors based on different diffusion devices, high-speed stirring or gas recirculation flow have been tested to enhance the H₂ mass transfer into the liquid phase.

Studies with gas diffusers on lab-scale CSTR were shown to require high stirring speed therefore considering the implementation of these systems at industrial scale, high energy needs and operational costs would be required. Membrane bioreactors are an attractive alternative in order to H₂ transfer by gas diffusion through the membrane material.

Literature on ex-situ biogas upgrading shows reactors at lab-scale with low H₂ loading rates so applied research should focus on developing viable bioreactor configurations that achieve both high H₂ loading rates and high methane yields on larger scales using efficient H₂ distribution systems.

In this study, the potential of a pilot hollow-fiber membrane bioreactor for the conversion of H₂ and CO₂ to CH₄ was evaluated and the feasibility of the bioconversion was assessed. The polymeric membrane was utilized to create a large sparging surface in order to overcome mass transfer limitations of H₂, which allows an efficient biogas upgrading while avoiding oversized energy consumption on larger scales. Noteworthy H₂ loading rates were studied and different gas recirculation rates were applied in order to evaluate mass transfer conditions and reactor performance. Molecular biology tools were used to study the microbial population.

4.2 MATERIALS AND METHODS

4.2.1 Pilot Plant

The description of the pilot plant used in the experiment has been performed in Chapter 3, section 3.1.1.1.a). As previously mentioned, it was a hollow-fiber membrane bioreactor with a working volume of 31 L with gas recirculation.

4.2.2 Operating conditions

The reactor was inoculated with 31 L of anaerobic sludge from a thermophilic pilot plant anaerobic digester at our laboratory treating activated sludge from Valladolid WWTP. We set up the reactor by supplying H₂ and CO₂ (ratio according to Eq. 1) at H₂ loading rate of 5.0 L_{H₂}/L_R·d with a gas recirculation rate of 3.2 L/L_R·d for 30 d. All the values of volumetric flow rates from this study are expressed at 55 °C and 1 atm.}

After the set-up period, the experiment started. The experiment was performed at thermophilic conditions (55 ± 1 °C) and divided into 6 stages (I–VI), each corresponding to a certain gas load rate, in order to determine the maximum H₂ loading rate that could be applied with a 95% conversion efficiency for H₂. Different gas recirculation rates were applied for some stages (Table 9) in order to evaluate mass transfer conditions and reactor performance.

Table 9. Operating conditions applied during the study.

	I		II		III		IV	V	VI			
	a	b	c	d	e	a	b		a	b		
t (d)	0	3	7	13	19	27	40	58	75	98	111	124
H₂ loading rate (L_{H₂}/L_R·d)}			10.1			20.1	30.2	45.2	25.1	40.2		
Gas recirculation rate (L/L_R·d)	3.2	6.5	12.9	25.8	51.9	51.9	51.9	77.7	155.8	70.0	142.9	155.8

Nutrients required for microbial activity and a phosphate buffer solution, were supplied when the NH₄⁺ concentration fell below 500 mg/L, specifically, during day 19, 52, 82 and 108. 200 mL of macronutrients solution, 20 mL of micronutrients solution

diluted in 180 mL of distilled water and 200 mL of buffer solution were added on the days mentioned.

The macronutrient solution was prepared like the stock solution A reported in Angelidaki and Sanders (2004), while the micronutrients solution was a version that was modified (by adding 500 mg/L of resazurine) from the trace-metal solution also from Angelidaki and Sanders (2004) and the phosphate buffer solution was prepared with $K_2HPO_4 \cdot 3H_2O$ and KH_2PO_4 to a final pH of 7.2 with a concentration of 1 mol/L PO_4^{3-} .

4.2.3 Monitoring and experimental analysis

The following parameters (Table 10) were monitored and analyzed during the experiment according to the materials and methods described in Chapter 3, section 3.3.:

Table 10. Parameters monitored and analyzed during the study.

Parameter	Measuring frequency
Headspace pressure Temperature	Continuous mode
Gas production rate Gas composition Liquid effluent	Daily
VFA concentration pH TSS/VSS NH_4^+	Weekly
Dissolved H_2 concentration	Periodically

4.2.4 Calculations

Calculations about efficiency of H_2 utilization (η_{H_2}), CH_4 yield (Y_{CH_4}), mass flow rate of H_2 transferred from gas to liquid phase ($\dot{m}_{H_2,G \rightarrow L}$), effluent mass flow rate of CH_4 gas as equivalent H_2 ($(\dot{m}_{CH_4,OUT})_{H_2eq}$), $k_L a_{H_2}$ and $k_L a_{CO_2}$ values, maximum specific utilization rate (U) and fraction of H_2 employed for methanogen growth (f_x) have been performed following the calculations described in Chapter 3, section 3.5.

4.2.5 Microbial analysis

In order to evaluate the evolution of the population during the experiment, samples from inoculum, end of stage III and end of stage VI were collected and extraction of genomic DNA, PCR and DGGE analysis were performed according to the materials and methods described in Chapter 3, sections 3.4.1. and 3.4.2.

4.3 RESULTS AND DISCUSSION

4.3.1 Performance of the conversion of H₂ and CO₂ to CH₄

The experiment started (stage I a) with a $\dot{m}_{H_2,IN}$ of 22.9 g/d and a gas recirculation rates of 3.2 L/L_R·d. The mass balance performed to the gas phase (Figure 26 a) showed that less than 90% of the H₂ fed was converted during these first days.

Next, gas recirculation rate was increased stepwise according to Table 9 until 51.9 L/L_R·d, with the purpose of raising η_{H_2} . The bioreactor presented an unstable behavior until day 20, η_{H_2} varied between 65% and 90% (Figure 26 b), and we found a significant difference between $\dot{m}_{H_2,G \rightarrow L}$ and $\left(\dot{m}_{OUT,GCH_4}\right)_{H_2eq}$ until day 9, which indicates that a large part of the H₂ fed in these first days was transferred to the liquid phase and consumed, but was not employed for CH₄ production, probably due to biomass adaptation to the substrate. The bioreactor converted at least 95% of the H₂ fed only after day 20. During stage I e, the average η_{H_2} was 97%, the average Y_{CH_4} was 0.20 L_{CH₄}/L_{H₂} and an average 82% CH₄ content was found in the output gas.

On day 27, $\dot{m}_{H_2,IN}$ was raised to 45.7 g/d while gas recirculation rate was maintained at 51.9 L/L_R·d (stage II). The increase in the mass flow rate provoked a slightly decrease in η_{H_2} , which remained around 95% for this period, thus indicating that mass transfer conditions were still acceptable even when the H₂ loading rate was doubled. Besides, the average Y_{CH_4} was 0.19 L_{CH₄}/L_{H₂}, somewhat lower than at the end of the previous period (Figure 26 b). CH₄ concentration in the output gas was on average 71%.

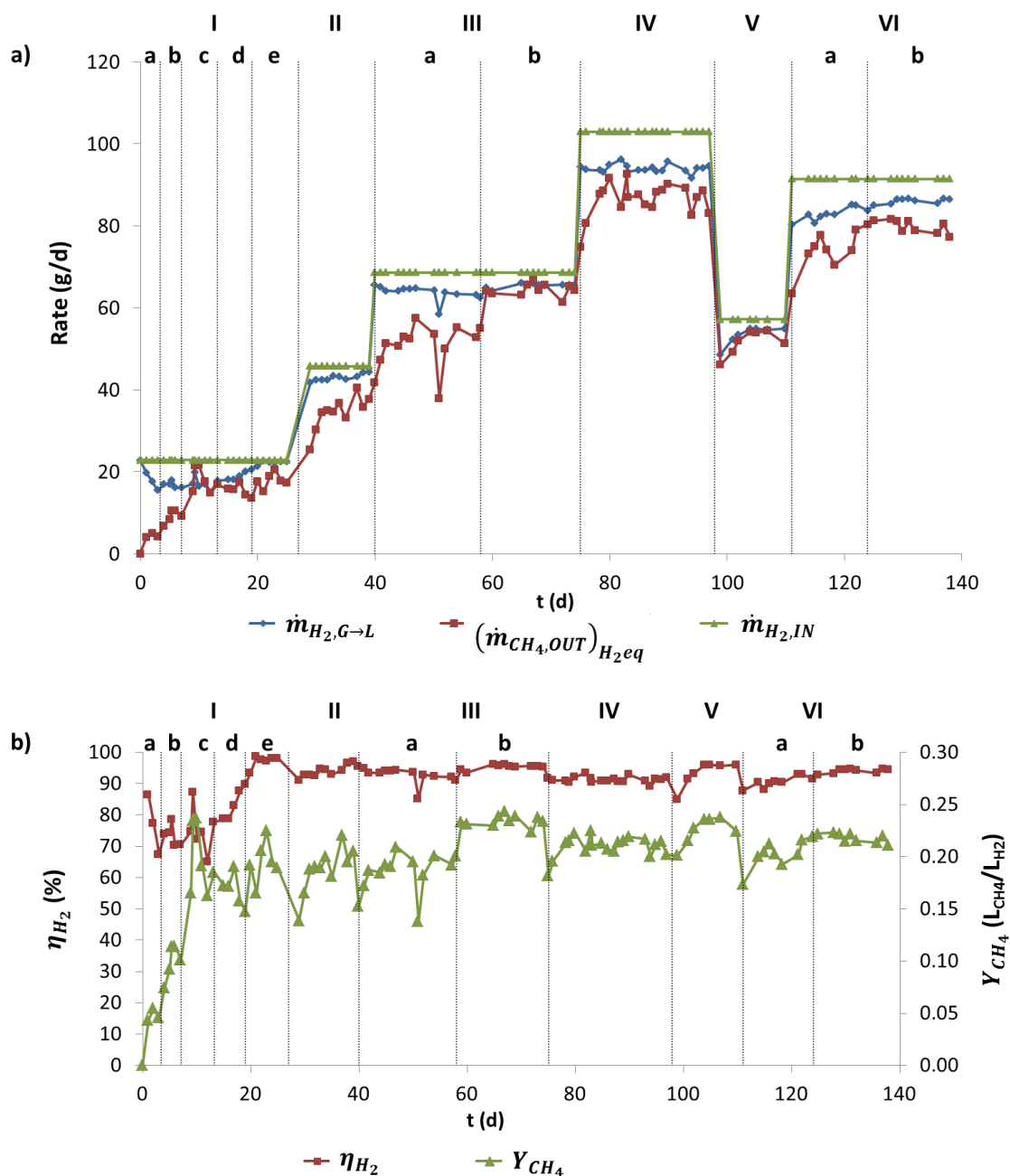


Figure 26. Performance of the bioconversion throughout the experiment.

a) H_2 and CH_4 as equivalent H_2 mass flow rates; **b)** Efficiency of H_2 utilization and CH_4 yield.

Given the fact that the conversion efficiency did not substantially fall during stage II, we increased $\dot{m}_{H_2, IN}$ to 68.6 g/d on day 40 (stage III a) and maintained gas recirculation rate. In this case, η_{H_2} decreased to an average 93% but the average Y_{CH_4} (Figure 26 b) and CH_4 concentration in the output gas (70%) were not altered.

On day 58, gas recirculation rate was augmented to 77.7 L/L_R·d (stage III b). Under these conditions, the performance of the bioreactor improved significantly, η_{H_2} reached 95% while Y_{CH_4} increased to 0.23 L_{CH₄}/L_{H₂}, much closer to the stoichiometric value (Figure 26 b). Furthermore, the difference between $\dot{m}_{H_2,G \rightarrow L}$ and $\left(\dot{m}_{OUT,GCH_4}\right)_{H_2eq}$ was drastically lower than in previous stages (Figure 26 a) thus indicating that *archaea* employed almost all H₂ transferred in order to produce CH₄. Moreover, average CH₄ concentration in the output gas increased to 79%.

The maximum $\dot{m}_{H_2,IN}$ supplied to the bioreactor was 103 g/d during stage IV, in combination with a gas recirculation rate of 155.8 L/L_R·d, the maximum capacity of gas pump. Throughout this period, η_{H_2} never reached the targeted 95%, instead averaging 91% while Y_{CH_4} was 0.21 L_{CH₄}/L_{H₂} (Figure 26b) and CH₄ concentration dropped to 67%. On day 98 (at the end of stage IV), the operation was stopped and the bioreactor opened in order to observe the state of the membrane.

There was no biomass attachment to the membrane, in contrast to the biofilm found on the MBRs employed for H₂ conversion to CH₄ in the literature (Ju et al., 2008; Wang et al., 2013), which operated without gas bubbles, probably due to the turbulence provoked by the high recirculation rates employed here to form bubbles while in Ju et al. (2008) and Wang et al. (2013) gas diffusion through the membrane was the transference mechanism.

The operation was restarted a few hours later with $\dot{m}_{H_2,IN}$ of 57.2 g/d (stage V). This lower rate was chosen because during the technical stop some liquid was lost and replaced with approximately 2 L of distilled water. η_{H_2} reached 96% after 2 days and Y_{CH_4} was 0.23 L_{CH₄}/L_{H₂}, similar values to those found on stage III b with a comparable H₂ loading rate.

In stage VI a, the rates of feed and recirculation were raised to 91.5 g/d and 142.9 L/L_R·d respectively on day 111 and the maximum recirculation capacity was applied from day 124 (stage VI b). During stage VI b, η_{H_2} was 95% in average while the Y_{CH_4} was 0.22 L_{CH₄}/L_{H₂} (Figure 26b). On average, 76% CH₄ content was observed in the output gas.

In brief, the bioreactor successfully transformed at least 95% of the H₂ fed at H₂ loading rate between 10 and 40.2 L_{H₂}/L_R·d adjusting the gas recirculation rate and 40.2 L_{H₂}/L_R·d is the maximum H₂ loading rate that could be supplied to the system while converting 95% of the H₂ fed since the application of a higher loading rate (as in stage IV) failed to achieve a such a conversion at the maximum recirculation rate provided by the gas pump.

This H₂ loading rate is higher than that achieved on similar pilot-scale bioreactors, such as packed column bioreactors (4.5 L_{H₂}/L_R·d) (Burkhardt and Busch, 2013) or CSTR (18 L_{H₂}/L_R·d) (Kim et al., 2013); on the other hand, Y_{CH_4} was somewhat lower than in those experiments, which found 0.26 and 0.23 L_{CH₄}/L_{H₂}, respectively. Nevertheless, H₂ loading rate during stage VI b was more than double that applied in Kim et al. (2013), while the reactor yield decreased only slightly. Hence, a membrane can be employed to transfer H₂ at a high rate, allowing the biological conversion to take place satisfactorily. Further research should focus on the long-term stability of the bioconversion rates found during this study.

4.3.2 Mass transfer capacity in the MBR

The concentration of dissolved H₂ in the liquid phase was below the detection limit during the whole experiment. As a consequence, the assumption that all the resistance to mass transfer is in the gas/liquid interphase was correct.

The correlation coefficient between the experimental data and the predicted values (Eq. 34) was 0.990, thus confirming that H₂ mass transfer to the liquid phase can be described accurately by Eq. 27 for the range of volumetric flow rates tested:

$$k_L a_{H_2} = 0.0645 \cdot (Q_{IN} + Q_R) + 1.1866 \quad (\text{Eq. 34})$$

where Q_{IN} is the volumetric gas feed rate (m³/d) and Q_R the volumetric gas recirculation rate (m³/d).

The $k_L a_{H_2}$ values observed (Figure 27) ranged from 30 h^{-1} for the lowest total gas flow through the membrane ($Q_{IN} + Q_R$) to 430 h^{-1} (for the highest) and the estimated $k_L a_{CO_2}$ from 20 to 300 h^{-1} .

It should be pointed out that this maximum $k_L a_{H_2}$ value is higher than $k_L a$ values found in bioreactors with traditional gas diffusers (at equivalent gas rates), and in the range of CSTR with high agitation speeds (700rpm) (Kreutzer et al., 2005). This is a consequence of the large sparging area of the membrane module employed (sparging area to reactor working volume ratio is 30 m^2/m^3), however, this ratio is lower than employed by Wang et al. (2013) when membranes were used to transfer H_2 by diffusion only (62 m^2/m^3). Nevertheless, gas sparging implies power consumption on gas recirculation to achieve a high $k_L a_{H_2}$ while this power input is prevented when H_2 is transferred only by diffusion through the membrane.

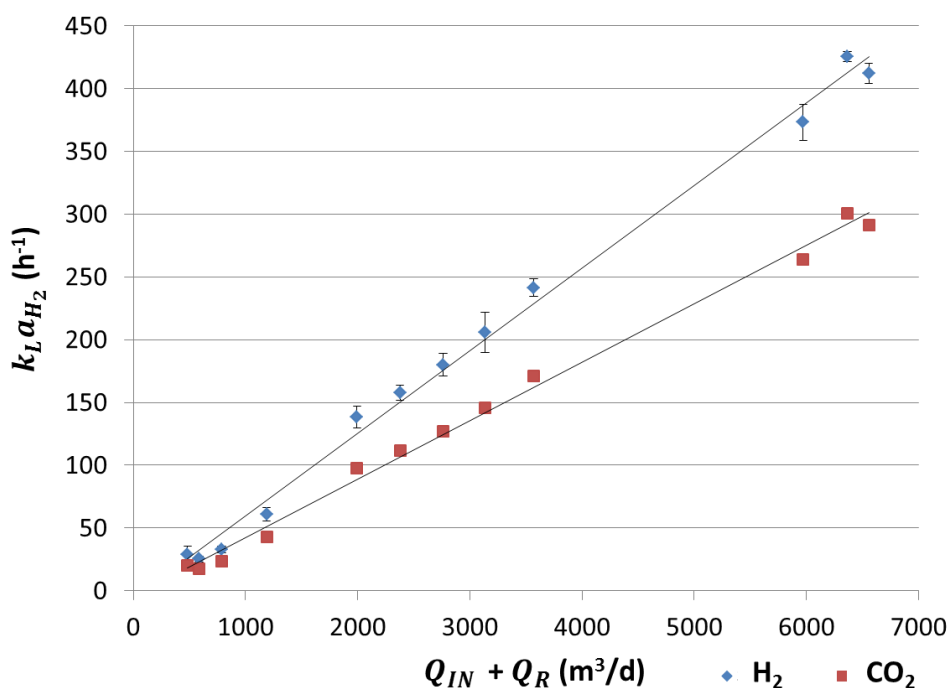


Figure 27. Linear fitting of experimental $k_L a_{H_2}$ and estimated $k_L a_{CO_2}$ values.

Conversely, much higher $k_L a$ values, as high as 3600 h^{-1} , were found in Peillex et al. (1990) using H_2 diffusion through porous glass and a Rushton impeller; however, the stirring speeds employed (over 1000 rpm) would presumably result in an extremely energy-consuming system on a larger scale.

A comparison between the maximum potential transfer rates ($k_L a (c_{G,membrane}/H)$) from the gas to the liquid phase showed that the ratio $k_L a_{H_2} (c_{H_2,G,membrane}/H_{H_2}) / k_L a_{CO_2} (c_{CO_2,G,membrane}/H_{CO_2})$ is around 0.01 g_{H₂}/h/g_{CO₂}/h under the experimental conditions. This is another indicator of H₂ transfer limitations in the bioreactor because 0.18 g of H₂ is required per g of CO₂ to perform the conversion according to stoichiometry (Eq. 1).

4.3.3 Biological activity

The maximum specific utilization rate observed during the study was around 7 g_{COD}/g_{VSS}·d (Figure 28). This experimental value is higher than the typical design value suggested for methanogens growing on H₂ and CO₂ (2.2 g_{COD}/g_{VSS}·d) (Rittman, 2001). Nevertheless, a review of kinetic parameters for different pure cultures of hydrogenotrophic *archaea* showed that U ranges from 2 – 90 g_{COD}/g_{VSS}·d depending on the specific strain (Pavlostathis and Giraldo-Gomez, 1991).

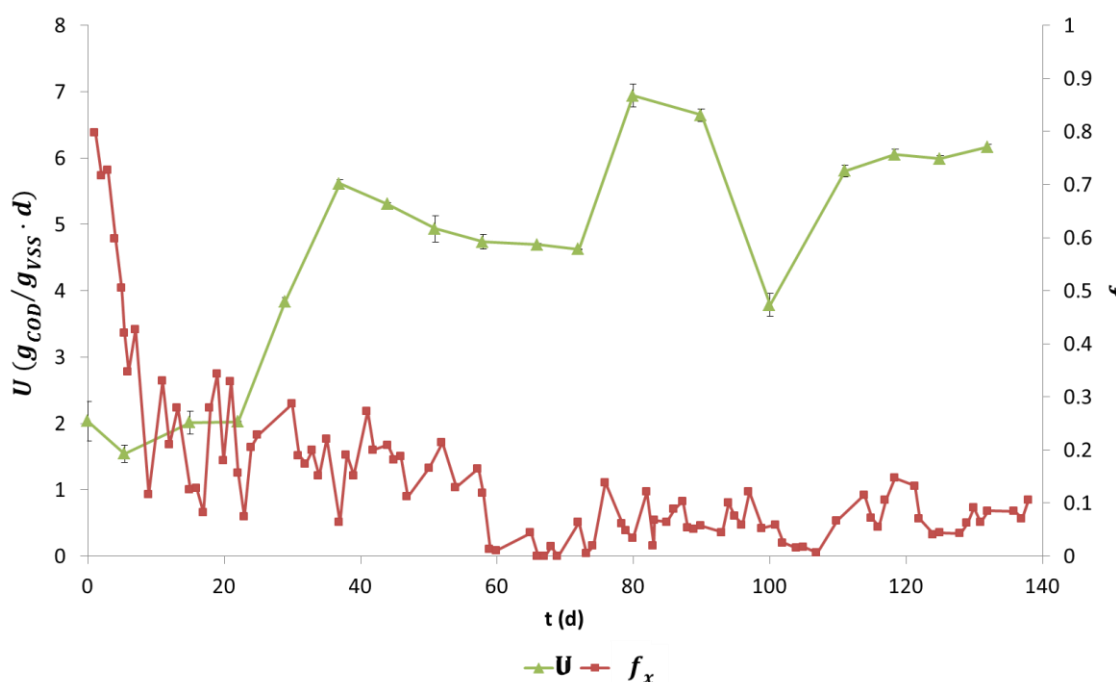


Figure 28. Specific H₂ utilization rate (U) and fraction of H₂ employed for microbial growth (f_x) during the experiment.

The higher the U , the larger the H_2 rate that can be converted to CH_4 in a specific bioreactor before the reaction's limiting factors overtake the H_2 mass transfer. Therefore, U values found during this experiment appear not to be the potential maximum, and are limited by H_2 mass transfer in the system, since the concentration of H_2 in the liquid phase was always below the detection limit, indicating a lack of limitations for the biological reaction.

A high concentration of H_2 in the liquid phase inhibits propionate and butyrate conversion to acetate or H_2 and CO_2 during anaerobic digestion occasioning lower yields or the whole process breakdown (Speece, 2008). Therefore, the fact that H_2 could be transferred at a high rate without any accumulation in the liquid phase is an important advantage of the technique studied, since it might be applied to the own anaerobic digester, thus avoiding additional units for biogas upgrading. In fact, in situ biogas upgrading was found feasible by Wang et al. (2013) but H_2 was transferred only through diffusion and a biofilm where H_2 and CO_2 were partly consumed developed over the membrane surface. Nevertheless, gas sparging impedes biofilm formation and methanogenesis takes place totally in the bulk phase; then, additional research is required to evaluate if the concentration of H_2 in the liquid phase would remain as low as in this experiment if anaerobic digestion and upgrading were combined.

From another point of view, the adaptation of an unspecific anaerobic sludge to H_2 and CO_2 led to the development of an acclimated population for the production of biomethane with yields of $0.22 L_{CH_4}/L_{H_2}$ at $40.2 L_{H_2}/L_R \cdot d$ and $0.23 L_{CH_4}/L_{H_2}$ at $30.2 L_{H_2}/L_R \cdot d$. These yields are larger than the yields achieved employing specific strains of *Methanobacterium thermoautotrophicum* (Jee et al., 1988; Peillex et al., 1990) (0.19 and $0.18 L_{CH_4}/L_{H_2}$) or *Methanococcus thermolithotrophicus* (Peillex et al., 1988) ($0.16 L_{CH_4}/L_{H_2}$) at high η_{H_2} values. This fact implies that the acquisition costs of specific strains of hydrogenotrophic methanogens could be avoided on an industrial scale by employing unspecific anaerobic sludge as inoculum instead, since higher yields could be reached, and given the fact that the current process is limited by H_2 mass transfer.

The fraction of H_2 employed for methanogen growth (f_x) calculated with Eq. 33 was larger during the first stages of the experiment than in the latter (Figure 28).

f_x dropped progressively from values around 0.7 at the beginning of the experiment to below 0.1 after day 60. This result is supported by the fact that VSS concentration (Figure 29) increased from 2.5 g/L, at the beginning of the study, to 3.6 g/L the day 58, and remained around this value during the rest of the experiment (Figure 29). This was also the reason underlying the fact that Y_{CH_4} was always below 0.20 L_{CH_4}/L_{H_2} until day 58, in spite of high η_{H_2} values, because an important fraction of H_2 was utilized for microbial growth. Then, f_x was higher when $\dot{m}_{H_2,G \rightarrow L}$ was low (also pointed by the important difference between $\dot{m}_{H_2,G \rightarrow L}$ and $(\dot{m}_{CH_4,OUT})_{H_2eq}$ in the first stages) whereas it was lower when $\dot{m}_{H_2,G \rightarrow L}$ rose, thus indicating an uncoupling of microbial growth (anabolism) and H_2 conversion to CH_4 (catabolism).

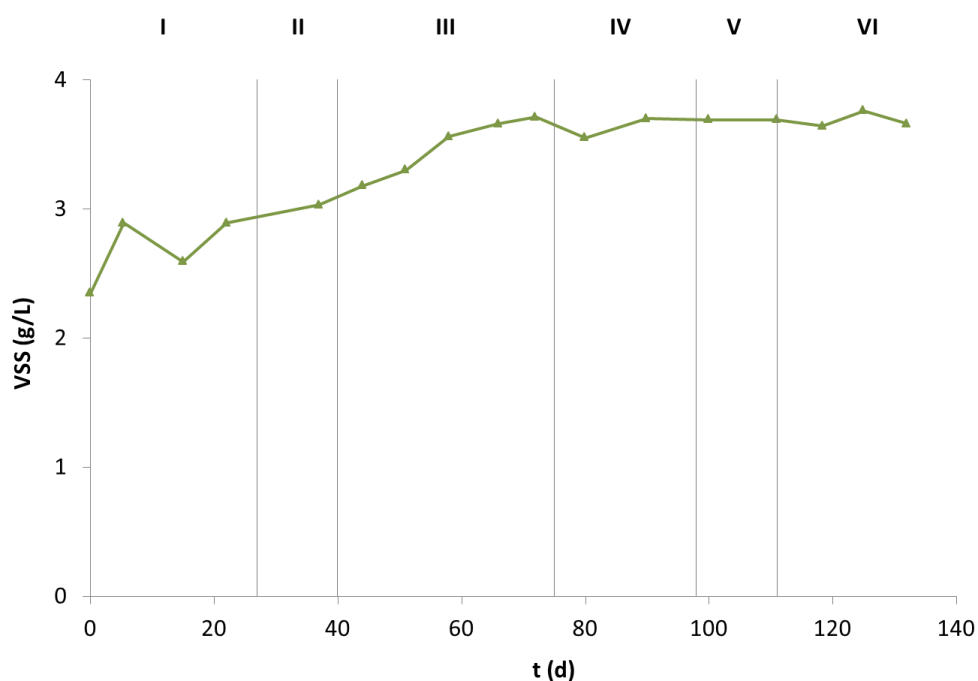


Figure 29. VSS concentrations in the bioreactor throughout the experiment.

This finding is in agreement with Fardeau and Belaich (1986) and with Schönheit et al. (1980), where this phenomenon had already been reported. An extensive discussion about not fixed stoichiometry in methanogenic environments from a biochemical point of view can be found in Kleerebezem and Stams (2000).

Additionally, since the inoculum employed in this study was adapted to the treatment of activated sludge prior to the beginning of the study, only a small fraction of the original microbial community was employed for the transformation of H₂ and CO₂ during the experiment. This fact may influence stoichiometry as well, especially on the first stages, and molecular biology tools has been considered in order to elucidate how the evolution of the microbial community influences the methane yield obtained.

From a technological point of view, the repercussions that arise from uncoupled growth and conversion are, at least initially, positive. A bioreactor can be inoculated and biomass adapted from an anaerobic sludge (treating a different substrate) directly inside the methanogenic bioreactor in a short period (as in this study). A low H₂ loading rate can be used, and an important fraction of H₂ and CO₂ will be employed for methanogens growth. Once the desired biomass concentration is achieved, H₂ loading rate can be raised, while most of the substrate will be employed for CH₄ production.

VFA concentration was very low during the whole experiment. Acetic acid concentration was under 100 mg/L, propionic acid was below 50 mg/L, and only traces of butyric acid were found. These concentrations are probably the result of microbial decay and endogenous activity. Acetate might also be produced, to some extent, by homoacetogenic bacteria, which use H₂ to reduce CO₂ to produce acetate. However, methanogenesis outcompeted homoacetogenesis in the present study, in contrast to Ju et al. (2008), where a VFA concentration over 4000 mg/L was found in combination with acetoclastic and hydrogenotrophic methanogenesis.

4.3.4 Microbial community

From the archaeal DGGE gel (Figure 30), 20 bands were sequenced. According to the RDP classifier (confidence threshold of 50%), all of them belonged to the *Euryarchaeota* phyla and they were ascribed to two classes, almost all to *Methanobacteria* (band 1-18) and only two bands to *Methanomicrobia* (band 19 and 20) (Table 11). The BLAST search tool provided consistent results with those given by the RDP classifier. *Methanothermobacter* and *Methanobacterium* were the two genus

assigned to *Methanobacteria* class and *Methanosarcina* genus to *Methanomicrobia* class (Table 11).

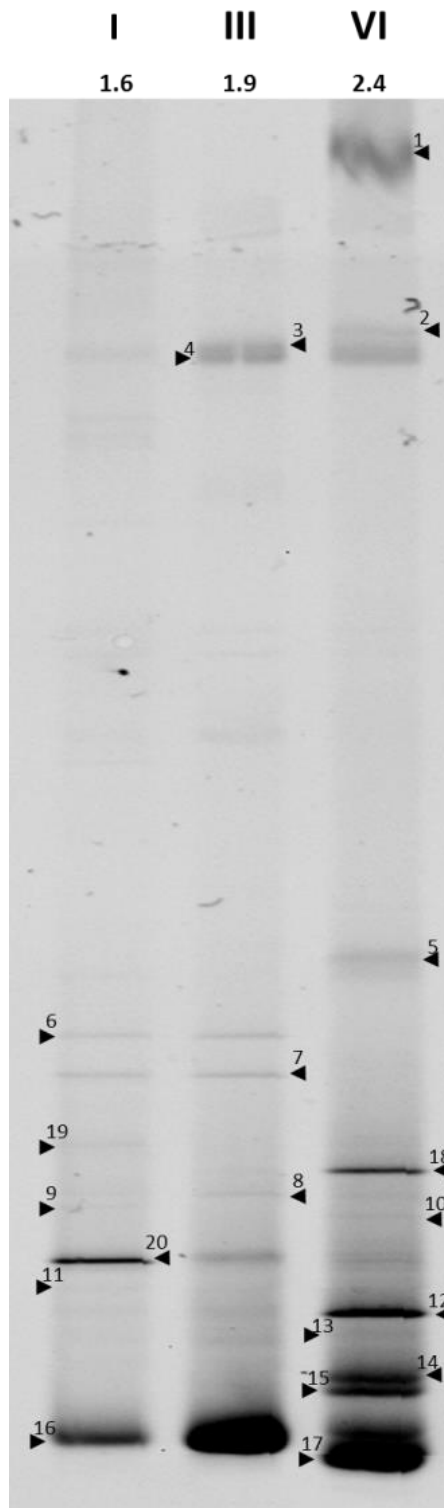


Figure 30. Archaeal DGGE profile of the 16S rRNA amplicons of the samples from inoculum (I), end of stage III (III) and end of stage VI (VI) with their respective diversity indices.

Some new *archaea* appeared during the experiment (bands 1, 2, 3, 5, 10, 13, 14, 15, 17 and 18, Figure 30) corresponding with uncultured *Methanothermobacter* archaeon (97-99% identity), *Methanobacteriaceae* sp. (91-93% identity) and *Methanothermobacter thermoautotrophicus* (99% identity) as a consequence of the H₂ and CO₂ supplied to the hydrogenotrophic reactor compared to the inoculum sample. This result is supported by the fact that VSS concentration (Figure 29) increased from 2.5 g/L at the beginning of the study to 3.6 g/L at stages III and VI.

Regarding the disappearance of *archaea* throughout the experiment, some of them disappeared progressively (bands 6, 7 and 9, Figure 30) corresponding with uncultured *Methanothermobacter* archaeon (97, 99% identity) and *Methanothermobacter tenebrarum* (99% identity) while others disappeared completely (bands 11 and 19, Figure 30) when comparing to the inoculum sample which were assigned to uncultured archaeon of *Methanothermobacter* and *Methanosarcina* genus (Table 11). Moreover, two *archaea* (bands 8 and 16) remained present with the same intensity during the whole experiment.

As is shown in Figure 30 and Table 11, bands 4 and 12 experienced an increasing trend throughout the experiment while band 20 (*Methanosarcina thermophila*, 99% identity) experienced a decrease.

Therefore, it was revealed the selection-effect of H₂ on archaeal community composition over time.

According to the results obtained in the archaeal DGGE analysis, inoculum was mainly composed by the hydrogenotrophic methanogen *Methanothermobacter tenebrarum* and the acetoclastic methanogen *Methanosarcina thermophila*. However, during the experiment and as the H₂ loading and gas recirculation rates were increased, *Methanothermobacter thermoautotrophicus*, a hydrogenotrophic *archaea*, was found to be present remarkably as well while the presence of the acetoclastic *Methanosarcina thermophila* was decreased notably (Figure 30, Table 11).

Table 11. RDP classification of the archaeal DGGE bands sequenced with a 50% of confidence level, and corresponding matches according to the BLAST search tool, with their similarity percentages, and environments from which they were retrieved.

Intensity < 35 = x, 35 ≤ intensity ≤ 80 = xx, intensity > 80 = xxx. Samples: Inoculum (I), end of stage III (III) and end of stage VI (VI).

Taxonomic placement (50% confidence level)	Band No.	I	III	VI	Closest relatives in Blast Name (Accession No.)	Similarity (%)	Source of origin
Phylum Euryarchaeota							
Class <i>Methanobacteria</i>							
Order <i>Methanobacteriales</i>							
Family <i>Methanobacteriaceae</i>							
Genus <i>Methanothermobacter</i>							
	1			xx	<i>Methanothermobacter thermautotrophicus</i> (NR_042782)	93	Presumptive identification of methanogens using 16S ribotyping
	2			x	<i>Methanothermobacter tenebrarum</i> (NR_113002)	92	gas-associated formation water
	3		xx	xx	<i>Methanothermobacter tenebrarum</i> (NR_113002)	91	gas-associated formation water
	4	x	xx	xx	<i>Methanothermobacter tenebrarum</i> (NR_113002)	96	gas-associated formation water
	5			x	Uncultured <i>Methanothermobacter</i> sp. (KF971873)	97	thermophilic sludge anaerobic digestion
	6	x	x		<i>Methanothermobacter tenebrarum</i> (NR_113002)	99	gas-associated formation water
					Uncultured archaeon (JF417883)	99	dry anaerobic digester
					Uncultured archaeon (HE805060)	99	anaerobic filter reactor of a thermophilic two-phase two-stage leach-bed biogas reactor supplied with rye silage in batches
	7	x	x		<i>Methanothermobacter tenebrarum</i> (NR_113002)	99	gas-associated formation water
					Uncultured archaeon (FN547930)	99	thermophilic biogas reactor fed with beet silage
					Uncultured archaeon (EF210848)	99	thermophilic biogas reactor fed with renewable biomass
	8	x	x	x	<i>Methanothermobacter tenebrarum</i> (NR_113002)	99	gas-associated formation water
					Uncultured archaeon (JF417888)	99	dry anaerobic digester
					Uncultured <i>Methanothermobacter</i> sp. (KJ744130)	99	methanogenic acetate-degrading consortium
	9	x	x		Uncultured archaeon (HE805068)	97	anaerobic filter reactor of a thermophilic two-phase two-stage leach-bed biogas reactor supplied with rye silage in batches
	10			x	Uncultured <i>Methanothermobacter</i> sp. (KF971873)	99	thermophilic sludge anaerobic digestion
					Uncultured <i>Methanothermobacter</i> sp. (AM418701)	99	compost
					Uncultured archaeon (AB234022)	99	anaerobic reactor
	11	x			<i>Methanothermobacter tenebrarum</i> (NR_113002)	99	gas-associated formation water
					Uncultured archaeon (JF417883)	99	dry anaerobic digester
					Uncultured archaeon (HE805060)	99	anaerobic filter reactor of a thermophilic two-phase two-stage leach-bed biogas reactor supplied with rye silage in batches
	12	x	x	xxx	<i>Methanothermobacter thermautotrophicus</i> (JQ346751)	99	culture_collection
					<i>Methanobacteriaceae</i> archaeon (GU129105)	99	primary culture of formation water from Gangxi oil bed (methanogens growing on H ₂ +CO ₂)
					Uncultured <i>Methanothermobacter</i> sp. (KF971873)	99	thermophilic sludge anaerobic digestion
	13			xx	<i>Methanothermobacter thermautotrophicus</i> (JX878361)	99	Formation water
					<i>Methanothermobacter thermautotrophicus</i> (JQ346751)	99	Culture collection
					Uncultured archaeon (EF512450)	100	expanded granular sludge bed reactor

Table 11. (Continued)

Taxonomic placement (50% confidence level)	Band No.	I	III	VI	Closest relatives in Blast Name (Accession No.)	Similarity (%)	Source of origin
Genus Methanobacterium	14			xxx	Uncultured archaeon (EF512442)	99	expanded granular sludge bed reactor
					Uncultured Methanothermobacter sp. (KF971873)	99	thermophilic sludge anaerobic digestion
					Uncultured archaeon (FJ189598)	98	Anaerobic reactor
	15			xxx	Methanothermobacter thermautotrophicus (JQ346751)	99	Culture collection
					Uncultured Methanothermobacter sp. (KF971873)	99	thermophilic sludge anaerobic digestion
	16	xxx	xxx	xxx	Methanothermobacter tenebrarum (NR_113002)	99	gas-associated formation water
					Uncultured archaeon (JF417883)	99	dry anaerobic digester
					Uncultured archaeon (HE805005)	99	anaerobic filter reactor of a thermophilic two-phase two-stage leach-bed biogas reactor supplied with rye silage in batches
	17			xxx	Methanothermobacter thermautotrophicus (JQ346751)	99	culture_collection
					Uncultured archaeon (EF512450)	99	expanded granular sludge bed reactor
					Uncultured archaeon (FN547954)	99	thermophilic biogas reactor fed with beet silage
	18		x	xx	Uncultured archaeon (AB447766)	91	PCR-derived sequence from anaerobic granule sludge developed at low temperature
Class Methanomicrobia							
Order Methanosarcinales							
Family Methanosarcinaceae							
Genus Methanosarcina	19	x			Uncultured methanogenic archaeon (JN864089)	93	anaerobic bioreactor
	20	xxx	xx	x	Methanosarcina thermophila (AB973357)	99	Deep diatomaceous shale formation
					Uncultured archaeon (KF419191)	99	biogas plant
					Uncultured archaeon (EF210882)	99	thermophilic biogas reactor fed with renewable biomass

As the DGGE profile was analyzed only for *archaea*, the possible presence of homoacetogens (bacteria) could not be determined. However, taking into account that the reactor was fed exclusively with H₂ and CO₂ and the presence of the acetoclastic methanogen *Methanosarcina thermophila* with a decreasing trend throughout the experiment, homoacetogens were presumably present in the process with a potential decreasing trend. Therefore, it seems that hydrogenotrophic methanogens outcompeted homoacetogens and the hydrogenotrophic pathway could be the main one to CH₄ production as the H₂ loading and gas recirculation rates were increased.

Further studies should include the bacterial DGGE profile in order to gain a deeper insight about the whole microbial community populating the ex-situ upgrading reactor, not only to verify the possible presence of homoacetogens but also to address the possible syntrophic association of bacteria with hydrogenotrophic methanogens.

Shannon-Wiener diversity index showed an increasing trend throughout the experiment (Figure 30), going from low *archaea* evenness and richness in the inoculum (1.6) to an intermediate value of *archaea* richness and evenness in the sample from stage VI (2.4). This is the result of the adaptation of the unspecific anaerobic sludge to H₂ and CO₂ performed in the experiment which led to the development of an acclimated population for the production of biomethane and the initial scarce *archaea* population present in the thermophilic anaerobic sludge used as inoculum.

The samples from stage III and VI presented lower similarity index of *archaea* compared to the inoculum (46.5% and 50.1%, respectively), which can be linked with the development of a hydrogenotrophic community from a conventional thermophilic sludge with the new H₂ and CO₂ substrates. Regarding the samples from the different stages with increasing H₂ loading and gas recirculation rates, the similarity index was not so different (83.9%).

Further studies should obtain samples from each stage of the upgrading experiment in order to study the evolution of the microbial population of the reactor depending on the operating conditions.

4.3.5 Application of the MBR for biogas upgrading

The biomethane concentration in upgraded biogas was simulated by assuming that the MBR studied here were employed for the upgrading of biogas under the following conditions:

- $k_L a_{H_2}$ values at similar volumetric flow rates through the membrane are the same when feeds of biogas and H_2 , and of pure CO_2 and H_2 are fed, since $k_L a$ is not dependent on the concentration of each compound.
- $Q_{IN} + Q_R$ must fall within the range of studied rates so that the $k_L a_{H_2}$ values can be calculated with Eq. 34 ($Q_{IN} + Q_R < 6.6 \text{ m}^3/\text{d}$).
- f_X is the same for biogas feed because the additional CH_4 supplied to the system will not alter the microbial activity (the concentration of dissolved CH_4 is that corresponding to the equilibrium in both cases).
- The CO_2 rate supplied as biogas and the H_2 rate are the same than those in stage VI of the experiment (the maximum H_2 loading rate that could be applied while achieving a 95% bioconversion efficiency of H_2).

The simulation was carried out using the mass balance equations for gas (Eq. 25 and Eq. 26) and liquid phases (Eq. 31 and Eq. 33), where the unknown variables are $\dot{m}_{CH_4,OUT}$ and $c_{H_2,OUT}$. f_X employed was 0.07, the average value found in the experiment after day 60 and $k_L a_{H_2}$ was calculated with Eq. 34.

The volumetric flow rates of biogas that could be upgraded with an equivalent CO_2 content to that of stage VI were 20 L/L_R·d (50/50 CH_4/CO_2), 25 L/L_R·d (60/40) and 34 L/L_R·d (70/30). The final CH_4 concentration as a function of recirculation to feed ratio was represented in Figure 31. Ratios between 1.75 and 2.25 were required to reach a 95% v. concentration of CH_4 and this was the maximum concentration achievable to comply with the previous second condition. However, this upgraded biogas fulfills the requirements for grid injection or for utilization as vehicle fuel in most European countries according to Petersson et al. (2007).

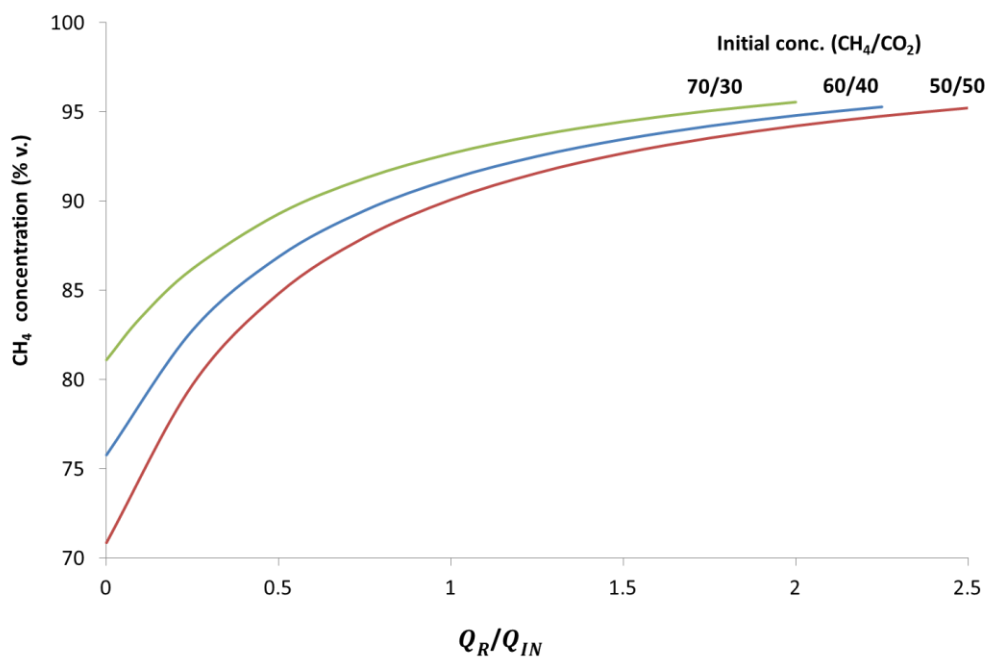


Figure 31. Simulation of the final CH₄ concentration in upgraded biogas for equivalent CO₂ rates to those of the study.

4.4 CONCLUSIONS

The bioconversion of H₂ and CO₂ to CH₄ was feasible at a maximum H₂ loading rate of 40.2 L_{H2}/L_R·d while achieving 95% efficiency in H₂ utilization and CH₄ yield of 0.22 L_{CH4}/L_{H2}, reaching a final concentration of biomethane of 76% and a CH₄ production rate of 8.84 L_{CH4}/L_R·d.

Gas sparging through the membrane resulted in a large capacity of H₂ mass transfer in the range of high-speeds-stirring lab-scale bioreactors. H₂ mass transfer to the liquid phase was identified as the limiting step for the conversion, and $k_L a$ values of 430 h⁻¹ were reached in the bioreactor by sparging gas through the membrane module.

The adaptation of an unspecific anaerobic sludge to H₂ and CO₂ led to the development of an acclimated population for the production of biomethane. *Methanothermobacter tenebrarum* and *Methanothermobacter thermoautotrophicus* were the hydrogenotrophic *archaea* found during the experiment.

The presence of the acetoclastic *Methanosarcina thermophila* was decreased notably throughout the experiment, suggesting that hydrogenotrophic methanogens outcompeted homoacetogens.

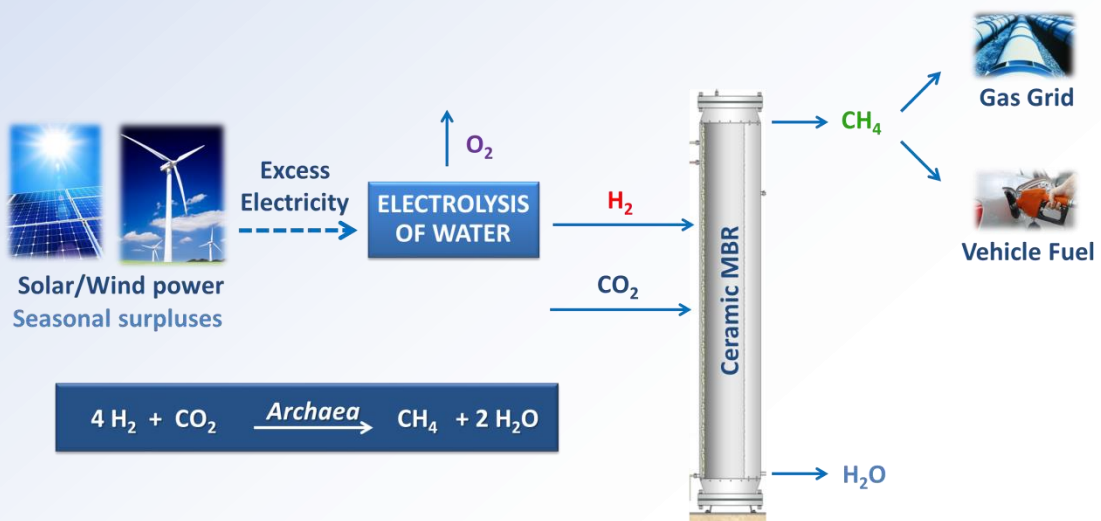
Methanogens showed higher ratios of conversion when the H₂ loading rate was increased, which entails a technological advantage when developing an efficient methanogenic population during the start-up, at low H₂ loading rates, while increasing energy conservation at high H₂ loading rates.

A simulation showed that the bioreactor could upgrade biogas at a rate of 25 L/L_R·d, increasing the CH₄ concentration from 60% to 95%.

Hence, this proof-of-concept study verified that a polymeric membrane can be employed to transfer H₂ at a high rate, allowing the biological conversion to take place satisfactorily.

Chapter 5

Evaluation of process performance, energy consumption and microbiota characterization in a ceramic membrane bioreactor for ex-situ biomethanation of H_2 and CO_2



5.1 INTRODUCTION

Polymeric membranes as the hollow-fiber experienced previously in Chapter 4 have a temperature work range up to 40 ° C (Suez Water Technologies – GE, 2014) so in a long-term they can produce operating problems being damaged on account of thermophilic conditions.

However, ceramic membrane modules are able to work with high temperatures up to 90 ° C (Atech Innovations, 2014). Therefore, from an industrial point of view, the working temperature challenge present in polymeric membranes can be solved with the use of ceramic MBRs allowing the biological conversion of H₂ and CO₂ into CH₄ to take place satisfactorily in a long-term.

The utilization of a ceramic membrane bioreactor to convert H₂ and CO₂ to biomethane to overcome the limitations to mass transfer of H₂ and the long-term operability was evaluated in this study. In addition, higher scale than which was used in previous studies of literature was experienced moving towards industrial scale. The ceramic membrane module was employed to create a large gas sparging surface and the feasibility of the technology was assessed. Total energy requirements for the upgrading process were determined. Dynamics of the microbial community were studied using molecular biology tools.

5.2 MATERIALS AND METHODS

5.2.1 Pilot Plant

The description of the pilot plant used in the experiment has been performed in Chapter 3, section 3.1.1.2. As previously mentioned, it was a ceramic membrane bioreactor with a working volume of 60 L with gas recirculation.

5.2.2 Operating conditions

Anaerobic sludge from a thermophilic anaerobic digester at the laboratory treating activated sludge from the WWTP of Valladolid (Spain) was used to inoculate the reactor in a total amount of 60 L. A set-up period was performed at thermophilic conditions by supplying H_2 and CO_2 in a ratio of 4:1 (according to the stoichiometric values of Eq. 1) at a H_2 loading rate of $5.0 L_{H_2}/L_R \cdot d$ with a gas recirculation rate of $192 L/L_R \cdot d$ for 30 d (all values expressed at $55^\circ C$ and 1 atm).

Afterwards, the experiment started maintaining thermophilic conditions in which a range between 10 and $30 L_{H_2}/L_R \cdot d$ was studied in four stages according to Table 12 with the objective of determining the maximum H_2 loading rate that could be applied with a 95% conversion efficiency for methane. In order to evaluate reactor performance and mass transfer conditions, different gas recirculation rates were applied in some stages.

Table 12. Operating conditions studied during the experiment.

	Stage 1	Stage 2		Stage 3
		2a	2b	
t (d)	0	26	86	137
H_2 loading rate ($L_{H_2}/L_R \cdot d$)	10	20	20	30
Gas recirculation rate ($L/L_R \cdot d$)	192	192	295.2	295.2

Nutrients required for microbial activity and a phosphate buffer solution were supplied when the concentration of NH_4^+ and PO_4^{3-} fell below 500 mg/L, macronutrients and micronutrients were added too. The macronutrient solution was prepared like the stock solution A reported in Angelidaki and Sanders (2004), while the micronutrients solution was a version that was modified (by adding 500 mg/L of resazurine) from the trace-metal solution also from Angelidaki and Sanders (2004).

Both solutions were used during the set-up period and stages 1-2a every 20 days approximately and the centrate wastewater from the centrifugation of anaerobically digested mixed sludge of the wastewater treatment plant of Valladolid (Spain) was used as nutrient solution during stages 2b-3 at a flow of 143 mL/d with a HRT of 420 d. The phosphate buffer solution was prepared with $K_2HPO_4 \cdot 3H_2O$ and KH_2PO_4 to a final pH of 7.4.

5.2.3 Monitoring and experimental analysis

The following parameters (Table 13) were monitored and analyzed during the experiment according to the materials and methods described in Chapter 3, section 3.3.:

Table 13. Parameters monitored and analyzed during the study.

Parameter	Measuring frequency
Headspace pressure Temperature	Continuous mode
Gas production rate Gas composition Liquid effluent	Daily
VFA concentration pH TSS/VSS NH ₄ ⁺	Weekly

5.2.4 Calculations

Calculations about efficiency of H₂ utilization (η_{H_2}), CH₄ yield (Y_{CH_4}), mass flow rate of H₂ transferred from gas to liquid phase ($\dot{m}_{H_2,G \rightarrow L}$), effluent mass flow rate of CH₄ gas as equivalent H₂ ($(\dot{m}_{CH_4,OUT})_{H_2eq}$), $k_L a_{H_2}$ and $k_L a_{CO_2}$ values, maximum specific utilization rate (U) and fraction of H₂ employed for methanogen growth (f_x) have been performed following the calculations described in Chapter 3, section 3.5.

To calculate the energy consumption of the system when upgrading biogas (CH₄/CO₂, 60%/40% v), a steady-state energy balance was performed according to the scheme shown in Figure 32.

The reference state is chosen to be $T_0 = 25$ °C and $P_0 = 1$ atm. The power (kW) required for gas compression (W_1 and W_2) was determined with Eq.35 (Perry et al., 1999):

$$W = 2.78 \cdot 10^{-4} \dot{V} P_1 \ln \frac{P_2}{P_1} \quad (\text{Eq. 35})$$

where \dot{V} is the volumetric flow rate of the stream (m³/s) and P_1 and P_2 the absolute inlet pressure and absolute discharge pressure (kPa) respectively.

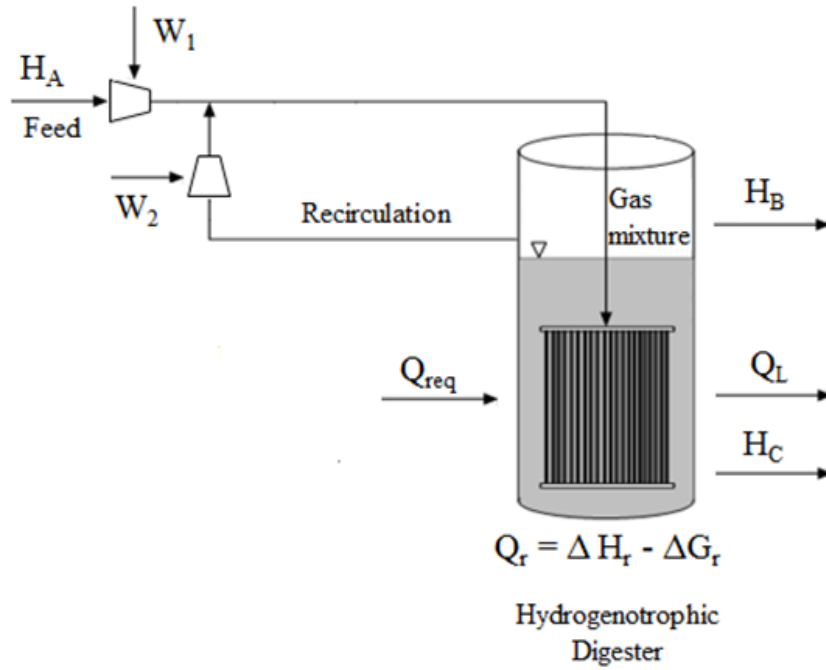


Figure 32. Diagram of the energy streams.

H_i (kW), the specific enthalpy of the stream i , is given by Eq. 36:

$$H_i = \dot{m}_i \cdot C_{p_i} (T_i - T_0) \quad (\text{Eq. 36})$$

where \dot{m}_i is the mass flow rate (kg/s) of stream i , C_{p_i} the specific heat (kJ/kg·K) of stream i , and T_i the temperature (K) of the stream. The values of C_p for the substances involved are 14.3, 0.8, 2.2, 2.08 and 4.184 kJ/kg·K for H_2 , CO_2 , CH_4 , H_2O vapor and H_2O liquid correspondingly (NIST Chemistry WebBook, NIST Standard Reference Database Number 69).

Heat losses in the vessel (Q_L) are defined by Eq. 37:

$$Q_L = U \cdot A (T_{IN} - T_{OUT}) \quad (\text{Eq. 37})$$

where U is the global heat transfer coefficient ($0.5 \cdot 10^{-3}$ kW/m²·K), A the specific heat transfer surface (m²) considering a 10 m length column (the diameter was adjusted to mass flow rate to fit a loading rate of 30 L_{H₂}/L_R·d), T_{IN} the temperature inside the vessel (328 K) and T_{OUT} the minimum ambient temperature (273K).

The heat rate (Q_r , kW) released by the biological reaction was approximated by Eq. 38, assuming that free enthalpy (ΔG_R^0) is the amount of enthalpy that can be employed by microorganisms (Madigan and Brock, 2009):

$$Q_r = 0.88 \frac{\dot{n}_{H_2}}{4} (\Delta H_R^0 - \Delta G_R^0) \quad (\text{Eq. 38})$$

where 0.88 is the efficiency of substrate conversion to CH_4 , \dot{n}_{H_2} is molar flow rate of H_2 supplied (mol/s), 4 the stoichiometric coefficient for H_2 in Eq. 1, and ΔH_R^0 and ΔG_R^0 the enthalpy and Gibbs free energy variations in Eq. 1, -165.0 and -113.6 kJ/mol correspondingly.

Then, the total energy consumption (kW) of the system shown in Figure 32 can be calculated as (Eq. 39):

$$\text{Total Energy consumption} = (H_A + H_B + H_C + Q_L + Q_r) + (W_1 + W_2) \quad (\text{Eq. 39})$$

where the terms within the first parenthesis correspond to enthalpy/heat rates and W_1 and W_2 the amount of work required for compressors.

5.2.5 Microbial analysis

In order to evaluate the evolution of the population during the experiment, samples during the different stages were collected and extraction of genomic DNA, PCR, DGGE and FISH analysis were performed according to the materials and methods described in Chapter 3, sections 3.4.1., 3.4.2. and 3.4.3.

Sequences were deposited in GenBank Data Library under accession numbers MG692444-MG692471 (*archaea*) and MG692472-MG692496 (*bacteria*).

5.3 RESULTS AND DISCUSSION

5.3.1 Conversion of H_2 and CO_2 to CH_4

Biomass adaptation to the substrate took place during the set-up period when the feed mass flow rate of H_2 gas ($\dot{m}_{H_2,IN}$) was 25.2 g/d (H_2 loading rate of 5.0 $L_{H_2}/L_R \cdot d$) and

gas recirculation rate 192 L/L_R·d. A large part of the H₂ fed in these first days was transferred to the liquid phase and consumed but was not employed for CH₄ production, probably due to biomass adaptation to the substrate.

Then, first stage started with a $\dot{m}_{H_2,IN}$ of 49.9 g/d (Figure 33) and the same gas recirculation rate than set-up period. The mass balance performed to the gas phase showed that the average η_{H_2} was 95% and an average Y_{CH_4} of 0.18 L_{CH₄}/L_{H₂} was observed. $\dot{m}_{H_2,G \rightarrow L}$ obtained was 44.6 g/d and $(\dot{m}_{CH_4,OUT})_{H_2eq}$ according to Eq. 1 in average of 35.0 g/d. An average 69% CH₄ content was found in the output gas.

On day 26, $\dot{m}_{H_2,IN}$ was raised to 99.9 g/d (Figure 33) while gas recirculation rate was maintained at 192 L/L_R·d (stage 2a). The increase in the mass flow rate provoked a slightly decrease in average η_{H_2} until 85.7% thus indicating that mass transfer conditions were still acceptable even when the H₂ loading rate was doubled. However, the average Y_{CH_4} obtained was slightly higher than in the previous stage, 0.19 L_{CH₄}/L_{H₂}. The difference between $\dot{m}_{H_2,G \rightarrow L}$ and $(\dot{m}_{CH_4,OUT})_{H_2eq}$ was almost exactly the same in stage 1 and stage 2a and the values obtained were 82.2 g/d and 72.5 g/d, respectively (Figure 33) and CH₄ concentration in the output gas was on average 57%.

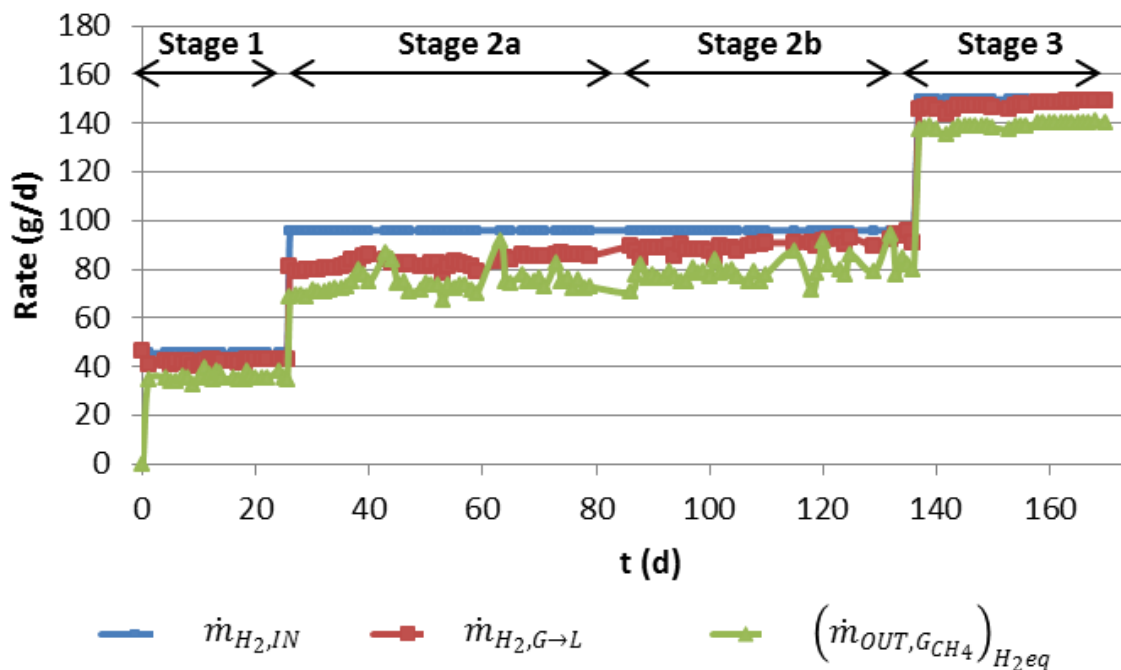


Figure 33. Bioconversion performance during the experiment.

Gas recirculation rate was increased to 295.2 L/L_R·d with the purpose of raising η_{H_2} and the stage 2b started. Under this conditions, the performance of the MBR improve significantly, reaching an average η_{H_2} value of 95% and Y_{CH_4} reached of 0.21 L_{CH₄}/L_{H₂}, the highest obtained up to then. In this case, $\dot{m}_{H_2,G \rightarrow L}$ observed was 89.2 g/d and 80.1 g/d of $(\dot{m}_{CH_4,OUT})_{H_2eq}$. The difference between them was in the same order of magnitude than the others (Figure 33). This values were somewhat higher than the ones obtained in stage 2a, thus indicating that recirculation improved the amount of H₂ transferred from gas to liquid phase, the amount of CH₄ produced and the CH₄ concentration in the output gas (73%).

Due to the high gas recirculation rate used in this stage, some foaming appeared in the reactor. This foaming disappeared naturally (without the use of antifoaming agents) after some weeks of the increase in the gas recirculation rate.

At this point, $\dot{m}_{H_2,IN}$ was augmented to 149.8 g/d in combination with a maintained gas recirculation rate of 295.2 L/L_R·d (stage 3). During this stage, η_{H_2} was 95% in average while Y_{CH_4} increased until 0.22 L_{CH₄}/L_{H₂}, much closer to the maximum stoichiometric value of 0.25 L_{CH₄}/L_{H₂}. The same Y_{CH_4} was obtained previously on the similar pilot-scale bioreactor described in Chapter 4. The difference between $\dot{m}_{H_2,G \rightarrow L}$ and $(\dot{m}_{CH_4,OUT})_{H_2eq}$ was lower than in previous stages meaning that *archaea* employed almost all H₂ transferred to produce CH₄ (Figure 33). On average, 81% CH₄ content was observed in the gas.

The MBR successfully transformed at least 95% of the H₂ fed at H₂ loading rate between 10 and 30 L_{H₂}/L_R·d adjusting the gas recirculation rate. This highest H₂ loading rate is similar than that achieved on the similar pilot-scale bioreactor (40 L_{H₂}/L_R·d) with a hollow fiber membrane module described in Chapter 4 and higher than those found in packed column bioreactors (4.5 L_{H₂}/L_R·d) (Burkhardt and Busch, 2013) or CSTR (18 L_{H₂}/L_R·d) (Kim et al., 2013).

Therefore, this membrane module can be employed to transfer H_2 at a high rate, allowing the biological conversion to take place satisfactorily in a long-term which is a challenge to polymeric MBRs because of the operating problems related with the damage on account of thermophilic conditions in the polymeric materials.

5.3.2 MBR mass transfer capacity

The average $k_L a_{H_2}$ values observed during the different stages in the experiment for the total gas flow thorough the membrane and the estimated $k_L a_{CO_2}$ values are shown in Table 14.

Table 14. Average of H_2 and CO_2 $k_L a$ values obtained in the different stages during the experiment.

	Stage 1	Stage 2		Stage 3
		2a	2b	
$k_L a_{H_2} (h^{-1})$	77	87	166	268
$k_L a_{CO_2} (h^{-1})$	54	61	117	190

It should be draw attention to the fact that this maximum $k_L a_{H_2}$ value is similar than those found in bioreactors with traditional gas diffusers (at equivalent gas rates), within the range of CSTR with high agitation speeds as 700 rpm (Kreutzer et al., 2005) and higher than the $k_L a_{H_2}$ value achieved on the similar pilot-scale bioreactor describe in Chapter 4 to the H_2 loading rate of $30 L_{H_2}/L_R \cdot d$.

In general, this is the result of the large sparging area of the membrane module employed, which produces a good gas-liquid mass transfer interfacial area. On the other side, between the two MBRs, this can be explained as a result of the higher pore of ceramic module ($0.8 \mu m$ versus $0.4 \mu m$ of polymeric module) and higher recirculation rate to transfer H_2 .

5.3.3 Biological activity

It is very important the fact that the adaptation of an unspecific anaerobic thermophilic sludge to H_2 and CO_2 was accomplished. As a result, a methanogenic *archaea* population was developed, which was capable of the bioconversion of H_2 and CO_2 into biomethane.

The methane yield of $0.22 L_{CH_4}/L_{H_2}$ is larger than the yields achieved employing specific strains of *M. thermoautotrophicum* (Jee et al., 1988; Peillex et al., 1990: 0.19 and 0.18 L_{CH_4}/L_{H_2} , respectively) or *Methanococcus thermolithotrophicus* (Peillex et al., 1998) at high efficiency of H_2 utilization values.

From an industrial point of view, it can be translated into lower acquisition costs of specific hydrogenotrophic methanogens because an unspecific anaerobic sludge could be used as inoculum.

The maximum average U and the f_x (fraction of H_2 consumed but not transformed to CH_4) are shown in Table 15. The maximum average specific utilization rate obtained was $7.7 g_{COD}/g_{VSS}\cdot d$ within the range of typical design value suggested from methanogens growing on H_2 and CO_2 (Rittman, 2001). At equivalent gas rates, the U obtained with this ceramic membrane bioreactor was always higher than the U value obtained on the similar pilot-scale bioreactor with hollow-fiber module described in Chapter 4.

Table 15. Maximum average specific utilization rate (U) and average fraction of H_2 employed for methanogen growth (f_x) in the different stages during the experiment.

	Stage 1	Stage 2		Stage 3
		2a	2b	
U ($g_{COD}/g_{VSS}\cdot d$)	6.0	7.7	4.7	3.53
f_x	0.22	0.12	0.11	0.09

According to the results shown in Table 15, it could be stated that the highest value of f_x was obtained during the first stage. This fraction has dropped along the experiment, and in the last stage a decrease of more than 50% appeared.

Then, the f_x was higher when mass flow rate of H_2 transferred from the gas to the liquid phase was low and vice versa thus indicating an uncoupling of microbial growth (anabolism) and H_2 conversion to CH_4 (catabolism). In addition, in the first stage of the experiments, the population of *archaea* in the sludge was not likely to be plentiful as a result of the characteristics of conventional sewage sludge about microbial population and the limitation of this sludge in hydrolysis step.

As it was described in the experiment of Chapter 4, this fact took place because at the beginning of the experiment, especially in the set-up period, an important fraction of H_2 was utilized for microbial growth but when the sludge was completely adapted to the gas substrates, only a small fraction of H_2 was used for methanogen growth, almost all H_2 transferred was used to produce CH_4 . At equivalent gas rates, the obtained f_x value with this ceramic MBR was always lower than the value obtained on the similar pilot-scale bioreactor with hollow-fiber membrane module described in Chapter 4.

VFA concentration was very low during the experiment: acetic acid concentration was under 100 mg/L and propionic acid was below 50 mg/L as it was in the experiment described in Chapter 4.

pH was over the experiment between 6.8-7.9 and it was observed that the use of centrate as a nutrient solution helped to balance the pH.

The initial content of SST and SSV in the inoculum was 5.63 and 3.13 g/L, respectively. After the set-up period, these values experienced a high decrease as a consequence of the biomass adaptation to the new substrate. Average total and volatile suspended solids concentration analyzed during the experiment in the several stages of the experiment are shown in Table 16.

Table 16. Average Total Suspended Solids (TSS) and average Volatile Suspended Solids (VSS) in the different stages during the experiment.

	Stage 1	Stage 2		Stage 3
		2a	2b	
TSS (g/L)	0.73	2.0	1.01	1.13
VSS (g/L)	0.44	1.6	0.91	1.02

These values showed an increasing trend from Stage 1 to Stage 2a (Table 16). However, a decrease was produced in stage 2b when the recirculation rate was increase (Table 16). This fact can be explained firstly, as a result of the high turbulence produced on account of the high recirculation rate employed and secondly, because of the appearance of foaming. This recirculation rate generated an obstacle to the growth of microorganisms being a breaking way for their and/or some losses of solids with the foaming. In the stage 3 of the experiment, it was observed a slightly increase in the content of VSS (Table 16).

5.3.4 Consumption of energy

The total energy requirements for the upgrading process are 0.44 kWh per m³ of biogas upgraded (Figure 34).

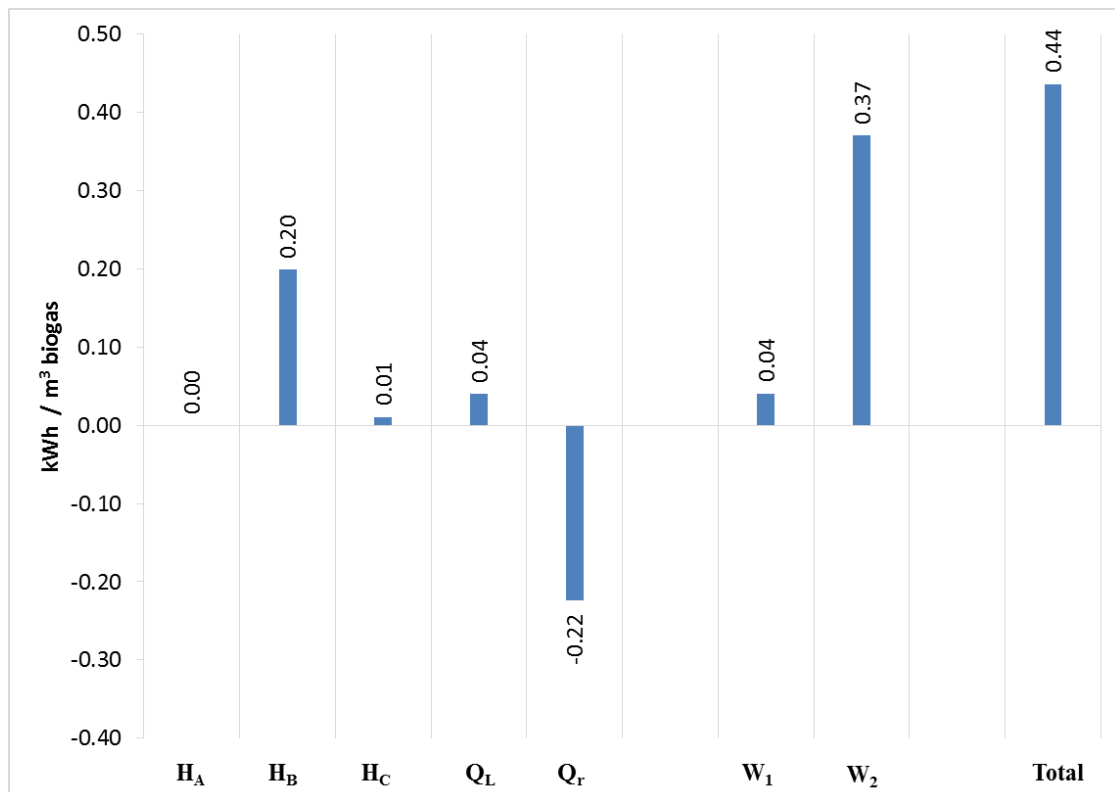


Figure 34. Energy balance of the upgrading process. Energy rates are normalized by the rate of the upgraded biogas.

Energy consumption is dominated by the work required for gas recirculation ($W_2 = 0.37 \text{ kWh/m}^3$ biogas), essential to transfer H_2 to the liquid phase at a high rate, while heat requirements (Q_{req}) are very low (0.025 kWh/m^3 biogas). These energy requirements are larger than those reported for the most used commercial technologies such as pressure-swing adsorption or water scrubbing (Bauer et al. 2013) in the range of $0.20 - 0.30 \text{ kWh per m}^3$ of biogas.

Nonetheless, it should be noted that 0.35 m^3 of new CH_4 can be formed per m^3 of biogas supplied to the system according to the maximum methane yield observed ($0.22 \text{ L}_{\text{CH}_4}/\text{L}_{\text{H}_2}$). Since the enthalpy of combustion of CH_4 is 9.95 kWh/Nm^3 (802 kJ/mol), the equivalent energy stored in new CH_4 would be 3.5 kWh per m^3 of biogas upgraded. Therefore, the total energy requirements represent approximately 13% of the energy that could be obtained from the combustion of new CH_4 formed, hence the energetic benefit of the hydrogenotrophic upgrading process.

From a different angle, the potential energy stored as CH_4 increases from $\sim 6.0 \text{ kWh per m}^3$, in the standard biogas plant (without upgrading) to $\sim 9.5 \text{ kWh per m}^3$ after the upgrading process. When discounted the total energy requirements of the upgrading process (0.44 kWh per m^3 of biogas), it can be observed an increase of $\sim 50\%$ in potential energy generation from CH_4 .

In this context, it is always worth mentioning that water electrolysis to produce H_2 for the upgrading process requires 7.2 kWh per m^3 of biogas, hence employing excess electricity production from wind and solar power, when they are in surplus, is a must in order that hydrogenotrophic upgrading can be applied. During these seasonal surpluses, the H_2 and CO_2 bioconversion processes, such as the studied, will be energetically beneficiaries.

Total energy consumption is slightly higher than the equivalent calculated for hollow-fiber membrane module of Chapter 4, 0.3 kWh per m^3 of biogas, as a result of the higher pressure drop within the ceramic module. Conversely, ceramic membranes are more resistant, long-lasting and easy cleaned than polymeric though its high economic cost. Additionally, ceramic membrane modules can withstand higher rates than hollow-fiber modules because a higher pressure can be applied for gas sparging.

5.3.5 Microbial community

From the archaeal DGGE gel (Figure 35 a), 28 bands were sequenced. According to the RDP classifier (confidence threshold of 50%), all of them belonged to the *Euryarchaeota* phyla and they were ascribed to two classes, almost all to *Methanobacteria* (band 1-27) and only one band to *Methanomicrobia* (band 28) (Table 17). The BLAST search tool provided consistent results with those given by the RDP classifier. *Methanothermobacter*, *Methanobacterium* and *Methanobrevibacter* were the three genus assigned to *Methanobacteria* class and *Methanosarcina* genus to *Methanomicrobia* class (Table 17).

After the biomass adaptation to the substrate during the set-up period, some new *archaea* appeared and were present since then (Figure 35 a): band 14, 22 and 26 corresponding with three uncultured archaeon (KJ209721 and KF630660) with an identity of 100% and 99%, respectively (Table 17). Other new appeared *archaea* (bands 2,5,9,11,15,17, 20 and 24) were present only in some stages but not in all of them (Figure 35 a). However, as a result of the set-up period, some *archaea* disappeared but later they appeared again and were present during the different stages of the experiment (band 6, 10, 25 and 28) and other disappeared completely (band 27) (Figure 35 a).

As is shown in Figure 35 a and Table 17, *Methanothermobacter thermautotrophicus* was the *archaea* found with high level of similarity in all the stages of the experiment after the initial acclimation to H₂ and CO₂. This *archaea* was used previously in pure culture studies as in Peillex et al. 1990.

From the bacterial DGGE gel (Figure 35 b) and according to the RDP classifier (confidence threshold of 50%), 25 bands belonging to three different phyla were sequenced: *Firmicutes* (band 1-18), *Proteobacteria* (band 19-23) and *Actinobacteria* (band 24) while one band remained unclassified (band 25) (Table 18). In general, the BLAST search tool provided consistent results with those given by the RDP classifier.

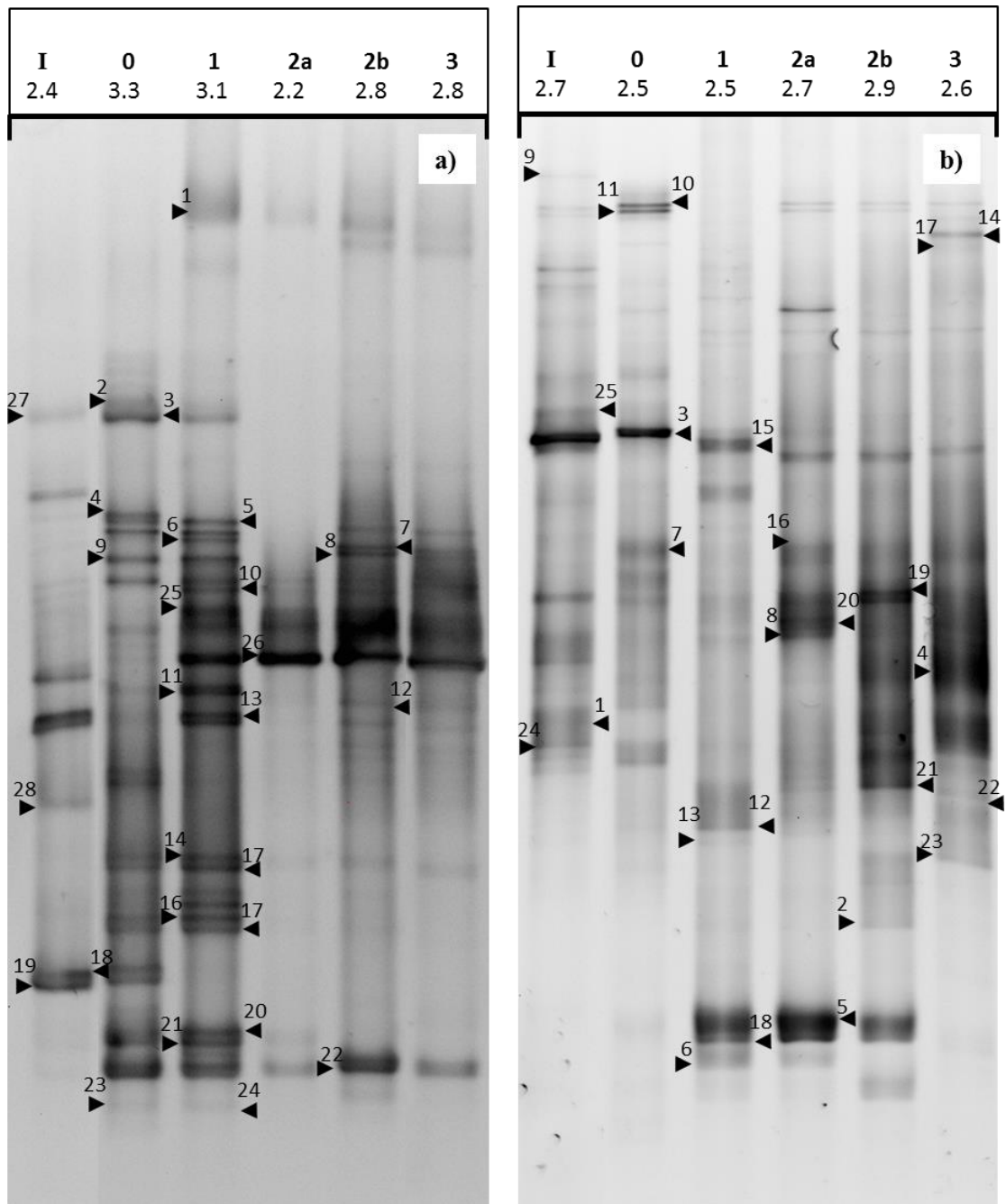


Figure 35. a) Archaeal DGGE profiles and **b)** Bacterial DGGE profiles of the 16S rRNA amplicons of the samples with their respective diversity indices.

Samples: Inoculum (I), set-up period (0) and stages 1-3 (1, 2a, 2b and 3).

Firmicutes was the predominant phylum with seven different genera. Two genera were assigned to *Proteobacteria* phylum and unclassified bacteria to *Actinobacteria* phylum.

After the biomass adaptation to the substrate during the set-up period, some new bacteria appeared and were present during the whole experiment (band 7, uncultured bacterium JF417907, (Table 18), others disappeared but they were founded again in other stages (band 1, 8 and 16, all of them uncultured bacterium) and other ones were maintained (bands 4, 10 and 11) (Figure 35 b).

From the *Proteobacteria* Phylum, the Blast search tool assigned the DGGE band 21 to the genus *Tepidiphilus* with an identity of 100%, which was appeared after the set-up period and maintained during the different stages of the experiment (Table 18). Although *Tepidiphilus thermophilus* could be a potential homoacetogen, acetoclastic methanogens (*Methanosarcina*) were not present in most of experiment stages (Table 17) and there was no VFA accumulation. Therefore, hydrogenotrophic pathway seems to be the main one to CH₄ production.

A moderately high *archaea* richness and evenness was found with Shannon-Wiener diversity index range between 2.2 and 3.3 having the maximum value after the set-up period of the experiment (Figure 35 a). The diversity index calculated from the bacterial DGGE gel were in the range of 2.5 to 2.9 showing a moderate bacterial richness and evenness (Figure 35 b).

The samples presented lower similarity index of *archaea* during the experiment in comparison with the inoculum (similarity index values between 12.5% and 27.3%), which can be linked with the development of a hydrogenotrophic community from a conventional thermophilic sludge with the new substrates (H₂ and CO₂).

After the set-up period and during the different stages with several H₂ loading rates, the similarity index was not so different (61.7% - 69.6%) even when the recirculation rate was increased in stage 2b.

Table 17. RDP classification of the archaeal DGGE bands sequenced with a 50% of confidence level, and corresponding matches according to the BLAST search tool, with their similarity percentages, and environments from which they were retrieved.

Intensity < 35 = x, 35 ≤ intensity ≤ 80 = xx, intensity > 80 = xxx. Samples: Inoculum (I), set-up period (O) and stages 1-3 (1, 2a, 2b and 3).

Taxonomic placement (50% confidence level)	Band No.	I	O	1	2a	2b	3	Closest relatives in Blast Name (Accession No.)	Similarity (%)	Source of origin
Phylum Euryarchaeota										
Class Methanobacteria										
Order Methanobacteriales										
Family Methanobacteriaceae										
Genus Methanothermobacter										
	1			xx	x	xx	x	Uncultured archaeon (JX853200)	94	Mixed culture fermentation reactor
	2		xx	xx				Uncultured archaeon (HE805060)	96	Anaerobic filter reactor of a thermophilic
								<i>Methanothermobacter tenebrarum</i> (NR_113002)	96	Gas-associated formation water
	3	xx	xxx	xx				<i>Methanothermobacter thermophilus</i> (LT626260)	99	Culture Collection
								<i>Methanothermobacter</i> <i>thermautotrophicus</i> (NR_074260)	99	Culture collection
								<i>Methanothermobacter</i> <i>thermautotrophicus</i> (JQ346751)	99	Culture collection
	4	x	xx					Uncultured archaeon (HE805060)	99	Anaerobic filter reactor of a thermophilic
								Uncultured archaeon (JF417888)	99	Dry thermophilic anaerobic digester
								<i>Methanothermobacter tenebrarum</i> (NR_113002)	99	Gas-associated formation water
	5		xx	xx		xx		<i>Methanothermobacter thermophilus</i> (LT626260)	96	Culture collection
	6	x		xx	x			<i>Methanobacteriaceae</i> archaeon (GU129105)	95	Primary culture of formation water from Gangxi oil bed
	7					xxx	xx	<i>Methanothermobacter</i> <i>thermautotrophicus</i> (NR_042782)	98	Culture collection
								<i>Methanothermobacter wolfeii</i> (LT608329)	98	Biogas sludge
								<i>Methanobacteriaceae</i> archaeon (GU129105)	98	Primary culture of formation water from Gangxi oil bed
	8					xxx	xxx	Uncultured archaeon (KX608586)	98	Anaerobic digester
								Uncultured archaeon (AB923516)	98	Anaerobic digester
								<i>Methanothermobacter wolfeii</i> (NR_040964)	98	Mixture of sewage sludge and river sediment
	9		xx	xxx				<i>Methanothermobacter</i> <i>marburgensis</i> (KU667127)	94	Thermophilic full-scale biogas plant

Table 17. (Continued)

Taxonomic placement (50% confidence level)	Band No.	I	0	1	2a	2b	3	Closest relatives in Blast Name (Accession No.)	Similarity (%)	Source of origin
	10	x		xx	xx	xxx	xxx	<i>Methanothermobacter thermautotrophicus</i> (JQ346751)	96	Culture collection
	11		xx	xxx	x		xx	<i>Methanothermobacter thermophilus</i> (LT626260)	99	Culture collection
								Uncultured <i>Methanothermobacter</i> sp. (KF971873)	99	Thermophilic sludge anaerobic digestion
	12					xx	xx	Uncultured archaeon (FNS47954)	99	Thermophilic biogas reactor
								<i>Methanothermobacter wolfeii</i> (LT608329)	98	Biogas sludge
								Uncultured archaeon (JF417882)	98	Dry thermophilic anaerobic digester
								<i>Methanothermobacter wolfeii</i> (NR_040964)	98	Mixture of sewage sludge and river sediment
	13	xxx	xx	xxx	x	xx	xx	<i>Methanothermobacter thermautotrophicus</i> (JQ346751)	99	Culture collection
								Uncultured <i>Methanothermobacter</i> sp. (KF971873)	99	Thermophilic sludge anaerobic digestion
								<i>Methanothermobacter thermautotrophicus</i> (NR_074260)	99	
	14		xx	xx	x	x	x	Uncultured archaeon (KJ209721)	100	Thermophilic two-phase anaerobic digester of SS-OFMSW
								<i>Methanothermobacter thermautotrophicus</i> (JQ346751)	99	Culture collection
								<i>Methanothermobacter thermautotrophicus</i> (NR_042782)	99	
	15		xx	xx	x		x	<i>Methanothermobacter thermautotrophicus</i> (JQ346751)	99	Culture collection
								Uncultured <i>Methanothermobacter</i> sp. (KF971873)	99	Thermophilic sludge anaerobic digestion
								<i>Methanothermobacter thermautotrophicus</i> (AE000666)	99	
	16	x	xx	xx		x		<i>Methanothermobacter thermautotrophicus</i> (JQ346751)	99	Culture collection
								Uncultured <i>Methanothermobacter</i> sp. (KF971873)	99	Thermophilic sludge anaerobic digestion
								<i>Methanobacteriaceae</i> archaeon (GU129105)	99	Primary culture of formation water from Gangxi oil bed
	17		xx	xx				<i>Methanothermobacter thermautotrophicus</i> (JQ346751)	99	Culture collection
								<i>Methanothermobacter</i> sp. (AP011952)	99	
	18	xxx	xx					Uncultured archaeon (JF417883)	98	Dry thermophilic anaerobic digester
								<i>Methanothermobacter tenebrarum</i> (NR_113002)	99	Gas-associated formation water
								Uncultured archaeon (EF210848)	98	Thermophilic biogas reactor fed with renewable biomass
	19	xx	xx					Uncultured <i>Methanobacteriales</i> (AB721089)	99	Thickened sewage sludge of methane fermentor
								Uncultured archaeon (JF417883)	99	Dry thermophilic anaerobic digester
								<i>Methanothermobacter tenebrarum</i> (NR_113002)	99	Gas-associated formation water

Chapter 5

Taxonomic placement (50% confidence level)	Band No.	I	0	1	2a	2b	3	Closest relatives in Blast Name (Accession No.)	Similarity (%)	Source of origin
	20		xxx	xx	x			<i>Methanobacteriaceae</i> archaeon (GU129105)	99	Primary culture of formation water from Gangxi oil bed
								<i>Methanothermobacter</i> sp. (AP011952)	99	
								<i>Methanothermobacter thermautotrophicus</i> (JQ346751)	99	Culture collection
	21	x	xxx	xxx	x			<i>Methanothermobacter thermautotrophicus</i> (DQ649328)	99	
								<i>Methanothermobacter thermautotrophicus</i> (AY196661)	99	
								Uncultured <i>Methanothermobacter</i> sp. (KF971873)	99	Thermophilic sludge anaerobic digestion
	22	x	xxx	xxx	xx	xxx	xx	Uncultured archaeon (KX608586)	99	Anaerobic digester
								Uncultured archaeon (AB923516)	99	Anaerobic digester
								<i>Methanothermobacter wolfeii</i> (LT608329)	99	Biogas sludge
	23					x		<i>Methanothermobacter wolfeii</i> (LT608329)	99	Biogas sludge
								Uncultured archaeon (LT546356)	99	Anaerobic digester
								Uncultured archaeon (EF210914)	99	Thermophilic biogas reactor fed with renewable biomass
	24		x	x				<i>Methanothermobacter thermautotrophicus</i> (JQ346751)	99	Culture collection
								<i>Methanothermobacter thermautotrophicus</i> (AY196661)	99	
								<i>Methanothermobacter thermautotrophicus</i> (LT626260)	99	
Genus <i>Methanobacterium</i>	25	x		xx	xxx	xxx	xxx	Uncultured archaeon (EF210881)	96	Thermophilic biogas reactor fed with renewable biomass
	26		x	xxx	xxx	xxx	xxx	Uncultured archaeon (KF630660)	99	Effluent liquor from the upflow anaerobic solid state reactor of a thermophilic two-phase two-stage biogas reactor
								Uncultured archaeon (EF210881)	99	Thermophilic biogas reactor fed with renewable biomass
								Uncultured archaeon (FN547934)	99	Thermophilic biogas reactor fed with beet silage
								<i>Methanobacterium formicicum</i> (CP006933)	99	Culture collection
Genus <i>Methanobrevibacter</i>	27	xx						Uncultured archaeon (GQ250588)	98	Thermophilic anaerobic digester
								Uncultured archaeon (EU838593)	98	Biogas-reactor
								<i>Methanobrevibacter acididurans</i> (NR_028779)	96	Anaerobic digester
Class <i>Methanomicrobia</i>										
Order <i>Methanosarcinales</i>										
Family <i>Methanosarcinaceae</i>										
Genus <i>Methanosarcina</i>	28	xx					x	<i>Methanosarcina thermophila</i> (AP017646)	98	Thermophilic anaerobic digester
								Uncultured archaeon (LT546330)	98	Biogas reactor
								<i>Methanosarcina</i> sp. (CP011449)	98	Anaerobic sludge

Table 18. RDP classification of the bacterial DGGE bands sequenced with a 50% of confidence level, and corresponding matches according to the BLAST search tool, with their similarity percentages, and environments from which they were retrieved.

Intensity < 35 = x, 35 ≤ intensity ≤ 80 = xx, intensity > 80 = xxx. Samples: Inoculum (I), set-up period (0) and stages 1-3 (1, 2a, 2b and 3).

Taxonomic placement (50% confidence level)	Band No.	I	0	1	2a	2b	3	Closest relatives in Blast Name (Accession No.)	Similarity (%)	Source of origin
Phylum <i>Firmicutes</i>	1	xx				xxx	xxx	Uncultured <i>Firmicutes</i> (KJ626489)	97	Thermophilic anaerobic sludge
	2			x	x	x		Uncultured <i>Thermoanaerobacteriaceae</i> (AM408563)	99	Thermophilic biohydrogen reactor
	3	xxx	xxx	xx	xx			Uncultured bacterium (AB434895) Uncultured bacterium (AY526502)	99 99	A hyperthermophilic anaerobic glucose degrading reactor Thermophilic anaerobic sludge from a methanol-fed lab scale bioreactor
Class <i>Clostridia</i>	4	xx	xx		x	xxx	xxx	Uncultured <i>Thermoanaerobacteriaceae</i> (AM408563)	99	Thermophilic biohydrogen reactor
	5			xxx	xxx	xxx		Uncultured bacterium (EF559032) Uncultured <i>Thermoanaerobacteriaceae</i> (AM408563)	96 99	Thermophilic anaerobic digester at 55 degrees celsius Thermophilic biohydrogen reactor
	6			xx	xx			Uncultured bacterium (AB221363) Uncultured bacterium (EF559038)	99 94	Thermophilic methanogenic bioreactor Thermophilic anaerobic digester at 55 degrees celsius
Order <i>Clostridiales</i>	7		xx		xx	xx	xxx	Uncultured bacterium (JF417907) Uncultured bacterium (AB299514)	98 98	Dry thermophilic anaerobic digester Thermophilic down-flow anaerobic packed-bed reactor (TDAPR)
	8	xx		x	xxx	xxx	xxx	Uncultured bacterium (KP150726)	98	Thermophilic chicken dung - cow slurry fermentation
Family <i>Lachnospiraceae</i> Genus <i>Hespellia</i>	9	x						Uncultured bacterium (CR933122) Uncultured bacterium (KU649795)	99 99	Evry municipal wastewater treatment plant Anaerobic full-scale reactors
Family <i>Gracilibacteraceae</i> Genus <i>Lutispora</i>	10	x	xxx		xx	x	x	<i>Lutispora thermophila</i> (LN881567)	97	Biogas plant
	11	x	xxx		x	x		Uncultured bacterium (KF990088) <i>Lutispora thermophila</i> (NR_041236)	98 98	Thermophilic anaerobic sludge treated with CH3F Methanogenic bioreactor
Family <i>Clostridiales_incertae_sedis III</i> Genus <i>Thermosediminibacter</i>	12	x	x	xx				Uncultured <i>Firmicutes</i> (KM819479)	99	Thermophilic electromethanogenic bioelectrochemical reactor biocathode
								Uncultured bacterium (EF198040) Anaerobic bacterium (AB232581)	99 99	Anaerobic thermophilic phenol-degrading enrichment Thermophilic anaerobic sludge treating palm oil mill effluent

Table 18. (Continued)

Taxonomic placement (50% confidence level)	Band No.	I	0	1	2a	2b	3	Closest relatives in Blast Name (Accession No.)	Similarity (%)	Source of origin
	13		x	x			xx	Uncultured <i>Fimicutes</i> (KM819479)	100	Thermophilic electromethanogenic bioelectrochemical reactor biocathode
Family <i>Clostridiaceae</i> 1								Uncultured bacterium (EF198040)	100	Anaerobic thermophilic phenol-degrading enrichment
								Anaerobic bacterium (AB232581)	100	Thermophilic anaerobic sludge treating palm oil mill effluent
								Uncultured <i>Thermoanaerobacterales</i> (EU638462)	97	Thermophilic microbial fuel cell control experiment with no acetate added
Genus <i>Oxobacter</i>	14						xx	Uncultured bacterium (KT798023)	99	Anaerobic reactor inoculated with sludge coming from a mesophilic WWTP anaerobic reactor
								Uncultured bacterium (AB220004)	98	Thermophilic Biofilm-based Reactor
Family <i>Ruminococcaceae</i>	15	xxx		xxx				<i>Oxobacter pfennigii</i> (NR_117689)	97	Rumen of cattle
Genus <i>Clostridium</i> III	16	x			xx			Uncultured bacterium (KM373124)	97	Hypermesophilic bioreactor
								Uncultured bacterium (KU652381)	99	Anaerobic full-scale reactors
								Uncultured bacterium (AM947536)	99	Anaerobically digested sludge
								Uncultured bacterium (KC493214)	99	Anaerobic thermophilic digester
Order <i>Thermoanaerobacterales</i>										
Family <i>Thermoanaerobacteraceae</i>										
Genus <i>Thermoanaerobacter</i>	17		x				x	<i>Thermoanaerobacter pseudethanolicus</i> (NR_121591)	93	Microbial mat
Genus <i>Thermoanaeromonas</i>	18			xxx	xxx	xx		Uncultured bacterium (KC493214)	94	High-temperature oil reservoir
Phylum Proteobacteria										
Class <i>Gamma</i> proteobacteria	19				xxx	xx		<i>Aeromonas</i> sp. (KR029256)	96	Bioaerosol emitted from wastewater treatment plant
Order <i>Pseudomonadales</i>										
Family <i>Pseudomonadaceae</i>										
Genus <i>Serpens</i>	20				xxx	xxx		Uncultured bacterium (GU389887)	99	Anaerobic digester treating feedstock
								<i>Pseudomonas</i> sp. (AY954288)	99	Anaerobic digestive reactor of waste water treatment plant
								Uncultured bacterium (KT251313)	99	Anaerobic full-scale farm reactor treating agricultural wastes
Class <i>Beta</i> proteobacteria										
Order <i>Hydrogenophilales</i>										
Family <i>Hydrogenophilaceae</i>										
Genus <i>Tepidiphilus</i>	21			xx	xx	xxx	xx	<i>Tepidiphilus thermophilus</i> (NR_125572)	100	Hot spring
								Uncultured bacterium (AF280864)	100	Mesophilic and thermophilic bioreactors
								Uncultured bacterium (AYS26504)	100	Thermophilic anaerobic sludge from a methanol-fed lab scale bioreactor
	22			xx			xx	<i>Tepidiphilus succinatimandens</i> (NR_025725)	99	Culture Collection
								Uncultured bacterium (AB374138)	99	A hyperthermophilic anaerobic glucose degrading reactor
	23					x	xx	Uncultured bacterium (KU654922)	99	Anaerobic full-scale reactors
								Uncultured bacterium (KT798020)	99	Anaerobic reactor inoculated with sludge coming from a mesophilic WWTP anaerobic reactor
								<i>Petrobacter succinatimandens</i> (KF000349)	99	Wastewater treatment plant
Phylum Actinobacteria	24	xx	x	x			xxx	Uncultured bacterium (EF559041)	95	Thermophilic anaerobic digester at 55 degrees celsius
Unclassified Bacteria	25	xx	xx					Uncultured bacterium (FN436184)	99	Thermophilic biogas reactor fed with renewable biomass

Archaea and bacteria were detected by FISH in all samples tested (Table 19). FISH micrographs can be found in Figure 36. *Archaea* appear red due to hybridization with the ARCH915 probe (red) while bacteria appear green due to hybridization with the EUB338 I and EUB338 plus probes (green) and DAPI (cyan).

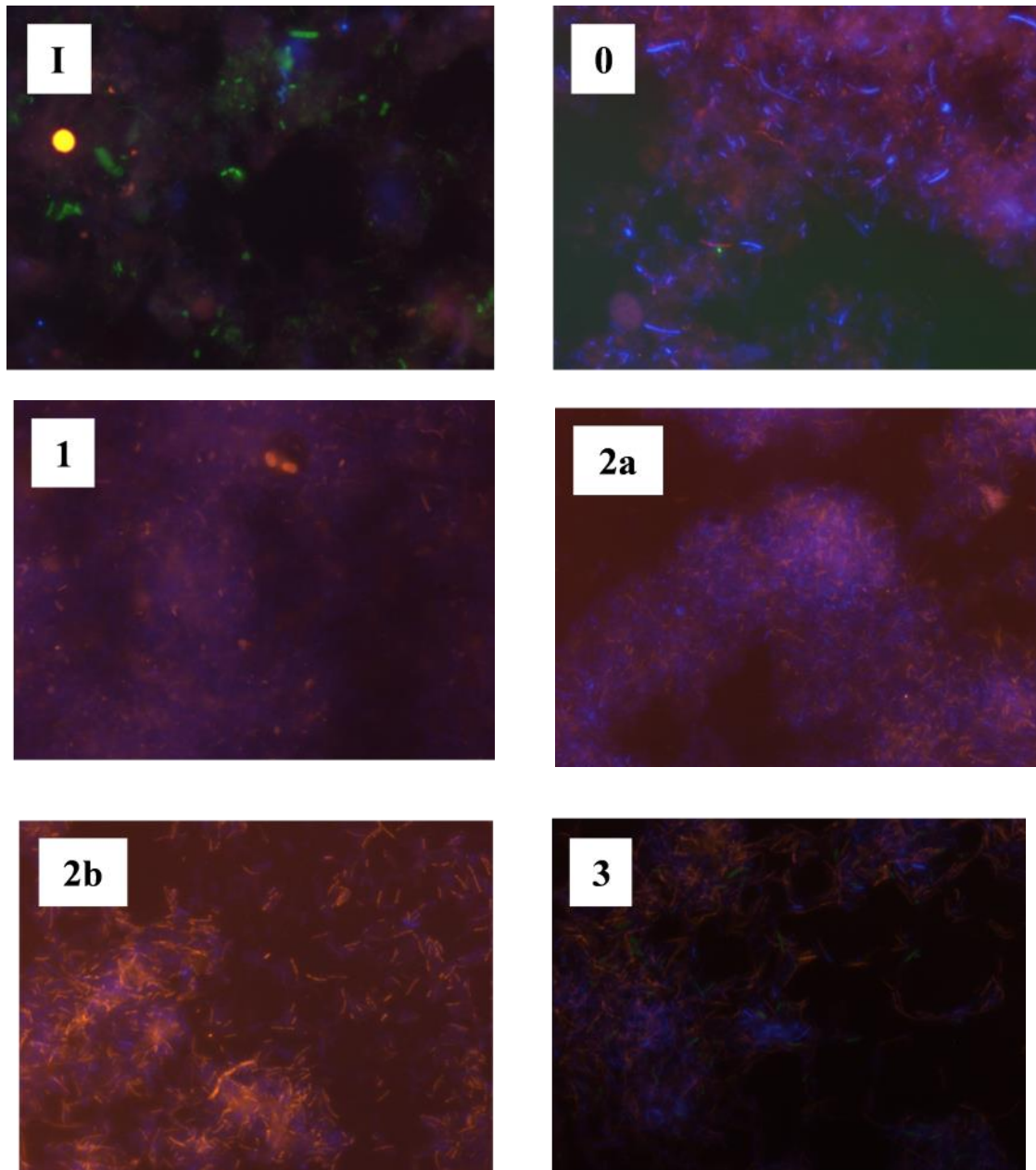


Figure 36. FISH micrographs 100x of *archaea* and bacteria during the experiment. Samples: Inoculum (I), set-up period (0) and stages 1-3 (1, 2a, 2b and 3).

In the inoculum, *archaea* accounted for 25.86% of the microbial population, while bacteria represented 24.47% with *archaea*/bacteria ratio of 51.37%.

Table 19. The abundances of *archaea* and bacteria related to the total biomass and *archaea*/bacteria ratio, in percentages. Samples: Inoculum (I), set-up period (0) and stages 1-3 (1, 2a, 2b and 3).

Sample	<i>Archaea</i> content(%)	Bacteria content (%)	<i>Archaea</i> /bacteria ratio (%)
I	25.86	24.47	51.37
0	1.76	0.015	99.15
1	11.14	0.07	99.37
2a	22.29	0.035	99.84
2b	9.03	0.00	100.00
3	10.70	0.02	99.86

After the set-up period, both *archaea* and bacteria content experienced a high decrease (being almost 0 the % of bacteria content, (Table 19) which can be linked with the decrease in the SSV above mentioned. Although the *archaea* content decreased in this period, the *archaea*/bacteria ratio was 99.15 joining with the acclimation process of the biomass previously explained to the new substrates (H₂ and CO₂) and the development of a methanogenic *archaea* population.

When the H₂ loading rate was augmented to 10 L_{H2}/L_R·d (stage 1) took place an increase in the content of *archaea* in comparison with the previous stage (more than 6 times, (Table 19). When this H₂ loading rate was doubled (stage 2a) the *archaea* content was doubled too (Table 19). However, when an increased in the recirculation rate was performed (stage 2b) with the purpose of raising the efficiency of H₂ utilization, the content of *archaea* decreased (Table 19). This could be explain as a result of the previously mentioned high turbulence produced on account of the high recirculation rate employed which could be an obstacle to the growth of microorganisms or a breaking way for their. The content of *archaea* experienced a slightly increase in stage 3 (Table 19).

All these results are in agreement with the SSV results showed previously. Otherwise, bacteria content had no significative changes since the set-up period (Table 19). As is showed in Table 19, after the acclimation biomass period, *archaea* were predominant against bacteria.

5.4 CONCLUSIONS

The bioconversion of H₂ and CO₂ into biomethane was feasible using an unspecific anaerobic thermophilic sludge as an inoculum after an adaptation period.

The system transformed 95% of H₂ fed at the maximum loading rate of 30 L_{H2}/L_R·d, reaching a final methane content of 81% and a CH₄ production rate of 6.60 L_{CH4}/L_R·d. The highest CH₄ yield found was 0.22 L_{CH4}/L_{H2}, close to the maximum stoichiometric value (0.25 L_{CH4}/L_{H2}) thus indicating that *archaea* employed almost all H₂ transferred to produce CH₄.

Gas sparging through the ceramic membrane showed a high capacity of H₂ mass transfer. $k_L a$ value of 268 h⁻¹ was reached at 30 L_{H2}/L_R·d.

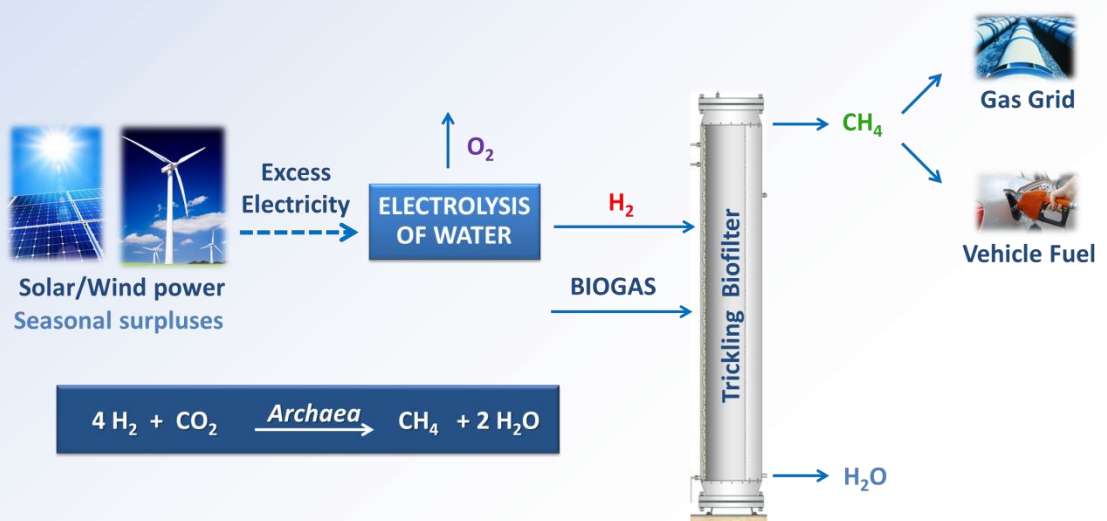
A remarkable *archaea* increase related to the selection-effect of H₂ on community composition over time was revealed by microbial analysis. *Methanothermobacter thermautotrophicus* was the *archaea* found with high level of similarity in all the experiment stages after the initial acclimation to H₂ and CO₂.

When discounted the total energy requirements of the upgrading process (0.44 kWh per m³ of biogas), it can be observed an increase of ~ 50% in potential energy generation from CH₄.

This study verified the successful application of ceramic membrane modules to efficiently transfer H₂ from gas to the liquid phase and the technical feasibility of the bioconversion.

Chapter 6

Process performance and microbial community structure in thermophilic trickling biofilter reactors for ex-situ biogas upgrading



6.1 INTRODUCTION

Considering the implementation of the biological biomethanation concept in industrial demonstration, reactors based on different diffusion systems (such as hollow-fiber membranes, ceramic membranes, stainless steel diffusers or sparger rings), high-speed stirring or gas recirculation would probably result in high parasitic energy needs and operational costs. In addition, diffusion modules are often fragile and/or subject to clogging.

For these reasons, TBF reactors have been proposed for the biomethanation of H₂ and CO₂. In a TBF reactor, the gases are forced through the packed bed either downwards or upwards and the liquid media is trickled and recycled over the packing material to provide moisture and nutrients, forming a thin liquid layer over the biofilm. Therefore, the TBF is composed of a three-phase system: a gas phase nearly filling the entire reactor, a liquid-phase trickling over the biofilm, and the biofilm itself attached to the packed-bed surfaces. The biofilm is composed of a specific arrangement of immobilized cells within a matrix of extracellular polymeric substances. This organization results in symbiotic behaviors that optimize microbial relations (Garrett et al., 2008).

The present study aimed at evaluating the process performance and determining the microbial ecology of thermophilic TBF reactors performing biological methanation of H₂ and CO₂. Progressively reduced gas retention times were applied by increasing the influent gas mixture to assess the stability and effectiveness of the process. Moreover, the gas mixture was injected in the reactors either with the flow or counter-flow to the liquid media to identify potential differences in biomethanation efficiency. Moreover, samples collected from the liquid phase and from the biofilm undergo high throughput 16S rRNA amplicon sequencing to gain a deeper understanding on how is the microbial community structured inside the trickling filter. Linking the microbial ecology information with the outcomes from the reactor monitoring can provide essential information for designing robust anaerobic systems for biological biogas upgrade.

6.2 MATERIALS AND METHODS

6.2.1 Reactors

The description of the reactors used in the experiment has been performed in Chapter 3, section 3.1.2.1. As previously mentioned, the gas mixture in R1 was injected in a counter-flow to the trickling media while the influent gas in R2 was directed with the flow of the recirculating liquid both in a single-pass plug flow operation (without gas recirculation).

6.2.2 Operating conditions

Enriched hydrogenotrophic culture obtained from laboratory biogas upgrading column reactors (Bassani et al., 2017) was used for the initial inoculation of the TBF reactors. The inoculum had a pH of 8.03, the concentration of total solids was 1.6 ± 0.0 % and the concentration of volatile solids was 0.6 ± 0.0 %. The total Kjeldahl nitrogen was measured to be 2.03 ± 0.11 g/L, the ammonia nitrogen equal to 1.63 ± 0.06 g/L and the concentration of volatile fatty acids was 304.8 ± 5.7 mg/L.

During the start-up period, the reactors were inundated for 24 hours with inoculum to enhance the initial microbial adhesion, and thus, biofilm formation (Langer et al., 2014) (Figure 37).



Figure 37. Biofilm formation after the inoculum inundation of the reactors.

Digestate collected from Snertinge biogas plant (Denmark), was used as nutrient source during the whole experimental work. The digestate was incubated at thermophilic conditions for a period of more than three months to ensure total degradation of the organic matter that would result in additional biogas generation inside the reactors influencing the mass balance.

During the experiment, TBF reactors were operated at thermophilic temperature ($54 \pm 1^\circ\text{C}$) and atmospheric pressure.

The feeding gas mixture was synthetically composed of 62% H_2 , 15% CO_2 and 23% CH_4 , replicating a mixture of biogas (about 60% CH_4 and 40% CO_2) and H_2 in stoichiometric proportions according to reaction of Eq. 1.

The experiment using both reactors lasted for a total of 94 d and was divided in four experimental periods (Table 20). During each period, the gas retention time of the reactors was reduced by increasing the H_2 loading rate of the reactors (Table 20).

Table 20. Operating conditions studied during the experiment.

	Period I	Period II	Period III	Period IV
t (d)	0	29	46	53
Gas retention time (h)	14	7	4.2	2.1
H_2 loading rate ($L_{\text{H}_2}/L_{\text{R}}\cdot\text{d}$)	1.1	2.2	3.6	7.2

Experimental operation was progressed from one period to the next one when steady state conditions were achieved (i.e. less than 5% variations of the output-gas composition).

6.2.3 Monitoring and experimental analysis

The following parameters (Table 21) were monitored and analyzed during the experiment according to the materials and methods described in Chapter 3, section 3.3. All measurements were performed in triplicate samples.

Table 21. Parameters monitored and analyzed during the study.

Parameter	Measuring frequency
Headspace pressure Temperature	Continuous mode
Gas production rate	Daily
Gas composition	Three times per week
VFA concentration	Three times per week
pH	Three times per week

pH, VFA, TS, VS, TKN and NH_4^+ were determined according to the materials and methods described in Chapter 3, section 3.3 in order to characterize the inoculum.

6.2.4 Calculations

Calculations about efficiency of H_2 utilization (η_{H_2}), CO_2 conversion efficiency (η_{CO_2}), CH_4 production rate and methane yield (Y_{CH_4}) have been performed following the calculations described in Chapter 3, section 3.5.

6.2.5 Microbial community analysis

At the end of the experiment triplicate samples from the liquid media and from the biofilm (Figure 38) that was created on the surface of the packing material in R2 were collected.



Figure 38. Biofilm created on the surface of the packing material in R2.

Extraction of genomic DNA and 16S rRNA gene sequencing analysis was performed according to the materials and methods described in Chapter 3, sections 3.4.1. and 3.4.4.

Raw reads were deposited in Sequence Read Archive (SRA) database of NCBI under the BioProject PRJNA481013.

6.3 RESULTS AND DISCUSSION

6.3.1 Process performance of trickling biofilter reactors

The TBF reactors achieved an output gas that was fulfilling the standards for substituting natural gas or could be used as transportation fuel in different countries.

The inoculation procedure with enriched hydrogenotrophic media was beneficial for the start-up process in the TBF reactors as it minimized the duration needed for the microbial adaptation. Indeed, the CH₄ content in the output gas after three days of initial operation reached 93%.

In general, it was demonstrated that the biomethanation efficiency of both reactors was similar (Table 22). More specifically, the CH₄ concentration of the upgraded biogas was progressively increasing to up to 4.2 h gas retention time (Period III) having a maximum CH₄ content of approximately 99%. The average CH₄ yield was 0.23-0.24 L_{CH₄}/L_{H₂} throughout the experiment in both reactors, close value to the stoichiometric maximum of 0.25 L_{CH₄}/L_{H₂}.

On average, the CH₄ production rate of the TBF reactors was 0.25 (Period I), 0.50 (Period II) and 0.88 L_{CH₄}/L_R·d (Period III). A further reduction of the gas retention time to almost 2 h led to an increment of the methane productivity to approximately 1.73 L_{CH₄}/L_R·d (Period IV); nevertheless, the quality of the output gas was lowered (i.e. on average 95% CH₄ concentration) (Table 22).

The decreased methane purity was attributed to the fact that the supplied H₂ and CO₂ was utilized for acetate production (homoacetogenesis) instead of methanogenesis.

Indeed, the results from the VFA determination showed that there was a strong accumulation of short chain fatty acids; especially the acetate concentration in R2 increased from 113 mg/L in Period I to 643 mg/L in Period IV (Table 22).

It is known that VFA-degradation requires low hydrogen partial pressure (Fukuzaki et al., 1990). Therefore, the observed VFAs accumulation suggests that the H₂:CO₂ ratio fed to the reactor (4.13:1) was slightly too high, resulting in an excess of H₂ that increased the H₂ partial pressure and hindered the degradation of VFA.

To verify the hypothesis, the gas mixture of R2 during Period IV was temporarily changed with pure nitrogen, and subsequently, the reactor was flushed for a three day period exclusively with nitrogen gas. It was shown that the decreased H₂ pressure led to an immediate degradation of VFA, whose final concentration reached 174 mg/L at the end of the flushed test.

However, once the gas feedstock was restored to the initial composition (i.e. 62% H₂, 15% CO₂ and 23% CH₄) the VFA content returned to the earlier levels. The fast response of the TBF reactors' performance concordantly with the change of gas composition could be attributed to the formation of a well-structured microbial biofilm.

It has been previously reported that the biofilm infrastructure is a key parameter in anaerobic biofilm systems whose high process productivity is depended on interspecies H₂ transfer (Annachhatre, 1996). In fact, at the end of the experiment a thin biofilm was created onto the surface of the packed material from which the microbial population was analyzed.

Another interesting remark extracted from the VFA monitoring was related with the effect of the directional flow gases inside the TBF reactors. It was demonstrated that the injection of the influent gas mixture with the directional flow of the liquid in R2 greatly enhanced acetate production compared to the reactor that the gases were directed counter-flow to the trickling media (R1) (Table 22).

Table 22. Overview of reactors' performance during their steady state operation at each experimental period.

	Period I		Period II		Period III		Period IV	
	R1	R2	R1	R2	R1	R2	R1	R2
CH₄ content (%)	97.3±0.6	97.0±0.1	98.0±0.4	98.1±0.2	98.7±0.3	99.1±0.1	95.1±0.5	94.9±0.6
CH₄ production rate (L_{CH₄}/L_R·d)	0.26±0.03	0.25±0.01	0.50±0.02	0.50±0.00	0.89±0.01	0.88±0.01	1.74±0.01	1.71±0.03
<i>Y</i>_{CH₄} (L_{CH₄}/L_{H₂})	0.24±0.01	0.23±0.00	0.23±0.01	0.23±0.00	0.25±0.00	0.24±0.00	0.24±0.00	0.24±0.00
<i>η</i>_{H₂} (%)	95.3±2.1	97.5±0.6	91.2±4.6	96.8±0.7	99.9±0.1	99.8±0.1	97.2±0.6	96.8±0.4
<i>η</i>_{CO₂} (%)	93.2±1.5	92.5±0.4	94.9±0.9	96.2±0.6	97.5±0.6	98.2±0.5	98.9±0.0	99.9±0.1
pH	8.56±0.18	8.58±0.17	8.60±0.09	8.63±0.11	8.58±0.04	8.59±0.06	8.29±0.03	8.12±0.14
VFA (mg/L)	49±14	132±24	36±2	89±2	65±2	159±41	117±20	759±25
Acetate (mg/L)	41±11	113±23	31±2	70±3	50±5	116±31	87±13	643±7

The down-flow operation could influence the process presumably due to the densities of the different gases passing through the reactor. Indeed, H₂ density is much lower than the ones of CH₄ and CO₂, and a downwards plug flow might involve higher H₂ partial pressure in the liquid, compared to up-flow operation, resulting in the promotion of homoacetogenesis.

Unlike the biomethanation trickle-bed research of Rachbauer et al. (2016), where the pH of the liquid media remained largely at neutral levels, in the present study, a continuous increment of pH was recorded even from the beginning of the experiment (Table 22). The maximum pH value reached 8.63 (R2 in Period II), which is above the optimum threshold for methanogenesis (Kougias and Angelidaki, 2018), and therefore, a pH adjustment was mandatory as countermeasure for maintaining stable pH values.

For this reason, 100 mL of liquid media were neutralized twice per week using HCl 1M and reintroduced in the nutrient glass vessel. The increment of the pH could be attributed to the H₂:CO₂ ratio fed to the reactors, which was slightly higher compared to the stoichiometric equation (i.e. H₂:CO₂ ratio was 4.13:1), resulting in an excess of H₂ that concomitantly reduced the CO₂ partial pressure.

It is known that the CO₂ produced during anaerobic digestion process reacts with the hydroxide ions (OH⁻) within the liquid, forming bicarbonate ions (HCO₃⁻) that increase the buffering capacity of the medium (Schnurer and Jarvis, 2010). However, in the current case the injected H₂ reacted with the CO₂, reducing the CO₂-partial pressure and provoking a loss of buffering capacity.

6.3.2 Microbial community profiles in the liquid media and biofilm

Illumina sequencing generated in total more than a million of raw reads with average length of 254 bp; results are summarized in Table 23. After quality filtering and pair merging, on average 63% of reads were taxonomically assigned to OTUs (Table 23). Rarefaction curves showed that the sequencing depth was adequate enough to cover the sample richness in the sample replicates. Microbial diversity was estimated and results showed 150 OTUs per replicate (on average).

Table 23. Summary of the sequencing data and results.

Sample ID	Sample Description	Raw Reads	Assigned Reads to OTUs	SRA accession IDs
L1	Liquid sample from R2	198594	58195	SAMN09655204
L2	Liquid sample from R2	236364	66295	SAMN09655204
L3	Liquid sample from R2	226410	64031	SAMN09655204
B1	Biofilm from R2	281440	78131	SAMN09655205
B2	Biofilm from R2	247640	68069	SAMN09655205
B3	Biofilm from R2	105686	25345	SAMN09655205

Principal coordinate analysis (PCoA) clearly indicated differences between the two samples, revealing a relative distance in their microbial beta diversity (Figure 39).

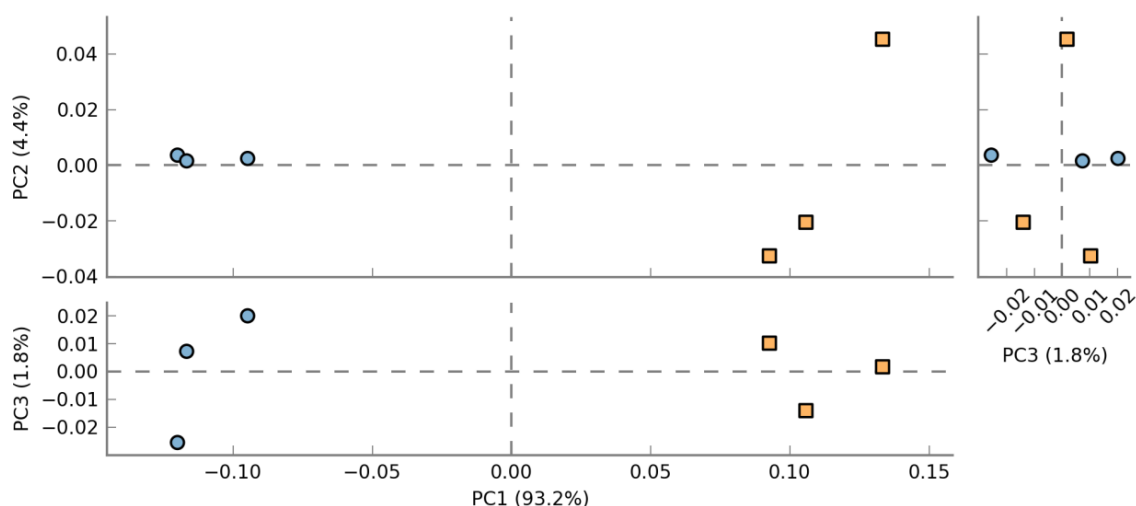


Figure 39. Principal coordinate analysis plot representing variations of the most abundant OTUs based on least squares method. Orange color represents the biofilm samples while blue color designates the liquid media samples.

The replicates from the liquid media sample were all clustered together. One replicate of the biofilm sample showed lower similarity (Figure 39) compared to the other two replicates (which clustered together) most probably due to technical issues (e.g. not homogenized sampling) and mainly influenced by the differences in only 3 abundant OTUs (*Clostridia* sp. 4, *Thermoanaerobacteraceae* sp. 10 and *Tissierella* sp. 11).

However, for the rest of OTUs, the PCoA results were consistent in the three replicates, and thus, all of them were maintained for the analysis.

As shown in Figure 39, two completely different clusters were obtained regarding the samples from the liquid media or from the biofilm.

Considering the most abundant microbes (>0.5% of relative abundance in at least one sample), 29 OTUs covered approximately 90% of the community in the samples.

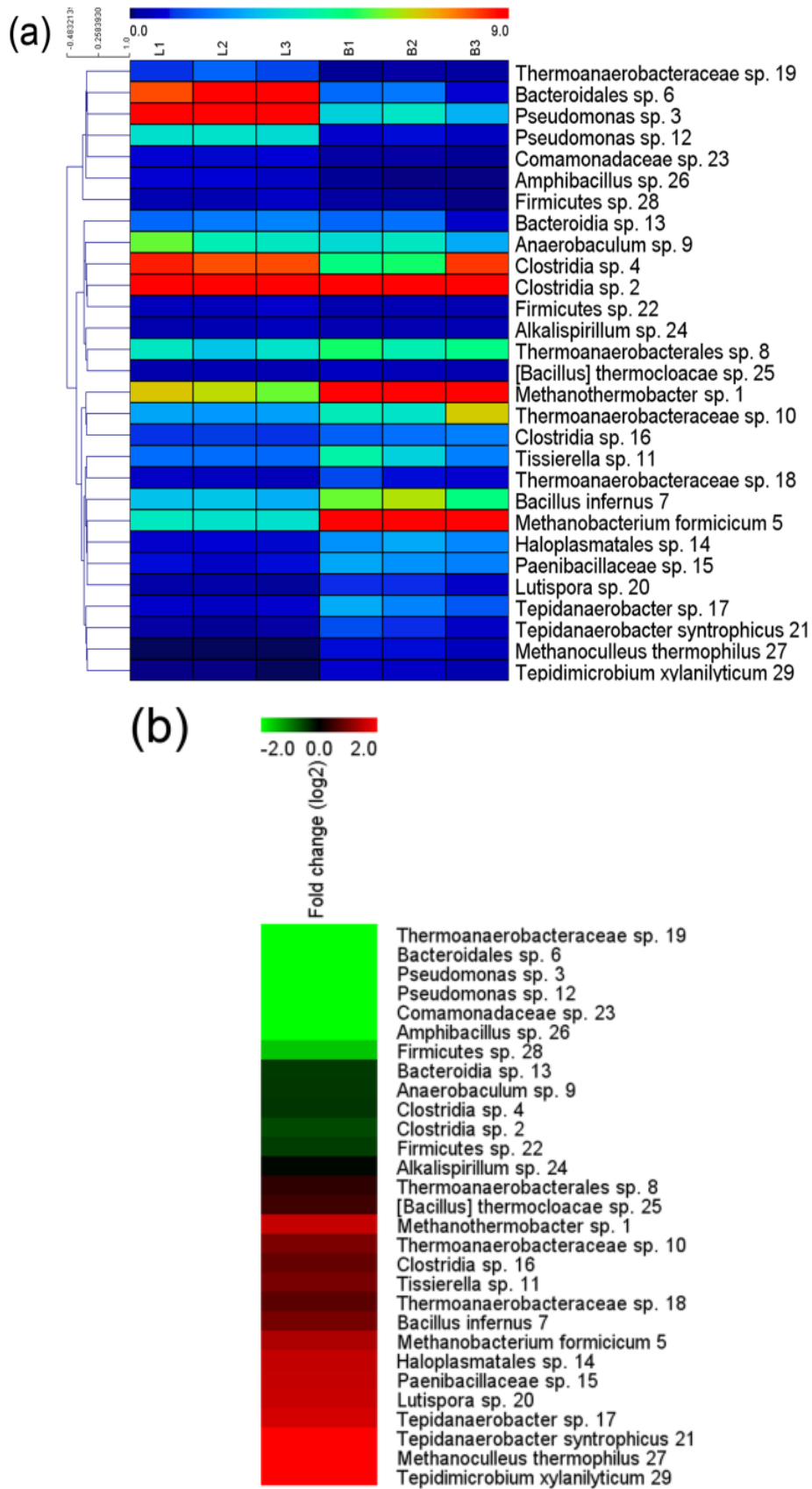
Among the selected OTUs, 8 were assigned at genus level and 6 at species level while the rest of the microbes were assigned only at higher taxonomic levels, suggesting the presence in the microbiome of numerous underexplored or undescribed taxa.

Taxonomic assignment, relative abundance and abundance variation (fold change) of the most abundant OTUs in the samples are reported in Figure 40. Correspondence between colors and relative abundance or fold change is reported in the scale at the top of each panel. Fold change is represented in red and green for increased and decreased OTUs, respectively.

The fold change of OTUs significantly changing in relative abundance is shown in Figure 41. The left part of the panel represents the relative abundance (>0.5%) while the right part shows the fold change of OTUs significantly changing in abundance (differences in mean proportions) as well as the confidence interval associated and the p-value.

Bacterial population covered on average 90% and 70% of the whole microbial community in liquid media and biofilm samples, respectively, whilst *archaea* accounted on average for 10% and 30%, respectively.

Two different communities were obtained as in agreement with the previously discussed PCoA results (Figure 39). In the liquid media samples, the most represented phyla were *Firmicutes* (40%), *Proteobacteria* (22%), *Bacteroidetes* (11%) and *Euryarchaeota* (10%), while the most abundant phyla in the biofilm samples were *Firmicutes* and *Euryarchaeota* (48% and 30%, respectively) with lower abundance of *Proteobacteria* (5%), *Bacteroidetes* (3%).



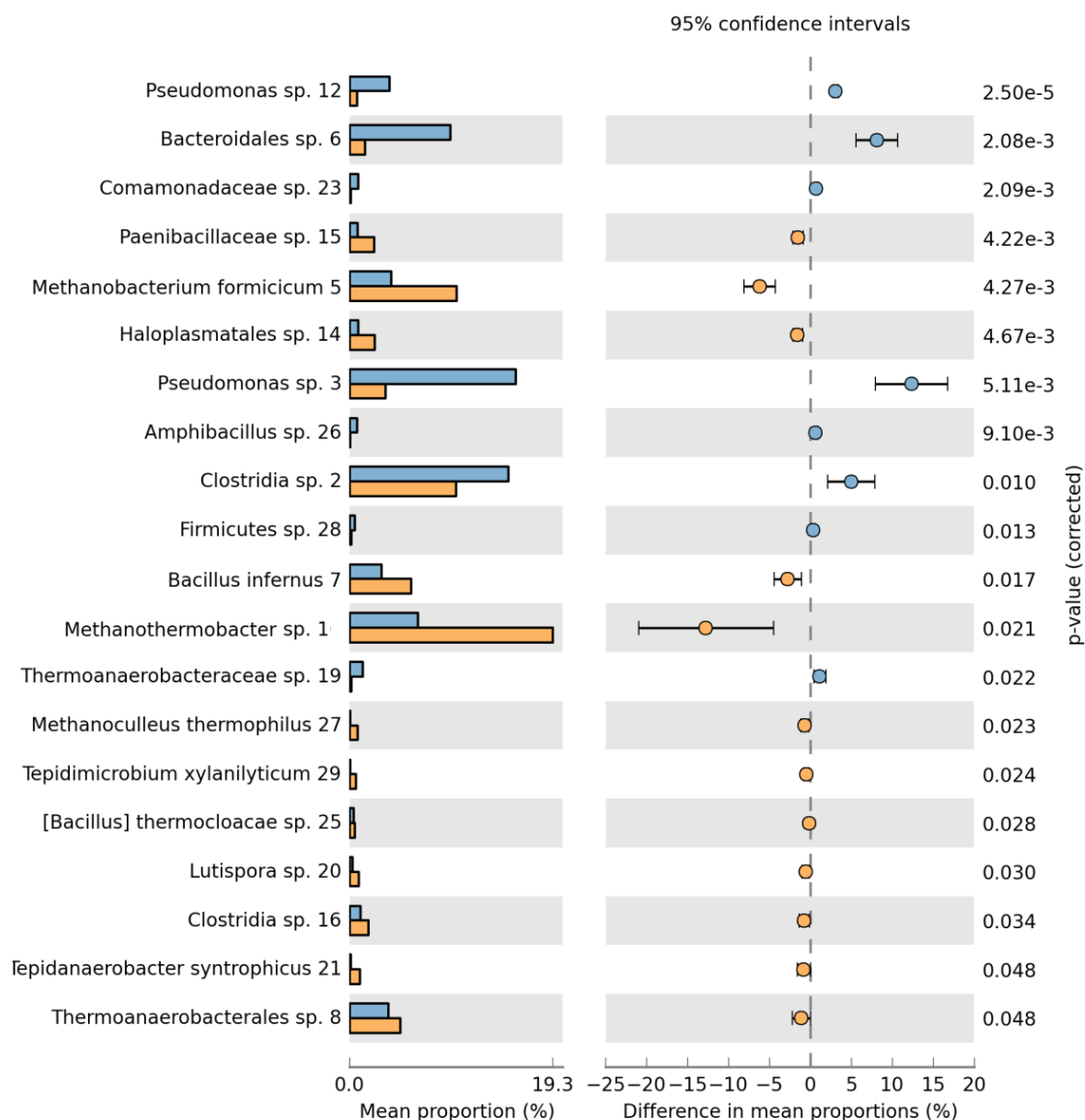


Figure 41. Statistical comparison between sample from the liquid media (blue color) and sample from the biofilm (orange color).

Among the most abundant OTUs, 3 of them were hydrogenotrophic methanogens assigned to *Methanothermobacter* sp. 1, *Methanobacterium formicicum* and *Methanoculleus thermophilus* (100, 97 and 100% similarity, respectively). BLASTn search against NCBI database revealed 100% similarity of *Methanothermobacter* sp. 1 with two microbial species, such as *Methanothermobacter thermautotrophicus* and *Methanothermobacter wolfeii*, indicating that the most abundant methanogen populating the archaeal and total community was represented by a new species.

Interestingly, these microorganisms were enriched in the biofilm compared to liquid media samples (Figure 40). This fact could be explained as a consequence of their higher proximity with the carbon and hydrogen source in the biofilm and/or their possible syntrophic relationship with biofilm forming bacteria.

Notably, *Methanothermobacter* sp. 1 was the most abundant microbe in the biofilm community (19%) followed by *M. formicicum* (10%) (Figure 40). The abundance of this two hydrogenotrophic *archaea* was shown to be statistically higher in the biofilm compared to the liquid media (Figure 41) and their ability to generate biofilms was reported in previous literature.

M. thermautotrophicus was found to be one of the only two microorganisms populating the biofilm formed on top of the diffuser surface of an ex-situ biogas upgrading reactor (bubble column) at thermophilic conditions (Kougias et al. 2017). Moreover, Rademacher et al., (2012) identified the prevalence of this archaeon on a methanogenic biofilm in a thermophilic biogas system (two-phase leach-bed).

In addition, the high abundance of *Methanothermobacter* sp. obtained in the present study in a TBF reactor is in agreement with previous studies which identified dominance of this hydrogenotrophic methanogen genus in biogas upgrading systems at thermophilic conditions in CSTR (Treu et al., 2018; Kougias et al., 2017), bubble columns (Kougias et al., 2017) and up-flow reactors (Bassani et al., 2017).

M. formicicum is known to be able to produce extracellular polysaccharides, which play various roles in structure and functions of biofilm communities (Veiga et al., 1997).

Although *Thermoanaerobacteraceae* sp. 10 was present in the liquid media (2%), its relative abundance was higher in the biofilm (5%) (Figure 40). Members of this family (e.g. *Moorella thermoacetica* and *Thermoanaerobacter kivui*) are known homoacetogenic bacteria using H₂ as electron donor to convert CO₂ into acetate (Pierce et al., 2008; Weghoff and Müller, 2016). The best hit with 91% similarity was a member of *Moorella* genus (*Moorella humiferrea*).

Thus, *Thermoanaerobacteraceae* sp. could be a possible homoacetogen which is in accordance with the high VFA content (mainly acetate) observed in R2 at the sampling moment for the microbial analysis.

Tepidanaerobacter syntrophicus (98% similarity) was found in all microbial communities (Figure 40). Previous studies (Sekiguchi et al., 2006) reported the syntrophic association of this microorganism with the hydrogenotrophic methanogen *M. thermoautotrophicus* and its ability to utilize ethanol, glycerol and lactate syntrophically for growth. Thus, the statistical higher relative abundance of *T. syntrophicus* in the biofilm samples compared to liquid media (Figure 41) was in agreement with the significant higher abundance of its partner *Methanothermobacter* sp. in the biofilm (Figure 40, Figure 41).

Bacillus infernus (100% similarity) was found to be enriched in the biofilm (Figure 40) with statistical relative abundance differences (Figure 41) compared to liquid media. This *B. infernus* richness in the biofilm agrees with the findings reported by Kougias et al. (2017) about higher relative abundance of this microbe in the biofilm compared to the liquid phase obtained in their ex-situ biogas upgrading bubble column reactor experiment at thermophilic conditions. *B. infernus*, a metal-reducing bacterium, is known to create biofilms in order to perform extracellular electron transfer (Badalamenti et al., 2013). In anaerobic digestion systems, the interspecies electron transfer is a fundamental feature between bacteria and *archaea* in order to maintain the redox reactions in sufficiently exergonic levels (Kougias et al., 2016).

Clostridia sp. 2 was the second (15%) and the third (10%) most abundant OTU of the community in liquid media and biofilm samples, respectively. This species was assigned to the recently discovered order MBA08, belonging to *Clostridia* class. BLAST results of this OTU's consensus sequence indicated a high similarity to *Hydrogenispora ethanolica* (90%) and confirmed the relevance of this uncharacterized OTU previously found in other works dealing with biogas upgrading (Bassani et al., 2017; Corbellini et al., 2018; Kougias et al., 2017; Treu et al., 2018).

In addition, Kougias et al. (2017) indicated the existence of a potential syntrophic interaction between the hydrogenotrophic methanogen *M. thermautotrophicus* and *Clostridia* sp. 2 (*H. ethanolica*) because of their concurrent remarkable high abundance. Interestingly, *Clostridia* sp. 2 was present in high abundance in the biofilm and the liquid media, thus suggesting its possible versatile metabolism.

The relative abundance differences of *Pseudomonas* sp. 3 and *Bacteroidales* sp. 6 were statistically higher in the liquid media than in the biofilm as shown in Figure 41. Both microorganisms presented high relative abundance values (16% and 10%, respectively) in the liquid media samples compared to biofilm samples and they were two of the highest abundant microbes in the liquid media (Figure 40).

The richness of *Pseudomonas* sp. in the liquid media compared to the biofilm was in agreement with the findings of Kougias et al. (2017) obtained in the samples from biofilm and liquid phase of their ex-situ biogas upgrading bubble column reactor experiment at thermophilic conditions. By performing a BLASTn search against the NCBI database, this OTU was similar to *Pseudomonas flexibilis* (95%). Literature reported not only a marked stimulated growth of *Pseudomonas flexibilis* utilizing lactate as a carbon and energy source but also stimulated growth by means of acetate and α -ketoglutarate (Herspell, 1977). Thus, as an acetate utilizer, its relative abundance was higher in the liquid media.

Bacteroidales sp.6 was the third most abundant OTU in liquid media samples (10%) and an “unclassified species” belonging to the order *Bacteroidales*. The taxonomic assignment could not be improved neither by BLASTn search against the NCBI database, nor by aligning the sequence against other public databases, such as RDP Classifier or SILVA ribosomal RNA gene database. The best hit with 81% similarity was with an obligatory anaerobic asaccharolytic member of *Porphyromonas* genus (*Porphyromonas circumdentaria*). This uncharacterized OTU was previously found in other works dealing with biogas upgrading (Kougias et al., 2017). Similarly to *Pseudomonas* sp. 3, *Bacteroidales* sp. 6 could be an acetate utilizer regarding its high abundance in the liquid media where high acetate concentration was present.

6.3.3 Practical considerations derived from the current study

The proposed biomethanation concept is becoming an attractive technology considering: a) the fact that H₂ used for the CO₂ hydrogenation can be generated from renewable energy sources via water electrolysis (Götz et al., 2015), and b) the high costs associated with H₂ storage (Gahleitner, 2013).

A question that needs to be addressed is related with the robustness of the process; commonly, renewable energy is a temporarily surplus, and thus, it is mandatory to elucidate the biomethanation efficiency during intermittent provision of H₂.

Therefore, a preliminary test was conducted in which the gas feed was interrupted for 22 h. After restarting the influx, a decline in output gas quality was observed (i.e. 91% of CH₄ content). The quality of the output gas was increased to 94% after approximately 3.5 h, while it fully recovered to 98% after 20 h.

This result is in accordance with other studies, which affirm that dormant cultures can be quickly reactivated in large-scale AD systems, and that methanogens can be fed intermittently (Lettinga, 1995; Martin et al., 2013). Moreover, this result agrees with the achievement potential recovery obtained in previous biogas upgrading TBF reactors after three days of H₂ suspension at mesophilic conditions (Burkhardt et al., 2015) and after one day of H₂ lack at thermophilic conditions (Strübing et al., 2017).

Nevertheless, further research related to the microbial tolerance towards periodical H₂ provision should be undertaken in order to draw conclusions on the dynamic operation of the presented system.

It is previously documented that the TBF reactors can produce high volumetric concentrations of CH₄ (Rittmann, 2015), and thus, are attractive configurations for the overall biomethanation process. The produced gas in all the experimental periods was of sufficient quality to be introduced in natural gas infrastructures (Muñoz et al., 2015).

Nevertheless, the tested TBF reactors could be considerably improved and optimized by enabling a faster process (i.e. lowering the gas retention time), or by reducing the specific reactor volume, which would lead to a decrease of the CAPEX.

For instance, optimization of the H₂:CO₂ ratio, together with adoption of more suitable packed-bed elements would involve inexpensive performance improvements.

Additionally, the liquid recirculation rate is considered as another key point for enhancing the efficiency of the system. In other studies (Burkhardt et al., 2015), reduction of the liquid recirculation rate was found to increase the performance of the TBF.

Previous works on biological biogas upgrading reported that the low gas liquid mass transfer is a bottleneck for achieving high bioconversion rates (Angelidaki et al., 2018). However, in the TBF reactors the gas-liquid boundary surface formed over the packed bed is maximized allowing a better and more homogenized dispersion of the injected gases. Moreover, given that biofilms rapidly consume accessible nutrients, high concentration gradients of the gases (in the current case H₂ and CO₂) are formed throughout the 3-phase system, triggering their favorable transport into the biofilm in accordance to Henry's law (Pauss et al., 1990). H₂ mass-transfer is therefore improved passively, without need of liquid stirring, diffusion devices or gas recirculation.

Additionally, pressurization of the reactors has been proven to reduce the H₂ mass transfer limitations (Martin et al., 2013). Nevertheless, an advantage of the presented concept is that the biomethanation occurs at atmospheric pressure, resulting in low technical requirements and economical costs.

Unlike catalytic methanation systems (Benjaminsson et al., 2013), it has been proven that chemical contaminants, such as H₂S or NH₃, do not disturb the biological methanation technologies, neither in trickle-bed reactors (Burkhardt et al., 2015), nor in liquid-phase systems (Martin et al., 2013). This aspect offers great a potential to the exploitation of biological methods for upgrading the quality of biogas.

Finally, considering all the outcomes from the present work, it can be extracted that the combination of biological methanation technology with the utilization of TBF reactor systems seems very convenient for application in the Power-to-Gas concept.

6.4 CONCLUSIONS

The present work demonstrates the suitability of thermophilic trickling biofilters for methanation of H₂ and the CO₂ fraction of biogas.

Stable and robust continuous operation was achieved through single-pass plug flow, without need for gas mixing or recirculation.

The investigated system upgraded biogas efficiently reaching a CH₄ concentration of 95%, CH₄ productivity of 1.74 L_{CH₄}/L_R·d and CH₄ yield of 0.24 L_{CH₄}/L_{H₂} (close to the stoichiometric maximum of 0.25 L_{CH₄}/L_{H₂}) for a H₂ loading rate of 7.2 L_{H₂}/L_R·d.

The quality of the output gas was comparable to the methane purity achieved by commercial biogas upgrading systems fulfilling the specifications to be used as substitute to natural gas.

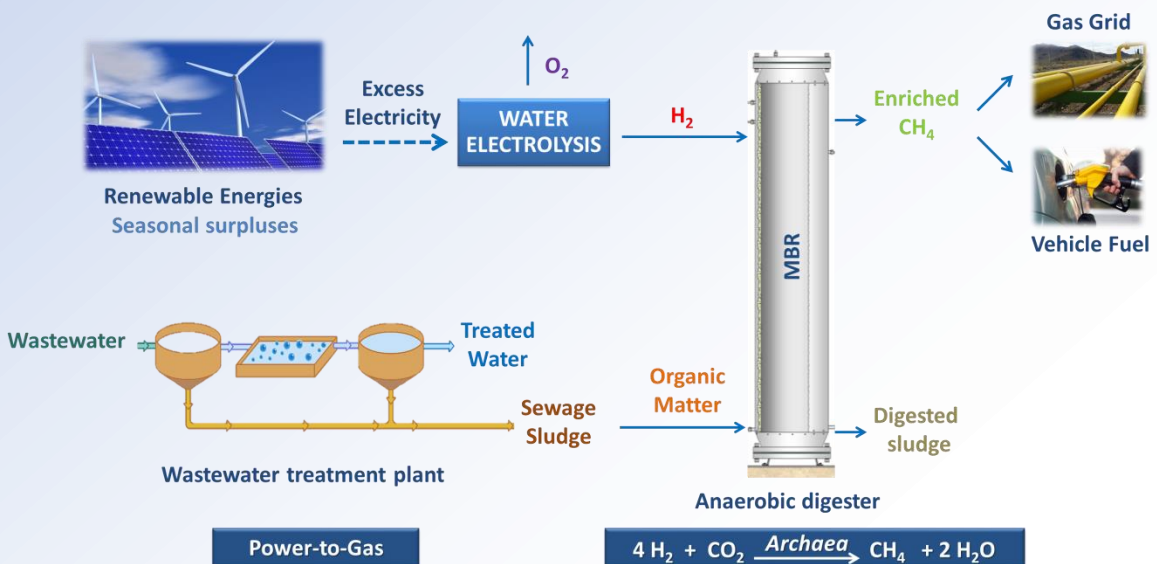
It was demonstrated that the injection of the influent gas mixture with the directional flow of the liquid media greatly enhanced acetate production compared to the injection in counter-flow to the trickling media.

The spatial distribution of the microbial consortia localized in the liquid media and biofilm enabled us to gain a deeper understanding on how the microbiome is structured inside the trickling biofilter.

Regarding the microbial community structure, it was shown that the most abundant methanogen populating the microbial community (*Methanothermobacter* sp.) was represented by a new species. Sequencing results revealed a significant predominance of *Methanothermobacter* sp. in the biofilm. Unknown members of the class *Clostridia* were highly abundant in biofilm and liquid media, while acetate utilizing bacteria predominated in liquid samples.

Chapter 7

H₂ addition through a submerged membrane for in-situ biogas upgrading in the anaerobic digestion of sewage sludge



7.1 INTRODUCTION

Power-to-Gas strategies have gained increased attention recently and several opportunities have been identified for the integration of Power-to-Gas in wastewater treatment plants (Patterson et al., 2017).

Mechanical stirring has been applied in previous in-situ studies to ease organic matter removal and H₂ conversion. An increase in mixing may also significantly increase the operation cost, though it could increase the hydrogen consumption rate.

Biogas recirculation or sludge recirculation are commonly employed for mixing in full-scale anaerobic digesters of organic matter (Appels et al., 2011). The application of biogas recirculation has shown to increase H₂ and CO₂ conversion (by increasing $k_L a_{H_2}$ values) in ex-situ MBRs (experiments of Chapters 4 and 5) and in the in-situ UASB reactor with H₂ supply of Bassani et al. (2016).

The aim of this work is to evaluate the feasibility of supplying H₂ to an anaerobic digester of sewage sludge through a submerged membrane module for in-situ upgrading of biogas. The effect of biogas recirculation rate on upgrading efficiency, performance of the organic matter removal and digested sludge dewaterability were assessed. Dynamics of the microbial community were studied using molecular biology tools.

7.2 MATERIALS AND METHODS

7.2.1 Pilot Plants

The description of the pilot plants used in the experiment has been performed in Chapter 3, section 3.1.1.1.b). As previously mentioned, R1 was used as upgrading reactor (equipped with a hollow-fiber membrane module) while R2 was utilized as control reactor both with 20 L working volume.

7.2.2 Operating conditions

Anaerobic sludge from a mesophilic anaerobic digester in the WWTP of Valladolid (Spain) was used to inoculate both reactors (20 L per reactor). The content of total and volatile solids in the inoculum was 22.0 g/kg and 12.8 g/kg, respectively.

R1 and R2 were fed at HRT of 20 d with sewage sludge (thickened mixed primary and secondary sludge) collected periodically from the afore mentioned WWTP and stored at 4 °C. Collected sludge composition varied seasonally, so did the OLR to the reactors (Table 24, Table 25).

Table 24. Operating conditions applied during the experiment.

	Set-up	Stage 1	Stage 2	Stage 3
t (d)	0	62	120	184
H₂ loading rate (L_{H₂}/L_R·d)	0	0.87	0.87	0.87
Gas recirculation rate (L/L_R·d)	0	50	101	202
OLR (g VS/L·d)	1.3 ± 0.1	1.3 ± 0.2	1.5 ± 0.2	1.8 ± 0.5

Table 25. Characteristics of raw sludge (sewage sludge) utilized during the experiment.

Parameter	Set-up	Stage 1	Stage 2	Stage 3
TS (g/kg)	31.7 ± 0.5	42.5 ± 1.7	38.3 ± 8.8	58.8 ± 2.3
VS/TS ratio	0.78 ± 0.13	0.75 ± 0.13	0.69 ± 0.11	0.69 ± 0.12
Acetate (mg/L)	350 ± 38	291 ± 42	489 ± 49	555 ± 48
NH₄⁺-N (mg/L)	102 ± 13	108 ± 16	125 ± 10	166 ± 36

A set-up period was performed at mesophilic conditions (35 ± 1 °C) for 60 d in both reactors by continuously feeding only thickened mixed sludge.

After the set-up period, H₂ was added to R1 (stage 1). H₂ addition at a flow rate of 0.87 L_{H₂}/L_R·d was maintained during the whole experiment in all stages, to achieve a ratio 4:1 (according to Eq. 1) to the average gaseous CO₂ production during the set-up period.

Gas recirculation rates applied to R1 ranged between 50 and 202 L/L_R·d in the different experimental stages (Table 24). All the values of flow rates from the study are expressed at 273.15 K and 1 atm.

7.2.3 Monitoring and experimental analysis

The following parameters (Table 26) were monitored and analyzed during the experiment according to the materials and methods described in Chapter 3, section 3.3.:

Table 26. Parameters monitored and analyzed during the study.

Parameter	Measuring frequency
Headspace pressure	Continuous mode
Temperature	
Gas production rate	Daily
Gas composition	
Liquid effluent	
VFA concentration	Weekly
pH	
TS/VS	
NH ₄ ⁺	
Dewaterability	Periodically

7.2.4 Calculations

Calculations about efficiency of H₂ utilization (η_{H_2}), H₂ gas-liquid mass transfer rate (r_t) and CH₄ production rate have been performed following the calculations described in Chapter 3, section 3.5 while specific gas transfer coefficient ($k_L a_{H_2}$) was calculated according to Eq. 3 of Chapter 1.

The methane evolution rate (MER), which expresses the increase in the specific CH₄ production rate ($L_{CH_4}/L_R \cdot d$) under H₂ supply with respect to the lack thereof, was calculated as follows (Eq. 40):

$$MER = CH_4 \text{ production rate in } R1 - CH_4 \text{ production rate in } R2 \quad (\text{Eq.40})$$

where R1 is the upgrading reactor (with H₂ addition) and R2 is the control reactor (without H₂ addition).

H₂ rate converted to methane ($L/L_R \cdot d$) was calculated according to Eq. 41:

$$H_2 \text{ rate to } CH_4 = 4 (CH_4 \text{ in output gas } R1 - CH_4 \text{ in output gas } R2) \quad (\text{Eq. 41})$$

where λ is the stoichiometric coefficient according to Eq. 1, CH_4 in output gas R1 ($L_{CH_4}/L_R \cdot d$) is the rate of CH_4 produced in R1 and CH_4 in output gas R2 ($L_{CH_4}/L_R \cdot d$) is the rate of CH_4 produced in R2.

The percentage of VS removal was calculated according to Eq. 42:

$$VS \text{ removal } (\%) = \frac{VS \text{ input} - VS \text{ output}}{VS \text{ input}} \cdot 100 \quad (\text{Eq. 42})$$

where $VS \text{ input}$ (g/Kg) is VS content in feed raw sludge (thickened mixed sludge) while $VS \text{ output}$ (g/Kg) is the VS concentration in the digested sludge.

7.2.5 Microbial analysis

Liquid samples, including inoculum, were collected at different stages of the process in order to evaluate the evolution of the microbial population during the experiment in both reactors. Extraction of genomic DNA, PCR, DGGE and FISH analysis were performed according to the materials and methods described in Chapter 3, sections 3.4.1., 3.4.2. and 3.4.3.

Sequences were deposited in GenBank Data Library under accession numbers MG383910 - MG383931 (*archaea*) and MG664852 - MG664869 (*bacteria*).

7.3 RESULTS AND DISCUSSION

7.3.1 Performance of the conversion of H_2 and CO_2 to CH_4

During the set-up period, the two reactors showed similar performance in terms of CH_4 production rates (Figure 42). The average CH_4 content in the biogas from R1 and R2 was around 66% (Table 27), which agrees with typical CH_4 concentration in biogas from sludge digestion as reported in literature (Metcalf and Eddy, 2003). Therefore, R2 was validated as control reactor to establish comparisons.

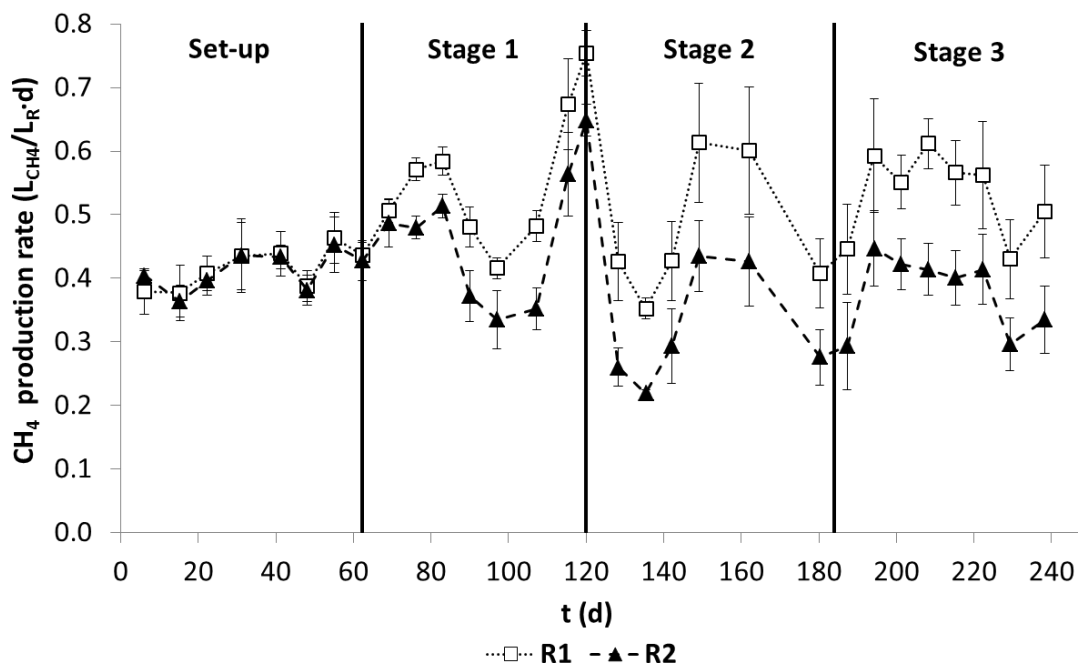


Figure 42. Methane production rates in R1 and R2 during the experiment.

After the set-up period (on day 62), the first stage started injecting $0.87 \text{ L}_{\text{H}_2}/\text{L}_R \cdot \text{d}$ into R1. In addition, a gas recirculation rate of $50 \text{ L}/\text{L}_R \cdot \text{d}$ was applied in R1. The conversion of H_2 and CO_2 to CH_4 took place at a low rate at the beginning of stage 1. The efficiency of H_2 utilization (η_{H_2}) and the H_2 flow rate converted to methane showed an increasing trend during this period (Figure 43). On average, only 55% of the H_2 injected was utilized, leading to a large concentration of unutilized H_2 in the output gas (Table 27). CH_4 production rate experienced an increase of 23% in R1 in comparison with R2 (Figure 42, Table 27) and MER reached $0.10 \text{ L}_{\text{CH}_4}/\text{L}_R \cdot \text{d}$. CO_2 flow rate in output gas in R1 was 43% lower than in R2 because of the reaction of H_2 with the in-situ produced CO_2 (Table 27).

Gas recirculation rate was increased to $101 \text{ L}/\text{L}_R \cdot \text{d}$ on day 120, marking the beginning of stage 2 of the experiment. Consequently, a significant improvement of the H_2 mass transfer in R1 was observed. 87% of the H_2 injected was transferred (Figure 43 and Table 27) thus reducing the unused concentration of H_2 in upgrading gas while CH_4 concentration rose to 71%. In R1, CH_4 production rate experienced an increase of 47% in comparison to R2 while CO_2 flow rate in output gas was 47% lower. MER also reached a larger value ($0.15 \text{ L}_{\text{CH}_4}/\text{L}_R \cdot \text{d}$) than in stage 1.

Table 27. Upgrading (R1) and control (R2) reactor performances.

	Set- up		Stage 1		Stage 2		Stage 3	
	R1	R2	R1	R2	R1	R2	R1	R2
Biogas production rate (L/L_R·d)	0.64 ± 0.08	0.63 ± 0.08	1.06 ± 0.18	0.67 ± 0.23	0.67 ± 0.22	0.47 ± 0.16	0.74 ± 0.16	0.56 ± 0.13
H ₂ (%)	/	/	36.5 ± 7.1	/	17.7 ± 3.9	/	7.2 ± 2.4	/
CO ₂ (%)	34.4 ± 1.4	34.4 ± 1.0	12.4 ± 1.9	34.1 ± 1.0	11.4 ± 4.8	32.0 ± 1.3	19.7 ± 3.0	32.9 ± 1.1
CH ₄ (%)	65.6 ± 1.4	66.0 ± 1.0	51.1 ± 6.5	65.8 ± 1.0	70.9 ± 3.6	68.0 ± 1.3	73.1 ± 3.4	67.1 ± 1.1
CH₄ production rate (L_{CH₄}/L_R·d)	0.42 ± 0.05	0.41 ± 0.05	0.54 ± 0.10	0.44 ± 0.10	0.47 ± 0.14	0.32 ± 0.11	0.54 ± 0.11	0.38 ± 0.08
CO₂ in output gas (L_{CO₂}/L_R·d)	0.22 ± 0.03	0.22 ± 0.03	0.13 ± 0.06	0.23 ± 0.05	0.08 ± 0.08	0.15 ± 0.05	0.15 ± 0.04	0.18 ± 0.04
η _{H₂} (%)	/	/	54.6 ± 9.4	/	86.2 ± 3.0	/	93.9 ± 2.9	/
H₂ transfer rate (L_{H₂}/L_R·d)	/	/	0.48 ± 0.09	/	0.75 ± 0.03	/	0.82 ± 0.03	/
k _L α _{H₂} (h ⁻¹)	/	/	2.7 ± 0.8	/	8.9 ± 1.9	/	24.9 ± 6.8	/
Acetate (mg/L)	35.6 ± 30.9	35.8 ± 42.0	45.0 ± 28.8	25.5 ± 15.2	25.3 ± 13.2	25.2 ± 22.2	31.1 ± 14.8	12.5 ± 11.4
pH	7.23 ± 0.12	7.45 ± 0.18	7.28 ± 0.14	7.41 ± 0.10	7.80 ± 0.23	7.42 ± 0.23	8.09 ± 0.23	7.41 ± 0.27
TS (g/kg)	21.5 ± 1.0	21.4 ± 1.5	21.1 ± 1.0	20.6 ± 1.8	22.3 ± 2.0	23.0 ± 3.5	27.6 ± 5.5	27.8 ± 3.9
VS/TS ratio	0.66 ± 0.05	0.66 ± 0.07	0.63 ± 0.06	0.63 ± 0.08	0.59 ± 0.07	0.60 ± 0.08	0.56 ± 0.05	0.57 ± 0.06
VS removal (%)	47.1 ± 4.9	47.4 ± 6.4	48.4 ± 7.7	49.4 ± 9.2	48.5 ± 15.0	48.5 ± 13.3	55.8 ± 9.3	55.7 ± 10.6
NH₄⁺-N (mg/L)	729 ± 106	780 ± 172	670 ± 117	692 ± 83	721 ± 99	702 ± 102	794 ± 105	756 ± 123

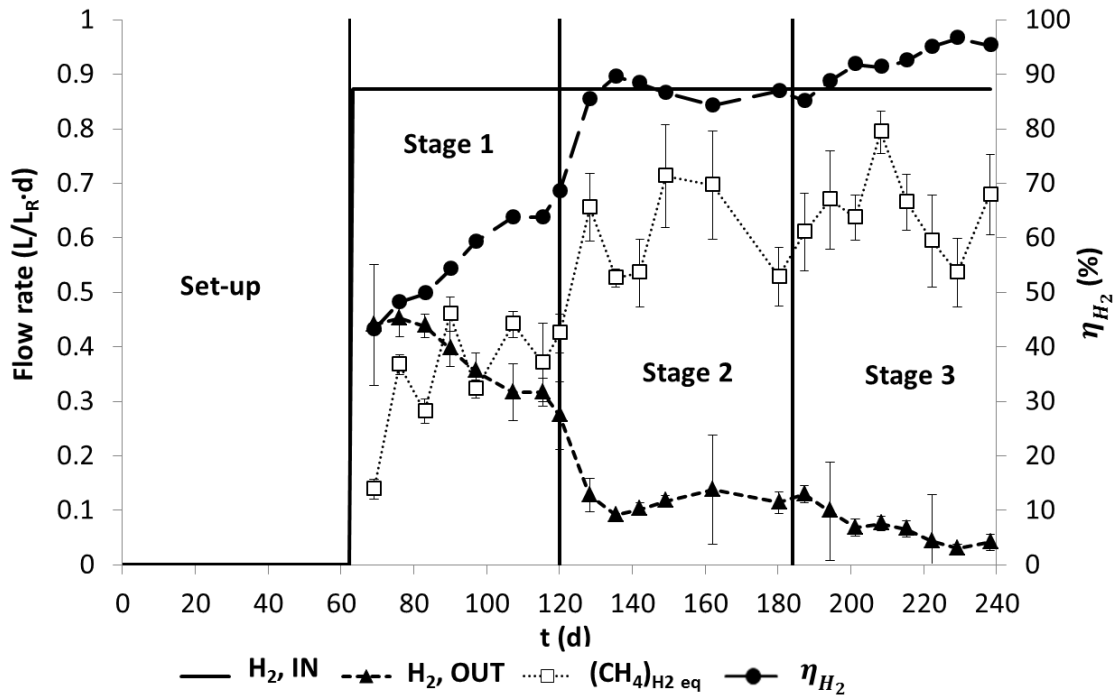


Figure 43. Gas flow rates and H₂ utilization efficiency in R1 throughout the experiment. H₂ supplied rate (H₂, IN), H₂ rate in biogas (H₂, OUT) and CH₄ as H₂ equivalent rate in biogas ((CH₄)_{H₂ eq}).

On day 181, gas recirculation rate was doubled to 202 L/L_R·d with the purpose of raising η_{H_2} (stage 3). In this stage, η_{H_2} increased to an average of 94%, thus showing larger H₂ utilization compared to stage 2 and 1 (Figure 43 and Table 27). Therefore, this stage showed an important improvement as almost all H₂ was transferred. CH₄ content in the biogas increased to 73% and H₂ content dropped to 7%. However, the CO₂ content increased (Table 27), probably because of the higher OLR applied during stage 3. CH₄ production rate of R1 was on average 42% higher (Table 27) compared to R2 and MER reached 0.16 L_{CH₄}/L_R·d.

H₂ converted to CH₄ can be calculated from a mass balance to H₂ according to Eq. 41 (Figure 44). The rate of converting H₂ to methane showed an increasing trend over the experiment, from an average H₂ conversion to methane of 46% during stage 1, to 72 and 76% in stages 2 and 3, respectively. This fact emphasizes the positive correlation between gas recirculation rate and the conversion of H₂ and CO₂ into CH₄.

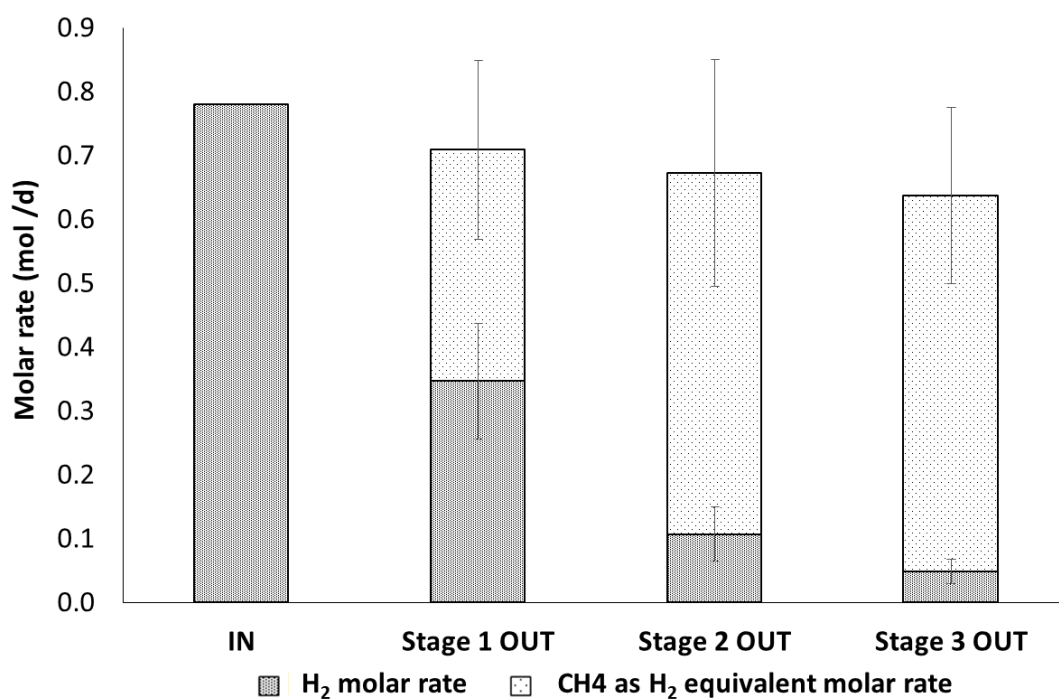


Figure 44. Balance of H₂.

H₂ utilization rate for microbial growth was estimated as the gap between H₂ supply rate (input) and the sum of H₂ rate and CH₄ as equivalent H₂ in the biogas (output). The portion of H₂ dedicated to microbial growth represented approximately 9, 14 and 18% of total H₂ supply and 16, 16 and 19% of transferred H₂ in stages 1, 2 and 3, respectively. These values are within the range of the two previous studies performed in ex-situ bioreactors with similar configurations described in Chapter 4 and Chapter 5.

In contrast, ex-situ study of Chapter 4 reached an asymptote of around 8-10% (of transferred H₂) after long time operation at low dilution rates, while microbial growth seemed to remain stable or slightly increase in this study. This can be the consequence of continuous biomass washout, as the amount of substrate used for growth has been reported to be larger at the beginning of the experiments, where the consumers of H₂ are in small proportion in the experiments of Chapters 4 and 5. The amount of acetate as H₂ equivalent can be neglected because of the low acetate concentrations observed during the study (Table 27).

In brief, the application of increasing gas recirculation rates successfully increased MER, the efficiency of H₂ utilization and the concentration of CH₄ in upgraded biogas up to 0.16 L_{CH₄}/L_R·d, 94% and 73%, respectively. This result is in accordance with the positive effect of gas recirculation on the increase of H₂ gas-liquid mass transfer rate}

previously described (Guiot et al., 2011). Gas recirculation prolonged the contact time between microorganisms and gases, enhancing H₂ addition and stimulating substrate conversion by hydrogenotrophic methanogens as it was previously described by Bassani et al. 2016.

Gas recirculation is frequently applied to mix anaerobic digesters of sludge and in-situ upgrading could benefit from that to avoid high-speed stirring to achieve efficient H₂ transfer and biogas upgrading (Agneessens et al., 2018; Agneessens et al., 2017). However, gas recirculation rates typically used for mixing in full-scale digesters are around 7.2 and 10 L/L_R·d (Appels et al., 2008), 5 to 20 times lower than those applied in this study, indicating that extra energy inputs for in-situ upgrading might still be required.

From another point of view, the CH₄ production rate and CH₄ content in biogas achieved in stage 3 are like those found in Luo and Angelidaki (2013a) under similar operating conditions but with a 24 times lower membrane area to reactor volume ratio in this study, showing an alternative biofilm formation over the membrane and pressure drop reported. On the contrary, biofilm formation could achieve a concentration of CH₄ of 99% CH₄ in another study (Wang et al., 2013).

In view of the results, a polymeric membrane can be employed to transfer H₂ allowing the biological conversion to take place satisfactorily. Although gas recirculation rate increased the transfer of H₂ to the liquid, thus improving the efficiency of the upgrading, CH₄ content in the output gas was not higher than 73%. This is the result of the excess of H₂ loading rate supplied in stages 2 and 3 (as it was maintained constant during the whole experiment at 0.87 L_{H₂}/L_R·d), leading to extra fed H₂ which could not couple with the real total amount of CO₂ produced in-situ during that stages. Thus, unutilized H₂ went out from the process producing a dilution effect on final CH₄ content in the produced biogas. Further studies should be conducted with regulated H₂ supply rates to fit the variable CO₂ production because of seasonal changes in OLR in order to maximize the CH₄ content in the biogas.

7.3.2 Mass transfer capacity in the MBR

$k_L a_{H_2}$ value showed an increasing trend during the experiment, in accordance with the positive effect of gas recirculation on $k_L a$ coefficient, increasing H_2 gas-liquid mass transfer rate as previously described (Guiot et al., 2011).

The average $k_L a_{H_2}$ values (h^{-1}) observed in the upgrading reactor are shown in Table 27. Literature on in-situ biogas upgrading reactors shows scarce $k_L a_{H_2}$ values. Employing a reactor of 0.6 L fed with a mixture of whey and cattle manure (OLR of 1.7 g VS/L·d) and H_2 loading rate of 1.7 $L_{H_2}/L_R \cdot d$ at thermophilic conditions, Luo and Angelidaki (2013b) found $k_L a_{H_2}$ values of 6.6 and 11.8 h^{-1} with a column diffuser and 16.0 h^{-1} with a ceramic diffuser.

In the present study, $k_L a_{H_2}$ values are the result of a good gas-liquid mass transfer interfacial area produced by the polymeric membrane module employed in the experiment generating fine small bubbles but several orders of magnitude lower than reported in the ex-situ experiments with a similar configuration described in Chapter 4 and Chapter 5. Despite everything, in-situ upgrading digesters with high HRT do not require specific mass transfer coefficients as high as the ex-situ process because of the lower specific CO_2 rates ($L_{CO_2}/L_R \cdot d$) to convert.

In fact, the H_2 concentration of 7.2% with a $k_L a_{H_2}$ value of 25 h^{-1} (stage 3) agrees with a modification of ADM1, to account for H_2 injection, that showed that $k_L a_{H_2}$ values around 21 h^{-1} should be achieved in in-situ digesters to reduce H_2 concentration to below 5% and around 35 h^{-1} to meet gas grid injection requirements (Bensmann et al., 2014). Thus, hollow-fiber membranes have potential advantages for in-situ biogas upgrading in comparison to other gas diffusion systems.

7.3.3 Anaerobic digestion performance

7.3.3.1 VFA evolution

During the set-up period, the two reactors showed similarly low VFA content with acetate concentration of 36 mg/L (Table 27), which agrees with literature of biogas production from sewage sludge (Metcalf and Eddy, 2003).

During the first HRT of stage 1, acetate concentration increased from 15 mg/L to 95 mg/L to decrease suddenly afterwards. This finding agrees with the statement of Agneessens et al. (2018) about the likelihood of acetate accumulation during the start-up phase of a continuous in-situ biogas upgrading reactor with the later stabilisation after 1 HRT.

During the rest of the experiment, VFA accumulation was not observed (Table 27). In contrast, acetate accumulation was reported during H₂ injection rates at 4:1 H₂:CO₂ ratio (Mulat et al., 2017) or higher ratios (Luo and Angelidaki, 2013a; Agneessens et al., 2018; Agneessens et al., 2017). Agneessens et al. (2017; 2018) showed that acetate accumulation was more likely during high H₂ (1.3 - 1.7 L_{H2}/L_R·d), low CO₂ (<7%) and high pH (>8.33) levels as H₂ was introduced in the headspace of the reactors in intermittent pulses. In these experiments, homoacetogenesis was stimulated by those conditions of H₂, CO₂ and pH, decreasing the activity of acetoclastic methanogens contributing to acetate accumulation and outcompeting methane production from H₂ and CO₂ by hydrogenotrophic methanogens.

High acetate accumulation (2070 mg/L) was also observed during the in-situ biogas upgrading experiment performed by Luo and Angelidaki (2013a) using a hollow-fiber membrane bioreactor with high H₂ loading rate (1.76 L_{H2}/L_R·d), high pH (8.31) and low CO₂ content in the output gas (4%). This accumulation was in accordance with the parameters affecting acetate concentrations during in-situ biogas upgrading described by Agneessens et al. (2018).

The present study was carried out with continuous H₂ injection (instead of sporadic pulses and lower H₂ load) in which CO₂ content ≥ 11% and pH reached lower values (≤ 8.1), thus avoiding the possible stimulation of homoacetogens, being outcompeted by

hydrogenotrophic methanogens. Agneessens et al. (2018) reported as well that more frequent H₂ injection rate reduces the possibility of acetate accumulation which can be linked to the lack of VFA accumulation obtained in the present experiment.

Contrary to previous studies (Speece, 2008; Liu et al., 2008), there was no accumulation of propionic acid despite the elevated H₂ partial pressure. Thus, the injection of H₂ through the hollow-fiber membrane module did not inhibit propionate degradation as in Luo and Angelidaki (2013a).

7.3.3.2 OLR

OLR is a critical parameter for anaerobic digestion reactor performance and it was recently shown to be an important parameter for in-situ biomethanation (Agneessens et al., 2018; Agneessens et al., 2017).

OLR had a slightly increasing trend during the experiment, ranging from 1.3 to 1.8 g VS/L·d (Table 24). Agneessens et al. (2018) found that increasing OLR (0.5 – 2 g VS/L·d) stimulates acetate accumulation due to an increased acetate production via homoacetogenesis, an incapability of acetoclastic methanogenesis to readily consume the present acetate or both.

The homoacetogens have previously been found to increase in abundance as the OLR increases (Ju et al., 2017; Li et al., 2016; Li et al., 2015). At an increasing OLR, the dissimilarity in conversion rate between the fast acidogenesis phase and slower methanogenic phase becomes more prominent which can contribute to acetate accumulation (Goux et al., 2015).

In the study of Agneessens et al. (2018), performed with pulse H₂ injections to the reactors, it was stated the influence of the increasing OLR, non-homogeneous H₂ distribution in the sludge and the pulse H₂ injections in favor of homoacetogens improving their contribution chances to H₂ consumption and thereby acetate production. In addition, Agneessens et al. (2018) stated that hydrogenotrophic methanogens, instead of homoacetogens, were benefited from repeated H₂ injections with an OLR of 2 g VS/L·d.

In the present study, there was no acetate accumulation because of good homogeneous H₂ distribution in the sludge obtained with the hollow-fiber membrane module with continuous H₂ injection, indicating hydrogenotrophic methanogens outcompeted homoacetogens. Under the studied conditions, the increasing OLR had no effect on the biomethanation process.

Conversely, in a previous experiment (Luo and Angelidaki, 2013a), at equivalent H₂ loading rates and similar OLR using a hollow-fiber membrane as H₂ diffusion system, acetate accumulation was observed. This may be explained as gas recirculation was not applied in the reactor thus, H₂ distribution was less homogeneous than in the present study leading to an important homoacetogen activity. Thus, gas recirculation rate seems to have a positive effect on the in-situ biomethanation when OLR is increasing.

7.3.3.3 pH, NH₄⁺ and solids removal

One of the main technical challenges of in-situ biogas upgrading technology is pH increase to values above 8.5, leading to the inhibition of methanogenesis (Angelidaki et al., 2018; Weiland, 2010).

During the set-up period, the two reactors showed similar pH values (~ 7.4) which are in accordance with literature reported on biogas production from sewage sludge (Metcalf and Eddy, 2003).

After the set-up period and throughout the experiment, the pH for R2 remained relatively unchanged, while a gradual pH increase to 8.1 was recorded in R1, as a result of CO₂ removal (Table 27). No inhibition was observed as previously reported in Agneessens et al. (2017; 2018) at pH 8.3, thus indicating adaptation of microorganisms to higher pH levels. Then, the direct H₂ addition to the anaerobic reactor had no effect on methanogenesis performance.

In contrast, previous experiments on in-situ biogas upgrading reactors (Luo et al., 2012; Luo and Angelidaki, 2013a; Luo and Angelidaki, 2013b) showed a slight inhibition of methanogenesis when pH was more than 8.3, verifying the argument that in

conventional biogas production systems, high pH levels inhibited or hampered biomethanation process.

During the experiment, the two reactors showed similar NH_4^+ concentrations (Table 27), in harmony with literature of biogas production from sewage sludge (Speece, 2008; Metcalf and Eddy, 2003). Thus, the H_2 addition to the anaerobic digestion of sewage sludge had no effect on NH_4^+ levels. As in the in-situ experiment performed by Luo and Angelidaki (2013b), NH_4^+ concentration was higher in the reactors than in the influent. Literature of in-situ biogas upgrading reactors shows no more NH_4^+ concentration results.

TS concentration, VS/TS ratio and %VS removal in feeding raw sludge, R1 and R2 are reported in Table 27. The two reactors showed similar performance in terms of solids removal (Table 27) during the set-up period, confirming the use of R2 as a control reactor for the in-situ upgrading process. This similarity of solids removal yield was maintained during the whole experiment regardless the injection of H_2 and the increase in the gas recirculation rate in R1. According to the results shown in Table 27, the removal of VS was not affected by the introduction of H_2 in any stage in R1 considering its high similarity with the VS removal results obtained in R2 with no significant differences. In addition, all these solids removal yields were within the normal range for the anaerobic digestion of sewage sludge (Speece, 2008; Metcalf and Eddy, 2003).

7.3.4 Dewaterability of digested sludge

The percentage of solids recovery by centrifugation was closely similar between the inoculum and the sample from R2 and slightly higher than the recovery showed in the sample from R1 (Table 28).

Table 28. Centrifugability and filterability of inoculum and digested sludge from R1 and R2 in stage 3.

	Inoculum	R1	R2
Centrifugability (% solids recovery)	99.20 ± 0.10	98.30 ± 0.10	99.10 ± 0.12
Filterability (filtration constant)	0.60 ± 0.00	0.25 ± 0.00	0.30 ± 0.00

The highest filtration constant was assigned to the initial inoculum being a double value of the one obtained in the sludges from both reactors (Table 28). R1 presented lower constant than R2 meaning worse filterability linked with the result of lower centrifugability mentioned above.

Additionally, the turbidity (by visual inspection, Figure 45) of the sludge from R1 was much higher than R2.

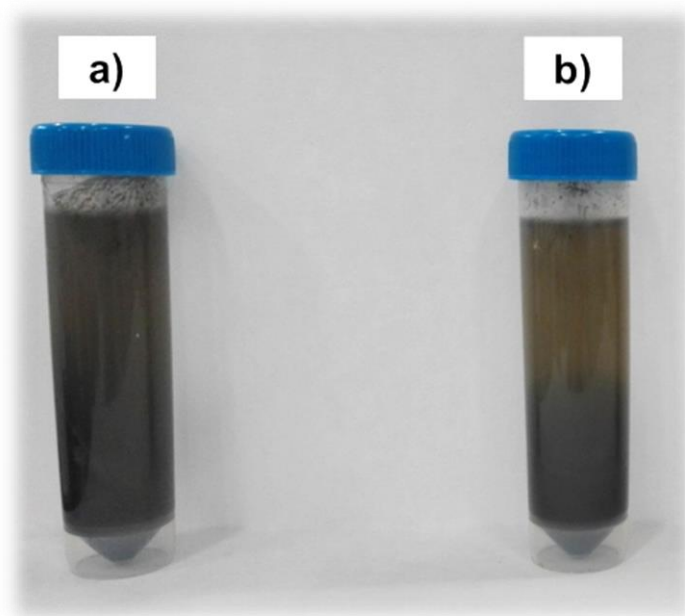


Figure 45. Turbidity visual inspection of samples from R1 (a) and R2 (b).

In short, R1 presented worse centrifugability, worse filterability and higher turbidity in comparison with the digested sludge from R2 as a result of the small particles and colloid materials present in the digested sludge. The presence of colloid materials was presumably a negative impact of the turbulence caused by high gas recirculation rate in R1. There was no literature data on dewaterability to compare the findings from this study to.

7.3.5 Microbial community

From the archaeal DGGE gel (Figure 46 a), 22 bands were sequenced. According to the RDP classifier (confidence threshold of 50%), they belonged to the *Euryarchaeota* and *Pacearchaeota* phyla. In the case of *Euryarchaeota* phyla, the bands were ascribed to

two classes, almost all to *Methanomicrobia* (band 1-15) and only one band to *Methanobacteria* (band 16). The *Pacearchaeota* phyla was found in bands 17-22 (Table 29). The BLAST search tool provided consistent results with those given by the RDP classifier.

Five families were present in which *Methanotrix*, *Methanospirillum*, *Methanoculleus* and *Methanolinea* were the four genus assigned to *Methanomicrobia* class and *Methanobacterium* genus to *Methanobacteria* class. The *Pacearchaeota* phyla ascribed the genus *Pacearchaeota Incertae Sedis AR13* (Table 29).

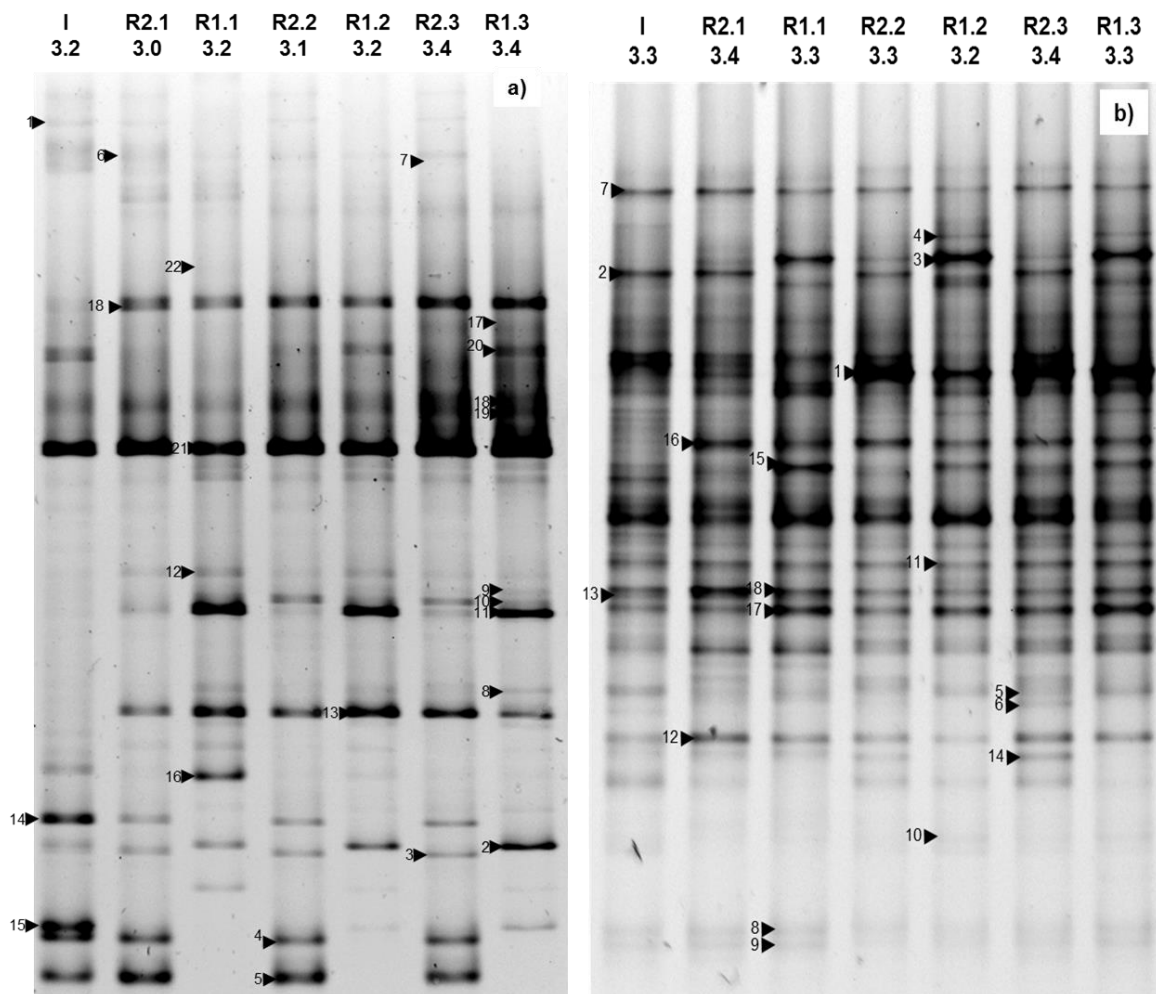


Figure 46. a) Archaeal DGGE profiles and b) Bacterial DGGE profiles of the 16S rRNA amplicons of the samples with their respective diversity indices. Samples: Inoculum (I), upgrading reactor (R1) and control reactor (R2) in the three stages (1-3) of the experiment.

During the experiment, some *archaea* disappeared corresponding only with the *Euryarchaeota* phyla (Figure 46 a). On the one hand, they disappeared completely in R1 (band 1, 3, 4, 5, 6 and 14) although they were present in the inoculum and R2. On the other hand, the missing *archaea* in R2 (band 2, 8 and 16) were present in R1 and with an increasing trend.

A new *archaea* appeared after the injection of H₂ in R1 and it was present since then (band 9), corresponding with an uncultured specie (*Methamicrobiales* CU916161.1 or archaeon KJ402292.1) with an identity of 99% (Table 29).

Methanobacterium sp. was an *archaea* present in inoculum and R1 during the experiment but not in R2. Therefore, it was revealed the selection-effect of H₂ on archaeal community composition over time.

Although *Methanoculleus sp.* was no present initially in the inoculum, it was highly present in R1 and R2 during the experiment (Figure 46 a, Table 29). This fact could be explained as it was not detected in the inoculum sample due to its low abundance or it could be introduced with the feed sludge (not analyzed).

With high values of abundance, both reactors had some common *archaea* (band 10, 11 and 12) belonging to *Euryarchaeota* phyla. *Pacearchaeota* phyla population was maintained during the experiment in R1 and R2 in terms of high abundance (Figure 46 a, Table 29).

According to the genus obtained in the archaeal DGGE analysis, some hydrogenotrophic *archaea* were present over the experiment in R1 as *Methanoculleus sp.*, *Methanospirillum sp.*, *Methanolinea sp.* and *Methanobacterium sp.* with *Pacearchaeota Incertae Sedis AR13* as a potential hydrogenotrophic methanogen as well. R1 had the possible presence of an acetoclastic methanogen, *Methanotrix sp.* present in R2 too.

No homoacetogens were found in R1, which links with the previous discussion of VFA and OLR results. Homoacetogens were potentially outcompeted by hydrogenotrophic methanogens because of the reactor configuration and operation (homogeneous H₂

distribution by hollow-fiber membrane module, use of gas recirculation rate, continuous H₂ injection and obtained pH and CO₂ levels).

From the bacterial DGGE gel (Figure 46 b) and according to the RDP classifier (confidence threshold of 50%), 18 bands belonging to seven different phyla were sequenced: *Proteobacteria* (band 1-4), *Firmicutes* (band 5-7), *Verrucomicrobia* (band 8-9), *Lentisphaerae* (band 10-11), *Actinobacteria* (band 12-13), *Acidobacteria* (band 14) and *Cloacimonetes* (band 15) while three bands remained unclassified (band 16-18) (Table 30). In general, the BLAST search tool provided consistent results with those given by the RDP classifier.

It was noted that there was no particular predominant phylum, but H₂ addition in R1 had an effect on the microbial community producing some changes on it. During the experiment, some new bacteria appeared in R1 but they were not present in R2 or in the initial inoculum (band 4, uncultured bacterium KU648653.1, Table 30) and they were present during the different stages.

Other bacteria disappeared from R1 but they were found in R2 (band 2 and 14 both uncultured bacterium) and vice versa (band 10) (Figure 46 b) and other ones disappeared completely in both reactors (band 13, uncultured *Propionibacteriaceae* EU812987.1, Table 30).

Some were maintained in the experiment in similar abundances in R1 and R2 in the different stages (bands 1, 5, 7, 8, 9, 11 and 12) but it can be observed that there was an increasing trend of other species in R1 (bands 3, 15, 17 and 18). Although it was not present initially in the inoculum, one unclassified bacterium (band 16, uncultured bacterium KU648637.1, Table 30) was highly present in R1 and R2 during the experiment.

Table 29. RDP classification of the archaeal DGGE bands sequenced with a 50% of confidence level, and corresponding matches according to the BLAST search tool, with their similarity percentages, and environments from which they were retrieved. Intensity < 20 = x, 20 ≤ intensity ≤ 100 = xx, intensity > 100 = xxx. Liquid samples from inoculum (I), upgrading reactor (R1) and control reactor (R2) during stages 1-3.

Taxonomic placement (50% confidence level)	Band No.	I	R2 Stage1	R1 Stage1	R2 Stage 2	R1 Stage 2	R2 Stage 3	R1 Stage 3	Closest relatives in Blast Name (Accession No.)	Similarity (%)	Source of origin
Phylum <i>Euryarcheota</i>	1	XX	X		X		X		Uncultured archaeon (CU917096.1)	98	Mesophilic anaerobic digester which treats municipal wastewater sludge
Class <i>Methanomicrobia</i>											
Order <i>Methanosarcinales</i>											
Family <i>Methanotrichaceae</i>											
Genus <i>Methanotrix</i>	2	X		XX		XX		XXX	Uncultured archaeon isolate (KJ402281.1)	99	Mesophilic reactor treating municipal sewage sludge under anaerobic and microaerobic conditions
									Uncultured archaeon clone (HM639832.1)	99	Activated sludge wastewater treatment plant
									Uncultured archaeon clone (EU926764.1)	99	Mesophilic anaerobic biogas reactor fed with corn silage
	3	X	XX		XX		XX		Uncultured Methanosarcinales (KF198804.1)	99	Mesophilic anaerobic digester which treats municipal wastewater sludge
									Uncultured Methanosarcinales (JX023141.1)	99	Sludge samples of anaerobic digesters treating sewage sludge or mixture of sewage sludge and food waste
									Uncultured archaeon clone (HM639831.1)	99	Activated sludge wastewater treatment plant
	4	XX	XX		XX		XX		Uncultured Methanosarcinales (JX023115.1)	99	Sludge samples of anaerobic digesters treating sewage sludge or mixture of sewage sludge and food waste
									Uncultured archaeon clone (HM639858.1)	99	Activated sludge wastewater treatment plant
									Uncultured archaeon clone (KT167063.1)	99	Anaerobic digestion of food waste

Chapter 7

Taxonomic placement (50% confidence level)	Band No.	I	R2 Stage1	R1 Stage1	R2 Stage 2	R1 Stage 2	R2 Stage 3	R1 Stage 3	Closest relatives in Blast Name (Accession No.)	Similarity (%)	Source of origin
	5	XXX	XXX		XXX		XXX		Uncultured Methanosarcinales (KF198726.1)	99	Mesophilic anaerobic digester which treats municipal wastewater sludge
									Uncultured archaeon clone (HM639848.1)	99	Activated sludge wastewater treatment plant
	6	XX	XX		XX		XX		Uncultured Methanosarcinales (JX023115.1)	99	Sludge samples of anaerobic digesters treating sewage sludge or mixture of sewage sludge and food waste
	7						X		Uncultured Methanosarcinales (CU916091.1)	96	Mesophilic anaerobic digester which treats municipal wastewater sludge
	8	X		XX		XX		XX	Uncultured Methanosarcinales (KF198646.1)	95	Mesophilic anaerobic digester which treats municipal wastewater sludge
	9			XX		XX		XX	Uncultured Methanosarcinales (CU916091.1)	94	Mesophilic anaerobic digester treating municipal wastewater sludge
Order <i>Methanomicrobiales</i>											
Family <i>Methanospirillaceae</i>											
Genus <i>Methanospirillum</i>											
	9			XX		XX		XX	Uncultured Methanomicrobiales (CU916161.1)	99	Mesophilic anaerobic digester which treats municipal wastewater sludge
									Uncultured archaeon isolate (KJ402292.1)	99	Mesophilic reactor treating municipal sewage sludge under anaerobic and microaerobic conditions
									Uncultured Methanomicrobiales (KF198627.1)	99	Mesophilic anaerobic digester treating municipal wastewater sludge
	10	X	X	XX	XX	XX	XX	XX	Uncultured Methanomicrobiales (KF198791.1)	99	Mesophilic anaerobic digester treating municipal wastewater sludge
									Uncultured archaeon isolate (KJ402292.1)	99	Mesophilic reactor treating municipal sewage sludge under anaerobic and microaerobic conditions
									Uncultured archaeon (FN547108.1)	99	Mesophilic biogas reactor fed with beet silage

Chapter 7

Taxonomic placement (50% confidence level)	Band No.	I	R2 Stage1	R1 Stage1	R2 Stage 2	R1 Stage 2	R2 Stage 3	R1 Stage 3	Closest relatives in Blast Name (Accession No.)	Similarity (%)	Source of origin
	11	X	XX	XXX	X	XXX	XX	XXX	Uncultured Methanomicrobiales (CU916161.1)	99	Mesophilic anaerobic digester which treats municipal wastewater sludge
									Uncultured archaeon isolate (KJ402288.1)	99	Mesophilic reactor treating municipal sewage sludge under anaerobic and microaerobic conditions
									Uncultured archaeon isolate (KJ402292.1)	99	Mesophilic reactor treating municipal sewage sludge under anaerobic and microaerobic conditions
Family <i>Methanomicrobiaceae</i>	12	X	X	XX	X	XX	X	X	Uncultured archaeon isolate (KJ402293.1)	96	Mesophilic reactor treating municipal sewage sludge under anaerobic and microaerobic conditions
Genus <i>Methanoculleus</i>	13		XX	XXX	XXX	XXX	XXX	XXX	Uncultured Methanomicrobiales (CU917425.1)	99	Mesophilic anaerobic digester which treats municipal wastewater sludge
									Uncultured archaeon isolate (KJ402293.1)	99	Mesophilic reactor treating municipal sewage sludge under anaerobic and microaerobic conditions
									Uncultured Methanomicrobiales (KF198785.1)	99	Mesophilic anaerobic digester treating municipal wastewater sludge
Family <i>Methanoregulaceae</i> Genus <i>Methanolinea</i>	14	XXX	XX		XX		XX		Uncultured Methanomicrobiales (CU917018.1)	99	Mesophilic anaerobic digester which treats municipal wastewater sludge
									Uncultured Methanomicrobiales (JX023133.1)	99	Sludge samples of anaerobic digesters treating sewage sludge or mixture of sewage sludge and food waste
									Uncultured Methanomicrobiales (KF198547.1)	99	Mesophilic anaerobic digester treating municipal wastewater sludge
	15	XXX	XX		XX	X	XX	XX	Uncultured Methanomicrobiales (CU917018.1)	97	Mesophilic anaerobic digester which treats municipal wastewater sludge

Chapter 7

Taxonomic placement (50% confidence level)	Band No.	I	R2 Stage1	R1 Stage1	R2 Stage 2	R1 Stage 2	R2 Stage 3	R1 Stage 3	Closest relatives in Blast Name (Accession No.)	Similarity (%)	Source of origin
Class <i>Methanobacteria</i>											
Order <i>Methanobacteriales</i>											
Family <i>Methanobacteriaceae</i>											
Genus <i>Methanobacterium</i>											
	16	XX		XXX		X		X	Uncultured archaeon clone (LN874179.1)	99	Mesophilic lab-scale biogas reactor
									Uncultured archaeon clone (KF670333.1)	99	Anaerobic digester sludge at mesophilic conditions
									Uncultured archaeon clone (EU926765.1)	99	Anaerobic biogas reactor fed with corn silage
Phylum <i>Paecearchaeota</i>											
Genus <i>Paecearchaeota Incertae</i>											
<i>Sedis AR13</i>											
	17				XX			XX	Uncultured archaeon clone (KX856562.1)	97	Upland soil
	18	X	XX	XX	XX	XX	XXX	XXX	Uncultured archaeon isolate (JF937221.1)	97	Anaerobic fluidized bed reactor treating vinasse
	19	XX	XX	XX	XX	XX	XX	XXX	Uncultured archaeon isolate (JF937221.1)	97	Anaerobic fluidized bed reactor treating vinasse
	20	XX				XX		XX	Uncultured archaeon isolate (JF937221.1)	96	Anaerobic fluidized bed reactor treating vinasse
	21	XXX	XX	XX	XX	XX	XXX	XXX	Uncultured archaeon isolate (JF937221.1)	96	Anaerobic fluidized bed reactor treating vinasse
	22		X	X			XX	XX	Uncultured archaeon (KX856574.1)	95	Upland soil

Table 30. RDP classification of the bacterial DGGE bands sequenced with a 50% of confidence level, and corresponding matches according to the BLAST search tool, with their similarity percentages, and environments from which they were retrieved. Intensity < 20 = x, 20 ≤ intensity ≤ 100 = xx, intensity > 100 = xxx. Liquid samples from inoculum (I), upgrading reactor (R1) and control reactor (R2) during stages 1-3.

Taxonomic placement (50% confidence level)	Band No.	I	R2 Stage1	R1 Stage1	R2 Stage 2	R1 Stage 2	R2 Stage 3	R1 Stage 3	Closest relatives in Blast Name (Accession No.)	Similarity (%)	Source of origin
Phylum Proteobacteria											
Class Deltaproteobacteria	1	XXX	XX	X	XXX	XXX	XXX	XX	Uncultured bacterium (CT574164.1)	90	Anaerobic sludge digester
Order Syntrophobacterales											
Family Syntrophaceae	2	XXX	XX		XX		XX		Uncultured Deltaproteobacteria (CU926157.1) Bacterium enrichment culture (FJ799158.1)	99	Mesophilic anaerobic digester which treats municipal wastewater sludge
									Uncultured bacterium (KF493716.1)	99	Anaerobic digestion systems containing propionate inoculated with sludge sample from cassava wastewater treatment plant
	3	XX	XX	XXX	XX	XXX	XX	XXX	Uncultured bacterium (KT797921.1)	99	Diversity of Microbial Community Responsible for Intermediates Degradation in Anaerobic Digestion System as Determined by 16S rDNA Sequence Analysis
	4			XX		XX		XX	Uncultured bacterium (KU648653.1)	97	Anaerobic reactor inoculated with sludge coming from a mesophilic WWTP anaerobic reactor
Phylum Firmicutes											
Class Clostridia											
Order Clostridiales	5	XX	XX	XX	X	XX	XX	XX	Uncultured Firmicutes (CU917543.1)	97	Anaerobic full-scale reactors
	6					X	XX		Uncultured Firmicutes (CU922958.1)	93	Mesophilic anaerobic digester which treats municipal wastewater sludge

Chapter 7

Taxonomic placement (50% confidence level)	Band No.	I	R2 Stage1	R1 Stage1	R2 Stage 2	R1 Stage 2	R2 Stage 3	R1 Stage 3	Closest relatives in Blast Name (Accession No.)	Similarity (%)	Source of origin
Family <i>Peptostreptococcaceae</i>	7	XX	XX	XX	XX	XX	XX	XX	Uncultured bacterium (KT834801.1)	95	Activated sludge
Phylum <i>Verrucomicrobia</i>											
Class Subdivision 5	8	X	X	X	X	X	X	X	Uncultured bacterium (KT798190.1)	93	Anaerobic reactor inoculated with sludge coming from a mesophilic WWTP anaerobic reactor
	9	X	X	X	X	X	X	X	Uncultured bacterium (KT798190.1)	92	Anaerobic reactor inoculated with sludge coming from a mesophilic WWTP anaerobic reactor
Phylum <i>Lentisphaerae</i>											
Class Oligosphaeria											
Order <i>Oligosphaerales</i>											
Family Oligosphaeraeaceae											
Genus Oligosphaera	10	X		X		X		X	Uncultured bacterium (KU648738.1)	99	Anaerobic full-scale reactors
									Uncultured bacterium (KT797693.1)	99	Anaerobic reactor inoculated with sludge coming from a mesophilic WWTP anaerobic reactor
	11	XX	XX	XX	XX	XX	XX	XX	Uncultured bacterium (KU651683.1)	97	Anaerobic full-scale reactors
Phylum <i>Actinobacteria</i>											
Class Actinobacteria											
Order Actinomycetales	12	XX	XXX	XX	XX	X	XX	XX	Uncultured bacterium (KT798074.1)	98	Anaerobic reactor inoculated with sludge coming from a mesophilic WWTP anaerobic reactor
									Uncultured Actinobacteria (CU926089.1)	98	Mesophilic anaerobic digester which treats municipal wastewater sludge
									Uncultured bacterium (EF029280.1)	98	Dewatered class B biosolids stabilized by anaerobic mesophilic digestion

Chapter 7

Taxonomic placement (50% confidence level)	Band No.	I	R2 Stage1	R1 Stage1	R2 Stage 2	R1 Stage 2	R2 Stage 3	R1 Stage 3	Closest relatives in Blast Name (Accession No.)	Similarity (%)	Source of origin
	13	XX							Uncultured Propionibacteriaceae (EU812987.1)	93	Biogas reactor fed with corn silage
Phylum Acidobacteria											
Class <i>Acidobacteria_Gp23</i>											
Genus <i>Thermoanaerobaculum</i>	14	XX	XX	XX	XX		XX		Uncultured bacterium (KT797190.1)	97	Anaerobic reactor inoculated with sludge coming from a mesophilic WWTP anaerobic reactor
Phylum Cloacimonetes											
Genus <i>Candidatus cloacamonas</i>	15	XX	XX	XXX	XX	XX	XX	XX	Uncultured bacterium (CU918359.1)	99	Mesophilic anaerobic digester which treats municipal wastewater sludge
Unclassified Bacteria											
	16	X	XXX	XXX	XXX	XX	XX	XX	Uncultured bacterium (KU648637.1)	96	Anaerobic full-scale reactors
	17	XX	XX	XXX	XX	XXX	XXX	XXX	Uncultured bacterium (CT574225.1)	91	Evry municipal wastewater treatment plant
	18	XX	XXX	XXX	XX	XX	XX	XXX	Uncultured bacterium (KT797785.1)	91	Anaerobic reactor inoculated with sludge coming from a mesophilic WWTP anaerobic reactor

High *archaea* richness and evenness found with Shannon-Wiener diversity index ranged between 3.2 and 3.4 (close to the upper range value of 3.5) in R1, having the maximum value in the last stage of the experiment with the highest gas recirculation rate (Figure 46 a). For *archaea*, H index of R1 was similar, but always slightly higher than the diversity index obtained in the inoculum and in R2 during the experiment. The diversity indices calculated from the bacterial DGGE gel were in the range of 3.2 to 3.3 in R1, showing a high bacterial richness and evenness (Figure 46 b). For bacteria, the diversity index of R1 was similar but always slightly lower to the H index obtained in the inoculum and in R2 during the experiment.

The liquid samples from the control reactor presented high similarity indices of *archaea* during the experiment in comparison with the inoculum as expected due to the same operating conditions in both cases (Table 31). During the different stages of the experiment in R2 the similarity indices were high and not so different (Table 31), indicating the maintenance of *archaea* population in the reactor over the time. In the upgrading reactor, similar high similarity indices were found between stage 1 and 2, and stage 2 and 3, although the gas recirculation rate was increased, in contrast to stage 1 and 3 for which the similarity index was significantly lower (Table 31).

Table 31. Archaeal similarity indices (%) between the liquid samples from inoculum (I), upgrading reactor (R1) and control reactor (R2) during stages 1-3.

	I	R2.1	R1.1	R2.2	R1.2	R2.3	R1.3
I	100	87.8	36.9	82.5	59.8	78.3	77.0
R2.1	-	100	57.9	96.0	79.1	92.4	86.3
R1.1	-	-	100	60.4	83.6	50.7	51.4
R2.2	-	-	-	100	82.2	96.2	89.1
R1.2	-	-	-	-	100	78.6	81.5
R2.3	-	-	-	-	-	100	93.5
R1.3	-	-	-	-	-	-	100

Comparing stage-by-stage similarity index of *archaea* found in R1 and R2 samples, it can be observed not only the highest difference in stage 1 as a result of the injection of H₂ in the upgrading reactor but also an increasing trend in stages 2 and 3 (Table 31). This increasing *archaea* similarity trend between R1 and R2 and the decreasing

similarity values in R1 cannot link with the increasing H₂ utilization efficiency obtained during the operation of the reactors described previously. These values might be explained by the appearance of a biofilm (not analyzed), around the hollow-fiber membrane module (Figure 47), which was likely to be created after stage 1, where some hydrogenotrophic *archaea* population potentially could be accumulated near the H₂ source and were responsible for the high process bioconversion.



Figure 47. Biofilm found around the hollow-fiber membrane module.

Kougias et al. (2017) reported the dominance of a hydrogenotrophic *archaea* in the biofilm formed on top of the H₂ diffuser surface for an ex-situ biogas upgrading experiment. However, the biofilm formed on the hollow-fiber membrane module employed by Luo and Angelidaki (2013a) was found not to be beneficial to the process since it increased the resistance of H₂ diffusion to the liquid. In their study, it was also demonstrated that the biofilm formed on the membrane only contributed 22-36% to the H₂ consumption, while most of the H₂ was consumed by the microorganisms in the liquid phase.

Thus, to ensure the contribution of the biofilm to H₂ consumption and CH₄ production, further research on in-situ biogas upgrading membrane bioreactors should focus on

the biofilm microbial analysis. In addition, further studies should include the determination of H₂ consumption rate by the biofilm formed on the membrane.

When compared to the inoculum, the liquid samples from the control reactor showed high similarity indices of bacteria during the experiment, with the same being observed in the upgrading reactor (Table 32). The similarity index of bacteria in R2 during the three experiment stages was high without too many differences indicating the bacteria population maintenance over the experiment time (Table 32). In this case, R1 showed the same behavior in bacteria similarity index having not significant bacteria population changes (Table 32).

Table 32. Bacterial similarity indices (%) between the liquid samples from inoculum (I), upgrading reactor (R1) and control reactor (R2) during stages 1-3.

	I	R2.1	R1.1	R2.2	R1.2	R2.3	R1.3
I	100	79.8	76.7	88.1	73.8	92.0	75.5
R2.1	-	100	82.8	78.0	68.9	82.3	76.7
R1.1	-	-	100	76.8	84.4	81.7	88.9
R2.2	-	-	-	100	80.4	96.3	86.0
R1.2	-	-	-	-	100	79.7	90.1
R2.3	-	-	-	-	-	100	86.0
R1.3	-	-	-	-	-	-	100

By comparing bacteria similarity index of R1 and R2 liquid samples, high similar values were observed (Table 32). However, it cannot be stated that H₂ injection had no effect on the bacteria population due to limitations of the employed microbial analysis techniques in the study. It was possible that differences in the bacterial community could have not been properly detected.

Thus, further studies should use Next Generation Sequencing (NGS) techniques to evaluate the effect of H₂ injection to anaerobic digestion of sewage sludge on bacteria community.

Archaea and bacteria were detected by FISH in all liquid samples tested for both reactors. FISH micrographs can be found in Figure 48. *Archaea* appear red due to hybridization with the ARCH915 probe (red) while bacteria appear green due to hybridization with the EUB338 I and EUB338 plus probes (green) and DAPI (cyan).

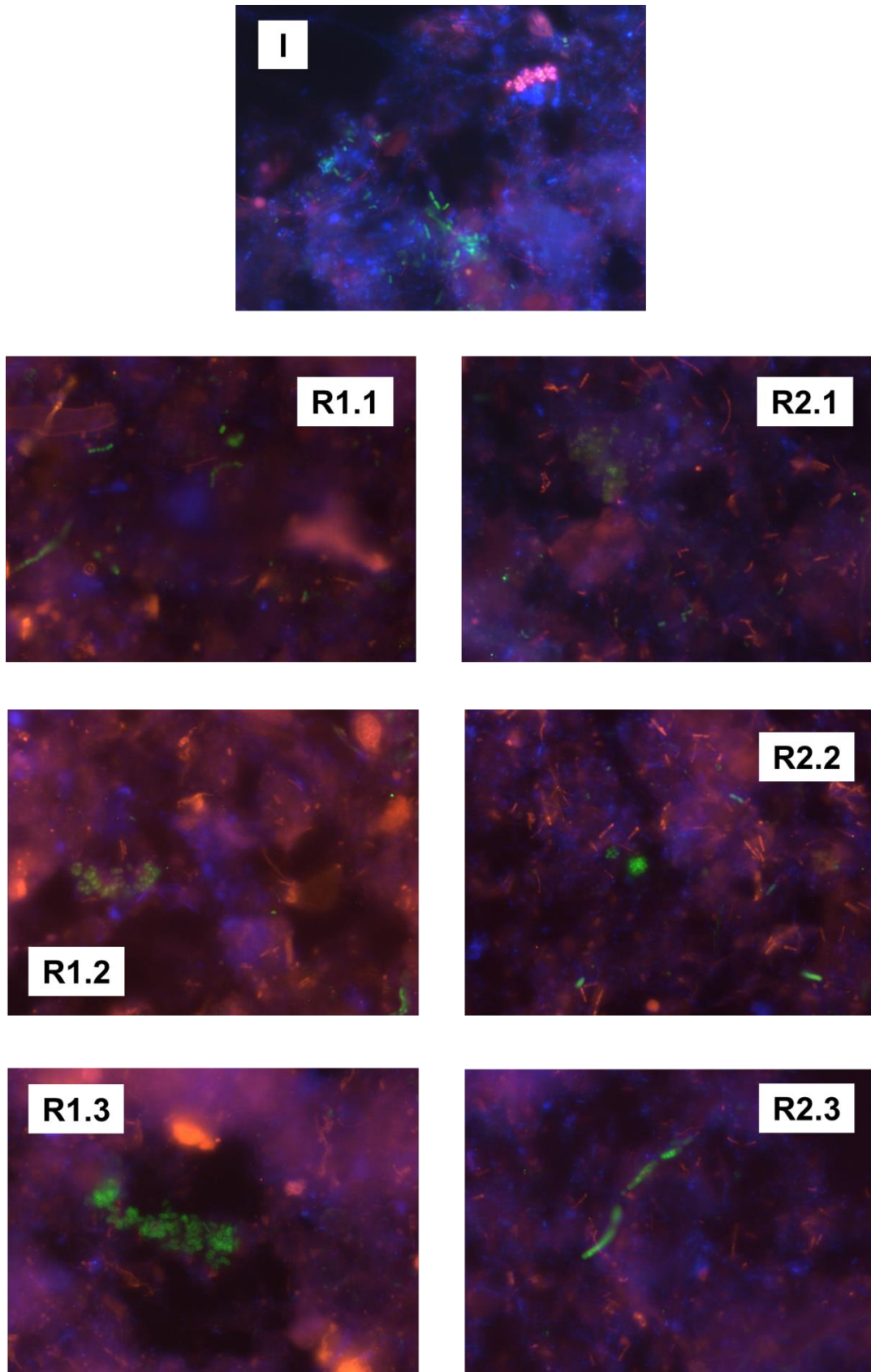


Figure 48. FISH micrographs 100x of *archaea* and bacteria during the experiment. Samples: inoculum (I), upgrading reactor (R1) and control reactor (R2), stages 1-3.

In the inoculum, *archaea* accounted for 10.48% of the microbial population, while bacteria represented 10.24%, with an *archaea*/bacteria ratio of 50.58% where any of both was predominant against the other. After the set-up period and during the different stages of the experiment in R1 and R2 both *archaea* and bacteria content experienced a slow progressive increase up to values of 16.92% and 16.61%, respectively, for R1 and 17.06% and 16.76%, respectively, for R2 but maintaining the *archaea*/bacteria ratio in close range in comparison to the inoculum.

This finding may be explained by the previously mentioned appearance of biofilm around the hollow-fiber membrane module which could concentrate hydrogenotrophic *archaea* due to the easy physical availability of H_2 thus not being in the liquid phase where samples were taken for FISH analysis.

7.4 CONCLUSIONS

Biological biogas upgrading by coupling CO_2 with external H_2 to upgrade methane was feasible in a mesophilic anaerobic digester of sewage sludge.

At H_2 loading rate of $0.87 L_{H_2}/L_R \cdot d$ and gas recirculation rate of $202 L/L_R \cdot d$, 94% efficiency in H_2 utilization was found. Under these rates, H_2 injection resulted in CH_4 production rate of $0.54 L_{CH_4}/L_R \cdot d$, which is a 42% increase in CH_4 production in comparison with the anaerobic digestion of sewage sludge and 73% CH_4 content was achieved in the biogas.

The biodegradation potential of the upgrading reactor was not compromised by H_2 supply or by the high pH level (8.1). No inhibition was observed indicating adaptation of microorganisms to higher pH levels.

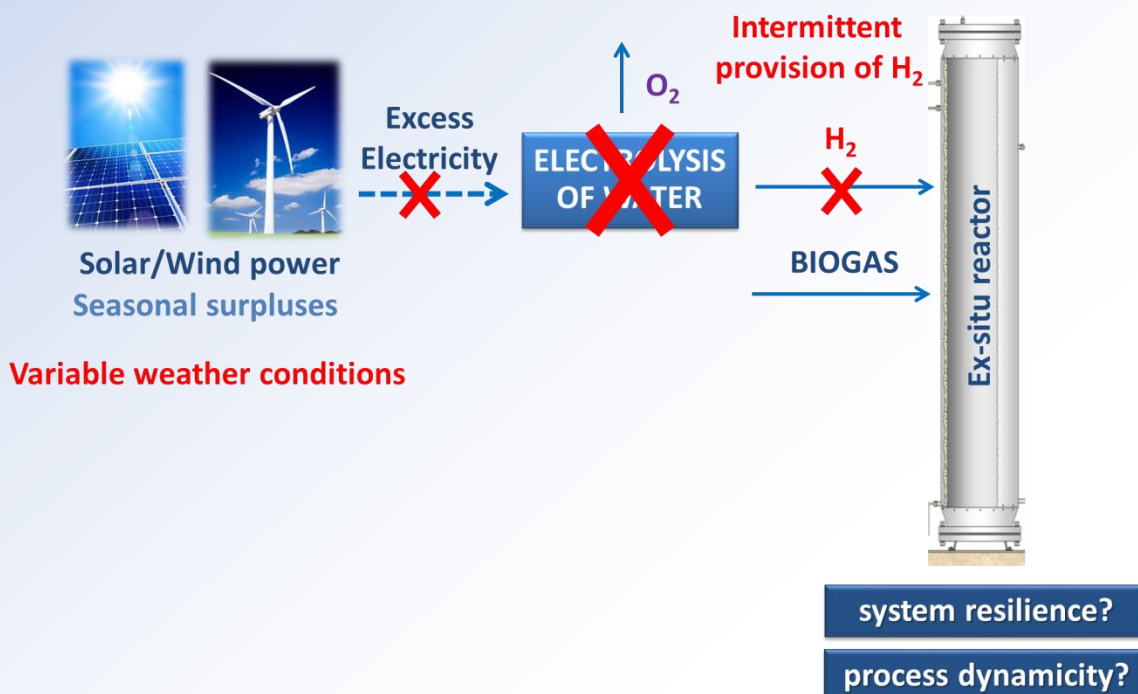
Hollow-fiber MBR showed good H_2 mass transfer capacity, reaching a $k_L a_{H_2}$ value of $25 h^{-1}$. Gas recirculation improved the H_2 gas-liquid mass transfer significantly and seemed to have a positive effect on the in-situ biomethanation when OLR increased.

VFA accumulation was not observed and H₂ rate converted to CH₄ showed an increasing trend over the experiment. Dewaterability of the sludge was negatively impacted by the turbulence caused by the high gas recirculation rate.

H₂ had influence on community composition and hydrogenotrophic methanogens outcompeted homoacetogens. *Methanoculleus* sp., *Methanospirillum* sp., *Methanolinea* sp. and *Methanobacterium* sp. were the hydrogenotrophic *archaea* present over the experiment.

Chapter 8

Intermittent provision of H_2 in up-flow reactors for ex-situ biogas upgrading



8.1 INTRODUCTION

Due to the fact that H₂ assisted biogas upgrading technology is based on the surplus of renewable electricity generated by wind or solar power, the system should be resilient to the natural variability of weather conditions and thus to different input H₂ flow rates even to the lack of H₂.

As mentioned in Chapter 1, some studies affirm that dormant cultures can be quickly reactivated in large-scale AD systems and that methanogens can be fed intermittently (Lettinga, 1995; Martin et al., 2013) and some introductory tests have been conducted in ex-situ biogas upgrading systems with TBF reactor configurations at thermophilic and mesophilic conditions, with one and three days of H₂ suspension, respectively (Strübing et al., 2017; Burkhardt et al., 2015). Moreover, in the experiment described in the Chapter 6, a preliminary test was performed in which the gas feed was interrupted for 22 h.

In all these tests, the system recovered the initial steady-state conditions of CH₄ content and production quickly. However, it is mandatory to elucidate the biomethanation efficiency during intermittent provision of H₂ in longer and repeated H₂ intermittent periods in order to perform the scaled up, a challenge of the biogas upgrading technology not studied yet.

The aim of the current work is to study the intermittent addition of H₂ for ex-situ biogas upgrading in order to evaluate the dynamicity of the process simulating real-cases during which renewable electricity is a temporary surplus. Different H₂ stop-feeding periods were experienced in three ex-situ up-flow reactors in a range of 1, 2 and 3 weeks. The reproducibility was assessed performing three replicates of H₂ stop-feeding periods in each reactor. The dispersion of gases in the reactors was performed using stainless steel diffusers combined with ceramic sponges. Microbial communities populating the upgrading reactors were studied during the different experimental stages to elucidate their plasticity against the lack of H₂.

8.2 MATERIALS AND METHODS

8.2.1 Reactors

The description of the reactors used in the experiment has been performed in Chapter 3, section 3.1.2.2. As previously mentioned, the experiment was performed using the same up-flow reactor configuration for three reactors (R1, R2 and R3) with working volume of 1.0 L for each setup. Each reactor was equipped with two stainless steel diffusers and two inert alumina ceramic sponges used as gas sparging surface.

8.2.2 Operating conditions

The three reactors were inoculated with an active enriched hydrogenotrophic thermophilic inoculum obtained from a previous ex-situ biogas upgrading reactor (Bassani et al., 2017) with the aim of having shorter set-up period. The chemical composition, elemental analysis and trace elements of the inoculum are given in Table 33 and Table 34.

The digestate used as nutrient solution was obtained from Snertinge biogas plant (Denmark). After arrival to the laboratory, the digestate was sieved using a 2 mm net in order to remove large particles and then stored at 55 °C at anaerobic conditions in 5 L bottles. The bottles were kept in one incubator at thermophilic conditions for two months in order to be completely degassed.

The chemical composition, elemental analysis and trace elements content of the digestate used as nutrient solution are shown in Table 33 and Table 34.

Before its use, pH was adjusted to 7.00 ± 0.04 in the digestate by the addition of approximately 3.5-4 mL of H_3PO_4 (34% vol) per 400 mL. Nutrient solution was introduced to the reactors from their bottom part with HRT of 50 d.

Table 33. Chemical composition of initial inoculum and digestate used as nutrient solution.

Parameter	Inoculum	Nutrient solution
pH	8.60±0.01	8.75±0.13
Total solids (g/L)	9.72±0.03	19.28±0.06
Volatile solids (g/L)	4.28±0.01	9.20±0.05
Total suspended solids (g/L)	7.70±0.28	11.51±0.45
Volatile suspended solids (g/L)	6.7±0.21	7.20±0.35
Total Kjeldahl nitrogen (g-N/L)	1.52±0.06	1.89± 0.02
Ammonium nitrogen, NH ₄ ⁺ (g-N/L)	1.53±0.02	1.63± 0.04
Total VFA (mg/L)	74.39±3.10	29.90±0.94
Acetate (mg/L)	60.34±3.37	29.90±0.94
Propionate (mg/L)	9.62±0.59	0.00±0.00
Iso-butyrate (mg/L)	0.48±0.07	0.00±0.00
Butyrate (mg/L)	3.35±0.38	0.00±0.00
Iso-valerate (mg/L)	0.28±0.12	0.00±0.00
Valerate (mg/L)	0.00±0.00	0.00±0.00
Hexanoate (mg/L)	0.32±0.12	0.00±0.00

Table 34. Elemental analysis and trace element content in the initial inoculum and in the digestate used as nutrient solution. N, C, H and S are expressed as % while the rest of the elements are expressed as mg/Kg of dry matter. DL= Detection Limit.

Element	Inoculum	Nutrient solution
N	6.31±0.06	5.01±0.41
C	25.51±0.56	23.55±0.48
H	4.45±0.02	3.35±0.17
S	5.02±0.19	4.77±0.34
Al	432±20	371±9
Ba	37±1	33±0
Ca	32039±157	26932±187
Co	481±4	46±0
Cu	197±2	215±2
Fe	3668±161	1925±55
K	88280±3427	118549±2471
Mg	11171±162	11851±398
Mn	318±3	305±9
Na	33748±339	17264±92
Ni	276±3	31±0
P	10770±38	13385±348
Sr	155±9	133±1
Zn	86±5	< DL

After the inoculation, a set-up period was performed in R1, R2 and R3 at thermophilic conditions by supplying a gas mixture of H₂, CO₂ and CH₄ with ratio 62:15:23 (%) at gas input rate of 2.23 L/L_R·d (H₂ loading rate of 1.38 L_{H₂}/L_R·d) and gas recirculation rate of 122.39 L/L_R·d for 5 d. Afterwards, the experiment started maintaining thermophilic conditions and the gas recirculation rate, with a gas retention time of 12 h.

During the experiment, each reactor experienced two different kind of experimental periods regarding H₂ intermittency: normal feeding period where H₂ was supplied to the reactors representing a normal ex-situ biogas upgrading period and H₂ stop-feeding period with no H₂ source simulating lack of H₂ as a consequence of no surplus of renewable energies. H₂ stop-feeding period was 1, 2 and 3 weeks to R1, R2 and R3, respectively. Three replicate H₂ stop-feeding periods were experienced in each up-flow reactor to assess the reproducibility of the process (Table 35).

Table 35. Operating conditions studied during the experiment.

Period	Feeding H₂/CO₂/CH₄ (%)	R1 Days	R2 Days	R3 Days
Set-up	62/15/23	0-5	0-5	0-5
First H₂ stop	0/40/60	6-12	6-19	6-26
Normal feeding	62/15/23	13-26	20-40	27-47
Second H₂ stop	0/40/60	27-33	41-54	48-68
Normal feeding	62/15/23	34-47	55-72	69-85
Third H₂ stop	0/40/60	48-54	73-86	86-104
Normal feeding	62/15/23	55-71	87-103	105-122

The gas input rate was maintained at 2.23 L/L_R·d during the whole experiment and the input gas mixture was composed of 15 % CO₂ and 60% H₂ according to the stoichiometry of hydrogenotrophic methanogenesis reaction (1:4, Eq. 1), 23% CH₄ in order to simulate typical biogas composition (40% CO₂ and 60% CH₄) and 2% extra H₂ as ground gas which was expected to remain unutilized during the normal feeding periods while a gas mixture of 40% CO₂ and 60% CH₄ was the input gas mixture during the H₂ stop-feeding periods.

8.2.3 Monitoring and experimental analysis

The following parameters (Table 36) were monitored and analyzed during the experiment according to the materials and methods described in Chapter 3, section 3.3. All analyses were done in duplicate samples.

Table 36. Parameters monitored and analyzed during the study.

Parameter	Measuring frequency
Headspace pressure	Continuous mode
Temperature	
Gas production rate	Daily
Gas composition	
VFA concentration	Twice per week
pH	

pH, VFA, TS, VS, TSS, VSS, TKN, NH_4^+ , elemental and trace elements analysis were determined according to the materials and methods described in Chapter 3, section 3.3 in order to characterize the inoculum and the digestate used as nutrient solution.

8.2.4 Calculations

Calculations about efficiency of H_2 utilization (η_{H_2}), CO_2 conversion efficiency (η_{CO_2}), CH_4 production rate and methane yield (Y_{CH_4}) have been performed following the calculations described in Chapter 3, section 3.5 while specific gas transfer coefficient ($k_L a_{\text{H}_2}$) was calculated according to Eq. 3 of Chapter 1.

H_2 utilization rate for microbial growth ($L_{\text{H}_2}/L_R \cdot d$) was estimated as the gap between H_2 loading rate (input) and the sum of H_2 rate and CH_4 as equivalent H_2 in the produced gas (output gas) according to Eq. 43:

$$H_2 \text{ rate to growth} = H_2 \text{ loading rate} - H_2 \text{ rate in output gas} - 4 \cdot CH_4 \text{ production rate} \text{ (Eq. 43)}$$

where H_2 loading rate ($L_{\text{H}_2}/L_R \cdot d$), H_2 rate in output gas ($L_{\text{H}_2}/L_R \cdot d$) and CH_4 production rate ($L_{\text{CH}_4}/L_R \cdot d$) were calculated according to the equations (Eq. 11, Eq. 12 and Eq. 23, respectively) described in Chapter 3, section 3.5 and 4 is the stoichiometric coefficient according to Eq. 1.

8.2.5 Microbial community analysis

In order to elucidate the plasticity of the microbial communities populating the upgrading reactors against the lack of H₂, samples were collected. Initially, a sample of the inoculum was taken before starting the experiment (1) and then several liquid samples (1-7) from each reactor were collected just at the end of each different experimental period to identify the microbial dynamics (Figure 49).

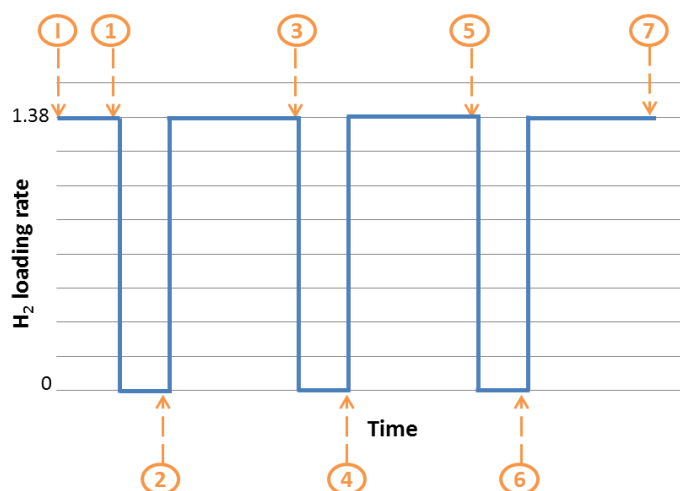


Figure 49. Sampling points in each reactor throughout the experiment for microbial analysis.

Extraction of genomic DNA of samples in triplicates and 16S rRNA gene sequencing analysis was performed according to the materials and methods described in Chapter 3, sections 3.4.1. and 3.4.4.

8.3 RESULTS AND DISCUSSION

During the first day of the experiment in the set-up period, foam was generated inside the three reactors as a consequence of the gas diffusion application which was suppressed by itself in all of them after one day.

The digestate used as nutrient solution had no residual biogas production as it had been previously degassed without any final effect on CH₄ production or VFA accumulation at all. In addition, its pH adjustment with H₃PO₄ from its high initial value of 8.75 ± 0.13 to a final value of 7.00 ± 0.04 was necessary before its use during the whole experiment in order to be within the optimum range for methanogenesis.

The three reactors, after the H₂-stop periods and once they recovered the previous initial conditions of CH₄ (production rate and content), were working some more days with H₂ source to assure reproducible and stable results before starting the next period of the experiment.

8.3.1 Performance of reactor 1

In the set-up period, CH₄ content increased from 23.0% in the input gas to 95.4% in the output flow in R1 achieving steady-state conditions in terms of stable methane production and composition in a short period of time (1 d). Approximately 2% H₂ in R1 remained unutilized and was recorded in the output gas (Table 37).

Average η_{H_2} , η_{CO_2} , Y_{CH_4} , pH and $k_L a_{H_2}$ values observed during the set-up period are shown in Table 37. Total VFA concentration decreased significantly being only composed by acetate and butyrate (Table 37). Average H₂ utilization rate for microbial growth was 0.07 L_{H₂}/L_R·d.

On day 6, the first H₂ stop-feeding period was applied by the only injection of CO₂ and CH₄ as gas feeding for a week and then (on day 13) R1 was fed again with the gas mixture containing H₂. Two more repetitions of these H₂ stop/start periods were performed according to Table 35.

During the three applied H₂ stop-feeding periods to R1 of one week, CH₄ production rate was approximately zero (Figure 50) and CH₄ content decreased to 61-64% approximately (Figure 51) being only CO₂ (36-39%) the other component of the produced biogas. These results were the expected ones as the gas substrate (H₂) for the bioconversion to CH₄ was not provided during these periods.

In the three replicate periods, as a consequence of lack of H₂ to react with CO₂, pH dropped (Figure 52) to an average range between 7.42±0.05 and 7.71±0.12.

Only during the first stop period, total VFA and acetate concentrations experienced an increase (from 84 to 140 mg/L and from 63 to 114 mg/L, respectively) while in the other two periods total VFA, acetate and butyrate concentrations did not experienced any significant change or accumulation.

Table 37. Performance of the reactors under steady state conditions.

Period	Reactor	Output gas composition (%)			Gas output rate L/L _R ·d	CH ₄ production rate L _{CH₄} /L _R ·d	Y _{CH₄} L _{CH₄} /L _{H₂}	η _{H₂} (%)	η _{CO₂} (%)	k _L a _{H₂} (h ⁻¹)	pH	Total VFA mg/L	Acetate mg/L	Butyrate mg/L
		H ₂	CO ₂	CH ₄										
Set-up	R1	2.3±1.8	2.3±0.5	95.4±1.3	0.87±0.01	0.32±0.01	0.24±0.01	98.7±0.5	96.0±0.1	167±12	8.56±0.13	92±16	63±8	26±4
	R2	3.0±0.8	2.4±0.7	94.6±0.1	0.85±0.04	0.32±0.00	0.24±0.00	98.7±0.4	98.9±0.1	172±7	8.53±0.12	126±15	93±10	32±4
	R3	6.6±0.2	3.4±0.2	90.0±0.0	0.91±0.01	0.30±0.00	0.22±0.00	97.4±0.0	93.4±0.1	87±2	8.53±0.01	138±16	89±15	33±1
First recovery	R1	1.8±0.8	2.8±0.6	95.4±0.6	0.86±0.02	0.31±0.02	0.23±0.01	98.3±0.7	92.4±0.1	167±21	8.57±0.09	77±11	44±0	32±11
	R2	3.6±0.4	1.9±0.1	94.5±0.5	0.88±0.01	0.31±0.00	0.24±0.00	98.4±0.7	95.4±0.7	179±7	8.61±0.06	85±8	55±7	28±1
	R3	6.3±0.3	3.2±0.2	90.5±0.1	0.88±0.01	0.29±0.01	0.21±0.00	95.7±0.1	91.9±0.5	91±2	8.79±0.02	90±13	53±12	25±1
Second recovery	R1	3.1±0.3	2.4±0.3	94.5±0.1	0.89±0.01	0.33±0.01	0.25±0.00	97.7±0.6	92.3±0.1	169±19	8.66±0.09	73±10	36±9	25±0
	R2	2.3±0.4	2.5±0.6	95.2±0.5	0.87±0.01	0.31±0.00	0.23±0.00	99.6±0.2	96.1±0.6	163±21	8.59±0.01	81±36	70±21	11±15
	R3	6.2±0.5	3.7±0.6	90.1±0.4	0.89±0.01	0.29±0.01	0.22±0.01	94.9±0.2	91.0±0.2	90±3	8.23±0.01	100±4	100±4	0±0
Third recovery	R1	3.5±0.6	1.8±0.7	94.7±0.2	0.90±0.05	0.33±0.01	0.25±0.01	97.6±0.3	94.9±1.4	165±19	8.55±0.02	50±1	41±2	9±12
	R2	2.6±0.7	1.6±0.7	95.7±0.6	0.87±0.01	0.32±0.00	0.24±0.00	98.3±0.1	96.4±1.3	180±22	8.54±0.06	60±6	60±6	0±0
	R3	6.3±0.5	3.5±0.4	90.2±0.2	0.88±0.00	0.29±0.00	0.21±0.00	95.8±0.4	91.9±0.1	86±5	8.26±0.13	122±1	109±1	13±1

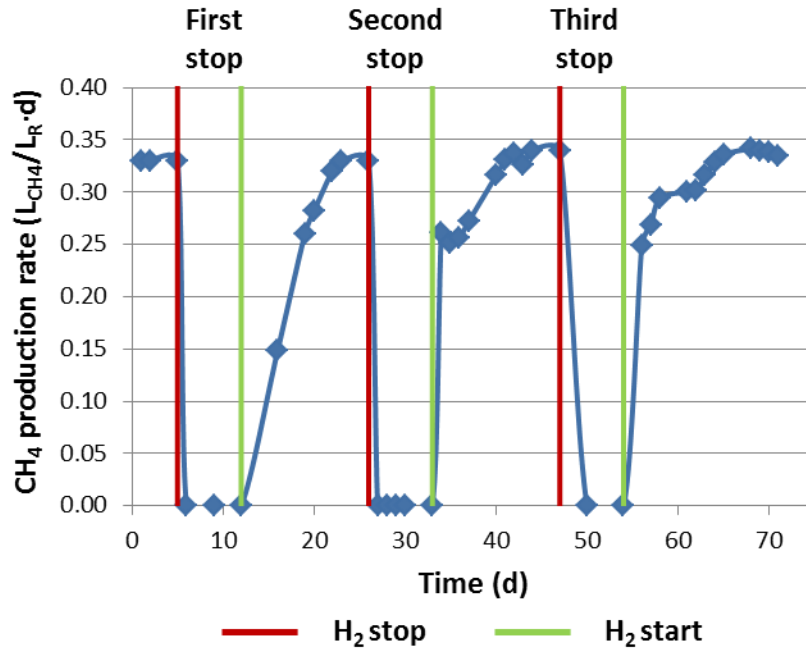


Figure 50. Methane production rate throughout the experiment in R1.

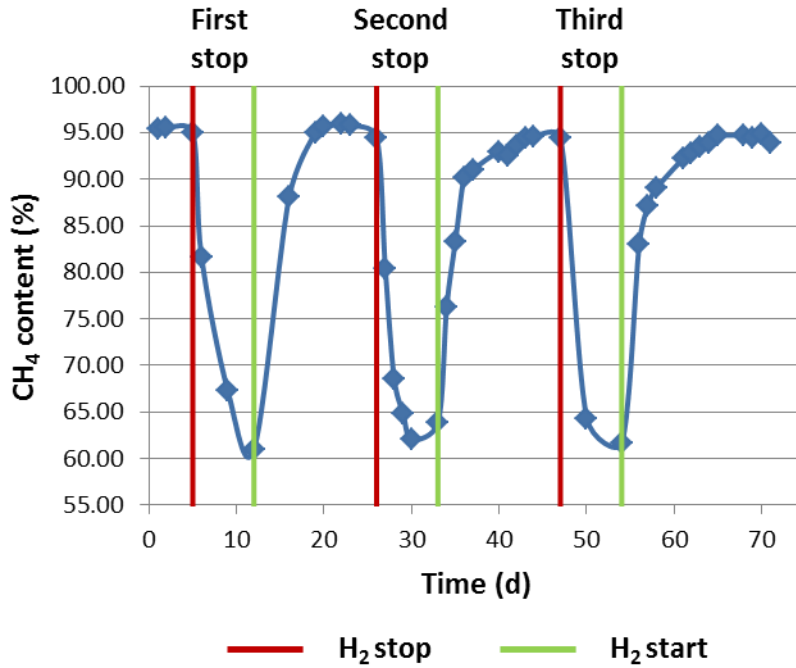


Figure 51. Methane content throughout the experiment in R1.

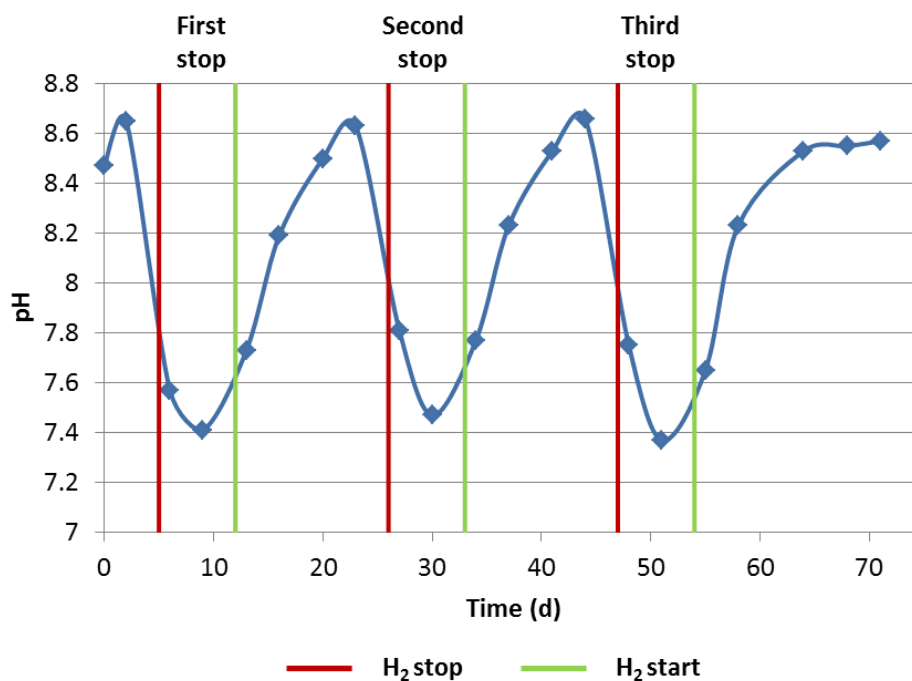


Figure 52. pH evolution throughout the experiment in R1.

After the reinjection of H_2 in the reactor, its transformation to CH_4 coupling with CO_2 took place since the beginning in all the recovery periods experienced.

In the three recovery periods, CH_4 production rate and CH_4 content gradually increased (Figure 50, Figure 51) reaching the initial values obtained during the set-up period (Table 37). The results from the three periods where H_2 was injected again to R1 showed exactly the same required time for the system to recover the initial steady conditions, 7 days (Figure 50, Figure 51).

As it was recorded during the set-up period, approximately 2-3% H_2 in R1 remained unutilized in the output gas in the three periods (Table 37). Approximate η_{H_2} values of 98% were obtained after the recoveries with no substantial differences with the initial efficiency values from the set-up period while slightly lower η_{CO_2} was found (92-95%) after the three recoveries in comparison with the initial value before the three H_2 stops (Table 37).

Y_{CH_4} gradually increased during the three recovery periods reaching the same values than the initial yield obtained during the set-up period (close to the maximum stoichiometric value of $0.25 L_{CH_4}/L_{H_2}$) (Table 37).

During all the recovery periods experienced, H_2 utilization rate for microbial growth dropped progressively throughout the recovery time, from average values of $0.49 L_{H_2}/L_R \cdot d$ at the beginning of the recovery period to $0.08 L_{H_2}/L_R \cdot d$ after the system recovery (close to the set-up value), supporting the gradually increased of Y_{CH_4} .

$k_L a_{H_2}$ values found during the three recovery periods had no significant differences each other or with the previous one obtained in the set-up period (Table 37).

As a result of the reaction of CO_2 with H_2 during these periods, pH experimented an increase in all of them (Figure 52, Table 37) with no biomethanation inhibition despite of high pH level.

Acetate dropped significantly during the first recovery therefore total VFA concentration decreased as well with no remarkable changes in butyrate concentration. During the second and third recovery periods, VFA accumulation took not place. H_2 and CO_2 utilized for VFA production were negligible.

Therefore, the H_2 intermittency had no effect on the capacity of the system to recover the initial CH_4 conditions or in the biomethanation process. The repetition of H_2 lack had not any positive or negative influence on the system recovery to reach the initial steady-state.

8.3.2 Performance of reactor 2

R2 achieved steady state conditions in terms of stable CH_4 (production and composition) in a short period of time (1 d) with an increase in its content from 23.0% in the input gas to 94.6% in the output flow during the set-up period. H_2 was reduced from 62.0% to 3.0% while CO_2 decreased from 15.0% to 2.4% (Table 37).

During the set-up period, η_{H_2} and η_{CO_2} reached 98.7% and 98.9%, respectively, $k_L a_{H_2}$ value was $172 h^{-1}$, Y_{CH_4} was $0.24 L_{CH_4}/L_{H_2}$ and average H_2 utilization rate for microbial growth was $0.07 L_{H_2}/L_R \cdot d$. pH ranged between 8.44 and 8.61 (Figure 53). Total VFA concentration decreased significantly being only composed by acetate and butyrate (Table 37).

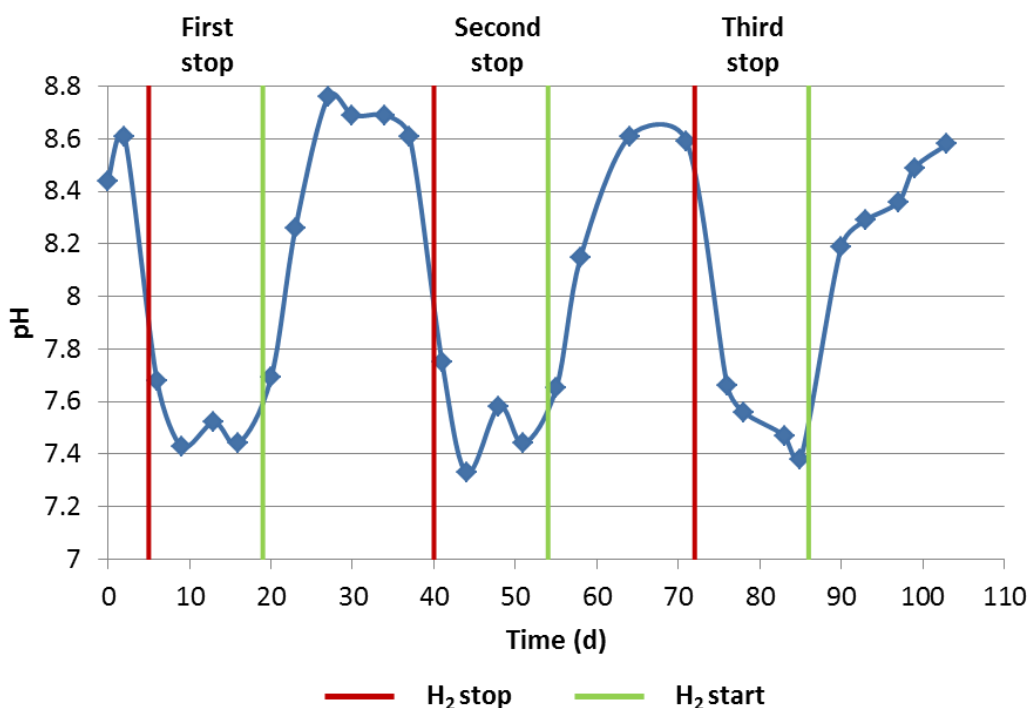


Figure 53. pH evolution throughout the experiment in R2.

On day 6, the first H₂ stop-feeding period was applied by the only injection of CO₂ and CH₄ as gas feeding for 2 weeks.

R2 was fed again with the H₂ gas mixture and the transformation of H₂ and CO₂ took place since the beginning of the period. CH₄ content and CH₄ production rate experienced a gradually increase (Figure 54 and Figure 55) reaching the same values than the initial values before the lack of H₂ (Table 37) after 17 days of H₂ presence in gas feeding. For this first recovery period, similar unutilized H₂ percentage in the output gas, Y_{CH_4} (which showed a gradual increase over the recovery period) and η_{H_2} were found in comparison to the initial values (Table 37) while η_{CO_2} was slightly lower compared to the value before the H₂ stop.

Then, on day 41, the second H₂ stop-feeding period was applied. After this second period of 2 weeks without H₂ source, R2 was fed again with the gas mixture composed by H₂, CO₂ and CH₄ (on day 55).

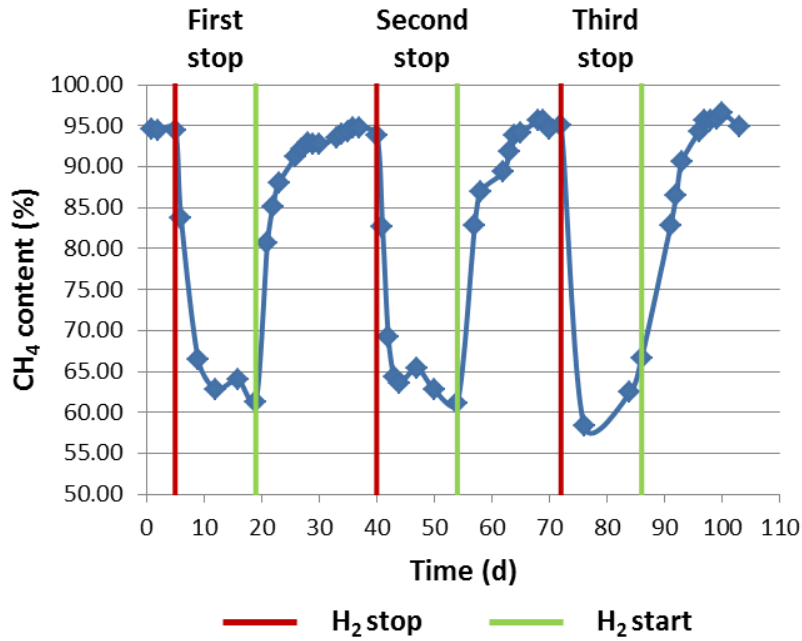


Figure 54. Methane content throughout the experiment in R2.

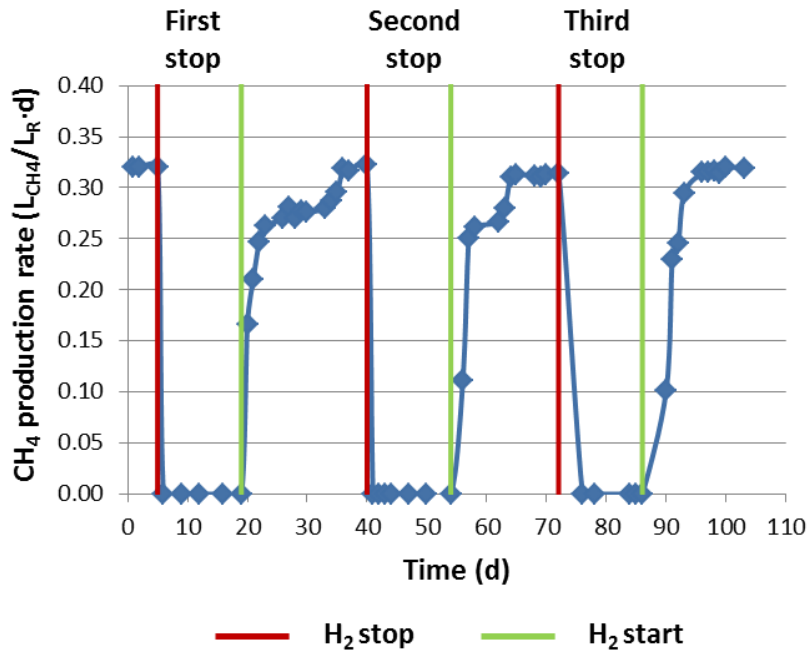


Figure 55. Methane production rate throughout the experiment in R2.

During this new second recovery period, 14 days were needed to R2 in order to recover the 95% CH₄ content in the output flow and the initial CH₄ production rate, 3 days less than the previous recovery time experienced (Figure 54 and Figure 55). It was shown that 99.6% of the injected H₂ was consumed, η_{CO_2} reached 96.1% and Y_{CH_4} was 0.23 L_{CH₄}/L_{H₂}.

On day 73, the last H₂ stop-feeding period was applied. Two weeks later, H₂ was injected again in the reactor, starting then the last period of the experiment (day 87). In this case, only 11 days were needed for recovering the initial steady conditions, the shortest required time for R2. η_{H_2} and η_{CO_2} were 98.3% and 96.4%, respectively, and Y_{CH_4} reached its previous value of 0.24 L_{CH₄}/L_{H₂}.

During the three H₂ stop-feeding periods of 2 weeks performed in R2, CH₄ production rate was zero (Figure 55) and CH₄ content decreased to 62-65% approximately (Figure 54) with CO₂ content of 35-38%.

In the three replicate periods, pH dropped (Figure 53) to a range between 7.38±0.05 and 7.70±0.05 as it was expected because of lack of H₂ to react with CO₂.

Only during the second stop period, total VFA and acetate concentrations experienced an exceptional increase (from 95 to 162 mg/L and from 55 to 131 mg/L, respectively) and subsequently decrease (to 64 and 41, respectively) while in the other two periods total VFA, acetate and butyrate concentrations did not experienced any significant accumulation or change.

The results from the three periods where H₂ was injected again to R2 showed a decreasing trend in the required time for the system to recover the previous initial steady conditions (Figure 54, Figure 55). Particularly, the first recovery in comparison with the second and the third showed a difference of three and six days meaning a reduction of 18% and 35% in the recovery time, respectively.

Therefore, the process was more resilient to the repeated lack of H₂ as more H₂ stop-feeding periods were experienced showing shorter recovery times for the system to reach again the initial steady conditions.

In the three periods after the H₂-stop and the recovery of the system, similar H₂ percentage in the output gas (2-4%), η_{H_2} (98-99%) and Y_{CH_4} (0.23-0.24 L_{CH₄}/L_{H₂}) values were found in comparison to the initial values (Table 37) while η_{CO_2} was slightly lower (95-96%) compared to the value before all the H₂ stops. $k_L a_{H_2}$ values found during the three recovery periods had similar values (Table 37). Biomethanation inhibition took not place despite of high pH level (Table 37, Figure 53). Acetate and total VFA

concentrations were found to be low and stable and butyrate was present in small concentration with a decreasing trend during the experiment and H₂ and CO₂ utilized for VFA production were negligible.

During all the recovery periods experienced and supporting the gradually increased of Y_{CH_4} , H₂ utilization rate for microbial growth dropped progressively throughout the recovery time, from average values of 0.45 L_{H2}/L_R·d at the beginning of the recovery period to 0.09 L_{H2}/L_R·d after the system recovery, slightly higher value compared to the value from the set-up period.

8.3.3 Performance of reactor 3

In the set-up period, CH₄ content increased from 23.0% in the input gas to 90.0% in the output flow in R3 achieving steady-state conditions in terms of stable methane production and composition in a short period of time (1 d). 6.6% H₂ and 3.4% CO₂ were recorded in the output gas (Table 37). Average η_{H_2} , η_{CO_2} , Y_{CH_4} , pH and $k_L a_{H_2}$ values observed during the set-up period are shown in Table 37. Total VFA concentration decreased significantly being only composed by acetate and butyrate. Average H₂ utilization rate for microbial growth was 0.13 L_{H2}/L_R·d.

On day 6, the first H₂ stop-feeding period was applied for 3 weeks restarting the feeding containing H₂ on day 27. Two more repetitions of these H₂ stop/start periods were performed according to Table 35.

As expected, during the three applied H₂ stop-feeding periods to R3 of 3 weeks, CH₄ production rate was approximately zero (Figure 56) and CH₄ content decreased to 61-63% approximately (Figure 57) and CO₂ was 37-39%.

In the three replicate periods, pH dropped (Figure 58) to an average range between 7.43±0.05 and 7.67±0.07 as a result of the lack of H₂ to react with CO₂. Total VFA and acetate concentrations experienced a slightly decrease during this H₂ stop periods while butyrate remained constant.

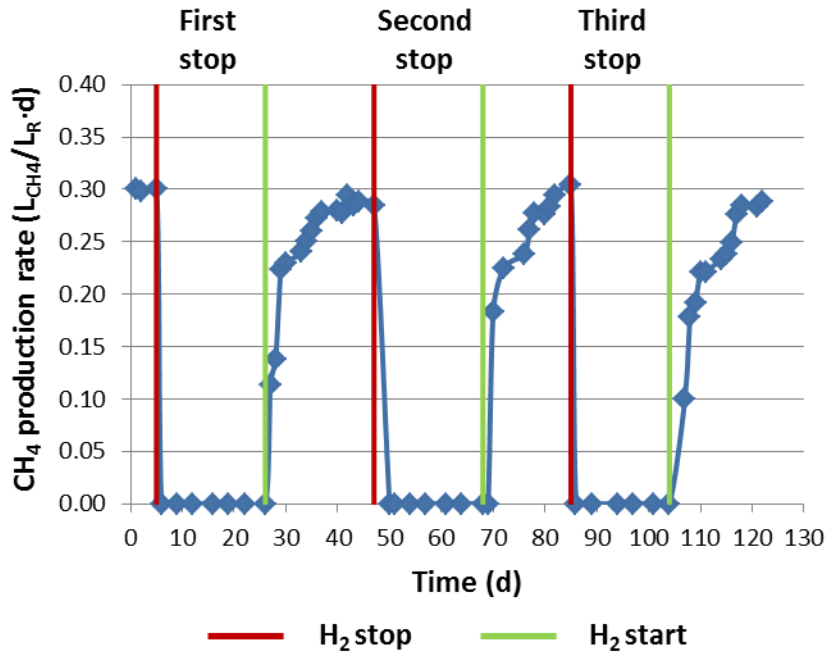


Figure 56. Methane production rate throughout the experiment in R3.

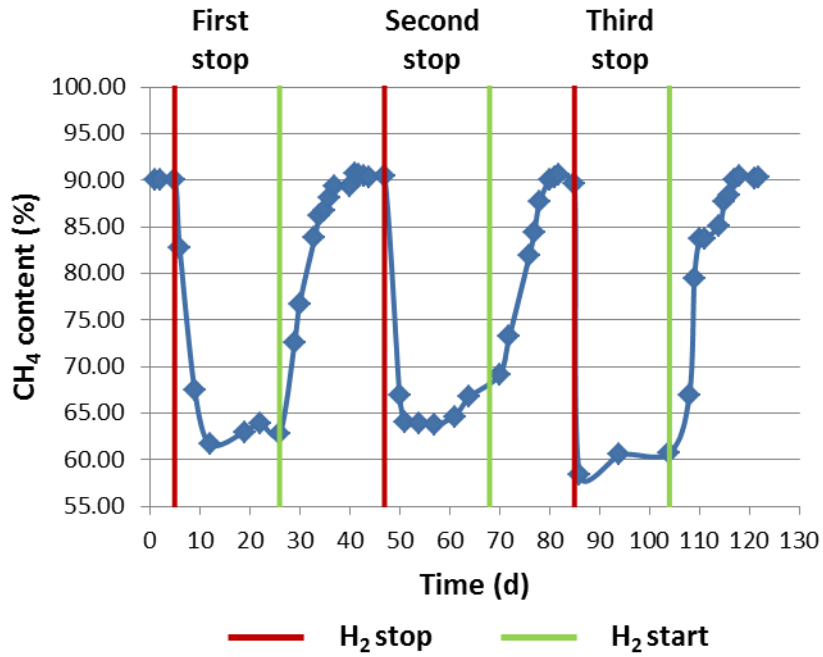


Figure 57. Methane content throughout the experiment in R3.

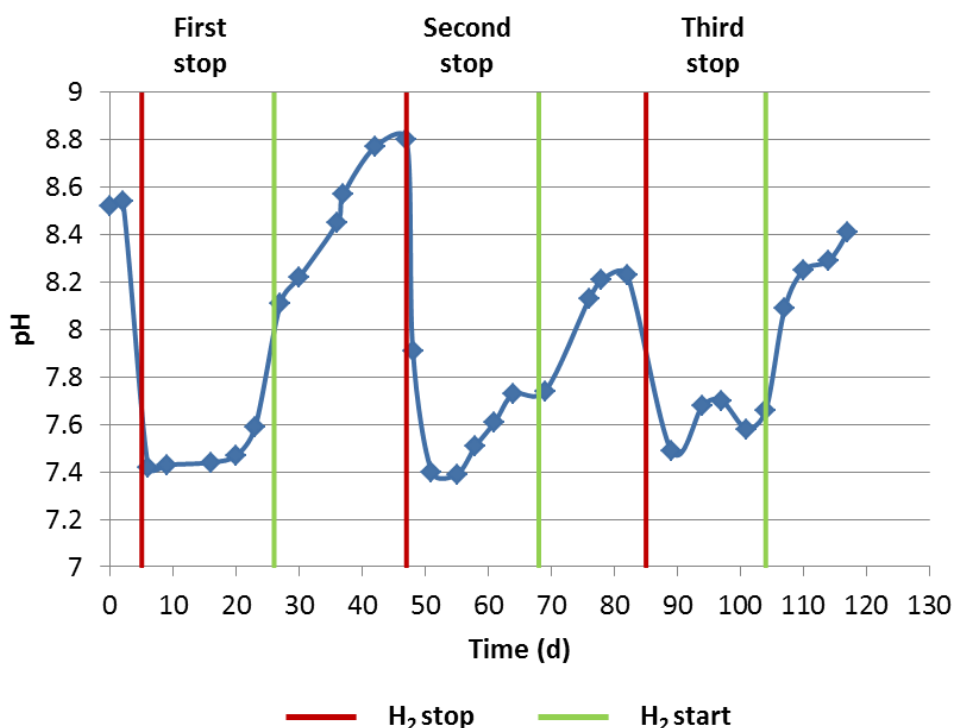


Figure 58. pH evolution throughout the experiment in R3.

After the reinjection of H₂ in R3, its transformation to CH₄ took place since the beginning for the three recovery periods experienced.

In the three recovery periods, CH₄ production rate and CH₄ content in the output gas gradually increased (Figure 56 and Figure 57) reaching the initial values obtained during the set-up period (Table 37). Similarly, Y_{CH_4} experimented a gradual increase.

The results showed a decreasing trend in the required time to recover the initial conditions (Figure 56 and Figure 57). 15, 12 and 11 days were needed for the CH₄ content and CH₄ production rate to reach steady conditions after the three consecutive applied H₂ stop-feeding periods, respectively, which can be translated into 20% and 27% reduction in the recovery time, respectively.

Therefore, H₂ intermittency had no effect on the system and on the biomethanation process as it recovered the initial CH₄ production conditions. Moreover, the repetition of the H₂ lack was shown to have a positive effect on the required recovery time of the system to reach the initial steady-state, shortening it.

Similarly to the set-up period, approximately 6% H₂ in R3 remained unutilized in the output gas in the three recovery periods (Table 37). Approximate η_{H_2} and η_{CO_2} values of 95-96% and 91-92% were obtained after the recoveries, respectively, close to the initial efficiency values from the set-up period (Table 37).

Similar Y_{CH_4} (0.21-0.22 L_{CH₄}/L_{H₂}) values were found in comparison to the initial values and $k_L a_{H_2}$ values were maintained throughout the experiment (Table 37). Biomethanation inhibition did not appear despite the high pH level (Table 37, Figure 58). Low total VFA, acetate and butyrate concentrations were found (Table 37) and H₂ and CO₂ utilized for VFA production were negligible.

During all the recovery periods experienced, H₂ utilization rate for microbial growth dropped progressively throughout the recovery time, from average values of 0.53 L_{H₂}/L_R·d at the beginning of the recovery period to 0.17 L_{H₂}/L_R·d after the system recovery (slightly higher value compared to the value from the set-up period), supporting the gradually increased of Y_{CH_4} .

8.3.4 Comparison of reactors' performance and H₂ intermittency

Although microbial community adaptation to the new operating conditions took place during the set-up period, microorganisms started to convert H₂ and CO₂ to CH₄ rapidly in R1, R2 and R3. The CH₄ content increased from 23%, in the input gas, to ≥90% in the output flow (approximately 95% in R1 and R2 and 90% in R3) achieving steady-state conditions in a short period of time.

During the set-up period, R1 and R2 showed similar performance in terms of CH₄ production rates and CH₄ content with similar Y_{CH_4} , η_{H_2} and η_{CO_2} values (Table 37). However, slightly lower values were obtained in R3 (Table 37), which could be attributed to the lower $k_L a_{H_2}$ value found probably due to some technical issues affecting the mass transfer conditions in the setup of R3. Similar pH and VFA content were observed.

The three reactors, after the first H₂-stop period and the subsequent H₂ reinjection, recovered their initial conditions of CH₄ (production, content and yield) thus biomethanation process was not affected by the intermittent provision of H₂ or the length of the H₂ lack (Table 37).

The stability of these results was shown during the days after achieving the initial conditions in which the reactors were working with H₂/CO₂/CH₄ gas mixture as feeding. The reproducibility and long-term feasibility of these results was demonstrated with the other two H₂ stop/start periods applied to the reactors, achieving the same outcomes (Table 37, Figure 50, Figure 51, Figure 54, Figure 55, Figure 56 and Figure 57).

After the first H₂-stop, more days were needed for the CH₄ content and CH₄ production rate to reach the initial steady conditions in R2 and R3 compared to R1 which can be linked with the longer period experienced without H₂ as gas substrate (Figure 50, Figure 51, Figure 54, Figure 55, Figure 56 and Figure 57).

After the second and third reinjection of H₂ in R1, the system showed the same required time to recover the initial conditions. Interestingly, the results from R2 and R3 showed a decreasing trend in the required time to the system recovery, reaching in both cases close values to R1 at the last periods experienced (Figure 50, Figure 51, Figure 54, Figure 55, Figure 56 and Figure 57).

Therefore, the repetition of the intermittent provision of H₂ in R2 and R3 was shown to have a positive effect on the recovery time of the system since the reactors recovered faster as more H₂-stop periods were applied. Moreover, R2 and R3 showed similar decreasing recovery times suggesting firstly the possible absence of significant effect of H₂-stop period length higher than 2 weeks on the system recovery time and secondly the possibility of reach lower recovery times (even closer to R1) if more H₂-stop periods were applied to the systems.

Further studies could evaluate the recovery times for H₂-stop periods higher than the currently experienced. More repetitions of H₂-stop periods of 2 and 3 weeks and H₂ restart would be interesting to assess more deeply the decreasing trend in the system recovery times observed in the current study.

During the whole experiments, VFA accumulation was not recorded. Moreover, no biomethanation inhibition was observed in the reactors during the different periods of the experiment despite the high pH (8.23-8.79) indicating adaptation of microorganisms to higher pH levels.

During all the recovery periods experienced in R1, R2 and R3, H₂ utilization rate for microbial growth showed an increase immediately after the H₂ reinjection to the system, presenting a decreasing trend throughout the recovery time to finally reach similar (R1) or slightly higher (R2 and R3) values compared to the initial ones observed in the set-up period, supporting the gradually increased of Y_{CH_4} over the period. In any case, these values are within the range of the three experiments performed in ex-situ and in-situ bioreactors described in Chapter 4, Chapter 5 and Chapter 7.

The increasing share of fluctuating renewable energy sources requires a demand-oriented operation of Power-to-Gas technologies, to provide flexible energy conversion for long-term storage. Biological methanation, using H₂ generated from excess electricity via water electrolysis and CO₂ emission streams, has the potential to become such a flexible energy conversion technology.

As discussed above, the ex-situ biogas upgrading reactors experienced had the capability to deal with the intermittent provision of H₂ so the technical feasibility of the future application of this technology as a demand-oriented and efficient energy conversion technology was accomplished at lab scale. Moreover, this study is the first demonstrating study of on-demand biomethanation in the biogas upgrading topic up to now.

8.3.5 Microbial community

Illumina sequencing generated in total more than 22 million of raw reads with average length of 249 bp; results are summarized in Table 38. After quality filtering and pair merging, on average 76% of reads were taxonomically assigned to OTUs (Table 38). Rarefaction curves (Figure 59) showed that the sequencing depth was adequate enough to cover the sample richness in the sample replicates. Microbial diversity was estimated and results showed 514 OTUs per replicate (on average).

Table 38. Summary of the sequencing data and results.

Sample ID	Raw Reads	Merged/Filtered	Assigned Reads to OTUs	% Assigned
I	294541	142138	100681	71
R1-1	340626	162429	129319	80
R1-2	273861	130867	102286	78
R1-3	288532	137231	105786	77
R1-4	405756	192575	140751	73
R1-5	395841	187583	142664	76
R1-6	396197	186663	136801	73
R1-7	348745	167037	128865	77
R2-1	314135	150745	116530	77
R2-2	277711	133068	97619	73
R2-3	255100	122934	96251	78
R2-4	334693	159948	107363	67
R2-5	349663	166274	123540	74
R2-6	382173	183109	136502	75
R2-7	388922	184153	140044	76
R3-1	276365	132900	106345	80
R3-2	287597	137269	101895	74
R3-3	242941	116723	91261	78
R3-4	393803	189149	141733	75
R3-5	357755	170336	131817	77
R3-6	385908	184779	139392	75
R3-7	358258	171546	129940	76

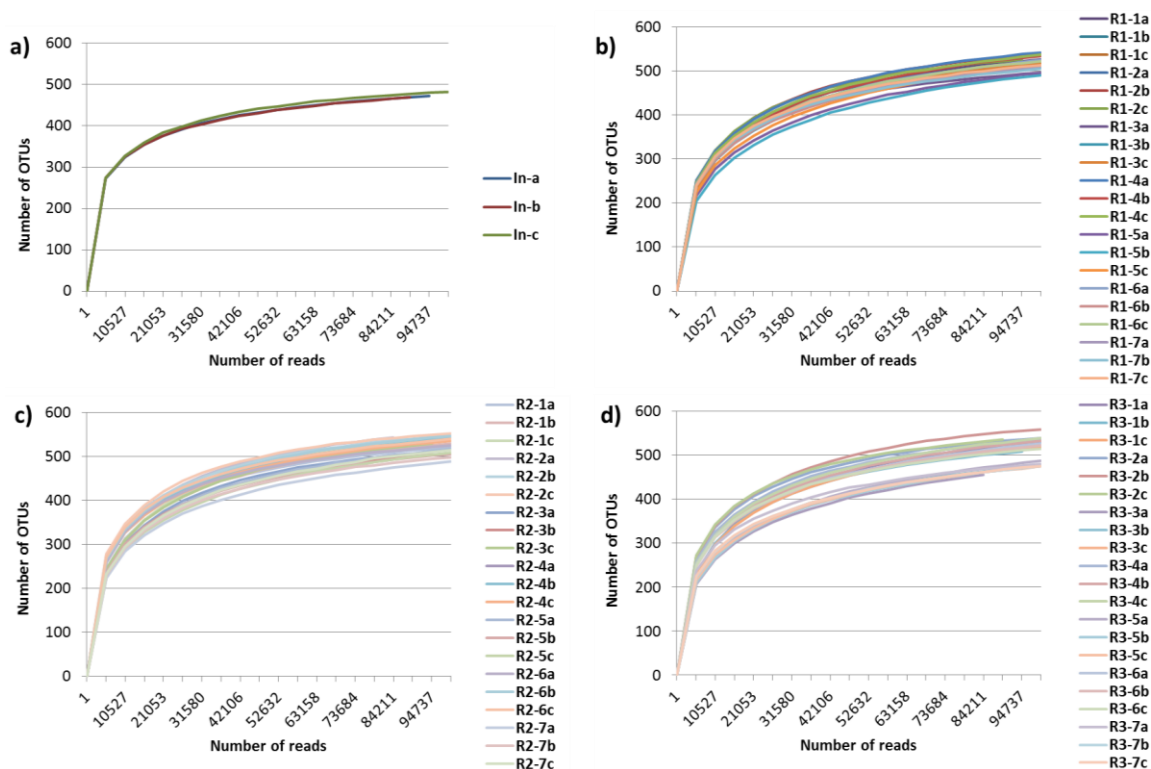


Figure 59. Rarefaction curves of annotated species richness.

a) Inoculum; **b)** R1; **c)** R2; **d)** R3. Sampling points: 1-7; a, b, c: replicates of each sample.

Considering the most abundant microbes (>1% of relative abundance in at least one sample), 48 OTUs covered approximately 71% and 83% of the community in the samples from inoculum and reactors, respectively. Among the selected OTUs, 8 were assigned at genus level and 6 at species level while the rest of the microbes were assigned only at higher taxonomic levels, suggesting the presence in the microbiome of numerous underexplored or undescribed taxa.

Taxonomic assignment and relative abundance of the most abundant OTUs in the samples of inoculum, R1, R2 and R3 are reported in Figure 60, Figure 61 and Figure 62, respectively. Correspondence between colors and relative abundance is reported in the scale at the top of the panel.

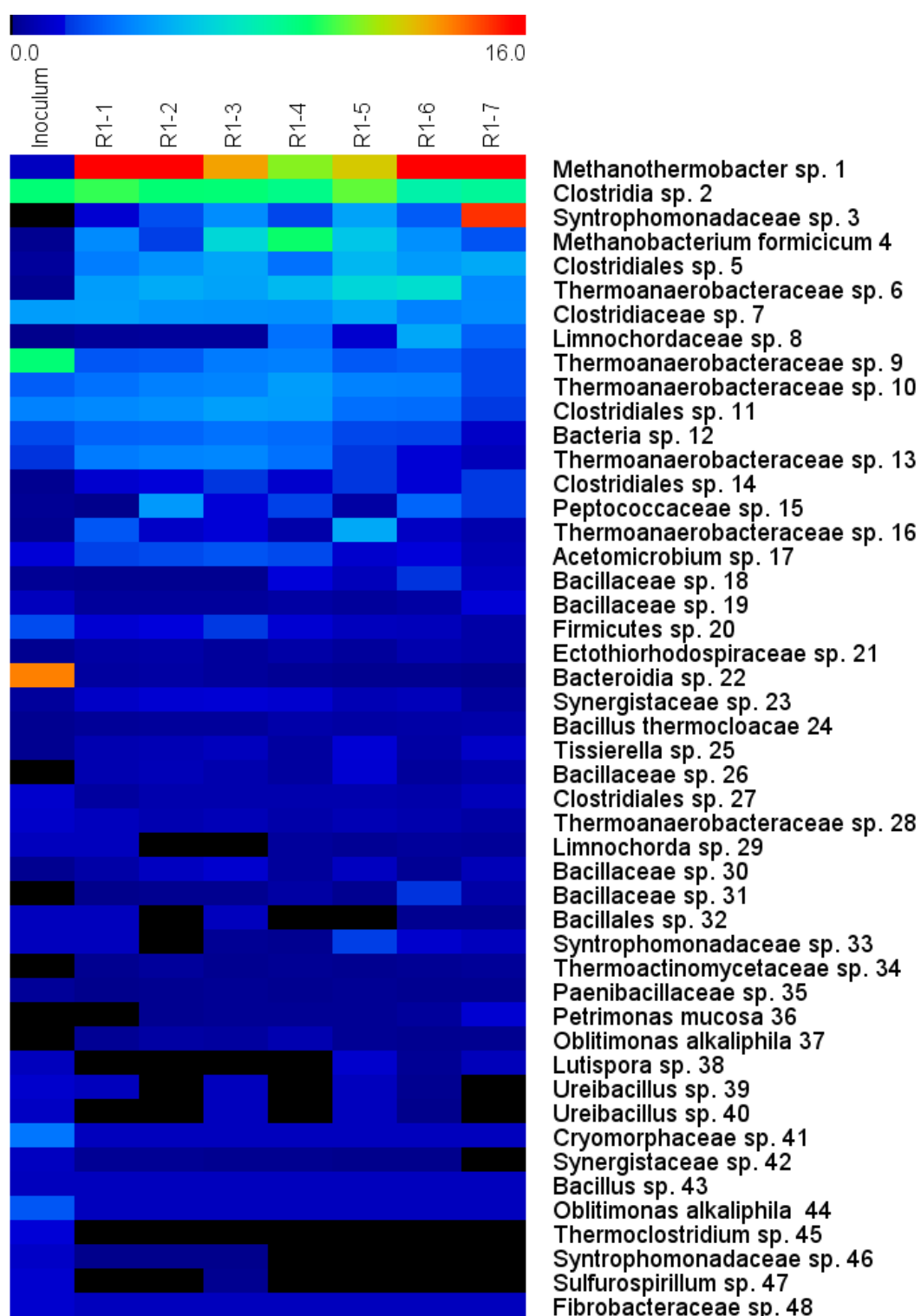


Figure 60. Heat maps of relative abundance (%) of the most abundant microorganisms populating R1 during the different experimental periods (1-7) and inoculum.

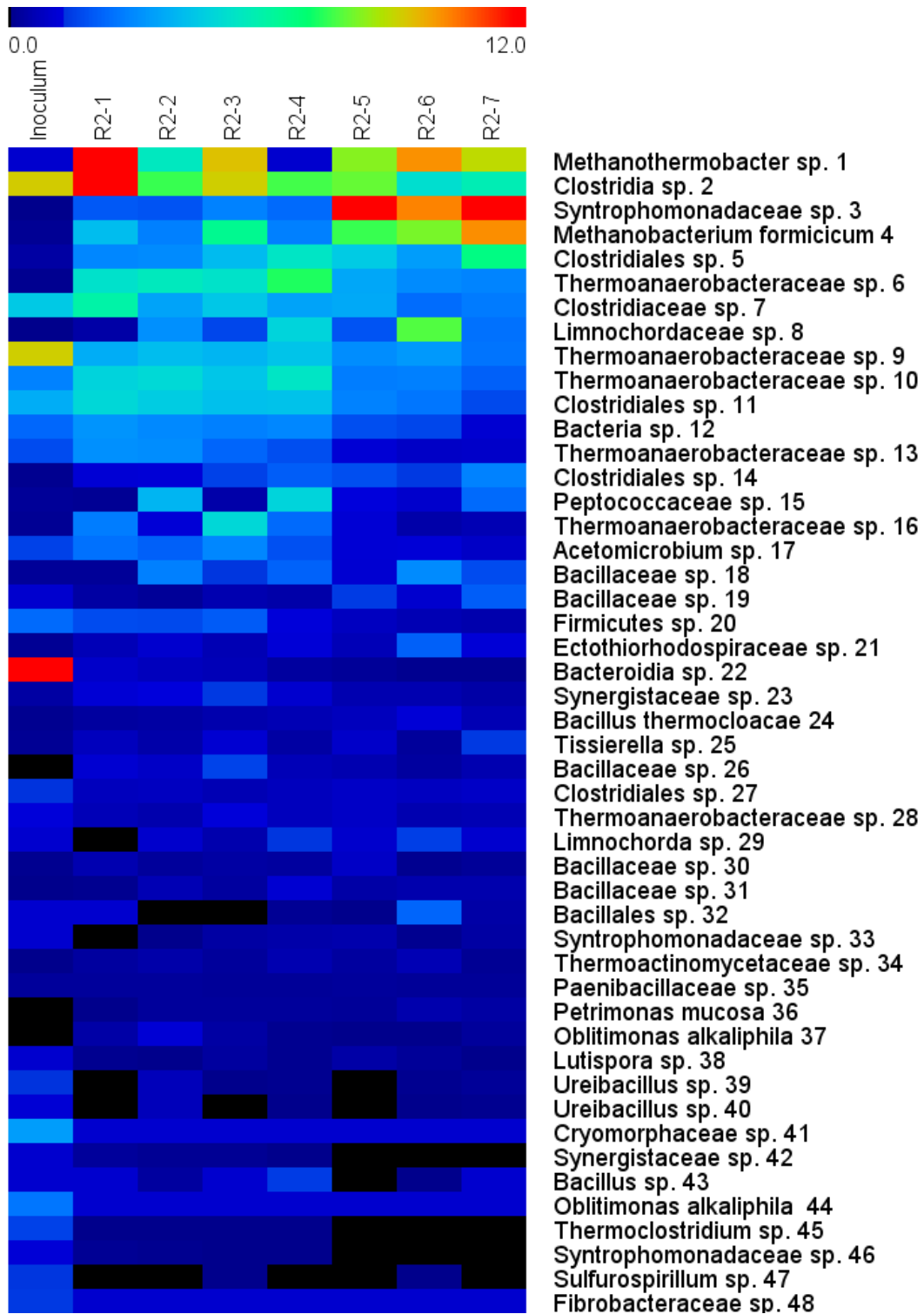


Figure 61. Heat maps of relative abundance (%) of the most abundant microorganisms populating R2 during the different experimental periods (1-7) and inoculum.

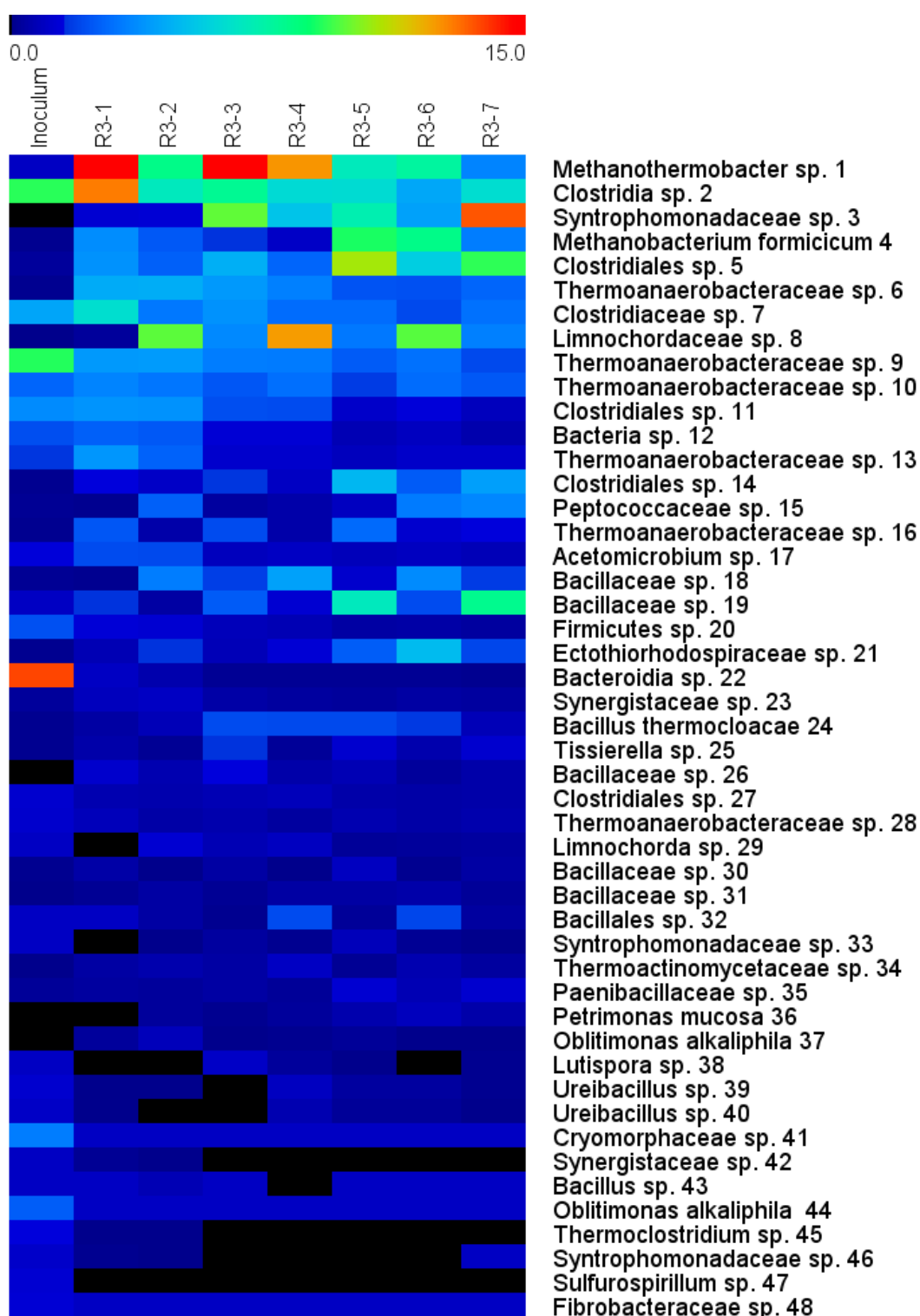


Figure 62. Heat maps of relative abundance (%) of the most abundant microorganisms populating R3 during the different experimental periods (1-7) and inoculum.

Bacterial population covered on average 70% of the whole microbial community in the inoculum whilst *archaea* accounted on average for only 1%. The most represented phyla were *Firmicutes* (43%), *Bacteroidetes* (17%) with lower abundance of *Proteobacteria* (4%), *Synergistetes* (3%), *Euryarchaeota* (1%) and *Fibrobacteres* (1%). The three most abundant OTUs of the inoculum community were *Bacteroidia* sp. 22 (14%), *Clostridia* sp. 2 (9%) and *Thermoanaerobacteraceae* sp. 9 (9%) (Figure 60).

As expected, during the set-up period, the specialization of the community took place with a remarkable increase of archaeal population in all the reactors (Figure 60, Figure 61 and Figure 62). After the set-up period (samples 1), archaeal species in the reactors represented on average 23% of the total microbial community.

Among the most abundant OTUs after the set-up period in all the reactors, 2 of them were hydrogenotrophic methanogens assigned to *Methanothermobacter* sp. 1 and *Methanobacterium formicicum* (100 and 97% similarity, respectively) with average relative abundances of 19% and 4%, respectively (Figure 60, Figure 61 and Figure 62). BLASTn search against NCBI database revealed 100% similarity of *Methanothermobacter* sp. 1 with two microbial species, such as *Methanothermobacter thermautotrophicus* and *Methanothermobacter wolfeii*, indicating that one of the most abundant methanogens populating the archaeal and total community in the reactors was represented by a new species.

The high abundance of *Methanothermobacter* sp. obtained in the present study is in agreement with previous studies which identified dominance of this hydrogenotrophic methanogen genus in biogas upgrading systems at thermophilic conditions in CSTR (Treu et al., 2018; Kougias et al., 2017), bubble columns (Kougias et al., 2017) and up-flow reactors (Bassani et al., 2017). Likewise, *Methanothermobacter* sp. was the most abundant hydrogenotrophic *archaea* found during the ex-situ experiments of Chapter 4, Chapter 5 and Chapter 6.

M. formicicum is known to be able to produce extracellular polysaccharides, which play various roles in structure and functions of biofilm communities (Veiga et al., 1997) so it is frequently found in systems with biofilms as in Chapter 6 where it was the second most abundant microbe in the biofilm community.

However, if the environmental conditions are favorable, *M. formicicum* is present in communities without biofilms, as in the present study.

After the set-up period, *Clostridia* sp. 2 was the second most abundant OTU of the community in the reactor samples (10-13%) (Figure 60, Figure 61 and Figure 62). This species was assigned to the recently discovered order MBA08, belonging to *Clostridia* class. BLAST results of this OTU's consensus sequence indicated a high similarity to *Hydrogenispora ethanolica* (89%) and confirmed the relevance of this uncharacterized OTU previously found in other works dealing with biogas upgrading (Bassani et al., 2017; Corbellini et al., 2018; Kougias et al., 2017; Treu et al., 2018; Chapter 6). In addition, Kougias et al. (2017) indicated the existence of a potential syntrophic interaction between the hydrogenotrophic methanogen *M. thermautotrophicus* and *Clostridia* sp. 2 (*H. ethanolica*) because of their concurrent remarkable high abundance, which could be observed in the experiment of Chapter 6 and in the present study after the set-up period in all the reactors.

Although *Thermoanaerobacteraceae* sp. 9 was the third most abundant OTU of the community in the inoculum, after the set-up period showed 3-4% relative abundance in the reactors (Figure 60, Figure 61 and Figure 62). Members of this family (e.g. *Moorella thermoacetica* and *Thermoanaerobacter kivui*) are known homoacetogenic bacteria using H₂ as electron donor to convert CO₂ into acetate (Pierce et al., 2008; Weghoff and Müller, 2016). The best hit with 91% similarity was *Moorella thermoacetica*. Thus, *Thermoanaerobacteraceae* sp. could be a possible homoacetogen.

Bacteroidia sp. 22 was an "unclassified species". The taxonomic assignment could not be improved neither by BLASTn search against the NCBI database, nor by aligning the sequence against other public databases, such as RDP Classifier or SILVA ribosomal RNA gene database. The best hit with 81% similarity was with an obligatory anaerobic asaccharolytic member of *Porphyromonas* genus (*Porphyromonas circumdentaria*). This uncharacterized OTU was previously found in other works dealing with biogas upgrading (Kougias et al., 2017; Chapter 6).

Although *Bacteroidia* sp. 22 was the most abundant OTU of the inoculum community, after the set-up period, its relative abundance dropped to 0-1% (Figure 60, Figure 61 and Figure 62).

The principal coordinate analysis (PCoA) results were consistent in the three replicates for each sample analyzed (which clustered together, Figure 63), and thus, all of them were maintained for the analysis. PCoA clearly indicated differences between the inoculum and all the samples from R1, R2 and R3, revealing a big distance in their microbial beta diversity, in agreement with the previously discussed specialization of the microbial community achieved during the set-up period (Figure 63).



Figure 63. Principal coordinate analysis plot (PC1 vs. PC2) representing variations of the most abundant OTUs based on least squares method in samples of R1, R2 and R3 during the different experimental periods (1-7) and inoculum.

During the different experimental H₂ stop/start periods, bacterial population covered on average 63%, 68% and 69% of the whole microbial community in R1, R2 and R3 samples, respectively, whilst *archaea* accounted on average for 21%, 14% and 15%, respectively. The most abundant phyla in the samples from the reactors were *Firmicutes* (56-63%), *Euryarchaeota* (14-21%) and *Synergistetes* (2-3%) with lower abundance of *Proteobacteria* (1-2%) and *Bacteroidetes* (1%).

A decrease in the relative abundance of *Methanothermobacter* sp. 1 and *M. formicicum* was observed in the samples obtained at the end of the first and second H₂-stop periods (samples 2 and 4) while an increase was obtained in the samples from the first and second H₂ reinjection periods (samples 3 and 5), for all the reactors. However, similar relative abundance was showed in the samples from the last H₂-stop and H₂ reinjection periods (samples 6 and 7) compared to the values of the second H₂ reinjection (samples 5) for the three reactors (Figure 60, Figure 61 and Figure 62).

These up and down oscillations in microbial relative abundance values can be observed more clearly in the samples from R2 (Figure 61) and especially R3 (Figure 62), due to the fact that the HRT of the systems was 40 d and these reactors operated with longer H₂ stop periods (14 and 21 d) compared to R1 (7 d).

All these behavior patterns were confirmed by PCoA (Figure 64) which clearly indicated differences between the samples from H₂ stop periods and H₂ reinjection periods for R1, R2 and R3 and their small or relative distance in their microbial beta diversity.

Therefore, H₂ lack and its subsequent injection produced a decrease and increase, respectively, in the relative abundance of the hydrogenotrophic *archaea* community during the first and the second periods. However, the archaeal community did not experience any significant change when the third H₂ stop/start period was applied, maintaining similar relative abundance values in their two hydrogenotrophic members (which were the most abundant OTUs in the total community), thus showing their resilience against the different H₂ conditions.

Methanothermobacter sp. 1 was dominant compared to *M. formicicum* in R1 throughout the experiment. Interestingly, this dominance disappeared in R2 and R3 as both hydrogenotrophic methanogens were present in close relative abundance (Figure 60, Figure 61 and Figure 62), thus suggesting the higher resilience of *M. formicicum* to longer H₂ lack periods and/or the higher adaptability of this species to different H₂ input rates and/or its faster growth after the H₂ reinjections compared to *Methanothermobacter* sp. 1. Further studies should study deeply the dynamicity of the hydrogenotrophic methanogens during the intermittent provision of H₂ to elucidate the possible dominance shift in a long-term observed in the present study.

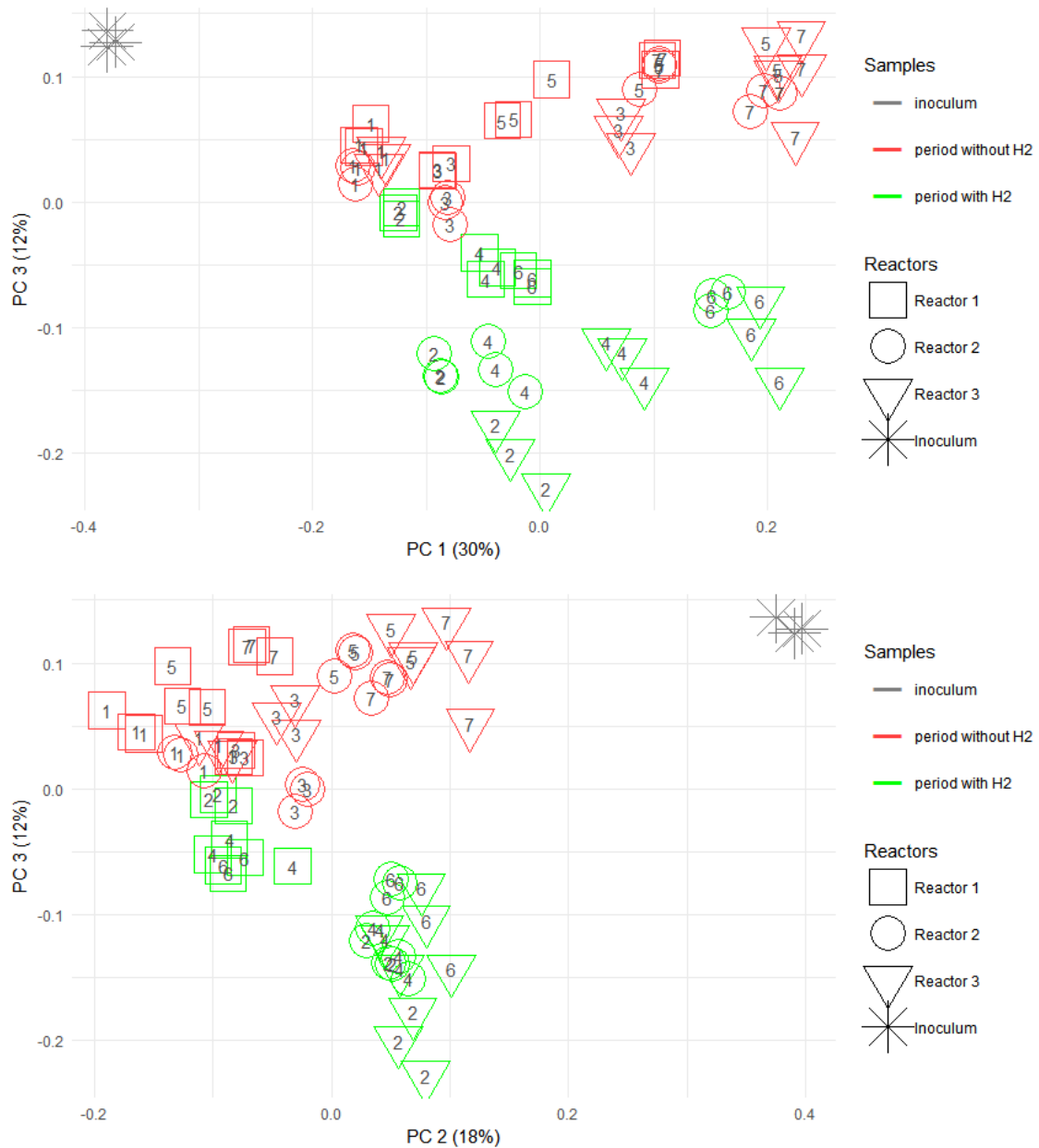


Figure 64. Principal coordinate analysis plot (PC1 vs. PC3 and PC2 vs. PC3) representing variations of the most abundant OTUs based on least squares method in samples of R1, R2 and R3 during the different experimental periods (1-7) and inoculum.

The existence of the potential syntrophic interaction between the hydrogenotrophic methanogen *M. thermotrophicus* and *Clostridia* sp. 2 (*H. ethanolic*) (because of their concurrent remarkable high abundance as indicated by Kougias et al. (2017)) was observed during the experiment in R1, R2 and R3. *Clostridia* sp. 2 showed constant relative abundance (8-10%) throughout the experiment dealing with the H₂ intermittency in R1 (Figure 60), while up and down oscillations in relative abundance

were found in R2 and R3 following the same behavior of the two hydrogenotrophic *archaea* (Figure 61 and Figure 62) thus confirming the potential syntrophic interaction between these microbes.

The potential homoacetogen *Thermoanaerobacteraceae* sp. was not affected by any of the H₂ stop periods in the three reactors, remaining constant its relative abundance throughout the experiment (Figure 60, Figure 61 and Figure 62).

Syntrophomonadaceae sp. 3 was an “unclassified species” and the best hit with 91% similarity was *Dethiobacter alkaliphilus*. This species has been reported to grow chemolithoautotrophically with H₂ as electron donor (Sorokin et al., 2008). Although *Syntrophomonadaceae* sp. 3 was scarcely present in the inoculum (<1%, Figure 60) and after the set-up period (1-2%) in the reactors (Figure 60, Figure 61 and Figure 62), it was the most abundant OUT after the third (in R1, Figure 60) and second H₂ reinjections (in R2 and R3, Figure 61 and Figure 62). Therefore, it was hypothesized that *Syntrophomonadaceae* sp. 3 had a regulatory role in the process, maintaining the balance of the system to perform the biomethanation. Further studies should focus on this microbe in order to elucidate if this syntrophic bacteria is critical for maintaining the biogas upgrading efficiency of the system.

8.4 CONCLUSIONS

The present work demonstrates the technical feasibility of the system recovery to reach the initial steady-state during the intermittent provision of H₂ in thermophilic up-flow reactors for ex-situ biogas upgrading.

The investigated systems, after the H₂-stop periods of 1, 2 and 3 weeks and the subsequent H₂ reinjections, recovered efficiently their initial conditions of CH₄ production rate, CH₄ content and CH₄ yield showing that the biomethanation process was not affected by the H₂ intermittency or the length of the H₂ lack.

The repeatability and long-term feasibility of these results was demonstrated with the two following H₂ stop/start periods applied to the reactors, achieving the same outcomes regarding the recovery of the systems.

The repetition of the intermittent provision of H₂ was shown to have a positive effect on the recovery time of the system for the experiments with H₂-stop periods of 2 and 3 weeks since the reactors recovered faster as more H₂-stop periods were applied. However, any effect of the repetition was observed in the system working with H₂-stop periods of 1 week, showing the same required time to reach its initial performance.

This study proved at lab scale the potential of up-flow ex-situ biogas upgrading reactors as a robust biological methanation technology, which is suitable for dynamic on-demand operation.

Archaeal microbial communities populating the upgrading reactors during the intermittent provision of H₂ showed their plasticity against the lack of H₂ regardless the length of the H₂ lack, without affecting the biomethanation potential of the systems.

After two H₂ stop/start periods applied to the systems, hydrogenotrophic *archaea* showed their resilience against the different H₂ conditions without significant changes in their relative abundance.

Sequencing results revealed the predominance of *Methanothermobacter* sp. on the archaeal community when 1 week H₂ stop periods were applied. However, *M. formicum* showed higher resilience to longer H₂ stop periods compared to *Methanothermobacter* sp. *Syntrophomonadaceae* sp. seemed to have a process regulatory role during the intermittent provision of H₂, maintaining the balance of the system to perform the biomethanation.

Chapter 9

Conclusions and future perspectives



9.1 CONCLUSIONS

The results obtained in the present thesis demonstrated the feasibility of H₂-mediated biological biogas upgrading in both ex-situ and in-situ concepts, overcoming the challenges of the technology. Biological biogas upgrading is a promising way to extend biomethane utilization and reduce the dependence on fossil fuels, providing enhanced environmental and economic benefits of biogas technologies.

The results verified that membrane modules can be employed to transfer H₂ efficiently, allowing the biological conversion to take place satisfactorily.

The ex-situ systems transformed 95% of H₂ fed at the maximum loading rates of 40.2 L_{H₂}/L_R·d (hollow-fiber MBR) and 30.0 L_{H₂}/L_R·d (ceramic MBR) reaching CH₄ production rates of 8.84 L_{CH₄}/L_R·d and 6.60 L_{CH₄}/L_R·d, CH₄ contents of 76% and 81% and $k_L a_{H_2}$ values of 430 h⁻¹ and 268 h⁻¹, respectively, both with CH₄ yield of 0.22 L_{CH₄}/L_{H₂}.

Ceramic membranes were proposed to address and solve the long-term bioconversion stability challenge of hollow-fiber membranes at thermophilic conditions.

Nonetheless, it should be noted the high energy consumption of the MBR systems, which is dominated for the power required for gas recirculation, essential to transfer H₂ to the liquid phase.

The TBF systems, by means of a single-pass gas flow, upgraded biogas efficiently reaching a CH₄ production rate of 1.74 L_{CH₄}/L_R·d for a H₂ loading rate of 7.2 L_{H₂}/L_R·d showing 97% H₂ utilization efficiency and CH₄ yield of 0.24 L_{CH₄}/L_{H₂}, close to the maximum stoichiometric value (0.25 L_{CH₄}/L_{H₂}). CH₄ content of 95% was reached, fulfilling the specifications to be used as substitute to natural gas or as transportation fuel. H₂ mass-transfer was improved passively, without need of liquid stirring, diffusion devices or gas recirculation.

The results demonstrated that the injection of the influent gas mixture with the directional flow of the liquid media greatly enhanced acetate production compared to

the injection in counter-flow to the trickling media, highlighting the convenience of working under H₂ up-flow operation in TBF systems.

TBF reactors resulted in attractive configurations with promising results for the overall biomethanation process. Higher CH₄ yield and CH₄ quality were achieved in TBFs with remarkable lower energy consumptions compared to the ex-situ MBRs.

In the in-situ experiment, H₂ injection resulted in a 42% increase in CH₄ production rate in comparison with the conventional anaerobic digestion of sewage sludge and 73% CH₄ content was achieved in the biogas. The biodegradation potential of the reactor was not compromised by H₂ supply. Hollow-fiber MBR showed good H₂ mass transfer capacity, reaching a $k_L a_{H_2}$ value of 25 h⁻¹ and 94% efficiency in H₂ utilization.

Gas recirculation was shown to improve the H₂ gas-liquid mass transfer significantly, increasing the amount of H₂ transferred from gas to the liquid phase thus raising the H₂ utilization efficiency and improving the performance of the reactors. Moreover, gas recirculation seemed to have a positive effect on the in-situ biomethanation when the OLR increased. However, dewaterability of the digested sludge was negatively impacted by the turbulence caused by the high gas recirculation rate employed.

The technical feasibility of the system recovery to reach the initial conditions of CH₄ (production, content and yield) during the intermittent provision of H₂ was demonstrated, regardless of the length of the H₂ lack. The repetition of the H₂ intermittent provision was shown to have a positive effect on the system recovery time, since the reactors recovered faster as more H₂ stop/start periods were applied for the experiments with H₂-stop periods of 2 and 3 weeks.

The selection-effect of H₂ on community composition over time was revealed by microbial analysis in the experiments with MBRs, in which hydrogenotrophic methanogens outcompeted homoacetogens, thus CH₄ production was via hydrogenotrophic methanogenesis pathway. *Methanothermobacter* sp. was the hydrogenotrophic archaea found during the ex-situ experiments while *Methanoculleus* sp., *Methanospirillum* sp., *Methanolinea* sp. and *Methanobacterium* sp. were present in the in-situ process.

Sequencing results revealed a significant predominance of *Methanothermobacter* sp. in the biofilm, which was the most abundant methanogen populating the microbial community in the TBF. Unknown members of the class *Clostridia* were highly abundant in biofilm and liquid media, while acetate utilizing bacteria predominated in liquid samples.

Archaeal microbial communities populating the upgrading reactors during the intermittent provision of H₂ showed their plasticity against the lack of H₂ regardless the length of the H₂ lack, without affecting the biomethanation potential of the systems.

9.2 FUTURE PERSPECTIVES

In this PhD project, several reactors' configurations were designed to study and optimize in-situ and ex-situ biogas upgrading processes. Despite the advances carried out in the present thesis, further research in the field of biogas upgrading should be necessary to gain a deeper knowledge of the technology.

Based on the achieved results, one of the future perspectives in terms of pilot plant scale reactor configuration and process optimization is the innovative hybrid setup exploiting the findings of both in-situ and ex-situ biogas upgrading concepts. The proposed configuration would consist of a double-stage reactor composed of a first reactor, working as a conventional anaerobic digester of organic matter and where the H₂ would be injected (in-situ biogas upgrading) and a second reactor, receiving the upgraded biogas from the first one, together with the unutilized H₂, to be further upgraded (ex-situ biogas upgrading) in order to develop strategies targeting the optimization of the biogas upgrading technology.

Other future perspective regarding the reduction of the H₂ mass transfer limitations is the pressurization of the reactors instead of working at atmospheric pressure. In a pressurized anaerobic digestion process, methanogenic microorganisms increase the pressure of the gas autogenatively, producing biomethane of natural gas quality inside the methane reactor, which could be fed directly into the gas grid. A study using

pressure in biogas upgrading technology would be useful to evaluate the process performance and their possible challenges.

For full scale process applications, further investigations would be necessary:

Firstly, the scale-up and optimization of the TBF reactors as they are attractive configurations for the biomethanation process. The tested TBF reactors could be considerably improved and optimized by enabling a faster process lowering the gas retention time (increasing the H₂ loading rate) or by reducing the specific reactor volume. For instance, optimization of the H₂/CO₂ ratio, together with adoption of more suitable packed-bed elements would involve inexpensive performance improvements.

Secondly, the feasibility of the intermittent H₂ feeding of the hydrogenotrophic culture and the recovery capacity of the system to reach the initial steady conditions after the H₂ stop periods and the plasticity of the microbial communities against the lack of H₂ have been assessed in this PhD thesis at lab scale ex-situ biogas upgrading reactors. However, further studies evaluating the H₂ intermittency for biogas upgrading configurations at higher scale would be necessary to confirm the full-scale technical feasibility.

In addition, a study evaluating the combination of intermittent provision of H₂ and different gas retention times (H₂ loading rates) would be interesting to evaluate the feasibility of the process for an industrial application not only addressing the H₂ lack but also different H₂ flow rates due to the fact that H₂ assisted biogas upgrading technology is based on the surplus electricity generated by wind and solar power which experiment uncontrollable natural fluctuations resulting in variable H₂ production rates.

Moreover, in order to implement biogas upgrading technology in a commercial application, an economic and environmental impact assessment of the proposed processes in the different chapters of the thesis would be beneficial.

Finally, further investigations are needed to achieve a deeper insight into the fundamentals of the biological biogas upgrading process and acquire a clearer knowledge of the complexity of the microbial consortium populating biogas upgrading

reactors (in-situ and ex-situ configurations). The necessity for an analysis of the community going beyond the identification of the microbial species, but focused on their function in the biomethane production process is stressed by the intricate network of interactions among the microorganisms resulting either in syntrophic relations or in competition. This deeper analysis of the microbial community focused on their biogas production functions would provide the basis for future metatranscriptomic and metaproteomic studies.

Chapter 10

References



REFERENCES

- Agler, M.T., Spirito, C.M., Usack, J.G., Werner, J.J., Angenent, L.T., 2012. Chain elongation with reactor microbiomes: upgrading dilute ethanol to medium-chain carboxylates. *Energy Environ. Sci.* 5, 8189.
- Agneessens, L.M., Ottosen, L.D.M., Voigt, N.V., Nielsen, J.L., de Jonge, N., Fischer, C.H., Kofoed, M.V.W., 2017. In-situ biogas upgrading with pulse H₂ additions: The relevance of methanogen adaption and inorganic carbon level. *Bioresour. Technol.* 233, 256–263.
- Agneessens, L.M., Ottosen, L.D.M., Andersen, M., Berg Olesen, C., Feilberg, A., Kofoed, M.V.W., 2018. Parameters affecting acetate concentrations during in-situ biological hydrogen methanation. *Bioresour. Technol.* 258, 33–40.
- Ahern, E.P., Deane, P., Persson, T., Ó Gallachóir, B, Murphy, J.D., 2015. A perspective on the potential role of renewable gas in a smart energy island system. *Renewable Energy.* 78, 648–656.
- Alitalo, A., Niskanen, M., Aura, E., 2015. Biocatalytic methanation of hydrogen and carbon dioxide in a fixed bed bioreactor. *Bioresour. Technol.* 196, 600–605.
- Andriani, D., Wresta, A., Atmaja, T.D., Saepudin, A., 2014. A review on optimization production and upgrading biogas through CO₂ removal using various techniques. *Appl. Biochem. Biotechnol.* 172, 1909–1928.
- Angelidaki, I., Sanders, W., 2004. Assessment of the anaerobic biodegradability of macropollutants. *Rev. Environ. Sci. BioTechnol.* 3, 117–129.
- Angelidaki, I., Treu, L., Tsapekos, P., Luo, G., Campanaro, S., Wenzel, H., Kougias, P.G., 2018. Biogas upgrading and utilization: Current status and perspectives. *Biotechnol. Adv.* 36, 452–466.
- Annachhatre, A. P., 1996. Anaerobic treatment of industrial wastewaters. *Resour. Conserv. Recycl.* 16, 161–166.
- APHA, AWWA, WPCF, 2005. *Standard Methods for the Examination of Water and Wastewater*, 21st ed., Washington, DC.
- Appels, L., Baeyens, J., Degrève, J., Dewil, R., 2008. Principles and potential of the anaerobic digestion of waste-activated sludge. *Prog. Energy Combust. Sci.* 34, 755–781.
- Appels, L., Lauwers, J., Degrève, J., Helsen, L., Lievens, B., Willems, K., Van Impe, J., Dewil, R., 2011. Anaerobic digestion in global bio-energy production: Potential and research challenges. *Renew. Sustain. Energy Rev.* 15, 4295–4301.
- Atech Innovations, 2014. Accessed January 2016. http://www.atech-innovations.com/fileadmin/downloads/Instructions_e_2014.pdf.

- Badalamenti, J.P., Krajmalnik-brown, R., Torres, C.I., 2013. Generation of High Current Densities by Pure Cultures of Anode- Respiring *Geoalkalibacter* spp. under Alkaline and Saline Conditions. *MBio* 4, 1–8.
- Bailera, M., Lisbona, P., Romeo, L.M., Espartolero, S., 2017. Power to Gas projects review: Lab, pilot and demo plants for storing renewable energy and CO₂. *Renew. Sust. Energ. Rev.* 69, 292–312.
- Bassani, I., Kougias, P.G., Treu, L., Angelidaki, I., 2015. Biogas Upgrading via Hydrogenotrophic Methanogenesis in Two-Stage Continuous Stirred Tank Reactors at Mesophilic and Thermophilic Conditions. *Environ. Sci. Technol.* 49, 12585–12593.
- Bassani, I., Kougias, P.G., Angelidaki, I., 2016. In-situ biogas upgrading in thermophilic granular UASB reactor: key factors affecting the hydrogen mass transfer rate. *Bioresour. Technol.* 221, 485–491.
- Bassani, I., Kougias, P. G., Treu, L., Porté, H., Campanaro, S., Angelidaki, I., 2017. Optimization of hydrogen dispersion in thermophilic up-flow reactors for ex-situ biogas upgrading. *Bioresour. Technol.* 234, 310–319.
- Batstone, D.J., Keller, J., Angelidaki, I., Kalyuzhnyi, S.V., Pavlostathis, S.G., Rozzi, A., Sanders, W.T., Siegrist, H., Vavilin, V.A., 2002. The IWA anaerobic digestion model no 1 (ADM1). *Water Sci. Technol.* 45, 65–73.
- Bauer, F., Hulteberg, C., Persson, T., Tamm, D., 2013. Biogas upgrading – review of commercial technologies (Biogasuppgradering – Granskning av kommersiella tekniker). Report from the Swedish Gas Technology Center, Malmö.
- Bekkering, J., Broekhuis, A., van Gemert, W.J.T., 2010. Optimisation of a green gas supply chain—a review. *Bioresour. Technol.* 101, 450–456.
- Benjaminsson, G., Benjaminsson, J., Rudberg, R.B., 2013. Power to Gas – a Technical Review. SGC - Sven. Gastek. Cent. AB, Malmö, Sweden, Rep. 256.
- Bensmann, A., Hanke-Rauschenbach, R., Heyer, R., Kohrs, F., Benndorf, D., Reichl, U., Sundmacher, K., 2014. Biological methanation of hydrogen within biogas plants: A model-based feasibility study. *Appl. Energy.* 134, 413–425.
- Bhandari, R., Trudewind, C.A., Zapp, P., 2014. Life cycle assessment of hydrogen production via electrolysis – a review. *J. Clean. Prod.* 85, 151–163.
- Bryant, M.P., 1979. Microbial methane production—theoretical aspects. *J. Anim. Sci.* 48, 193–201.
- Burkhardt, M., Busch, G., 2013. Methanation of hydrogen and carbon dioxide. *Appl. Energy.* 111, 74–79.
- Burkhardt, M., Koschack, T., Busch, G., 2015. Biocatalytic methanation of hydrogen and carbon dioxide in an anaerobic three-phase system. *Bioresour. Technol.* 178, 330–333.

- Collet, P., Flottes, E., Favre, A., Raynal, L., Pierre, H., Capela, S., Peregrina, C., 2017. Techno-economic and Life Cycle Assessment of methane production via biogas upgrading and power to gas technology. *Appl. Energy*. 192, 282–295.
- Corbellini, V., Kougias, P.G., Treu, L., Bassani, I., Malpei, F., Angelidaki, I., 2018. Hybrid biogas upgrading in a two-stage thermophilic reactor. *Energy Convers. Manag.* 168, 1–10.
- Cruz, I., 2008. Energy storage technologies. Technical Business Conference. Department of eolic power. CIEMAT. Spain.
- Daims, H., Brühl, A., Amann, R., Schleifer, K.H., Wagner, M., 1999. The domain-specific probe EUB338 is insufficient for the detection of all Bacteria: development and evaluation of a more comprehensive probe set. *Syst. Appl. Microbiol.* 22(3), 434–444.
- Daims, H., Lücker, S., Wagner, M., 2006. Daime, a novel image analysis program for microbial ecology and biofilm research. *Environ Microbiol.* 8, 200–213.
- Demirel, B., Scherer, P., 2008. The roles of acetotrophic and hydrogenotrophic methanogens during anaerobic conversion of biomass to methane: a review. *Rev. Environ. Sci. Biotechnol.* 7, 173–190.
- Deng, L., Hägg, M.B., 2010. Techno-economic evaluation of biogas upgrading process using CO₂ facilitated transport membrane. *Int. J. Greenhouse Gas Control.* 4, 638–646.
- Deublein, D., Steinhauser, A., 2011. *Biogas from Waste and Renewable Resources: An Introduction*. Wiley.
- Díaz, I., Lopes, A.C., Pérez, S.I., Fdz-Polanco, M., 2010. Performance evaluation of oxygen, air and nitrate for the microaerobic removal of hydrogen sulphide in biogas from sludge digestion. *Bioresour. Technol.* 101, 7724–7730.
- Dupnock, T., Deshusses, M.A., 2017. High-Performance Biogas Upgrading Using a Biotrickling Filter and Hydrogenotrophic Methanogens. *Appl. Biochem. Biotechnol.* 183, 488–502.
- EurObservER, L'Observatoire des énergies renouvelables, 2013. The state of renewable energies in Europe. ISSN 2101–9622.
- EurObserver, 2014. Biogas barometer. Accessed October 2015. <http://www.eurobserver.org/biogas-barometer-2014/>.
- European Commission, Proposal for a directive of the European Parliament and of the council on the promotion of the use of energy from renewable sources (recast), Off. J. Eur. Union. 0382. Accessed June 2018. http://eur-lex.europa.eu/resource.html?uri=cellar:3eb9ae57-faa6-11e6-8a35-01aa75ed71a1.0007.02/DOC_1&format=PDF%0A; <http://eur-lex.europa.eu/legal-content/EN/TXT/?uri=CELEX:52016PC0767R%2801%29>.

- Fardeau, M., Belaich, J., 1986. Energetics of the growth of *Methanococcus thermolithotrophicus*. Arch. Microbiol. 144, 381–385.
- Fukuzaki, S., Nishio, N., Shobayashi, M., Nagai, S., 1990. Inhibition of the fermentation of propionate to methane by hydrogen, acetate, and propionate. Appl. Environ. Microbiol. 56, 719–723.
- Gahleitner, G., 2013. Hydrogen from renewable electricity: An international review of power-to-gas pilot plants for stationary applications. Int. J. Hydrogen Energy. 38, 2039–2061.
- Garrett, T.R., Bhakoo, M., Zhang, Z., 2008. Bacterial adhesion and biofilms on surfaces. Prog. Nat. Sci. 18, 1049–1056.
- Götz, M., Lefebvre, J., Mörs, F., McDaniel Koch, A., Graf, F., Bajohr, S., Reimert, R., Kolb, T., 2015. Renewable Power-to-Gas: A technological and economic review. Renew. Energy. 85, 1371–1390.
- Goux, X., Calusinska, M., Lemaigre, S., Marynowska, M., Klocke, M., Udelhoven, T., Benizri, E., Delfosse, P., 2015. Microbial community dynamics in replicate anaerobic digesters exposed sequentially to increasing organic loading rate, acidosis, and process recovery. Biotechnol. Biofuels. 8, 122.
- Granovskii, M., Dincer, I., Rosen, M.A., 2006. Economic and environmental comparison of conventional, hybrid, electric and hydrogen fuel cell vehicles. J. Power Source. 159, 1186–1193.
- Guinot, B., Montignac, F., Champel, B., Vannucci, D., 2015. Profitability of an electrolysis based hydrogen production plant providing grid balancing services. Int. J. Hydrogen Energy. 40, 8778–8787.
- Guiot, S.R., Cimpoaia, R., Carayon, G., 2011. Potential of wastewater-treating anaerobic granules for biomethanation os synthesis gas. Environ. Sci. Technol. 45, 2006–2012.
- Guneratnam, A.J., Ahern, E., FitzGerald, J.A., Jackson, S.A., Xia, A., Dobson, A.D.W., Murphy, J.D., 2017. Study of the performance of a thermophilic biological methanation system. Bioresour. Technol. 225, 308–315.
- Häne, B.G., Jäger, K., Drexler, H.G., 1993. The Pearson product-moment correlation coefficient is better suited for identification of DNA fingerprint profiles than band matching algorithms. Electrophoresis. 14, 967–972.
- Heide, D., von Bremen, L., Greiner, M., Hoffmann, C., Speckmann, M., Bofinger, S., 2010. Seasonal optimal mix of wind and solar power in a future, highly renewable Europe. Renewable Energy. 35, 2483–2489.
- Herspell, R.B., 1977. *Serpens flexibilis* gen. nov., sp. nov., an unusually flexible, lactate-oxidizing bacterium. Int. J. Syst. Evol. Microbiol. 27, 371–381.
- Hori, K., Matsumoto, S., 2010. Bacterial adhesion: From mechanism to control. Biochem. Eng. J. 48, 424–434.

- Jee, H.S., Nishio, N., Nagai, S., 1988. Continuous CH₄ production from H₂ and CO₂ by *Methanobacterium thermoautotrophicum* in a fixed-bed reactor. J. Ferment. Technol. 66, 235–238.
- Ju, D., Shin, J., Lee, H., Kong, S., 2008. Effects of pH conditions on the biological conversion of carbon dioxide to methane in a hollow-fiber membrane biofilm reactor (Hf – MBfR). Desalination. 234, 409–415.
- Ju, F., Lau, F., Zhang, T., 2017. Linking Microbial Community, Environmental Variables, and Methanogenesis in Anaerobic Biogas Digesters of Chemically Enhanced Primary Treatment Sludge. Environ. Sci. Technol. 51, 3982–3992.
- Jürgensen, L., Ehimen, E.A., Born, J., Holm-Nielsen, J.B., 2014. Utilization of surplus electricity from wind power for dynamic biogas upgrading: northern Germany case study. Biomass Bioenergy. 66, 126–132.
- Kim, S., Choi, K., Chung, J., 2013. Reduction in carbon dioxide and production of methane by biological reaction in the electronics industry. Int. J. Hydrog. Energy. 38, 3488–3496.
- Kleerebezem, R., Stams, a J., 2000. Kinetics of syntrophic cultures: a theoretical treatise on butyrate fermentation. Biotechnol. Bioeng. 67, 529–43.
- Kopp, J., Dichtl, N., 2001. Characterization, in: L. Spinosa, P.A. Vesilind (Eds.), Sludge into Biosolids – Processing, Disposal, Utilization, IWA Publishing, United Kingdom, Chapter 2.
- Kougiyas, P.G., Boe, K., Einarsdottir, E.S., Angelidaki, I., 2015. Counteracting foaming caused by lipids or proteins in biogas reactors using rapeseed oil or oleic acid as antifoaming agents. Water Res. 79, 119–127.
- Kougiyas, P.G., Treu, L., Campanaro, S., Zhu, X., Angelidaki, I., 2016. Dynamic functional characterization and phylogenetic changes due to Long Chain Fatty Acids pulses in biogas reactors. Sci. Rep. 6, 28810.
- Kougiyas, P.G., Treu, L., Peñailillo Benavente, D., Boe, K., Campanaro, S., Angelidaki, I., 2017. Ex-situ biogas upgrading and enhancement in different reactor systems. Bioresour. Technol. 225, 429–437.
- Kougiyas, P.K., Angelidaki, I., 2018. Biogas and its opportunities – A review. Front. Environ. Sci. Eng. 12:14.
- Kreuzer, M.T., Kapteijn, F., Moulijn, J.A., Ebrahimi, S., Kleerebezem, R., Loosdrecht, M.C.M. Van, 2005. Monoliths as Biocatalytic Reactors : Smart Gas - Liquid Contacting for Process Intensification. Ind. Eng. Chem. Res. 44 (25), 9646–9652.
- Langer, S., Schropp, D., Bengelsdorf, F.R., Othman, M., Kazda, M., 2014. Dynamics of biofilm formation during anaerobic digestion of organic waste. Anaerobe. 29, 44–51.

- Lecker, B., Illi, L., Lemmer, A., Oechsner, H., 2017. Biological hydrogen methanation – A review. *Bioresour. Technol.* 245, 1220–1228.
- Lee, J.C., Kim, J.H., Chang, W.S., Pak, D., 2012. Biological conversion of CO₂ to CH₄ using hydrogenotrophic methanogen in a fixed bed reactor. *J. Chem. Technol. Biotechnol.* 87, 844–847.
- Lettinga, G., 1995. Anaerobic digestion and wastewater treatment systems. *Antonie Van Leeuwenhoek. Anaerobic.* 67, 3–28.
- Levene, J.I., Mann, M.K., Margolis, R.M., Milbrandt, A., 2007. An analysis of hydrogen production from renewable electricity sources. *Sol. Energy.* 81, 773–780.
- Li, L., He, Q., Ma, Y., Wang, X., Peng, X., 2015. Dynamics of microbial community in a mesophilic anaerobic digester treating food waste: relationship between community structure and process stability. *Bioresour. Technol.* 189, 113–120.
- Li, L., He, Q., Ma, Y., Wang, X., Peng, X., 2016. A mesophilic anaerobic digester for treating food waste: process stability and microbial community analysis using pyrosequencing. *Microb. Cell Fact.* 15, 1–11.
- Liu, Y., Whitman, W.B., 2008. Metabolic, phylogenetic, and ecological diversity of the methanogenic archaea. *Ann. N. Y. Acad. Sci.* 1125, 171–189.
- Lovley, D.R., Nevin, K.P., 2013. Electrobiocommodities: powering microbial production of fuels and commodity chemicals from carbon dioxide with electricity. *Curr. Opin. Biotechnol.* 24, 385–390.
- Luo, G., Angelidaki, I., 2012. Integrated biogas upgrading and hydrogen utilization in an anaerobic reactor containing enriched hydrogenotrophic methanogenic culture. *Biotechnol. Bioeng.* 109, 2729–2736.
- Luo, G., Johansson, S., Boe, K., Xie, L., Zhou, Q., Angelidaki, I., 2012. Simultaneous hydrogen utilization and in situ biogas upgrading in an anaerobic reactor. *Biotechnol. Bioeng.* 109, 1088–1094.
- Luo, G., Angelidaki, I., 2013a. Hollow fiber membrane based H₂ diffusion for efficient in situ biogas upgrading in an anaerobic reactor. *Appl. Microbiol. Biotechnol.* 97, 3739–3744.
- Luo, G., Angelidaki, I., 2013b. Co-digestion of manure and whey for in situ biogas upgrading by the addition of H₂: process performance and microbial insights. *Appl. Microbiol. Biotechnol.* 97, 1373–1381.
- Luo, G., Wang, W., Angelidaki, I., 2014. A new degassing membrane coupled upflow anaerobic sludge blanket (UASB) reactor to achieve in-situ biogas upgrading and recovery of dissolved CH₄ from the anaerobic effluent. *Appl. Energy.* 132, 536–542.

- Madigan, M.T., Brock, T.D., 2009. Brock biology of microorganisms. Pearson/Benjamin Cummings, San Francisco, CA. ISBN 0-13-2232460-1.
- Martin, M.R., Fornero, J.J., Stark, R., Mets, L., Angenent, L.T., 2013. A Single-Culture Bioprocess of *Methanothermobacter thermautotrophicus* to Upgrade Digester Biogas by CO₂-to-CH₄ Conversion with H₂. *Archaea*. 2013, 1–11.
- Mc. Donald, G., 2003. Biogeography: introduction to space, time and life, Wiley, New York.
- Mc. Ginnis, S., Madden, T.L., 2004. BLAST: at the core of a powerful and diverse set of sequence analysis tools. *Nucleic Acids Res.* 32.
- MeGa-stoRE, 2016. Final Report of Project No 12006. [WWW Document]. Accessed July 2018. <http://www.lemvigbiogas.com/MeGa-stoREfinalreport.pdf>.
- Metcalf & Eddy, 2003. Wastewater Engineering: Treatment and Reuse, McGraw-Hill, New York.
- Mulat, D.G., Mosbæk, F., Ward, A.J., Polag, D., Greule, M., Keppler, F., Nielsen, J.L., Feilberg, A., 2017. Exogenous addition of H₂ for an in situ biogas upgrading through biological reduction of carbon dioxide into methane. *Waste Manag.* 68, 146–156.
- Muñoz, R., Meier, L., Díaz, I., Jeison, D., 2015. A review on the state-of-the-art of physical/chemical and biological technologies for biogas upgrading. *Rev. Environ. Sci. Biotechnol.* 14, 727–759.
- Ni, M., Leung, M., Sumathy, K., Leung, D., 2006. Potential of renewable hydrogen production for energy supply in Hong Kong. *Int. J. Hydrogen Energy.* 31 (10), 1401–1412.
- Parks, D.H., Beiko, R.G., 2010. Identifying biologically relevant differences between metagenomic communities. *Bioinformatics.* 26, 715–721.
- Patterson, T., Savvas, S., Chong, A., Law, I., Dinsdale, R., Esteves, S., 2017. Integration of Power to Methane in a waste water treatment plant – A feasibility study. *Bioresour. Technol.* 245, 1049–1057.
- Pauss, A., Andre, G., Perrier, M., Guiot, S.R., 1990. Liquid-to-gas mass transfer in anaerobic processes: inevitable transfer limitations of methane and hydrogen in the biomethanation process. *Appl. Environ. Microbiol.* 56, 1636–1644.
- Pavlostathis, S.G., Giraldo-Gomez, E., 1991. Kinetics of anaerobic treatment. *Water Sci. Technol.* 24, 35–59.
- Peillex, J., Fardeau, M., Boussand, R., Navarro, J., Belaich, J.P., 1988. Growth of *Methanococcus thermolithotrophicus* in batch and continuous culture on H₂ and CO₂: influence of agitation. *Appl. Microbiol. Biotechnol.* 29, 560–564.

- Peillex, J.P., Fardeau, M.L., Belaich, J.P., 1990. Growth of *Methanobacterium thermoautotrophicum* on H₂ & CO₂: High CH₄ productivities in continuous culture. *Biomass*. 21, 315–321.
- Perry, R.H., Green, D.W., Maloney, J.O., 1999. Perry's Chemical Engineers' Handbook, 7th ed, McGraw-Hill CD-ROM Handbooks. McGraw-Hill. ISBN 0-07-049841-5.
- Persson, T., Murphy, J., Jannasch, A.-K., Liebetrau, J., Toya, J., Ahern, E., Trommler, M., 2015. A Perspective on the Potential Role of Biogas in Smart Energy Grids, 2014. IEA Bioenergy, Dublin 9.
- Petersson, A., Holm-nielsen, J.B., Baxter, D., 2007. Biogas upgrading technologies – developments and innovations. IEA Bioenergy report.
- Petersson, A., Wellinger, A., 2009. Biogas upgrading technologies–developments and innovations. IEA Bioenergy 20.
- Pierce, E., Xie, G., Barabote, R.D., Saunders, E., Han, C.S., Detter, J.C., Richardson, P., Brettin, T.S., Das, A., Ljungdahl, L.G., Ragsdale, S.W., 2008. The complete genome sequence of *Moorella thermoacetica* (f. *Clostridium thermoaceticum*). *Environ. Microbiol.* 10, 2550–2573.
- Power to Gas Strategy, 2011. Accessed April 2018.
<https://www.dena.de/en/topics-projects/projects/energy-systems/power-to-gas-strategy-platform/>.
- Rachbauer, L., Voitl, G., Bochmann, G., Fuchs, W., 2016. Biological biogas upgrading capacity of a hydrogenotrophic community in a trickle-bed reactor. *Appl. Energy*. 180, 483–490.
- Rademacher, A., Zakrzewski, M., Schlüter, A., Schönberg, M., Szczepanowski, R., Goesmann, A., Pühler, A., Klocke, M., 2012. Characterization of microbial biofilms in a thermophilic biogas system by high-throughput metagenome sequencing. *FEMS Microbiol. Ecol.* 79, 785–799.
- Rittmann, B.E., McCarty, P.L., 2001. *Environmental Biotechnology: Principles and Applications*, McGraw Hill, New York.
- Rittmann, S.K., 2015. A critical assessment of microbiological biogas to biomethane upgrading systems. *Adv Biochem Eng Biotechnol.* 151, 117–135.
- Roest, K., Heilig, H.G., Smidt, H., de Vos, W.M., Stams, A.J.M., Akkermans, A.D.L., 2005. Community analysis of a full-scale anaerobic bioreactor treating paper mill wastewater. *Syst. Appl. Microbiol.* 28, 175–185.
- Ryckebosch, E., Drouillon, M., Vervaeren, H., 2011. Techniques for transformation of biogas to biomethane. *Biomass Bioenergy*. 35, 1633–1645.
- Saeed, A., Bhagabati, N., Braisted, J., Liang, W., Sharov, V., Howe, E., 2006. TM4 microarray software suite. *Methods Enzymol.* 411, 134–193.

- Savvas, S., Donnelly, J., Patterson, T., Chong, Z.S., Esteves, S.R., 2017. Biological methanation of CO₂ in a novel biofilm plug-flow reactor: a high rate and low parasitic energy process. *Appl. Energy*. 202, 238–247.
- Schnurer, A., Jarvis, A., 2010. Microbiological handbook for biogas plants. Avfall Sverige and Swedish Gas Centre (SGC).
- Schönheit, P., Moll, J., Thauer, R.K., 1980. Growth Parameters (K_s , μ_{max} , Y_s) of *Methanobacterium thermoautotrophicum*. *Arch. Microbiol.* 65, 59–65.
- Schuchmann, K., Müller, V., 2014. Autotrophy at the thermodynamic limit of life: a model for energy conservation in acetogenic bacteria. *Nat. Rev. Microbiol.* 12, 809–821.
- Seifert, A.H., Rittmann, S., Bernacchi, S., Herwig, C., 2013. Method for assessing the impact of emission gasses on physiology and productivity in biological methanogenesis. *Bioresour. Technol.* 136, 747–751.
- Sekiguchi, Y., Imachi, H., Susilorukmi, A., Muramatsu, M., Ohashi, A., Harada, H., Hanada, S., Kamagata, Y., 2006. *Tepidanaerobacter syntrophicus* gen. nov., sp. nov., an anaerobic, moderately thermophilic, syntrophic alcohol- and lactate degrading bacterium isolated from thermophilic digested sludges. *Int. J. Syst. Evol. Microbiol.* 56, 1621–1629.
- Sensfuss, F., Pfluger, B., 2014. Optimized Pathways Towards Ambitious Climate Protection in the European Electricity System (EU Long-Term Scenarios 2050 II). Karlsruhe [Online]. Accessed January 2017. <http://www.isi.fraunhofer.de/isi-wAssets/docs/x/en/projects/Optimized-pathways-final.pdf>.
- Serejo, M.L., Posadas, E., Boncz, M.A., Blanco, S., Garcia-Encina, P., Muñoz, R., 2015. Influence of biogas flow rate on biomass composition during the optimization of biogas upgrading in microalgal-bacterial processes. *Environ. Sci. Technol.* 49, 3228–3236.
- Sorokin, D.Y., Tourova, T.P., Mussmann, M., Muyzer, G., 2008. *Dethiobacter alkaliphilus* gen. nov. sp. nov., and *Desulfurivibrio alkaliphilus* gen. nov. sp. nov.: two novel representatives of reductive sulfur cycle from soda lakes. *Extremophiles*. 12, 431–439.
- Speece, R.E., 2008. Anaerobic biotechnology and odor/corrosion control for municipalities and industries. Archaea Press, Nashville Tennessee, EEUU.
- Stams, A.J.M., Plugge, C.M., 2009. Electron transfer in syntrophic communities of anaerobic bacteria and archaea. *Nat. Rev. Microbiol.* 7, 568–577.
- Strevett, K.A., Vieth, R.F., Grasso, D., 1995. Chemo-autotrophic biogas purification for methane enrichment: mechanism and kinetics. *Chem. Eng. J. Biochem. Eng. J.* 58, 71–79.

- Strübing, D., Huber, B., Lebuhn, M., Drewes, J.E., Koch, K., 2017. High performance biological methanation in a thermophilic anaerobic trickle bed reactor. *Bioresour. Technol.* 245, 1176–1183.
- Suez Water Technologies – GE, 2014. Accessed January 2018. <https://www.suezwatertechnologies.com/products/zeeweed-hollow-fiber-membranes>.
- Sun, Q., Li, H., Yan, J., Liu, L., Yu, Z., Yu, X., 2015. Selection of appropriate biogas upgrading technology-a review of biogas cleaning, upgrading and utilisation. *Renew. Sust. Energ. Rev.* 51, 521–532.
- Toledo-Cervantes, A., Madrid-Chirinos, C., Cantera, S., Lebrero, R., Muñoz, R., 2017. Influence of the gas-liquid flow configuration in the absorption column on photosynthetic biogas upgrading in algal-bacterial photobioreactors. *Bioresour. Technol.* 225, 336–342.
- Treu, L., Kougias, P.G., de Diego-Díaz, B., Campanaro, S., Bassani, I., Fernández-Rodríguez, J., Angelidaki, I., 2018. Two-year microbial adaptation during hydrogen-mediated biogas upgrading process in a serial reactor configuration. *Bioresour. Technol.* 264, 140-147.
- Turner, J., Sverdrup, G., Mann, M.K., Maness, P.C., Kroposki, B., Ghirardi, M., Evans, R.J., Blake, D., 2008. Renewable hydrogen production. *Int. J. Energy Res.* 32, 379–407.
- Van Eerten-Jansen, M.C.A.A., Ter Heijne, A., Buisman, C.J.N., Hamelers, H.V.M., 2012. Microbial electrolysis cells for production of methane from CO₂: long-term performance and perspectives. *Int. J. Energy Res.* 36, 809–819.
- Veiga, M.C., Jain, M.K., Wu, W.M., Hollingsworth, R.I., Zeikus, J.G., 1997. Composition and role of extracellular polymers in methanogenic granules. *Appl. Environ. Microbiol.* 63, 403–407.
- Wall, D.M., Dumont, M., Murphy, J.D. GREEN GAS Facilitating a future green gas grid through the production of renewable gas. Accessed June 2018. <http://www.attero.nl/klanten-leveranciers/locaties/wijster>.
- Wang, Q., Garrity, G.M., Tiedje, J.M., Cole, J.R., 2007. Naïve Bayesian classifier for rapid assignment of rRNA sequences into the new bacterial taxonomy. *Appl. Environ. Microbiol.* 73, 5261–5267.
- Wang, W., Xie, L., Luo, G., Zhou, Q., Angelidaki, I., 2013. Performance and microbial community analysis of the anaerobic reactor with coke oven gas biomethanation and in situ biogas upgrading. *Bioresour. Technol.* 146, 234–239.
- Weghoff, M.C., Müller, V., 2016. CO metabolism in the thermophilic acetogen *Thermoanaerobacter kivui*. *Appl. Environ. Microbiol.* 82, 2312–2319.

- Weiland, P., 2010. Biogas production: current state and perspectives. *Appl. Microbiol. Biotechnol.* 85, 849–860.
- Wilke, C.R., Chang, P., 1955. Correlation of diffusion coefficients in dilute solutions. *AIChE J.* 1, 264–270.
- Wu, B., Zhang, X., Xu, Y., Bao, D., Zhang, S., 2015. Assessment of the energy consumption of the biogas upgrading process with pressure swing adsorption using novel adsorbents. *J. Clean Prod.* 101, 251–261.
- Yu, Y., Ramsay, J.A., Ramsay, B.A., 2006. On-line estimation of dissolved methane concentration during methanotrophic fermentations. *Biotechnol. Bioeng.* 95, 788–793.
- Yun, Y.M., Sung, S., Kang, S., Kim, M.S., Kim, D.H., 2017. Enrichment of hydrogenotrophic methanogens by means of gas recycle and its application in biogas upgrading. *Energy.* 135, 294–302.
- Zabranska, J., Pokorna, D., 2018. Bioconversion of carbon dioxide to methane using hydrogen and hydrogenotrophic methanogens. *Biotechnol. Adv.* 36, 707–720.
- Zhang, Y., Angelidaki, I., 2014. Microbial electrolysis cells turning to be versatile technology: recent advances and future challenges. *Water Res.* 56, 11–25.

Annexes

Publications





Evaluation of process performance, energy consumption and microbiota characterization in a ceramic membrane bioreactor for ex-situ biomethanation of H₂ and CO₂



Natalia Alfaro, María Fdz-Polanco, Fernando Fdz-Polanco, Israel Díaz*

Department of Chemical Engineering and Environmental Technology, Escuela de Ingenierías Industriales, Sede Dr. Mergelina, University of Valladolid, Dr. Mergelina s/n, 47011 Valladolid, Spain

GRAPHICAL ABSTRACT



ARTICLE INFO

Keywords:

Ex-situ upgrading
Biomethane
MBR
Hydrogenotrophic archaea
Methanation

ABSTRACT

The performance of a pilot ceramic membrane bioreactor for the bioconversion of H₂ and CO₂ to bioCH₄ was evaluated in thermophilic conditions. The loading rate was between 10 and 30 m³ H₂/m³ reactor d and the system transformed 95% of H₂ fed. The highest methane yield found was 0.22 m³ CH₄/m³ H₂, close to the maximum stoichiometric value (0.25 m³ CH₄/m³ H₂) thus indicating that archaeas employed almost all H₂ transferred to produce CH₄. k_{1,a} value of 268 h⁻¹ was reached at 30 m³ H₂/m³ reactor d. DGGE and FISH revealed a remarkable archaeas increase related to the selection-effect of H₂ on community composition over time. *Methanothermobacter thermautotrophicus* was the archaea found with high level of similarity. This study verified the successful application of membrane technology to efficiently transfer H₂ from gas to the liquid phase, the development of a hydrogenotrophic community from a conventional thermophilic sludge and the technical feasibility of the bioconversion.

1. Introduction

The production of biomethane is gaining attention within the countries of the European Union, because of two reasons; firstly, it allows to reduce reliance on natural gas imports (EurObserver, 2014) and

secondly, permitting its transport and utilization far from the place where it is obtained. In this context, the bioconversion of H₂ and CO₂ to biomethane by means of methanogenic archaea according to reaction



* Corresponding author.

E-mail address: israel.diaz@iq.uva.es (I. Díaz).

<https://doi.org/10.1016/j.biortech.2018.02.087>

Received 28 December 2017; Received in revised form 16 February 2018; Accepted 17 February 2018

Available online 23 February 2018

0960-8524/ © 2018 Elsevier Ltd. All rights reserved.

has an important economic, environmental and energetic interest; specially in the actual context of renewable energies implementation because the bioconversion of CO₂ (or biogas) into biomethane can create a synergy between renewable energies. On the one side, H₂ generation from water electrolysis from wind and solar power can be the solution of the variable wind power production, site-specificity of this source and electricity storage (Levene et al., 2007; Ni et al., 2006). EU countries with high implementation of renewable energies, suffer of seasonal surpluses where production exceeds demand and an appreciable portion of electricity production is lost in most cases. H₂ obtained from water electrolysis from excess electricity production from wind and solar power allows long-term energy storage and avoids energy squandering (Cruz, 2008), which is an important and remarkable point nowadays in the idea of environmental conservation and responsible use of energy. However, H₂ limitations and drawbacks are linked to its transportation and management (Granovskii et al., 2006) because of its low density which requires high storage volumes and the technology for direct utilization is not developed yet. Then, the direct transformation of H₂ into biomethane by coupling it with CO₂/biogas permits renewable energy in the form of biomethane to be stored, injected and distributed through the natural gas grid or employed as fuel for vehicles (Deublein and Steinhauser, 2011; Deng and Hägg, 2010). Additionally, anaerobic digestion of biomass, organic wastes and by-products is an effective and well-established renewable energy technology for bioenergy production in the EU (EurObservER, 2013) which produces a biogas with a typical content of 30–40% CO₂ and 70–60% CH₄. This biogas can be upgraded by means of hydrogenotrophic *archaeas* and an external source of H₂ from water electrolysis from surplus wind and solar power (according to Eq. (1) and then, the rate of biomethane increased, increasing its heating value and its potential applications as alternative to natural gas (Deng and Hägg, 2010). At the same time, this technology fixes CO₂ by means of its chemoautotrophic conversion with H₂ to biomethane, decreasing the CO₂ emissions to the atmosphere and then the greenhouse gases, reducing by this way its impact in the global warming which can be translated into an effective CO₂ mitigation technology. Biomethane production from the synergy between the above mentioned renewable energies is a promising and effective method for bioenergy production. Commercial technologies (as PSA, membrane separation, scrubbing, absorption, cryogenic separation or chemical treatment) only separate CH₄ from CO₂ thus requiring further steps to avoid CO₂ emissions, the use of chemical substances, high pressures and temperatures and energy input increasing process costs (Bauer et al., 2013; Luo and Angelidaki, 2012). However, biological biogas upgrading constitutes a cheaper and environmentally friendly alternative technology moving towards sustainable energy production.

Two different approaches are shown in literature in order to remove CO₂ by hydrogenotrophic methanogenesis. The first approach is the addition of H₂ to conventional anaerobic digesters of organic matter with the aim of removing CO₂ from biogas while increasing the production of biomethane named in-situ biogas upgrading (Luo et al., 2012; Wang et al., 2013; Luo and Angelidaki, 2013; Bassani et al., 2016). The second is ex-situ biogas upgrading, the supply of H₂ and CO₂ (or biogas) to an exclusively methanogenic bioreactor rich in methanogenic *archaeas* (Burkhardt and Busch, 2013; Kim et al., 2013; Lee et al., 2012; Luo and Angelidaki, 2012; Ju et al., 2008; Peillex et al., 1990; Kougiyas et al., 2017; Bassani et al., 2017; Bassani et al., 2015).

The gas-liquid mass transfer of H₂ was found to be the main constraint to the successful development of the technology in both approaches due to its low solubility (dimensionless Henry's constant = 55 g/L_G/g/L_{H₂O} at 55 °C). Different methods of gas-liquid mass transfer of H₂ have been performed up to now. Gas diffusers on lab-scale CSTR were shown to require high stirring speed employing a pure culture of *Methanobacterium thermoautotrophicum* at 65 °C (Peillex et al., 1990) or mixed methanogens cultures at thermophilic conditions (55 °C) (Luo and Angelidaki, 2012; Bassani et al., 2015). Lab-scale packed columns bioreactors at mesophilic conditions (35 °C) with a

mixed culture were studied as well (Lee et al., 2012). Moreover, up-flow reactors were experienced in lab-scale (Kougiyas et al., 2017; Bassani et al., 2017). Membrane bioreactors (MBR) were also evaluated for the transfer of H₂ by gas diffusion through the membrane material (Díaz et al., 2015; Strevett et al., 1995; Wang et al., 2013; Ju et al., 2008; Bassani et al., 2016). Scant literature of reactors with volume higher than 10 L has been found: Burkhardt and Busch (2013) used a trickled-bed bioreactor in a 26.8 L of reactor working volume at 35 °C; Kim et al. (2013) studied in a 100 L CSTR at moderate stirring speed at mesophilic conditions and Díaz et al. (2015) performed the biogas upgrading in a membrane bioreactor of 31 L working volume at 55 °C using a polymeric membrane as gas-liquid mass transfer method.

Polymeric membranes as the hollow-fiber experienced previously have a temperature work range up to 40 °C (Suez Water Technologies – GE, 2014) so in a long-term they can produce operating problems being damaged on account of thermophilic conditions. However, ceramic membrane modules are able to work with high temperatures up to 90 °C (Atech Innovations, 2014). Therefore, from an industrial point of view, the working temperature challenge present in polymeric membranes can be solved with the use of ceramic MBRs allowing the biological conversion to take place satisfactorily in a long-term. The utilization of a ceramic membrane bioreactor (MBR) to convert H₂ and CO₂ to bioCH₄ in thermophilic conditions to overcome the limitations to mass transfer of H₂ and the long-term operability was evaluated in this study. In addition, higher scale than which was used in previous studies of literature was experienced moving towards industrial scale. The ceramic membrane module was employed to create a large gas sparging surface and the feasibility of the technology was assessed.

2. Materials and methods

2.1. Pilot plant

The experiment was performed using one insulated cylindrical membrane bioreactor with a working volume of 60 L in which an electric resistance was used to heat reactor walls. Reactor was equipped with a ceramic tubular membrane module (ATECH, Germany) consisted of 28 tubes of Al₂O₃ with 0.8 μm pore size and an area of approximately 1 m² which was used as gas sparging surface in order to generate fine small bubbles. Hydrogenotrophic reactor was fed continuously with H₂ and CO₂ from gas cylinders and two mass-flow controllers (Aalborg, USA) were used to regulate the rate of both gases. Feed and recirculation lines were mixed and then preheated in a thermostatic bath at 55 °C. The gas mixture was injected in the reactor through upper part of ceramic membrane as given in schematic representation of the reactor in Fig. 1. The reactor counted with a compressor to recirculate biogas from the reactor's headspace through the membrane module. A peristaltic pump was employed to avoid solids deposition at a rate of 1000 mL/min.

2.2. Operating conditions

Anaerobic sludge from a thermophilic anaerobic digester at the laboratory treating activated sludge from the WWTP of Valladolid (Spain) was used to inoculate the reactor in a total amount of 60 L. A set-up period was performed at thermophilic conditions by supplying H₂ and CO₂ in a ratio of 4:1 (according to the stoichiometric values of Eq. (1) at a loading rate (LR) of 5.0 m³H₂/m³reactor·d with a gas recirculation rate (Q_R) of 11.6 m³/d for 30 days (all values expressed at 55 °C and 1 atm). Afterwards, the experiment started maintaining thermophilic conditions in which a range between 10 and 30 m³H₂/m³reactor·d was studied in four stages according to Table 1 with the objective of determining the maximum LR that could be applied with a 95% conversion efficiency for methane. In order to evaluate reactor performance and mass transfer conditions different recirculation rates were applied in some stages. Nutrients required for microbial activity and a phosphate buffer

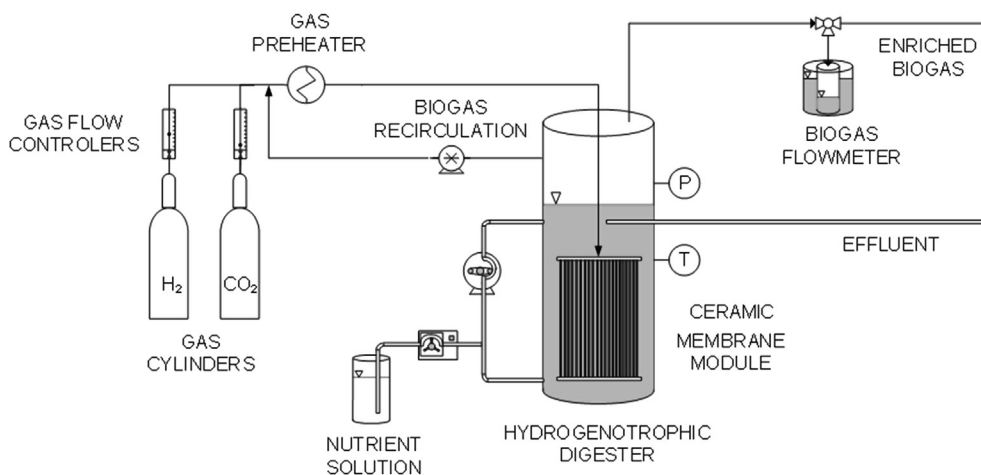


Fig. 1. Diagram of the MBR studied in the experiment.

Table 1
Operating conditions studied during the experiment.

	Stage 1	Stage 2		Stage 3
		2a	2b	
t (d)	0	26	86	137
LR (m ³ H ₂ /m ³ reactor d)	10	20	20	30
Q _R (L/min)	8.0	8.0	12.3	12.3

solution were supplied when the concentration of NH₄⁺ and PO₄³⁻ fell below 500 mg/L as in Díaz et al., 2015, macronutrients and micronutrients were added too. The macronutrient solution was prepared like the stock solution A reported in Angelidaki and Sanders (2004), while the micronutrients solution was a version that was modified (by adding 500 mg/L of resazurine) from the trace-metal solution also from Angelidaki and Sanders (2004). Both solutions were used during the set-up period and stages 1-2a every 20 days approximately and the centrate wastewater from the centrifugation of anaerobically digested mixed sludge of the wastewater treatment plant of Valladolid (Spain) was used as nutrient solution during stages 2b-3 at a flow of 143 mL/day with a HRT of 420 days. The phosphate buffer solution was prepared with K₂HPO₄·3H₂O and KH₂PO₄ to a final pH of 7.4 like in Díaz et al. (2015).

2.3. Monitoring and analysis

Temperature was maintained at 55 ± 1 °C during the experiment and was controlled with a PID and a PT100 probe. For this purpose the walls of the insulated reactor were heated with an electric resistance. Headspace pressure was monitored with an Endress Hauser Cerabar PMC131 probe. A gas flowmeter was employed to measure the effluent gas rate by liquid displacement and the composition of the obtained biogas (dry basis) was determined by gas chromatography (GC-TCD) as described in Díaz et al. (2010) on a daily basis using gas sample point to obtain the biogas sample. A graduate cylinder was used to collect liquid effluent daily. pH, total suspended solids (TSS), volatile suspended solids (VSS), total solids (TS), volatile solids (VS) and NH₄⁺ values were analyzed on a week basis according to Standard Methods (APHA, 2005). VFA concentration was analyzed weekly by gas chromatography (GC-FID) following the method reported in Díaz et al. (2010). Liquid sample was collected in liquid sample point in order to obtain above physicochemical parameters.

2.4. Calculations

Calculations about efficiency of H₂ utilization, methane yield, mass flow rate of H₂ transferred from gas to liquid phase, effluent mass flow rate of CH₄ gas as equivalent H₂, k_La_{H₂} and k_La_{CO₂} values, maximum specific utilization rate and fraction of H₂ employed for methanogen growth have been performed following calculations in Díaz et al. (2015). CH₄ and H₂ in the liquid effluent can be neglected due to the low solubility of CH₄ in water (Adimensional Henry's constant is 43 at 55 °C) and H₂ is several orders of magnitude lower than the H₂ mass flow rates in gaseous streams. In steady state conditions, assuming all the resistance to mass transfer is in the gas/liquid interphase, mass flow rate of H₂ transferred from gas to liquid phase was calculated. H₂ concentration in the liquid phase is negligible as a result of H₂ complete consumption by methanogens in this phase.

To calculate the energy consumption of the system when upgrading biogas (CH₄/CO₂, 60/40 %v.), a steady-state energy balance was performed according to the scheme shown in Fig. 2. The reference state is chosen to be T₀ = 25 °C and P₀ = 1 atm. The power (kW) required for gas compression (W₁ and W₂) was determined with Eq. (2) (Perry et al., 1999):

$$W = 2.78 \cdot 10^{-4} \dot{V} P_1 \ln \frac{P_2}{P_1} \quad (2)$$

where \dot{V} is the volumetric flowrate of the stream (m³/s) and P₁ and P₂

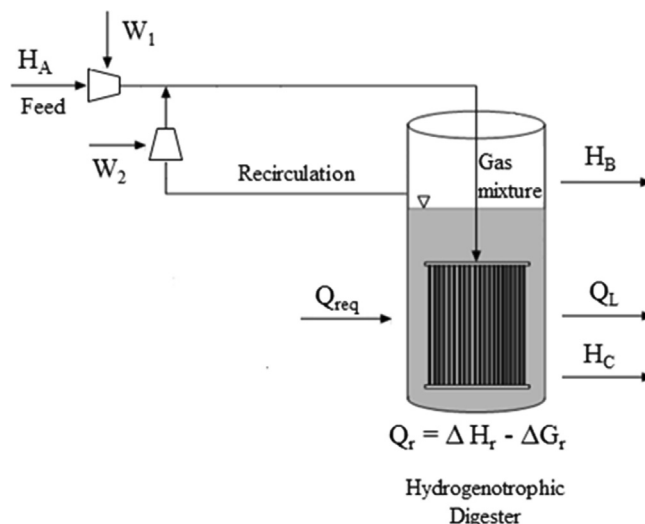


Fig. 2. Diagram of energy streams.

the absolute inlet pressure and absolute discharge pressure (kPa) respectively.

H_i (kW), the specific enthalpy of the stream i , is given by Eq. (3):

$$H_i = \dot{m}_i \cdot C_{p_i} (T_i - T_0) \quad (3)$$

where \dot{m}_i is the mass flow rate (kg/s) of stream i , C_{p_i} the specific heat (kJ/kg K) of stream i , and T_i the temperature (K) of the stream. The values of C_p for the substances involved are 14.3, 0.8, 2.2, 2.08 and 4.184 kJ/kg K for H_2 , CO_2 , CH_4 , H_2O vapor and H_2O liquid correspondingly (NIST Chemistry WebBook, NIST Standard Reference Database Number 69).

Heat losses in the vessel (Q_L) are defined by Eq. (4):

$$Q_L = UA(T_{IN} - T_{OUT}) \quad (4)$$

where U is the global heat transfer coefficient ($0.5 \cdot 10^{-3}$ kW/m² K), A the specific heat transfer surface (m²) considering a 10 m length column (the diameter was adjusted to mass flow rate to fit a loading rate of $30 \text{ m}^3 H_2 / \text{m}^3_{\text{reactor}} \text{ d}$), T_{IN} the temperature inside the vessel (328 K) and T_{OUT} the minimum ambient temperature (273 K).

The heat rate (kW) released by the biological reaction was approximated by Eq. (5), assuming that free enthalpy (ΔG_R^0) is the amount of enthalpy that can be employed by microorganisms (Madigan and Brock, 2009):

$$Q_r = 0.88 \frac{n_{H_2}}{4} (\Delta H_R^0 - \Delta G_R^0) \quad (5)$$

where 0.88 is the efficiency of substrate conversion to CH_4 , n_{H_2} is molar flow rate of H_2 supplied (mol/s), 4 the stoichiometric coefficient for H_2 in Eq. (1), and ΔH_R^0 and ΔG_R^0 the enthalpy and Gibbs free energy variations in Eq. (1), -165.0 and -113.6 kJ/mol correspondingly.

Then, the total energy consumption (kW) of the system shown in Fig. 2 can be calculated as (Eq. (6)):

$$\text{Total Energy Consumption} = (H_A + H_B + H_C + Q_L + Q_r) + (W_1 + W_2) \quad (6)$$

where the terms within the first parenthesis correspond to enthalpy/heat rates and W_1 and W_2 the amount of work required for compressors.

2.5. Microbial analysis

In order to evaluate the evolution of the population during the experiment, samples during the different stages were collected in sterile polypropylene tubes and immediately stored at -20 °C. Extraction of genomic DNA, polymerase chain reaction (PCR) amplification and denaturing gradient gel electrophoresis (DGGE) analysis were performed. The protocol described in the Fast[®] DNA Spin Kit for Soil (MP Biomedicals, LLC) handbook was used to extract DNA. The V6–V8 region of the bacterial 16S rRNA genes was amplified by PCR using the universal bacterial primers 968-F-GC and 1401-R (Sigma-Aldrich, St. Louis, MO, USA). The DGGE analysis of the amplicons was performed with a D-Code Universal Mutation Detection System (Bio Rad Laboratories) using 8%(w/v) polyacrylamide gels with a urea/formamide denaturing gradient of 45 to 65%. DGGE running conditions were applied according to Roest et al. (2005). The gels were stained with GelRed Nucleic Acid Gel Stain (biotium) and the most relevant bands were excised from the DGGE gel in order to identify the microorganisms present in the samples. Using the GelCompar IITM software (Applied Maths BVBA, Sint-Martens-Latem, Belgium) DGGE profiles were compared. After image normalization, bands were defined for each sample using the bands search algorithm within the program. Similarity indices were calculated from the densitometric curves of the scanned DGGE profiles by using the Pearson product-moment correlation coefficient (Häne et al., 1993). The peak heights in these densitometric curves were also used to determine the Shannon–Wiener diversity index (H). This index reflects the relative number of DGGE bands (sample richness) and relative intensity of every band (evenness).

It ranges from 1.5 to 3.5 (low and high species evenness and richness, respectively) according to McDonald (2003). The taxonomic position of the sequenced DGGE bands was obtained using the RDP classifier tool (50% confidence level) (Wang et al., 2007). The closest cultured and uncultured relatives to each band were obtained using the BLAST search tool at the NCBI (National Centre for Biotechnology Information) (McGinnis and Madden, 2004). Sequences were deposited in GenBank Data Library under accession numbers MG692444–MG692471 (*archaeas*) and MG692472–MG692496 (bacteria).

In addition, Fluorescence *in situ* hybridization (FISH) was performed. First of all, samples were centrifuged during 5 min and 10000 rpm at 4 °C removing the supernatant. Paraformaldehyde (4% w/v) was used to fix biomass samples (250 μ L) during 3 h. Then, they were washed three times with phosphate-buffered saline (PBS). Aliquots of 10 μ L of samples were deposited on the wells of gelatin-coated, acid-washed, glass microscope slides and dehydrated by passing through a 50%, 80% and 100% (v/v) ethanol series. Hybridization with formamide (30% v/v) and the oligonucleotide probes was at 46 °C for 2 h. The following probes were used: EUB338 I (for most of bacteria, 5'-GCTGCCTCCCGTAGGAGT-3'), EUB338 plus (for Planctomycetales and Verrucomicrobiales, 5'-GCWGCCACCCGTAGGTGT-3') and ARCH915 (for most of *archaea*, 5'-GTGCTCCCCGCCAATTCCT-3') (Daims et al., 1999). After hybridization step, and once the slides were washed and dried, the specimens were counter-stained for 5 min at room temperature with the DNA stain DAPI to quantify the total number of cells. 28 images were randomly acquired from inside each well on the slides using a Leica DM4000B microscope (Leica Microsystems, Wetzlar, Germany) for quantitative FISH analysis. *Archaea* appear red due to hybridization with the ARCH915 probe (red) while bacteria appear green due to hybridization with the EUB338 I and EUB338 plus probes (green) and DAPI (cyan). DAIME software was used to calculate the relative biovolumes of total *archaea* and total bacteria from the total DAPI-stained biomass. They were split into individual colour channels before image segmentation (Daims et al. 2006).

3. Results and discussion

3.1. Conversion of H_2 and CO_2 to CH_4

Biomass adaptation to the substrate took place during the set-up period when the feed mass flow rate of H_2 gas ($m_{H_2, IN}$) was 25.2 g/d (LR of $5.0 \text{ m}^3 H_2 / \text{m}^3_{\text{reactor}} \text{ d}$) and Q_R 8.0 L/min. A large part of the H_2 fed in these first days was transferred to the liquid phase and consumed but was not employed for CH_4 production, probably due to biomass adaptation to the substrate. Then, first stage started with a $m_{H_2, IN}$ of 49.9 g/d (Fig. 3) and the same Q_R than set-up period. The mass balance performed to the gas phase showed that the average efficiency of H_2 utilization (η_{H_2}) was 95% and an average methane yield (Y_{CH_4}) of $0.18 \text{ m}^3 CH_4 / \text{m}^3 H_2$ was observed. Average mass flow rate of H_2 transferred from gas to liquid phase ($m_{H_2, G \rightarrow L}$) obtained was 44.6 g/d and an effluent mass flow rate of CH_4 gas as equivalent H_2 ($(m_{CH_4, OUT})_{H_2eq}$) according to Eq. (1) in average of 35.0 g/d. On day 26 $m_{H_2, IN}$ was raised to 99.9 g/d (Fig. 3) while Q_R was maintained at 8.0 L/min (stage 2a). The increase in the mass flow rate provoked a slightly decrease in average η_{H_2} until 85.7% thus indicating that mass transfer conditions were still acceptable even when the LR was doubled. However, the average Y_{CH_4} obtained was slightly higher than in the previous stage, $0.19 \text{ m}^3 CH_4 / \text{m}^3 H_2$. The difference between $m_{H_2, G \rightarrow L}$ and $(m_{CH_4, OUT})_{H_2eq}$ was almost exactly the same in stage 1 and 2a and the values obtained were 82.2 g/d and 72.5 g/d respectively (Fig. 3). Biogas recirculation rate was increased to 12.3 L/min with the purpose of raising η_{H_2} and the stage 2b started. Under this conditions, the performance of the MBR improve significantly, reaching an average η_{H_2} value of 95% and Y_{CH_4} reached of $0.21 \text{ m}^3 CH_4 / \text{m}^3 H_2$, the highest obtained up to then. In this case, $m_{H_2, G \rightarrow L}$ observed was 89.2 g/d and 80.1 g/d of (m

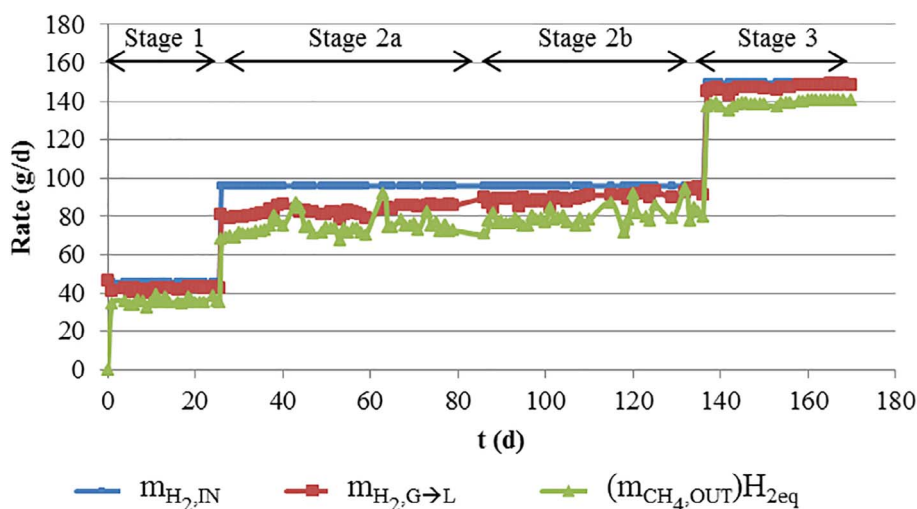


Fig. 3. Bioconversion performance during the experiment.

Table 2

Average k_{La} obtained in the different stages during the experiment of H_2 and CO_2 .

	Stage 1	Stage 2		Stage 3
		2a	2b	
$k_{La_{H_2}}$ (h^{-1})	77	87	166	268
$k_{La_{CO_2}}$ (h^{-1})	54	61	117	190

Table 3

Maximum average specific utilization rate (U), average fraction of H_2 employed for methanogen growth (f_x), average Total Suspended Solids (TSS) and average Volatile Suspended Solids (VSS) in the different stages during the experiment.

	Stage 1	Stage 2		Stage 3
		2a	2b	
U ($g_{COD}/g_{VSS}d$)	6.0	7.7	4.7	3.53
f_x	0.22	0.12	0.11	0.09
TSS (g/L)	0.73	2.0	1.01	1.13
VSS (g/L)	0.44	1.6	0.91	1.02

CH_4 , OUT) H_{2eq} . The difference between them was in the same order of magnitude than the others (Fig. 3). These values were somewhat higher than the ones obtained in stage 2a, thus indicating that recirculation improved the amount of H_2 transferred from gas to liquid phase and the amount of CH_4 produced. Due to the high Q_R used in this stage, some foaming appeared in the reactor. This foaming disappeared naturally (without the use of antifoaming agents) after some weeks of the increase in the Q_R . At this point, $m_{H_2,IN}$ was augmented to 149.8 g/d in combination with a maintained Q_R of 12.3 L/min (stage 3). During this stage, η_{H_2} was 95% in average while Y_{CH_4} increased until 0.22 m^3CH_4/m^3H_2 , much closer to the maximum stoichiometric value of 0.25 m^3CH_4/m^3H_2 . The same methane yield was obtained previously on a similar pilot-scale bioreactor (Díaz et al., 2015). The difference between $m_{H_2, G \rightarrow L}$ and $(m_{CH_4, OUT})H_{2eq}$ was lower than in previous stages meaning that *archaeas* employed almost all H_2 transferred to produce CH_4 (Fig. 3).

The MBR successfully transformed at least 95% of the H_2 fed at LR between 10 and 30 $m^3H_2/m^3_{reactor}d$ adjusting the gas recirculation rate. This highest LR is similar than that achieved on a similar pilot-scale bioreactor (40 $m^3H_2/m^3_{reactor}d$ in Díaz et al., 2015) with a hollow fiber membrane module and higher than those found in packed column bioreactors (4.5 $m^3H_2/m^3_{reactor}d$) (Burkhardt and Busch, 2013) or CSTR (18 $m^3H_2/m^3_{reactor}d$) (Kim et al., 2013). Therefore, this membrane

module can be employed to transfer H_2 at a high rate, allowing the biological conversion to take place satisfactorily in a long-term which is a challenge to polymeric MBRs because of the operating problems related with the damage on account of thermophilic conditions in the polymeric materials.

3.2. MBR mass transfer capacity

The average $k_{La_{H_2}}$ values observed during the different stages in the experiment for the total gas flow through the membrane and the estimated $k_{La_{CO_2}}$ values are shown in Table 2. It should be drawn attention to the fact that this maximum $k_{La_{H_2}}$ value is similar than those found in bioreactors with traditional gas diffusers (at equivalent gas rates), within the range of CSTR with high agitation speeds as 700 rpm (Kreutzer et al., 2005) and higher than the $k_{La_{H_2}}$ value achieved on a similar pilot-scale bioreactor (Díaz et al., 2015) to the LR of 30 $m^3H_2/m^3_{reactor}d$. In general, this is the result of the large sparging area of the membrane module employed, which produces a good gas-liquid mass transfer interfacial area. On the other side, between the two MBRs, this can be explained as a result of the higher pore of ceramic module (0.8 μm versus 0.4 μm of polymeric module) and higher recirculation rate to transfer H_2 .

3.3. Biological activity

It is very important the fact that the adaptation of an unspecific anaerobic thermophilic sludge to H_2 and CO_2 was accomplished. As a result, a methanogenic *archaeas* population was developed, which was capable of the bioconversion of H_2 and CO_2 into bio CH_4 . The methane yield of 0.22 m^3CH_4/m^3H_2 is larger than the yields achieved employing specific strains of *M. thermoautotrophicum* (Jee et al., 1988; Peillex et al., 1990: 0.19 and 0.18 m^3CH_4/m^3H_2 respectively) or *Methanococcus thermolithotrophicus* (Peillex et al., 1988) at high efficiency of H_2 utilization values. From an industrial point of view, it can be translated into lower acquisition costs of specific hydrogenotrophic methanogens because an unspecific anaerobic sludge could be used as inoculum. The maximum specific utilization rate (U) and the fraction of H_2 employed for methanogen growth (fraction of H_2 consumed but not transformed to CH_4 , f_x) are shown in Table 3. The maximum average specific utilization rate obtained was 7.7 $g_{COD}/g_{VSS}d$ within the range of typical design value suggested from methanogens growing on H_2 and CO_2 (Rittman, 2001). At equivalent gas rates, the specific utilization rate obtained with this ceramic membrane bioreactor was always higher than the U value obtained on a similar pilot-scale bioreactor (Díaz et al., 2015) with hollow-fiber module.

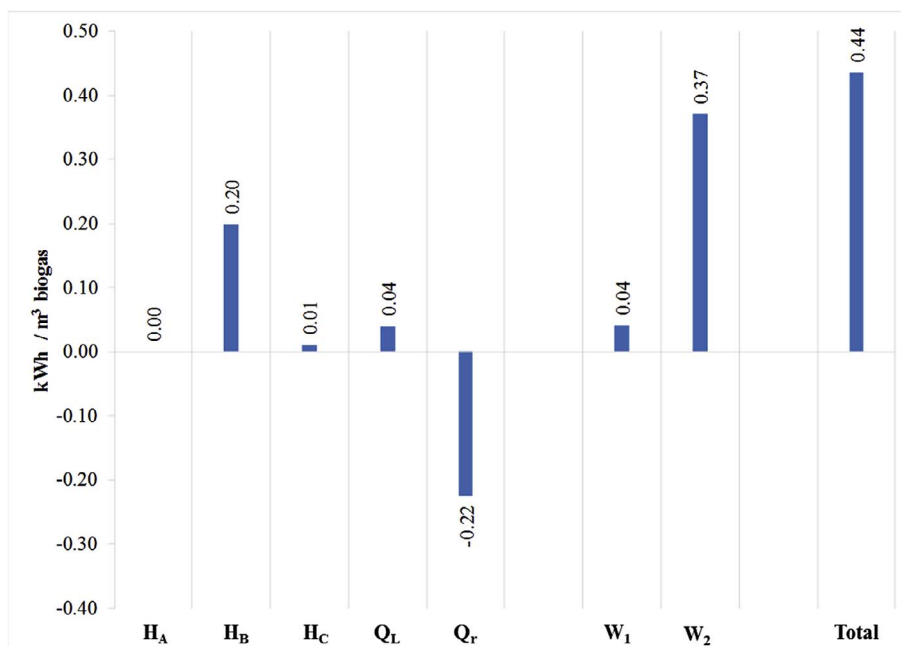


Fig. 4. Energy balance of the upgrading process. Energy rates are normalized by the rate of the upgraded biogas.

According to the results shown in Table 3, it could be stated that the highest value of f_x was obtained during the first stage. This fraction has dropped along the experiment, and in the last stage a decrease of more than 50% appeared. Then, this fraction was higher when mass flow rate of H₂ transferred from the gas to the liquid phase was low and vice versa thus indicating an uncoupling of microbial growth (anabolism) and H₂ conversion to CH₄ (catabolism). In addition, in the first stage of the experiments, the population of *archaeas* in the sludge was not likely to be plentiful as a result of the characteristics of conventional sewage sludge about microbial population and the limitation of this sludge in hydrolysis step. As was described in Díaz et al. (2015) previously, this fact took place because at the beginning of the experiment, especially in the set-up period, an important fraction of H₂ was utilized for microbial growth but when the sludge was completely adapted to the gas substrates, only a small fraction of H₂ was used for methanogen growth, almost all H₂ transferred was used to produce CH₄. At equivalent gas rates, the obtained f_x value with this ceramic MBR was always lower than the value obtained on a similar pilot-scale bioreactor (Díaz et al., 2015) with hollow-fiber membrane module.

VFA concentration was very low during the experiment: acetic acid concentration was under 100 mg/L and propionic acid was below 50 mg/L as it was in Díaz et al., 2015. pH was over the experiment between 6.8 and 7.9 and it was observed that the use of centrate as a nutrient solution helped to balance the pH.

The initial content of SST and SSV in the inoculum was 5.63 and 3.13 g/L respectively. After the set-up period, these values experienced a high decrease as a consequence of the biomass adaptation to the new substrate. Average total and volatile suspended solids concentration analyzed during the experiment in the several stages of the experiment are shown in Table 3. These values showed an increasing trend from Stage 1 to Stage 2a. However, a decrease was produced in stage 2b when the recirculation rate was increase. This fact can be explained firstly, as a result of the high turbulence produced on account of the high recirculation rate employed and secondly, because of the appearance of foaming. This recirculation rate generated an obstacle to the growth of microorganisms being a breaking way for their and/or some losses of solids with the foaming. In the stage 3 of the experiment, it was observed a slightly increase in the content of VSS.

3.4. Consumption of energy

The total energy requirements for the upgrading process are 0.44 kWh per m³ of biogas upgraded (Fig. 4). Energy consumption is dominated by the work required for gas recirculation ($W_2 = 0.37$ kWh/m³ biogas), essential to transfer H₂ to the liquid phase at a high rate, while heat requirements (Q_{req}) are very low (0.025 kWh/m³ biogas). These energy requirements are larger than those reported for the most used commercial technologies such as pressure-swing adsorption or water scrubbing (Bauer et al. 2013) in the range of 0.20–0.30 kWh per m³ of biogas. Nonetheless, it should be noted that 0.35 m³ of new CH₄ can be formed per m³ of biogas supplied to the system according to the maximum methane yield observed (0.22 m³ CH₄/m³ H₂). Since the enthalpy of combustion of CH₄ is 9.95 kWh/Nm³ (802 kJ/mol), the equivalent energy stored in new CH₄ would be 3.5 kWh per m³ of biogas upgraded. Therefore, the total energy requirements represent approximately 13% of the energy that could be obtained from the combustion of new CH₄ formed, hence the energetic benefit of the hydrogenotrophic upgrading process.

From a different angle, the potential energy stored as CH₄ increases from ~6 kWh per m³, in the standard biogas plant (without upgrading) to ~9.5 kWh per m³ after the upgrading process. When discounted the total energy requirements of the upgrading process (0.44 kWh per m³ of biogas), it can be observed an increase of ~50% in potential energy generation from CH₄. In this context, it is always worth mentioning that water electrolysis to produce H₂ for the upgrading process requires 7.2 kWh per m³ of biogas, hence employing excess electricity production from wind and solar power, when they are in surplus, is a must in order that hydrogenotrophic upgrading can be applied. During these seasonal surpluses, the H₂ and CO₂ bioconversion processes, such as the studied, will be energetically beneficiaries.

Total energy consumption is slightly higher than the equivalent calculated for hollow-fiber membrane modules (Díaz et al., 2015), 0.3 kWh per m³ of biogas, as a result of the higher pressure drop within the ceramic module. Conversely, ceramic membranes are more resistant, long-lasting and easy cleaned than polymeric though its high economic cost. Additionally, ceramic membrane modules can withstand higher rates than hollow-fiber modules because a higher pressure can be applied for gas sparging.

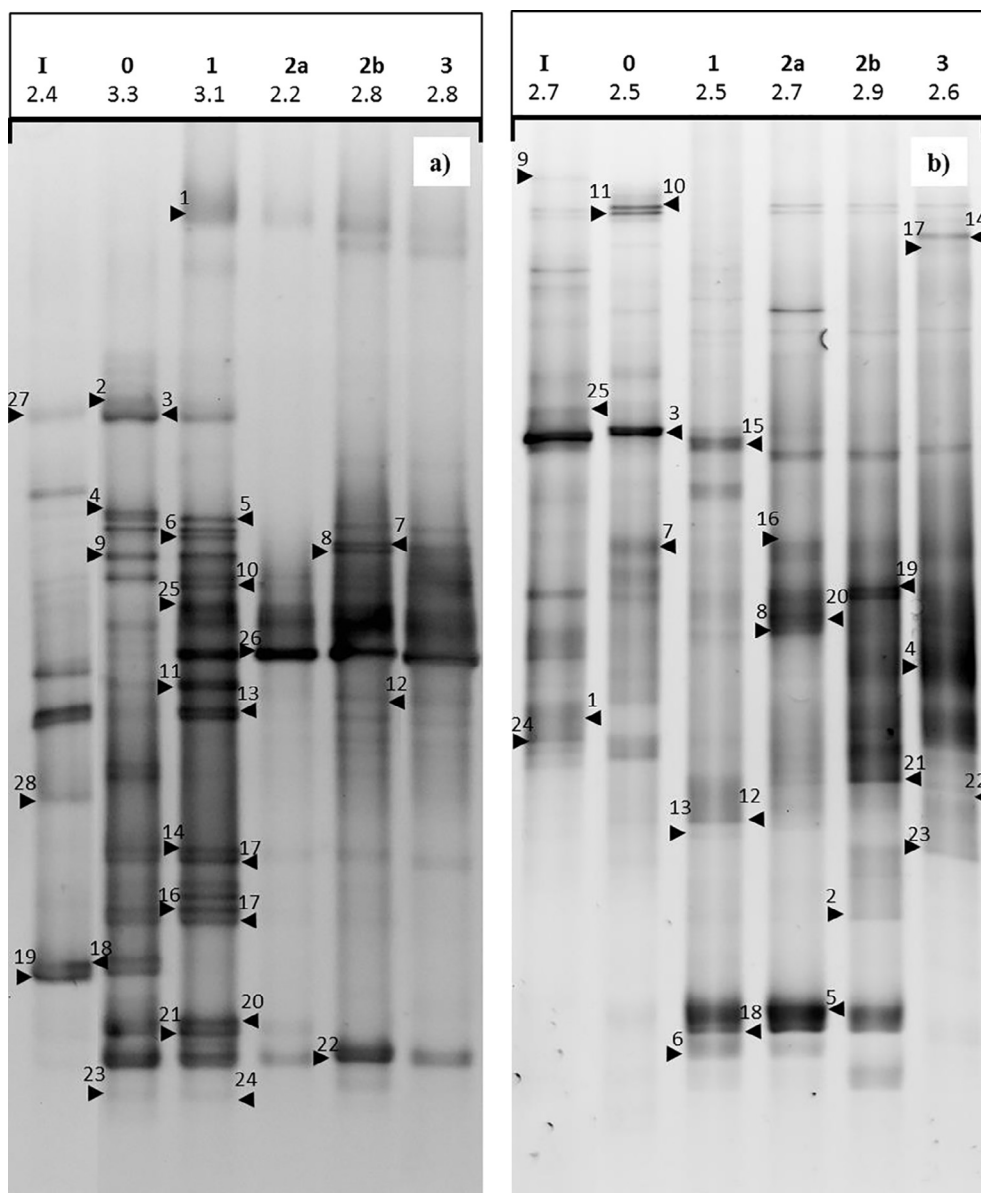


Fig. 5. a) Archaeal DGGE profiles and b) Bacterial DGGE profiles of the 16S rRNA amplicons of the samples with their respective diversity indices. Samples: Inoculum (I), set-up period (0) and stages 1–3 (1, 2a, 2b and 3).

Table 4

The abundances of archaea and bacteria related to the total biomass and ratio archaea/bacteria, in percentages. Samples: Inoculum (I), set-up period (0) and stages 1–3 (1, 2a, 2b and 3).

Sample	Archaea content (%)	Bacteria content (%)	Archaea/bacteria (%)
I	25.86	24.47	51.37
0	1.76	0.015	99.15
1	11.14	0.07	99.37
2a	22.29	0.035	99.84
2b	9.03	0.00	100.00
3	10.70	0.02	99.86

3.5. Microbial community

From the archaeal DGGE gel (Fig. 5a), twenty-eight bands were sequenced. According to the RDP classifier (confidence threshold of 50%), all of them belonged to the *Euryarchaeota* phyla and they were ascribed to two classes, almost all to *Methanobacteria* (band 1–27) and only one band to *Methanomicrobia* (band 28). The BLAST search tool

provided consistent results with those given by the RDP classifier. *Methanothermobacter*, *Methanobacterium* and *Methanobrevibacter* were the three genus assigned to *Methanobacteria* class and *Methanosarcina* genus to *Methanomicrobia* class. After the biomass adaptation to the substrate during the set-up period, some new archaeas appeared and were present since then: band 14, 22 and 26 corresponding with three uncultured archaeon (KJ209721 and KF630660) with an identity of 100% and 99% respectively. Other new appeared archaeas (bands 2, 5, 9, 11, 15, 17, 20 and 24) were present only in some stages but not in all of them. However, as a result of the set-up period, some archaeas disappeared but later they appeared again and were present during the different stages of the experiment (band 6, 10, 25 and 28) and other disappeared completely (band 27). As is showed in Fig. 5a, *Methanothermobacter thermautotrophicus* was the archaea found with high level of similarity in all the stages of the experiment after the initial acclimation to H₂ and CO₂. This archaea was used previously in pure culture studies as in Peillex et al. (1990).

From the bacterial DGGE gel (Fig. 5b) and according to the RDP classifier (confidence threshold of 50%), twenty-five bands belonging to

three different phyla were sequenced: *Firmicutes* (band 1–18), *Proteobacteria* (band 19–23) and *Actinobacteria* (band 24) while one band remained unclassified (band 25). In general, the BLAST search tool provided consistent results with those given by the RDP classifier. *Firmicutes* was the predominant phylum with seven different genera. Two genera were assigned to *Proteobacteria* phylum and unclassified bacteria to *Actinobacteria* phylum. After the biomass adaptation to the substrate during the set-up period, some new bacteria appeared and were present during the whole experiment (band 7, uncultured bacterium JF417907), others disappeared but they were founded again in other stages (band 1, 8 and 16, all of them uncultured bacterium) and other ones were maintained (bands 4, 10 and 11). From the *Proteobacteria* Phylum, the Blast search tool assigned the DGGE band 21 to the genus *Tepidiphilus* with an identity of 100%, which was appeared after the set-up period and maintained during the different stages of the experiment. Although *Tepidiphilus thermophilus* could be a potential homoacetogen, acetoclastic methanogens (*Methanosarcina*) were not present in most of experiment stages and there was no VFA accumulation. Therefore, hydrogenotrophic pathway seems to be the main one to methane production.

A moderately high *archaea* richness and evenness was found with Shannon-Wiener diversity index range between 2,2 and 3,3 having the maximum value after the set-up period of the experiment (Fig. 5a). The diversity index calculated from the bacterial DGGE gel were in the range of 2,5 to 2,9 showing a moderate bacterial richness and evenness (Fig. 5b). The samples presented lower similarity index of *archaeas* during the experiment in comparison with the inoculum (similarity index values between 12.5 and 27.3), which can be linked with the development of a hydrogenotrophic community from a conventional thermophilic sludge with the new substrates (H_2 and CO_2). After the set-up period and during the different stages with several LR the similarity index was not so different (61.7–69.6) even when the recirculation rate was increased in stage 2b.

Archaea and bacteria were detected by FISH in all samples tested (Table 4). In the inoculum, *archaea* accounted for 25.86% of the microbial population, while bacteria represented 24.47% with ratio *archaea*/bacteria of 51.37%. After the set-up period, both *archaea* and bacteria content experienced a high decrease (being almost 0 the % of bacteria content) which can be linked with the decrease in the SSV above mentioned. Although the *archaea* content decreased in this period, the ratio *archaea*/bacteria was 99.15 joining with the acclimation process of the biomass previously explained to the new substrates (H_2 and CO_2) and the development of a methanogenic *archaeas* population. When the LR was augmented to $10\text{ m}^3\text{H}_2/\text{m}^3_{\text{reactor}}\text{d}$ (stage 1) took place an increase in the content of *archaea* in comparison with the previous stage (more than 6 times). When this LR was doubled (stage 2a) the *archaea* content was doubled too. However, when an increased in the recirculation rate was performed (stage 2b) with the purpose of raising the efficiency of H_2 utilization, the content of *archaea* decreased (9.03%). This could be explain as a result of the previously mentioned high turbulence produced on account of the high recirculation rate employed which could be an obstacle to the growth of microorganisms or a breaking way for their. The content of *archaea* experienced a slightly increase in stage 3. All this results are in agreement with the SSV results showed previously. Otherwise, bacteria content had no significative changes since the set-up period. As is showed in Table 4, after the acclimation biomass period, *archaea* were predominant against bacteria.

4. Conclusions

The bioconversion of H_2 and CO_2 into bio CH_4 was feasible using an unspecific anaerobic thermophilic sludge as an inoculum after an adaptation period. The maximum loading rate of $30\text{ m}^3\text{H}_2/\text{m}^3_{\text{reactor}}\text{d}$ had a 95% efficiency in H_2 utilization and a methane yield of $0.22\text{ m}^3\text{CH}_4/\text{m}^3\text{H}_2$. Gas sparging through the ceramic MBR showed a

high capacity of H_2 mass transfer. k_La value of 268 h^{-1} was reached at $30\text{ m}^3\text{H}_2/\text{m}^3_{\text{reactor}}\text{d}$. *Methanothermobacter thermoautotrophicus* was the *archaea* found with high level of similarity in all the experiment stages after the initial acclimation to H_2 and CO_2 .

Acknowledgments

This research was supported by the Spanish Ministry of Education, Culture and Sports (FPU13/04680 Grant) and the funding company FCC-Aqualia in the project Smart Green Gas. The authors also thank the researchers Elisa Rodríguez, Patricia Ayala and Rebeca Pérez.

Appendix A. Supplementary data

Supplementary data associated with this article can be found, in the online version, at <https://doi.org/10.1016/j.biortech.2018.02.087>.

References

- Angelidaki, I., Sanders, W., 2004. Assessment of the anaerobic biodegradability of macropollutants. *Rev. Environ. Sci. BioTechnol.* 3, 117–129.
- APHA, AWWA, WPCF, 2005. Standard Methods for the Examination of Water and Wastewater, 21st ed., Washington, DC.
- Atech Innovations, 2014. http://www.atech-innovations.com/fileadmin/downloads/Instructions_e_2014.pdf Accessed January 2016.
- Bassani, I., Kougias, P.G., Treu, L., Angelidaki, I., 2015. Biogas upgrading via hydrogenotrophic methanogenesis in two-stage continuous stirred tank reactors at mesophilic and thermophilic conditions. *Environ. Sci. Technol.* 49 (20), 12585–12593.
- Bassani, I., Kougias, P.G., Angelidaki, I., 2016. In-situ biogas upgrading in thermophilic granular UASB reactor: key factors affecting the hydrogen mass transfer rate. *Bioresour. Technol.* 221, 485–491.
- Bassani, I., Kougias, P.G., Treu, L., Porté, H., Campanaro, S., Angelidaki, I., 2017. Optimization of hydrogen dispersion in thermophilic up-flow reactors for ex-situ biogas upgrading. *Bioresour. Technol.* 234, 310–319.
- Bauer, F., Hultberg, C., Persson, T., Tamm, D., 2013. Biogas upgrading – review of commercial technologies (Biogasupgradering – Granskning av kommersiella tekniker). Report from the Swedish Gas Technology Center, Malmö.
- Burkhardt, M., Busch, G., 2013. Methanation of hydrogen and carbon dioxide. *Appl. Energy* 111, 74–79.
- Cruz, I., 2008. Energy storage technologies. Technical Business Conference. Department of eolic power. CIEMAT. Spain.
- Daims, H., Brühl, A., Amann, R., Schleifer, K.H., Wagner, M., 1999. The domain-specific probe EUB338 is insufficient for the detection of all Bacteria: development and evaluation of a more comprehensive probe set. *Syst. Appl. Microbiol.* 22 (3), 434–444.
- Daims, H., Lückner, S., Wagner, M., 2006. Daime, a novel image analysis program for microbial ecology and biofilm research. *Environ. Microbiol.* 8, 200–213.
- Deng, L., Hägg, M.B., 2010. Techno-economic evaluation of biogas upgrading process using CO_2 facilitated transport membrane. *Int. J. Greenhouse Gas Control.* 4, 638–646.
- Deublein, D., Steinhauser, A., 2011. *Biogas from Waste and Renewable Resources: An introduction*. Wiley.
- Díaz, I., Lopes, A.C., Pérez, S.I., Fdz-Polanco, M., 2010. Performance evaluation of oxygen, air and nitrate for the microaerobic removal of hydrogen sulphide in biogas from sludge digestion. *Bioresour. Technol.* 101, 7724–7730.
- Díaz, I., Pérez, C., Alfaro, N., Fdz-Polanco, F., 2015. A feasibility study on the bio-conversion of CO_2 and H_2 to biomethane by gas sparging through polymeric membranes. *Bioresour. Technol.* 185, 246–253.
- EurObservER, L'Observatoire des énergies renouvelables, 2013. The state of renewable energies in Europe. ISSN 2101–9622.
- EurObserver, 2014. Biogas barometer. Accessed October 2015. <http://www.euroobserver.org/biogas-barometer-2014/>.
- Granovskii, M., Dincer, I., Rosen, M.A., 2006. Economic and environmental comparison of conventional, hybrid, electric and hydrogen fuel cell vehicles. *J. Power Source* 159, 1186–1193.
- Häne, B.G., Jäger, K., Drexler, H.G., 1993. The Pearson product-moment correlation coefficient is better suited for identification of DNA fingerprint profiles than band matching algorithms. *Electrophoresis* 14, 967–972.
- Jee, H.S., Nishio, N., Nagai, S., 1988. Continuous CH_4 production from H_2 and CO_2 by *Methanothermobacter thermoautotrophicus* in a fixed-bed reactor. *J. Ferment. Technol.* 66, 235–238.
- Ju, D., Shin, J., Lee, H., Kong, S., 2008. Effects of pH conditions on the biological conversion of carbon dioxide to methane in a hollow-fiber membrane biofilm reactor (HF-MBfR). *Desalination* 234, 409–415.
- Kim, S., Choi, K., Chung, J., 2013. Reduction in carbon dioxide and production of methane by biological reaction in the electronics industry. *Int. J. Hydrogen Energy* 38, 3488–3496.
- Kougias, P.G., Treu, L., Peñailillo Benavente, D., Boe, K., Campanaro, S., Angelidaki, I., 2017. Ex-situ biogas upgrading and enhancement in different reactor systems. *Bioresour. Technol.* 225, 429–437.

- Kreutzer, M.T., Kapteijn, F., Moulijn, J.A., Ebrahimi, S., Kleerebezem, R., Van Loosdrecht, M.C.M., 2005. Monoliths as biocatalytic reactors: smart gas–liquid contacting for process intensification. *Ind. Eng. Chem. Res.* 44 (25), 9646–9652.
- Lee, J.C., Kim, J.H., Chang, W.S., Pak, D., 2012. Biological conversion of CO₂ to CH₄ using hydrogenotrophic methanogen in a fixed bed reactor. *J. Chem. Technol. Biotechnol.* 87, 844–847.
- Levene, J.I., Mann, M.K., Margolis, R.M., Milbrandt, A., 2007. An analysis of hydrogen production from renewable electricity sources. *Sol. Energy* 81, 773–780.
- Luo, G., Angelidaki, I., 2012. Integrated biogas upgrading and hydrogen utilization in an anaerobic reactor containing enriched hydrogenotrophic methanogenic culture. *Biotechnol. Bioeng.* 109, 729–2736.
- Luo, G., Angelidaki, I., 2013. Co-digestion of manure and whey for in situ biogas upgrading by the addition of H₂: process performance and microbial insights. *Appl. Microbiol. Biotechnol.* 97, 1373–1381.
- Luo, G., Johansson, S., Boe, K., Xie, L., Zhou, Q., Angelidaki, I., 2012. Simultaneous hydrogen utilization and in situ biogas upgrading in an anaerobic reactor. *Biotechnol. Bioeng.* 109, 1088–1094.
- Madigan, M.T., Brock, T.D., 2009. *Brock Biology of Microorganisms*. Pearson/Benjamin Cummings, San Francisco, CA.
- McDonald, G., 2003. *Biogeography: Introduction to Space, Time and Life*. Wiley, New York.
- McGinnis, S., Madden, T.L., 2004. BLAST: at the core of a powerful and diverse set of sequence analysis tools. *Nucl. Acids Res.* 32.
- Ni, M., Leung, M., Sumathy, K., Leung, D., 2006. Potential of renewable hydrogen production for energy supply in Hong Kong. *Int. J. Hydrogen Energy.* 31 (10), 1401–1412.
- Peillex, J., Fardeau, M., Boussand, R., Navarro, J., Belaich, J.P., 1988. Growth of *Methanococcus thermolithotrophicus* in batch and continuous culture on H₂ and CO₂: influence of agitation. *Appl. Microbiol. Biotechnol.* 29, 560–564.
- Peillex, J.P., Fardeau, M.L., Belaich, J.P., 1990. Growth of *Methanobacterium thermoautotrophicum* on H₂ & CO₂: High CH₄ productivities in continuous culture. *Biomass* 21, 315–321.
- Perry, R.H., Green, D.W., Maloney, J.O., 1999. *Perry's Chemical Engineers' Handbook*. McGraw-Hill CD-ROM Handbooks, 7th ed. McGraw-Hill.
- Rittman, B., 2001. *Environmental Biotechnology: Principles and Applications*. McGraw Hill, New York.
- Roest, K., Heilig, H.G., Smidt, H., de Vos, W.M., Stams, A.J.M., Akkermans, A.D.L., 2005. Community analysis of a full-scale anaerobic bioreactor treating paper mill wastewater. *Syst. Appl. Microbiol.* 28, 175–185.
- Strevett, K.A., Vieth, R.F., Grasso, D., 1995. Chemo-autotrophic biogas purification for methane enrichment: mechanism and kinetics. *Chem. Eng. J. Biochem. Eng. J.* 58, 71–79.
- Suez Water Technologies – GE, 2014. <https://www.suezwatertechnologies.com/products/zeeweed-hollow-fiber-membranes> Accessed January 2018.
- Wang, Q., Garrity, G.M., Tiedje, J.M., Cole, J.R., 2007. Naïve Bayesian classifier for rapid assignment of rRNA sequences into the new bacterial taxonomy. *Appl. Environ. Microbiol.* 73, 5261–5267.
- Wang, W., Xie, L., Luo, G., Zhou, Q., Angelidaki, I., 2013. Performance and microbial community analysis of the anaerobic reactor with coke oven gas biomethanation and in situ biogas upgrading. *Bioresour. Technol.* 146, 234–239.



A feasibility study on the bioconversion of CO₂ and H₂ to biomethane by gas sparging through polymeric membranes



I. Díaz^{a,*}, C. Pérez^b, N. Alfaro^a, F. Fdz-Polanco^a

^a Department of Chemical Engineering and Environmental Technology, Escuela de Ingenierías Industriales, Sede Dr. Mergelina, University of Valladolid, Dr. Mergelina s/n, 47011 Valladolid, Spain

^b Department of Process Engineering, Ros Roca Indox Cryo Energy S.L., Spain

HIGHLIGHTS

- A hollow-fiber MBR was evaluated for the bioconversion of CO₂ and H₂ to biomethane.
- Gas sparging resulted in $k_L a$ values up to 430 h⁻¹ for H₂.
- Biomethane yield reached 0.22–0.23 m³ per m³ of H₂ supplied.
- Biogas could be upgraded up to a 95% CH₄ concentration.

ARTICLE INFO

Article history:

Received 20 January 2015

Received in revised form 25 February 2015

Accepted 27 February 2015

Available online 6 March 2015

Keywords:

Biomethane

Biogas upgrading

Hydrogenotrophic archaea

MBR

Methanation

ABSTRACT

In this study, the potential of a pilot hollow-fiber membrane bioreactor for the conversion of H₂ and CO₂ to CH₄ was evaluated. The system transformed 95% of H₂ and CO₂ fed at a maximum loading rate of 40.2 m³_{H₂}/m³_d and produced 0.22 m³ of CH₄ per m³ of H₂ fed at thermophilic conditions. H₂ mass transfer to the liquid phase was identified as the limiting step for the conversion, and $k_L a$ values of 430 h⁻¹ were reached in the bioreactor by sparging gas through the membrane module. A simulation showed that the bioreactor could upgrade biogas at a rate of 25 m³/m³_d, increasing the CH₄ concentration from 60 to 95%v. This proof-of-concept study verified that gas sparging through a membrane module can efficiently transfer H₂ from gas to liquid phase and that the conversion of H₂ and CO₂ to biomethane is feasible on a pilot scale at noteworthy load rates.

© 2015 Elsevier Ltd. All rights reserved.

1. Introduction

The emissions of greenhouse gases are a major concern for environmental conservation as they are directly linked to climate change; most of the recent global warming can be attributed to the release of CO₂ and other heat-trapping gases from human activities (NRC, 2010). Decreasing CO₂ emissions can be achieved by reducing the amount of CO₂ produced and by managing the utilization of CO₂ or the storage and fossilization of CO₂ (Yang et al., 2008). Although technology that can increase the efficiency of combustion processes and hence reduce the amount of fossil fuels burnt is evolving, only the development of mitigation technologies can decrease the actual CO₂ concentration from its current value (370 ppm) to the pre-industrial concentration (280 ppm). For this reason, several technologies are subject of ongoing research to

better capture, transform, utilize and storage CO₂ (Mikkelsen et al., 2010), with a particular focus on biological alternatives, as these can achieve carbon fixation with low or none use of chemical products, while also avoiding extreme operational conditions, such as high pressure or temperature (Burkhardt and Busch, 2013; Lam et al., 2012).

The technology to fix CO₂ by means of the chemoautotrophic conversion of CO₂ and H₂ to biomethane (Eq. (1)) by methanogenic archaea is still undeveloped because most of the H₂ production worldwide comes from steam reforming of CH₄ (Ullman, 2000). However, it is gaining attention in the actual context of renewable energies implementation. On the one hand, H₂ production from wind and solar power through water electrolysis has been proposed in order to circumvent the limitations of intermittency and site-specificity associated with these sources (Levene et al., 2007). Furthermore, the low density of H₂ requires high storage volumes, and the technology for transportation and direct utilization is still under development. As a consequence, its transformation to biomethane, which can be injected into natural gas

* Corresponding author. Tel.: +34 983423166; fax: +34 983423013.

E-mail address: israel.diaz@iq.uva.es (I. Díaz).

Notation

C_{GmemH_2}	concentration of H_2 in the stream supplied to the membrane (g/m^3)	\dot{m}_{OUT,GH_2}	effluent mass flow rate of H_2 gas (g/d)
C_{IN,GH_2}	concentration of H_2 in the feed gas (g/m^3)	\dot{m}_{OUT,LH_2}	effluent mass flow rate of dissolved H_2 (g/d)
C_{LH_2}	concentration of H_2 in the liquid phase (g/m^3)	η_{H_2}	efficiency of H_2 utilization (%)
C_{OUT,GH_2}	concentration of H_2 in the effluent gas (g/m^3)	OLR	organic loading rate ($m^3_{H_2}/m^3_R d$)
f_X	fraction of H_2 employed for microorganisms growth	Q_{IN,GH_2}	gas feed rate of H_2 (m^3/d)
H_{CH_4}	dimensionless Henry's law constant for CH_4	$Q_{RC,G}$	gas recirculation rate (m^3/d)
H_{H_2}	dimensionless Henry's law constant for H_2	$Q_{OUT,G}$	gas effluent rate (m^3/d)
$k_L a_{CO_2}$	liquid film mass transfer coefficient for CO_2 (h^{-1})	Q_{OUT,GH_2O}	gas effluent rate of water vapor (m^3/d)
$k_L a_{H_2}$	liquid film mass transfer coefficient for H_2 (h^{-1})	r_{utH_2}	H_2 utilization rate (g/h)
$\dot{m}_{G \rightarrow LH_2}$	mass flow rate of H_2 transferred from gas to liquid phase (g/d)	U	specific substrate utilization rate ($g_{COD}/g_{VSS}d$)
\dot{m}_{IN,GH_2}	feed mass flow rate of H_2 gas (g/d)	V_{mCO_2}	molecular volume of CO_2 (mL/mol)
\dot{m}_{OUT,GCH_4}	effluent mass flow rate of CH_4 gas (g/d)	V_{mH_2}	molecular volume of H_2 (mL/mol)
$(\dot{m}_{OUT,GCH_4})_{H_2eq}$	effluent mass flow rate of CH_4 gas as equivalent H_2 according to Eq. (1) (g/d)	V_R	working volume of the bioreactor (L)
		X	concentration of microorganisms (g_{VSS}/L)
		x_{CH_4}	molar fraction of CH_4
		Y_{CH_4}	methane yield ($m^3_{CH_4}/m^3_{H_2}$)

(NG) grids or employed as fuel for vehicles, is very attractive (Deublein and Steinhauser, 2011). On the other hand, biogas production, with a typical content of 60% CH_4 and 40% CO_2 from the anaerobic digestion (AD) of organic wastes and by-products, is a well-established renewable energy technology in the EU (EurObservER, 2013). Incentives and feed-in tariffs initially boosted electricity generation from biogas, despite the low engines efficiency when using this feed, however recent cuts and European policies to develop alternative fuels which reduce energetic dependence are leading to the fast development of biogas upgrading plants that remove CO_2 and produce biomethane (Pettersson et al., 2007). By upgrading biogas with hydrogenotrophic archaeas through Eq. (1), and an external source of H_2 from wind or solar power, a synergy could be reached due to the fact that commercial upgrading plants are based on physical/chemical processes (i.e. absorption, adsorption and membrane separation) that only separate CH_4 from CO_2 , thus requiring further steps to avoid carbon emissions (Bauer et al., 2013):



Literature shows two different approaches when considering the development of a technology that takes advantage of hydrogenotrophic methanogenesis to remove CO_2 . Firstly, the addition of H_2 to anaerobic digesters of organic matter in order to remove CO_2 from biogas while increasing the production of biomethane (Luo and Angelidaki, 2013; Luo et al., 2012; Wang et al., 2013) and, secondly, the supply of H_2 and a CO_2 (or biogas) to an exclusively methanogenic bioreactor rich in hydrogenotrophic archaeas (Burkhardt and Busch, 2013; Ju et al., 2008; Kim et al., 2013; Lee et al., 2012; Luo and Angelidaki, 2012; Peillex et al., 1990). Both lines of research found that the barrier to the successful development of the technology on an industrial scale is the gas–liquid mass transfer of H_2 , due to its low solubility (dimensionless Henry's constant, $H_{H_2} = 50$ and $55 \text{ g/L}_G/\text{g/L}_{H_2O}$ at 35 and 55 °C, respectively). Studies with gas diffusers on lab-scale CSTR were shown to require high stirring speed; Peillex et al. (1990) attained an organic loading rate (OLR) of $1488 \text{ m}^3_{H_2}/\text{m}^3_R d$ with a methane yield of $0.19 \text{ m}^3_{CH_4}/\text{m}^3_{H_2}$ employing a pure culture of *Methanobacterium thermoautotrophicum* at 65 °C. More modest loads were found when employing mixed methanogens cultures at thermophilic conditions (55 °C) (Luo and Angelidaki, 2012), increasing the content of CH_4 in biogas from 60% to 90% at a rate

of $14.4 \text{ m}^3_{H_2}/\text{m}^3_R d$. Another experiment with packed columns bioreactors reported a load of $5.7 \text{ m}^3_{H_2}/\text{m}^3_R d$ with a mixed culture at mesophilic conditions obtaining a yield of $0.23 \text{ m}^3_{CH_4}/\text{m}^3_{H_2}$ (Lee et al., 2012) (close to the stoichiometric maximum). Membrane bioreactors (MBR) were also evaluated for the transfer of H_2 by gas diffusion through the membrane material, reaching a final concentration of biomethane in upgraded biogas of more than 95% (Strevett et al., 1995; Wang et al., 2013), as well as high methanogenic activity even at low pH values or high concentrations of reaction intermediates (Ju et al., 2008).

Literature on reactors with a working volume larger than 10 L is scarce, and limited to mesophilic temperature. Employing a 26.8 L, Burkhardt and Busch (2013) found a yield of $0.26 \text{ m}^3_{CH_4}/\text{m}^3_{H_2}$ in a trickled-bed bioreactor at a rate of $4.52 \text{ m}^3_{H_2}/\text{m}^3_R d$ and in Kim et al. (2013) a load of $18 \text{ m}^3_{H_2}/\text{m}^3_R d$ was reached in a 100 L CSTR at moderate stirring speed, showing a slightly lower yield ($0.23 \text{ m}^3_{CH_4}/\text{m}^3_{H_2}$). Consequently, applied research should focus on developing viable bioreactor configurations that achieve both a high load and a high CH_4 yield on larger scales. This paper aims to study the feasibility of producing CH_4 from H_2 and CO_2 at thermophilic conditions on a pilot scale MBR.

2. Methods

2.1. Pilot plant description

One 40 L cylindrical reactor (176 mm × 1200 mm) with a working volume of 31 L was taken. The reactor was insulated and the walls were heated with electric resistance. Feed gas was obtained from gas cylinders, and the rate was regulated with rotameters. Feed line was preheated in a thermostatic bath (55 °C), mixed with the recirculation, filtered by 0.45 μm (Millex, Millipore) and connected to the upper part of the membrane module as shown in Fig. 1. The hollow-fiber membrane module (Porous fibers, Spain) was placed in the bioreactor to generate gas bubbles. The module consisted of 232 polymeric fibers (PVDF) with a pore size of 0.4 μm and fiber length of 550 mm. The total membrane surface was 0.93 m² and the module occupied 2.6 L. The bioreactor was equipped with a gas pump to recirculate biogas from the headspace through the membrane module, and one peristaltic pump to mix the liquid at a constant rate of 700 mL/min.

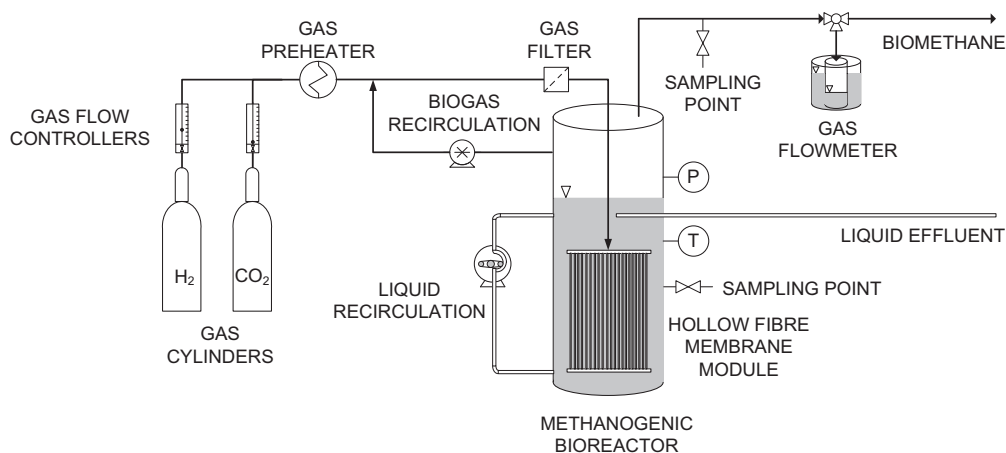


Fig. 1. Pilot plant diagram.

Table 1
Operating conditions applied during the study.

	I					II	III		IV	V	VI	
	a	b	c	d	e		a	b			a	b
<i>t</i> (d)	0	3	7	13	19	27	40	58	75	98	111	124
OLR (m ³ _{H₂} /m ³ _R d)	10.1					20.1	30.2		45.2	25.1	40.2	
Q _{RC,G} (m ³ /d)	0.10	0.20	0.40	0.80	1.61	1.61	1.61	2.41	4.83	2.17	4.43	4.83

2.2. Operating conditions

The reactor was inoculated with 31 L of anaerobic sludge from a thermophilic pilot plant anaerobic digester at our laboratory treating activated sludge from Valladolid WWTP. We set up the reactor by supplying H₂ and CO₂ (ratio according to Eq. (1)) at an organic loading rate of 5.03 m³_{H₂}/m³_Rd with a gas recirculation rate (Q_{RC,G}) of 0.10 m³/d for 30 d. All the values of volumetric flow rates from the study are expressed at 55 °C and 1 atm.

After the set-up period, the experiment started. The experiment was performed at thermophilic conditions (55 ± 1 °C) and divided into 6 stages (I–VI), each corresponding to a certain gas load rate, in order to determine the maximum OLR that could be applied with a 95% conversion efficiency for H₂ (η_{H₂}). Different Q_{RC,G} were applied for some stages (Table 1) in order to evaluate mass transfer conditions and reactor performance. Nutrients required for microbial activity, and a phosphate buffer solution, were supplied when the NH₄⁺ concentration fell below 500 mg/L, specifically, during day 19, 52, 82 and 108. 200 mL of macronutrients solution, 20 mL of micronutrients solution diluted in 180 mL of distilled water and 200 mL of buffer solution were added on the days mentioned. The macronutrient solution was prepared like the stock solution A reported in Angelidaki and Sanders (2004), while the micronutrients solution was a version that was modified (by adding 500 mg/L of resazurine) from the trace-metal solution also from Angelidaki and Sanders (2004) and the phosphate buffer solution was prepared with K₂HPO₄·3H₂O and KH₂PO₄ to a final pH of 7.2 with a concentration of 1 mol/L PO₄³⁻.

2.3. Monitoring and experimental analysis

Headspace pressure was monitored with a Cerabar PMC131 probe (Endress Hauser) and temperature was controlled with a PID and a PT100 probe. Effluent gas rate was measured daily by liquid displacement, and gas composition (dry basis) was determined

by gas chromatography (GC–TCD) as described in Díaz et al. (2010). The liquid effluent was collected and measured daily in a graduated cylinder.

Volatile fatty acids concentration was measured weekly by gas chromatography (GC–FID) following the method reported in Alcántara et al. (2014).

Dissolved H₂ concentration (c_{L,H₂}) was measured periodically by gas–liquid partition with a modified version of the method described in Yu et al. (2006). 8 mL of liquid were sampled from the reactor and subsequently injected into a 10 mL gas-tight serological bottle. The bottles contained 200 μL of concentrated H₂SO₄ in order to prevent any biological activity in the sample. They were closed with butyl septa, sealed with aluminum caps and degassed with helium prior to the sample injection. H₂ in the headspace of the bottles was measured 8 h after sample injection by GC–TCD and liquid concentration was estimated through mass balances. A higher variability between replicates is expected in this modified version since analyses were only performed in duplicate in comparison to the original method where triplicate aqueous samples were withdrawn. Due to the nature of the GC detection limit for H₂ (1% in volume), the minimum c_{L,H₂} that can be measured is 0.022 mg/L.

pH, TSS (total suspended solids), VSS (volatile suspended solids) and NH₄⁺ concentration were measured weekly according to standard methods (APHA et al., 2005).

3. Calculation

Methane yield (Y_{CH₄}) was defined as the volume of CH₄ generated per volume of H₂ fed to the bioreactor, and was calculated with Eq. (2). CH₄ in the liquid effluent can be neglected due to the low solubility of CH₄ in water (H_{CH₄} = 43 at 55 °C) and the low liquid effluent rate:

$$Y_{CH_4} = (Q_{OUT,G} - Q_{OUT,G,H_2O}) \cdot x_{CH_4} / Q_{IN,G,H_2} \quad (2)$$

where $Q_{OUT,G}$ is the volumetric gas effluent rate, $Q_{OUT,G_{H_2O}}$ the volumetric flow rate of water in the gas effluent (calculated with vapor pressure given by Antoine equation), x_{CH_4} the molar fraction of CH_4 (dry basis) in gas effluent and $Q_{IN,G_{H_2}}$ volumetric gas feed rate of H_2 .

In a similar way, the efficiency of H_2 utilization was defined by Eq. (3):

$$\eta_{H_2} = 100 \cdot \left(\dot{m}_{IN,G_{H_2}} - \dot{m}_{OUT,G_{H_2}} \right) / \dot{m}_{IN,G_{H_2}} \quad (3)$$

where $\dot{m}_{IN,G_{H_2}}$ is the mass flow rate of H_2 fed and $\dot{m}_{OUT,G_{H_2}}$ the mass flow rate of H_2 in the effluent gas. H_2 in the liquid effluent can be neglected as well as it is several orders of magnitude lower than the mass flow rates of H_2 in gaseous streams.

A mass balance to the gas phase in the bioreactor (Eq. (4)) was performed to calculate the mass transfer coefficient for H_2 , $k_L a_{H_2}$:

$$\dot{m}_{IN,G_{H_2}} = \dot{m}_{OUT,G_{H_2}} + \dot{m}_{G \rightarrow L_{H_2}} \quad (4)$$

where $\dot{m}_{G \rightarrow L_{H_2}}$ is the mass flow rate of H_2 transferred from the gas to the liquid phase in the bioreactor. In steady-state conditions, $\dot{m}_{G \rightarrow L_{H_2}}$ is given by Eq. (5) assuming that all the resistance to mass transfer is in the gas/liquid interphase:

$$\dot{m}_{G \rightarrow L_{H_2}} = V_R \cdot k_L a_{H_2} \left(c_{G_{mem_{H_2}}} / H_{H_2} - c_{L_{H_2}} \right) \quad (5)$$

where $c_{L_{H_2}} \approx 0$ when the high turbulence provoked by gas sparging rate prevents a concentration gradient in the liquid phase and dissolved H_2 is consumed completely by methanogens. Then, combining Eqs. (4) and (5), $k_L a_{H_2}$ can be obtained (Eq. (6)):

$$k_L a_{H_2} = \frac{\dot{m}_{IN,G_{H_2}} - \dot{m}_{OUT,G_{H_2}}}{V_R \left(c_{G_{mem_{H_2}}} / H_{H_2} \right)} \quad (6)$$

where V_R is the reactor working volume (31 L). $c_{G_{mem_{H_2}}}$ is given by Eq. (7):

$$c_{G_{mem_{H_2}}} = \frac{c_{IN,G_{H_2}} \cdot Q_{IN,G} + c_{OUT,G_{H_2}} \cdot Q_{RC,G}}{Q_{IN,G} + Q_{RC,G}} \quad (7)$$

$c_{IN,G_{H_2}}$ and $c_{OUT,G_{H_2}}$ are the H_2 concentrations in feed and effluent gas respectively, Q_{IN} the volumetric gas feed rate and $Q_{RC,G}$ the volumetric gas recirculation rate.

Yu et al. (2006) demonstrated that the mass transfer coefficient for a given gaseous substrate can be estimated when the coefficient for a reference gas is known in the same reactor and under the same operating conditions (Eq. (8)); thus, the mass transfer coefficient for CO_2 ($k_L a_{CO_2}$) was estimated:

$$k_L a_{CO_2} / k_L a_{H_2} = \left(1 / V_{m_{CO_2}} \right)^{0.4} / \left(1 / V_{m_{H_2}} \right)^{0.4} \quad (8)$$

where $V_{m_{H_2}}$ and $V_{m_{CO_2}}$ are the molecular volume of H_2 and CO_2 (14.3 and 34 mL/mol, respectively) (Wilke and Chang, 1955).

From $\dot{m}_{G \rightarrow L_{H_2}}$, some parameters of the biological kinetics and stoichiometry were calculated performing a mass balance to H_2 in the liquid phase of the bioreactor (Eq. (9)):

$$\dot{m}_{G \rightarrow L_{H_2}} = \dot{m}_{OUT,L_{H_2}} + r_{ut_{H_2}} \quad (9)$$

where $r_{ut_{H_2}}$ is the H_2 utilization rate. From $r_{ut_{H_2}}$, U , the specific substrate utilization rate, was obtained with Eq. (10) including the conversion factors: $8 \text{ g}_{COD} / \text{g}_{H_2}$ and 24 h/d :

$$U = 0.33 \cdot r_{ut_{H_2}} / (X V_R) \quad (10)$$

where X is the microorganisms concentration.

Finally, f_X , the fraction of H_2 employed for microorganisms growth (anabolism), was estimated (Eq. (11)) given the fact that

the mass flow rate of H_2 consumed to produce energy (catabolism) can be obtained from the methane production rate ($\dot{m}_{OUT,G_{CH_4}}$) according to Eq. (1):

$$f_X = \frac{r_{ut,H_2} - \left(\dot{m}_{OUT,G_{CH_4}} / 2 \right)}{r_{ut,H_2}} \quad (11)$$

where the term $\dot{m}_{OUT,G_{CH_4}} / 2$ is defined as the mass flow rate of CH_4 as equivalent H_2 $\left(\dot{m}_{OUT,G_{CH_4}} \right)_{H_2,eq}$ according to Eq. (1).

4. Results and discussion

4.1. Performance of the conversion of H_2 and CO_2 to CH_4

The experiment started (stage Ia) with a $\dot{m}_{IN,G_{H_2}}$ of 22.9 g/d and a $Q_{RC,G}$ of 0.10 m³/d. The mass balance performed to the gas phase (Fig. 2a) showed that less than 90% of the H_2 fed was converted during these first days. Next, biogas recirculation rate was increased stepwise according to Table 1 until 1.61 m³/d, with the purpose of raising η_{H_2} . The bioreactor presented an unstable behavior until day 20, η_{H_2} varied between 65% and 90% (Fig. 2b), and we found a significant difference between $\dot{m}_{G \rightarrow L_{H_2}}$ and $\left(\dot{m}_{OUT,G_{CH_4}} \right)_{H_2,eq}$ until day 9, which indicates that a large part of the H_2 fed in these first days was transferred to the liquid phase and consumed, but was not employed for CH_4 production, probably due to biomass adaptation to the substrate. The bioreactor converted at least 95% of the H_2 fed only after day 20. During stage Ie, the average η_{H_2} was 97% and the average Y_{CH_4} was 0.20 m³_{CH₄} / m³_{H₂}.

On day 27, $\dot{m}_{IN,G_{H_2}}$ was raised to 45.7 g/d while $Q_{RC,G}$ was maintained at 1.61 m³/d (stage II). The increase in the mass flow rate provoked a slightly decrease in η_{H_2} , which remained around 95% for this period, thus indicating that mass transfer conditions were still acceptable even when the OLR was doubled. Besides, the average Y_{CH_4} was 0.19 m³_{CH₄} / m³_{H₂}, somewhat lower than at the end of the previous period. Given the fact that the conversion efficiency did not substantially fall during stage II, we increased $\dot{m}_{IN,G_{H_2}}$ to 68.6 g/d on day 40 (stage IIIa) and maintained $Q_{RC,G}$. In this case, η_{H_2} decreased to an average 93% but the average Y_{CH_4} was not altered.

On day 58, $Q_{RC,G}$ was augmented to 2.41 m³/d (stage IIIb). Under these conditions, the performance of the bioreactor improved significantly, η_{H_2} reached 95% while Y_{CH_4} increased to 0.23 m³_{CH₄} / m³_{H₂}, much closer to the stoichiometric value. Furthermore, the difference between $\dot{m}_{G \rightarrow L_{H_2}}$ and $\left(\dot{m}_{OUT,G_{CH_4}} \right)_{H_2,eq}$ was drastically lower than in previous stages (Fig. 2a) thus indicating that *archaea* employed almost all H_2 transferred in order to produce CH_4 .

The maximum $\dot{m}_{IN,G_{H_2}}$ supplied to the bioreactor was 103 g/d during stage IV, in combination with a recirculation flow rate of 4.83 m³/d, the maximum capacity of gas pump. Throughout this period, η_{H_2} never reached the targeted 95%, instead averaging 91% while Y_{CH_4} was 0.21 m³_{CH₄} / m³_{H₂}. On day 98 (at the end of stage IV), the operation was stopped and the bioreactor opened in order to observe the state of the membrane. There was no biomass attachment to the membrane, in contrast to the biofilm found on the MBRs employed for H_2 conversion to CH_4 in the literature (Ju et al., 2008; Wang et al., 2013), which operated without gas bubbles, probably due to the turbulence provoked by the high recirculation rates employed here to form bubbles while in Ju et al. (2008) and Wang et al. (2013) gas diffusion through the membrane was the transference mechanism.

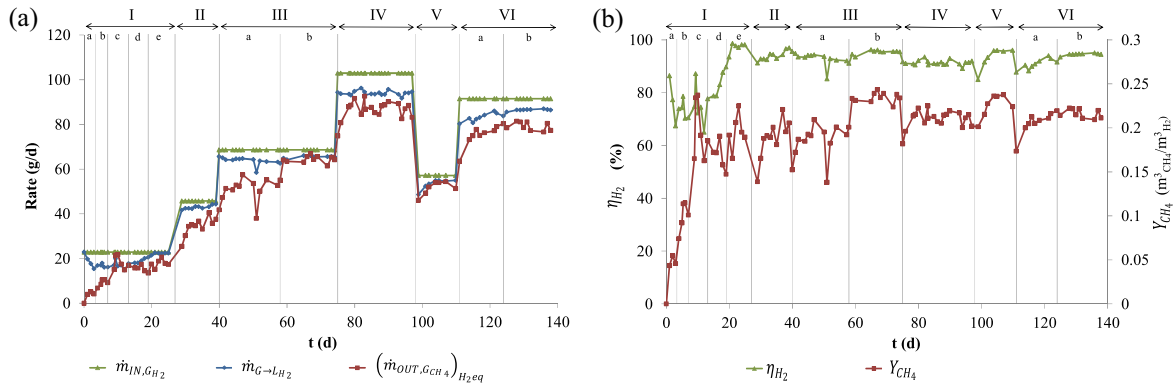


Fig. 2. Performance of the bioconversion throughout the experiment. H_2 and CH_4 as equivalent H_2 mass flow rates (a). Efficiency of H_2 utilization and CH_4 yield (b).

The operation was restarted a few hours later with \dot{m}_{IN,GH_2} of 57.2 g/d (stage V). This lower rate was chosen because during the technical stop some liquid was lost and replaced with approximately 2 L of distilled water. η_{H_2} reached 96% after 2 days and Y_{CH_4} was 0.23 $m^3_{CH_4}/m^3_{H_2}$, similar values to those found on stage IIIb with a comparable OLR. In stage VIa, the rates of feed and recirculation were raised to 91.5 g/d and 4.43 m^3/d , respectively on day 111 and the maximum recirculation capacity was applied from day 124 (stage VIb). During stage VIb, η_{H_2} was 95% in average while the CH_4 yield was 0.22 $m^3_{CH_4}/m^3_{H_2}$. In brief, the bioreactor successfully transformed at least 95% of the H_2 fed at OLR between 10 and 40.2 $m^3_{H_2}/m^3_R/d$ adjusting the gas recirculation rate and 40.2 $m^3_{H_2}/m^3_R/d$ is the maximum OLR that could be supplied to the system while converting 95% of the H_2 fed since the application of a higher loading rate (as in stage IV) failed to achieve a such a conversion at the maximum recirculation rate provided by the gas pump.

This OLR is higher than that achieved on similar pilot-scale bioreactors, such as packed column bioreactors (4.5 $m^3_{H_2}/m^3_R/d$) (Burkhardt and Busch, 2013) or CSTR (18 $m^3_{H_2}/m^3_R/d$) (Kim et al., 2013); on the other hand, Y_{CH_4} was somewhat lower than in those experiments, which found 0.26 and 0.23 $m^3_{H_2}/m^3_R/d$, respectively. Nevertheless, OLR during stage VIb was more than double that applied in Kim et al. (2013), while the reactor yield decreased only slightly. Hence, a membrane can be employed to transfer H_2 at a high rate, allowing the biological conversion to take place satisfactorily. Further research should focus on the long-term stability of the bioconversion rates found during this study.

4.2. Mass transfer capacity in the MBR

The concentration of dissolved H_2 in the liquid phase was below the detection limit during the whole experiment (Fig. 3). As a consequence, the assumption that all the resistance to mass transfer is in the gas/liquid interphase was correct. The correlation coefficient between the experimental data and the predicted values (Eq. (12)) was 0.990, thus confirming that H_2 mass transfer to the liquid phase can be described accurately by Eq. (6) for the range of volumetric flow rates tested:

$$k_L a_{H_2} = 0.0645(Q_{IN,G} + Q_{RC,G}) + 1.1866 \quad (12)$$

The $k_L a_{H_2}$ values observed (Fig. 4) ranged from 30 h^{-1} for the lowest total gas flow through the membrane ($Q_{IN,G} + Q_{RC,G}$) to 430 h^{-1} (for the highest) and the estimated $k_L a_{CO_2}$ from 20 to 300 h^{-1} .

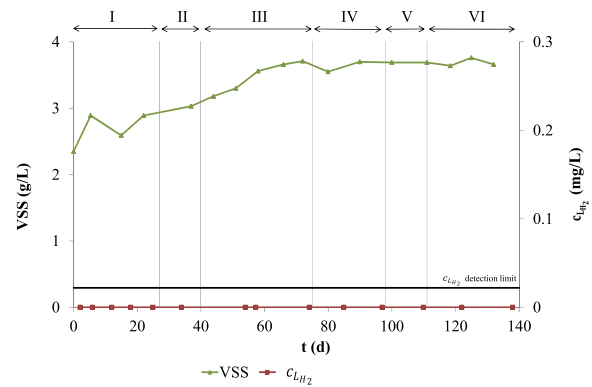


Fig. 3. VSS and dissolved H_2 concentrations in the bioreactor.

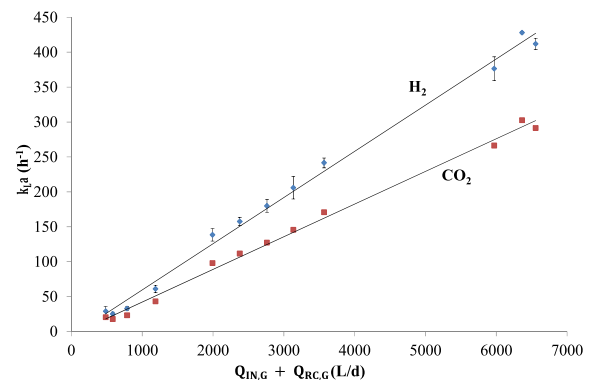


Fig. 4. Linear fitting of experimental $k_L a_{H_2}$ and estimated $k_L a_{CO_2}$ values.

It should be pointed out that this maximum $k_L a_{H_2}$ value is higher than $k_L a$ values found in bioreactors with traditional gas diffusers (at equivalent gas rates), and in the range of CSTR with high agitation speeds (700 rpm) (Kreutzer et al., 2005). This is a consequence of the large sparging area of the membrane module employed (sparging area to reactor working volume ratio is 30 m^2/m^3_R), however, this ratio is lower than employed by Wang et al. (2013) when membranes were used to transfer H_2 by diffusion only (62 m^2/m^3_R). Conversely, gas sparging implies power consumption on gas recirculation to achieve a high $k_L a_{H_2}$ while this power input is prevented when H_2 is transferred only by diffusion through the membrane.

Conversely, much higher $k_L a$ values, as high as 3600 h^{-1} , were found in Peilleux et al. (1990) using H_2 diffusion through porous

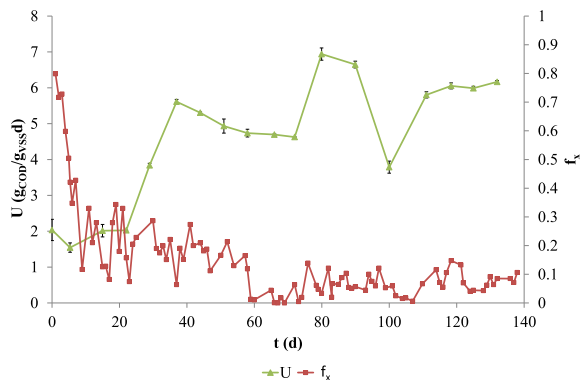


Fig. 5. Specific H₂ utilization rate (U) and fraction of H₂ employed for microbial growth during the experiment.

glass and a Rushton impeller; however, the stirring speeds employed (over 1000 rpm) would presumably result in an extremely energy-consuming system on a larger scale.

A comparison between the maximum potential transfer rates ($k_L a(c_{G\text{mem}}/H)$) from the gas to the liquid phase showed that the ratio $k_{L\text{H}_2}(c_{G\text{memH}_2}/H_{\text{H}_2})/k_{L\text{CO}_2}(c_{G\text{memCO}_2}/H_{\text{CO}_2})$ is around 0.01 g_{H₂}/h/g_{CO₂}/h under the experimental conditions. This is another indicator of H₂ transfer limitations in the bioreactor because 0.18 g of H₂ is required per g of CO₂ to perform the conversion according to stoichiometry (Eq. (1)).

4.3. Biological activity

The maximum specific utilization rate (U) observed during the study was around 7 g_{COD}/g_{VSSd} (Fig. 5). This experimental value is close to the typical design value suggested for methanogens growing on H₂ and CO₂ (8.8 g_{COD}/g_{VSSd}) (Rittman, 2001). Nevertheless, a review of kinetic parameters for different pure cultures of hydrogenotrophic archaea showed that U ranges from 2 to 90 g_{COD}/g_{VSSd} depending on the specific strain (Pavlostathis and Giraldo-Gomez, 1991). The higher the U , the larger the H₂ rate that can be converted to CH₄ in a specific bioreactor before the reaction's limiting factors overtake the H₂ mass transfer. Therefore, U values found during this experiment appear not to be the potential maximum, and are limited by H₂ mass transfer in the system, since c_{H_2} was always below the detection limit, indicating a lack of limitations for the biological reaction.

A high c_{H_2} inhibits propionate and butyrate conversion to acetate or H₂ and CO₂ during anaerobic digestion occasioning lower yields or the whole process breakdown (Speece, 2008). Therefore, the fact that H₂ could be transferred at a high rate without any accumulation in the liquid phase is an important advantage of the technique studied, since it might be applied to the own anaerobic digester, thus avoiding additional units for biogas upgrading. In fact, in situ biogas upgrading was found feasible by Wang et al. (2013) where H₂ was transferred only through diffusion and H₂ and CO₂ were partly consumed in the biofilm developed over the membrane surface. Conversely, gas sparging impedes biofilm formation and methanogenesis takes place totally in the bulk phase; then, additional research is required to evaluate if c_{H_2} would remain as low as in this experiment if anaerobic digestion and upgrading were combined.

From another point of view, the adaptation of an unspecific anaerobic sludge to H₂ and CO₂ led to the development of an acclimated population for the production of biomethane with yields of 0.22 m³_{CH₄}/m³_{H₂} at 40.2 m³_{H₂}/m³_Rd and 0.23 m³_{CH₄}/m³_{H₂} at 30.2 m³_{H₂}/m³_Rd. These yields are larger than the yields achieved

employing specific strains of *M. thermoautotrophicum* (Jee et al., 1988; Peillex et al., 1990) (0.19 and 0.18 m³_{CH₄}/m³_{H₂}) or *Methanococcus thermolithotrophicus* (Peillex et al., 1988) (0.16 m³_{CH₄}/m³_{H₂}) at high η_{H_2} values. This fact implies that the acquisition costs of specific strains of hydrogenotrophic methanogens could be avoided on an industrial scale by employing unspecific anaerobic sludge as inoculum instead, since higher yields could be reached, and given the fact that the current process is limited by H₂ mass transfer.

The fraction of H₂ employed for methanogen growth (f_x) calculated with Eq. (11) was larger during the first stages of the experiment than in the latter (Fig. 5). f_x dropped progressively from values around 0.7 at the beginning of the experiment to below 0.1 after day 60. This result is supported by the fact that VSS concentration increased from 2.5 g/L, at the beginning of the study, to 3.6 g/L the day 58, and remained around this value during the rest of the experiment (Fig. 3). This was also the reason underlying the fact that Y_{CH_4} was always below 0.20 m³_{CH₄}/m³_{H₂} until day 58, in spite of high η_{H_2} values, because an important fraction of H₂ was utilized for microbial growth. Then, f_x was higher when $\dot{m}_{G \rightarrow \text{LH}_2}$ was low (also pointed by the important difference between $\dot{m}_{G \rightarrow \text{LH}_2}$ and $(\dot{m}_{\text{OUT.GCH}_4})_{\text{H}_2\text{eq}}$ in the first stages) whereas it was lower when $\dot{m}_{G \rightarrow \text{LH}_2}$ rose, thus indicating an uncoupling of microbial growth (anabolism) and H₂ conversion to CH₄ (catabolism). This finding is in agreement with Fardeau and Belaich (1986) and with Schönheit et al. (1980), where this phenomenon had already been reported. An extensive discussion about not fixed stoichiometry in methanogenic environments from a biochemical point of view can be found in Kleerebezem and Stams (2000). Additionally, since the inoculum employed in this study was adapted to the treatment of activated sludge prior to the beginning of the study, only a small fraction of the original microbial community was employed for the transformation of H₂ and CO₂ during the experiment. This fact may influence stoichiometry as well, especially on the first stages, and molecular biology tools should be considered in further research in order to elucidate how the evolution of the microbial community influences the methane yield obtained.

From a technological point of view, the repercussions that arise from uncoupled growth and conversion are, at least initially, positive. A bioreactor can be inoculated and biomass adapted from an anaerobic sludge (treating a different substrate) directly inside the methanogenic bioreactor in a short period (as in this study). A low OLR can be used, and an important fraction of H₂ and CO₂ will be employed for methanogens growth. Once the desired biomass concentration is achieved, OLR can be raised, while most of the substrate will be employed for CH₄ production.

VFA concentration was very low during the whole experiment. Acetic acid concentration was under 100 mg/L, propionic acid was below 50 mg/L, and only traces of butyric acid were found. These concentrations are probably the result of microbial decay and endogenous activity. Acetate might also be produced, to some extent, by homoacetogenic bacteria, which use H₂ to reduce CO₂ to produce acetate. However, methanogenesis outcompeted homoacetogenesis in the present study, in contrast to Ju et al. (2008), where a VFA concentration over 4000 mg/L was found in combination with acetoclastic and hydrogenotrophic methanogenesis.

4.4. Application of the MBR for biogas upgrading

The biomethane concentration in upgraded biogas was simulated by assuming that the MBR studied here were employed for the upgrading of biogas under the following conditions:

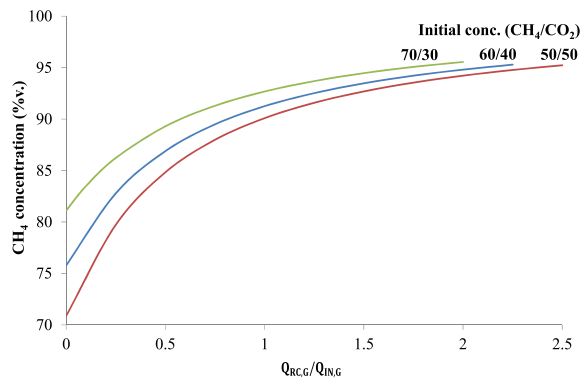


Fig. 6. Simulation of the final CH₄ concentration in upgraded biogas for equivalent CO₂ rates to those of the study.

- (i) $k_{L}a_{H_2}$ values at similar volumetric flow rates through the membrane are the same when feeds of biogas and H₂, and of pure CO₂ and H₂ are fed, since $k_{L}a$ is not dependent on the concentration of each compound.
- (ii) $Q_{IN,G} + Q_{RC,G}$ must fall within the range of studied rates so that the $k_{L}a_{H_2}$ values can be calculated with Eq. (12) ($Q_{IN,G} + Q_{RC,G} < 6.6 \text{ m}^3/\text{d}$).
- (iii) f_X is the same for biogas feed because the additional CH₄ supplied to the system will not alter the microbial activity (the concentration of dissolved CH₄ is that corresponding to the equilibrium in both cases).
- (iv) The CO₂ rate supplied as biogas and the H₂ rate are the same than those in stage VI of the experiment (the maximum OLR that could be applied while achieving a 95% bioconversion efficiency of H₂).

The simulation was carried out using the mass balance equations for gas (Eqs. (4) and (5)) and liquid phases (Eqs. (9) and (11)), where the unknown variables are m_{OUT,GCH_4} and c_{OUT,GH_2} . f_X employed was 0.07, the average value found in the experiment after day 60 and $k_{L}a_{H_2}$ was calculated with Eq. (12).

The volumetric flow rates of biogas that could be upgraded with an equivalent CO₂ content to that of stage VI were 20 m³/m³d (50/50 CH₄/CO₂), 25 m³/m³d (60/40) and 34 m³/m³d (70/30). The final CH₄ concentration as a function of recirculation to feed ratio was represented in Fig. 6. Ratios between 1.75 and 2.25 were required to reach a 95%v. concentration of CH₄ and this was the maximum concentration achievable to comply with condition (ii). However, this upgraded biogas fulfills the requirements for grid injection or for utilization as vehicle fuel in most European countries according to Petersson et al. (2007).

5. Conclusions

The bioconversion of H₂ and CO₂ to CH₄ was feasible at a maximum loading rate of 40.2 m³_{H₂}/m³d while achieving a 95% efficiency in H₂ utilization. Gas sparging through the membrane resulted in a large capacity of H₂ mass transfer in the range of high-speeds-stirring lab-scale bioreactors. Methanogens showed higher ratios of conversion when the load rate was increased, which entails a technological advantage when developing an efficient methanogenic population during the start-up, at low load rates, while increasing energy conservation at high load rates. The system could upgrade biogas efficiently reaching a final concentration of biomethane of 95%v.

Acknowledgements

This research was supported by the Spanish Ministry of Education, Culture and Sports (FPU13/04680 Grant).

References

- Alcántara, C., Fernández, C., García-Encina, P., Muñoz, R., 2014. Mixotrophic metabolism of *Chlorella sorokiniana* and algal-bacterial consortia under extended dark-light periods and nutrient starvation. *Appl. Microbiol. Biotechnol.* 99, 2393–2404.
- Angelidaki, I., Sanders, W., 2004. Assessment of the anaerobic biodegradability of macropollutants. *Rev. Environ. Sci. BioTechnol.* 3, 117–129.
- APHA, AWWA, WPCF, 2005. Standard Methods for the Examination of Water and Wastewater, 21st ed., Washington, DC.
- Bauer, F., Hultberg, C., Persson, T., Tamm, D., 2013. Biogas upgrading – review of commercial technologies (Biogasupgradering – Granskning av kommersiella tekniker). Report from the Swedish Gas Technology Center, Malmö.
- Burkhardt, M., Busch, G., 2013. Methanation of hydrogen and carbon dioxide. *Appl. Energy* 111, 74–79.
- Deublein, D., Steinhauser, A., 2011. Biogas from Waste and Renewable Resources: An Introduction. Wiley.
- Díaz, I., Lopes, A.C., Pérez, S.I., Fdz-Polanco, M., 2010. Performance evaluation of oxygen, air and nitrate for the microaerobic removal of hydrogen sulphide in biogas from sludge digestion. *Bioresour. Technol.* 101, 7724–7730.
- EurObservER, L'Observatoire des énergies renouvelables, 2013. The state of renewable energies in Europe. ISSN 2101–9622.
- Fardeau, M., Belaich, J., 1986. Energetics of the growth of *Methanococcus thermolithotrophicus*. *Arch. Microbiol.* 144, 381–385.
- Jee, H.S., Nishio, N., Nagai, S., 1988. Continuous CH₄ production from H₂ and CO₂ by *Methanobacterium thermoautotrophicum* in a fixed-bed reactor. *J. Ferment. Technol.* 66, 235–238.
- Ju, D., Shin, J., Lee, H., Kong, S., 2008. Effects of pH conditions on the biological conversion of carbon dioxide to methane in a hollow-fiber membrane biofilm reactor (Hf – MBfR). *Desalination* 234, 409–415.
- Kim, S., Choi, K., Chung, J., 2013. Reduction in carbon dioxide and production of methane by biological reaction in the electronics industry. *Int. J. Hydrogen Energy* 38, 3488–3496.
- Kleerebezem, R., Stams, a.J., 2000. Kinetics of syntrophic cultures: a theoretical treatise on butyrate fermentation. *Biotechnol. Bioeng.* 67, 529–543.
- Kreutzer, M.T., Kapteijn, F., Moulijn, J.A., Ebrahimi, S., Kleerebezem, R., Van Loosdrecht, M.C.M., 2005. Monoliths as biocatalytic reactors: smart gas–liquid contacting for process intensification. *Ind. Eng. Chem. Res.* 9646–9652.
- Lam, M.K., Lee, K.T., Mohamed, A.R., 2012. Current status and challenges on microalgae-based carbon capture. *Int. J. Greenh. Gas Control* 10, 456–469.
- Lee, J.C., Kim, J.H., Chang, W.S., Pak, D., 2012. Biological conversion of CO₂ to CH₄ using hydrogenotrophic methanogen in a fixed bed reactor. *J. Chem. Technol. Biotechnol.* 87, 844–847.
- Levene, J.J., Mann, M.K., Margolis, R.M., Milbrandt, A., 2007. An analysis of hydrogen production from renewable electricity sources. *Sol. Energy* 81, 773–780.
- Luo, G., Angelidaki, I., 2012. Integrated biogas upgrading and hydrogen utilization in an anaerobic reactor containing enriched hydrogenotrophic methanogenic culture. *Biotechnol. Bioeng.* 109, 2729–2736.
- Luo, G., Angelidaki, I., 2013. Co-digestion of manure and whey for in situ biogas upgrading by the addition of H₂: process performance and microbial insights. *Appl. Microbiol. Biotechnol.* 97, 1373–1381.
- Luo, G., Johansson, S., Boe, K., Xie, L., Zhou, Q., Angelidaki, I., 2012. Simultaneous hydrogen utilization and in situ biogas upgrading in an anaerobic reactor. *Biotechnol. Bioeng.* 109, 1088–1094.
- Mikkelsen, M., Jørgensen, M., Krebs, F.C., 2010. The teraton challenge. A review of fixation and transformation of carbon dioxide. *Energy Environ. Sci.* 3, 43–81.
- NRC, The National Research Council, 2010. Advancing the Science of Climate Change. A report from The National Academies, Washington, DC.
- Pavlostathis, S.G., Giraldo-Gomez, E., 1991. Kinetics of anaerobic treatment. *Water Sci. Technol.* 24, 35–59.
- Peillex, J., Fardeau, M., Boussand, R., Navarro, J., Belaich, J.P., 1988. Growth of *Methanococcus thermolithotrophicus* in batch and continuous culture on H₂ and CO₂: influence of agitation. *Appl. Microbiol. Biotechnol.* 29, 560–564.
- Peillex, J.-P., Fardeau, M.-L., Belaich, J.-P., 1990. Growth of *Methanobacterium thermoautotrophicum* on H₂ & CO₂: High CH₄ productivities in continuous culture. *Biomass* 21, 315–321.
- Petersson, A., Holm-nielsen, J.B., Baxter, D., 2007. Biogas upgrading technologies – developments and innovations. IEA Bioenergy Report.
- Rittman, B., 2001. Environmental Biotechnology: Principles and Applications. McGraw Hill, New York.
- Schönheit, P., Moll, J., Thauer, R.K., 1980. Growth Parameters (K_s, μ_{max}, Y_s) of *Methanobacterium thermoautotrophicum*. *Arch. Microbiol.* 65, 59–65.
- Speece, R.E., 2008. Anaerobic biotechnology and odor/corrosion control for municipalities and industries. *Archaea Press*.
- Strevett, K.A., Vieth, R.F., Grasso, D., 1995. Chemo-autotrophic biogas purification for methane enrichment: mechanism and kinetics. *Chem. Eng. J. Biochem. Eng. J.* 58, 71–79.
- Ullman, F., 2000. Ullmann's Encyclopedia of Industrial Chemistry, seventh ed. Wiley, Weinheim.

- Wang, W., Xie, L., Luo, G., Zhou, Q., Angelidaki, I., 2013. Performance and microbial community analysis of the anaerobic reactor with coke oven gas biomethanation and in situ biogas upgrading. *Bioresour. Technol.* 146, 234–239.
- Wilke, C.R., Chang, P., 1955. Correlation of diffusion coefficients in dilute solutions. *AIChE J.* 1, 264–270.
- Yang, H., Xu, Z., Fan, M., Gupta, R., Slimane, R.B., Bland, A.E., Wright, I., 2008. Progress in carbon dioxide separation and capture: a review. *J. Environ. Sci. (China)* 20, 14–27.
- Yu, Y., Ramsay, J.A., Ramsay, B.A., 2006. On-line estimation of dissolved methane concentration during methanotrophic fermentations. *Biotechnol. Bioeng.* 95, 788–793.

About the Author



About Me



Natalia Alfaro Borjabad (Soria, 1988) started her **Chemical Engineering** studies in 2006 at the University of Zaragoza with the specialization in Environmental Technology. She was awarded in April 2012 with the **Extraordinary End of Degree Award** by the University of Zaragoza.

She collaborated as a **researcher** in the **Department of Biomass Thermal Conversion** of the National Research Center “**CEDER-CIEMAT**” (Lubia, Soria) headed by Dr. Raquel Ramos in 2009 **for 3 months** working on the demonstration of the feasibility of energy production from the combustion process of the rockrose with or without additives in different scale pilot plants.



Afterwards, in 2010, Natalia spent **8 months** at “**CEDER-CIEMAT**” in the **Department of Energy**, headed by Dr. Juan E. Carrasco, successfully developing her **Final Degree Project** on “Influence of lignosulphonate addition on poplar palletization and combustion” within the frame of the European Singular Strategy Project PSE OnCultivos which was focus on the development, demonstration and evaluation of the feasibility of energy production in Spain from energy crops. She was awarded in May 2011 with the **Award of the Best Final Degree Project** by the University of Zaragoza and the School of Industrial Engineers of Aragón.

In September 2011, she started a **Master’s Program in Chemical Engineering and Environmental Technologies** at the University of Zaragoza. Between 2011 and 2012, Natalia collaborated as a researcher in the Research Group “**Quality and Treatments of Water**” from the **Regional Government of Aragón** for **9 months** at Professor José Luis Ovelleiro Narvi3n’s lab at the **Department of Chemical Engineering and Environmental Technologies** of the University of Zaragoza working on Environmental Microbiology with the specialization in Microbiology of Wastewater and Sludge.

Natalia performed her **master’s thesis** at the Industrial Engineering School of the University of Valladolid in the **Environmental Technology Research Group of the**

Department of Chemical Engineering and Environmental Technology, supervised by Professor Fernando Fdz-Polanco in February 2013, where she developed a research project focused on the study of the “Hygienization of sewage sludge during Anaerobic Digestion processes”, which was her first contact with the Anaerobic Digestion research. As a result of this research, she was awarded in November 2013 with the **accesit award of the XII National Competition Arquímedes – Introduction to Scientific Research** by the Spanish Government and in May 2014 with the **accesit award of the IX Cátedra Ideconsa de Construcción of the University of Zaragoza**.

In March 2013, Natalia fully joined the **Anaerobic Digestion Group** headed by Professor Fernando Fdz-Polanco in the **Environmental Technology Research Group (Department of Chemical Engineering and Environmental Technology of the University of Valladolid)**. She carried out research in several projects funded by public organizations (Spanish Ministry of Science and Innovation) and private companies (Cadagua and Urbaser). Her researches were focused on the anaerobic digestion topic: microbial analysis of sewage sludge, sludge pre-treatment (thermal hydrolysis process and ultrasounds), pre-treatment and anaerobic treatment of the organic fraction of urban solid waste, biochemical methane potential of organic wastes, anaerobic treatment of organic wastes and by-products, energetic optimization in wastewater treatment plant by biological control (activated sludge) and foaming control in anaerobic digesters.

In **September 2014**, Natalia was **awarded with a PhD Grant (FPU)** by the Spanish Ministry of Education, Culture and Sport. Her **PhD thesis** focused on the study of the biogas upgrading technology by biological conversion of H_2 and CO_2 into CH_4 .

Natalia carried out within her PhD studies a **ten-month research stay** (May 2017 – March 2018) at the **Department of Environmental Engineering of the Technical University of Denmark (DTU - Environment)** in the **Bioenergy Research Group** under the supervision of Professor Irini Angelidaki and Associate Professor Panagiotis Kougiaris focused on the study of the intermittent provision of H_2 for ex-situ biogas upgrading and the study of trickling biofilter reactors for biogas upgrading.

Additionally, Natalia worked in the **private sector** for **7 months** as an **environmental consultant** in 2012 at **TECOPYSA** (Parque Tecnológico de Boecillo, Valladolid).

PUBLICATIONS

1. **Alfaro, N.**, Fdz-Polanco, M., Fdz-Polanco, F., Díaz, I., 2018. Evaluation of process performance, energy consumption and microbiota characterization in a ceramic membrane bioreactor for ex-situ biomethanation of H₂ and CO₂. *Bioresource Technology*. 258, 142-150.
2. Porté, H., Kougias, P.G., **Alfaro, N.**, Treu, L., Campanaro, S., Angelidaki, I., 2018. Process performance and microbial community structure in thermophilic trickling biofilter reactors for biogas upgrading. *Science of the Total Environment* (submitted for publication, under revision).
3. Khoshnevisan, B., Tsapekos, P., **Alfaro, N.**, Díaz, I., Fdz-Polanco, M., Rafiee, S., Angelidaki, I., 2017. A review on prospects and challenges of biological H₂S removal from biogas with focus on biotrickling filtration and microaerobic desulfurization. *Biofuel Research Journal*. 16, 741-750.
4. Díaz, I., Pérez, C., **Alfaro, N.**, Fdz-Polanco, F., 2015. A feasibility study on the bioconversion of CO₂ and H₂ to biomethane by gas sparging through polymeric membranes. *Bioresource Technology*. 185, 246-253.
5. **Alfaro, N.**, Cano, R., Fdz-Polanco, F., 2014. Effect of thermal hydrolysis and ultrasounds pretreatments on foaming in anaerobic digesters. *Bioresource Technology*. 170, 477-482.

Publications in preparation

1. **Alfaro, N.**, Kougias, P.G., Treu, L., Campanaro, S., Fdz-Polanco, M., Fdz-Polanco, F., Angelidaki, I., 2018. Intermittent provision of H₂ in up-flow reactors for ex-situ biogas upgrading.

2. **Alfaro, N.**, Fdz-Polanco, M., Fdz-Polanco, F., Díaz, I., 2018. H₂ addition through a submerged membrane for in-situ biogas upgrading in the anaerobic digestion of sewage sludge.
3. **Alfaro, N.**, Díaz, I., Fdz-Polanco, F., Fdz-Polanco, M., 2018. Methanogenesis from H₂ and CO₂ in sewage sludge. Hydrogen acclimation and an approach to hydrogenotrophic activity determination.
4. **Alfaro, N.**, Tsapekos, P., Khoshnevisan, B., Kougias, P.G., Treu, L., Angelidaki, I. Effect of organic load on biogas production and microbial populations during the anaerobic digestion of urban organic waste.
5. Tsapekos, P., **Alfaro, N.**, Kougias, P.G., Khoshnevisan, B., Treu, L., Angelidaki, I. Microbial diversity and dynamicity of continuous anaerobic digesters during start up, stress and stable conditions.

CONFERENCES

Oral presentations

1. **Alfaro, N.**, Kougias, P.G., Treu, L., Fdz-Polanco, M., Fdz-Polanco, F., Angelidaki, I. Intermittent provision of H₂ and CO₂ in up-flow reactors for ex-situ biogas upgrading. Sustain 2017 Conference - Creating Technology for a Sustainable Society, 6 December 2017, Lyngby (Denmark).
2. Díaz, I., Romero-Güiza, M., Icaran, P., Poza, A., **Alfaro, N.**, Fdz-Polanco, M. Start-up of microaerobic removal of H₂S from biogas in full-scale digestion of sewage sludge. AD15 IWA World Conference on Anaerobic Digestion, 17-20 October 2017, Beijing (China).
3. **Alfaro, N.** Del residuo al recurso: soluciones biotecnológicas para el medio ambiente. Ciclo de Conferencias Investigadoras de la UVA en la Aventura de la Ciencia y la Tecnología, 10 March 2017, Valladolid (Spain).

4. **Alfaro, N.** ¿Cómo transformar el viento en gas natural?. Ciclo de Conferencias Investigadoras de la UVa en la Aventura de la Ciencia y la Tecnología, 10 March 2017, Valladolid (Spain).
5. **Alfaro, N.**, Díaz, I., Fdz-Polanco, F., Fdz-Polanco, M. Application of membrane technology to improve mass transfer for the bioconversion of H₂ and CO₂/biogas to bioCH₄. XII DAAL - XII Latin American Workshop and Symposium on Anaerobic Digestion, 23-27 October 2016, Cusco (Perú).
6. **Alfaro, N.**, Díaz, I., Fdz-Polanco, M., Fdz-Polanco, F. Thermal hydrolysis as foaming controlling tool in anaerobic digesters. XII DAAL - XII Latin American Workshop and Symposium on Anaerobic Digestion, 23-27 October 2016, Cusco (Perú).
7. **Alfaro, N.**, Díaz, I., Fdz-Polanco, F., Fdz-Polanco, M. Application of MBR to convert H₂ and CO₂/biogas into bioCH₄. 1st International Conference on Bioenergy and Climate Change – Towards a Sustainable Development, 6-7 June 2016, Soria (Spain).
8. **Alfaro, N.** Enriquecimiento de biogás por conversión biológica de H₂ y CO₂. Ciclo de Conferencias Investigadoras de la UVa en la Aventura de la Ciencia y la Tecnología, 4 March 2016, Valladolid (Spain).
9. Díaz, I., **Alfaro, N.**, Pérez. C., Fdz-Polanco, F. Application of membrane modules to improve mass transfer for the chemoautotrophic biogas upgrading. AD14 World Congress on Anaerobic Digestion, 15-18 November 2015, Viña del Mar (Chile).
10. **Alfaro, N.** Estudio de la higienización de fangos de EDAR en procesos de digestión anaerobia. XII Certamen Universitario Arquímedes de Introducción a la Investigación Científica, 18-20 November 2013, Madrid (Spain).
11. Mediavilla, I., **Alfaro, N.**, Esteban, L.S., Carrasco, J.E. Influence of lignosulphonate addition on poplar pelletisation and combustion. 19th European Biomass Conference and Exhibition, 6-10 June 2011, Berlin (Germany).

Poster presentations

1. **Alfaro, N.**, Fdz-Polanco, M., Fdz-Polanco, F., Díaz, I. Use of membranes for H₂ sparging into sludge digestion: Interactions with organic matter removal and effect of gas recirculation rate on biogas upgrading. 3rd International Conference on Alternative Fuels, Energy and Environment (ICAFEE): Future and Challenges, 28-31 October 2018, Nanjing (China).
2. **Alfaro, N.**, Fdz-Polanco, M., Fdz-Polanco, F., Díaz, I. Application of membrane technology to improve mass transfer for ex-situ biogas upgrading. 2nd International Conference on Alternative Fuels & Energy (ICAFE), 23-25 October 2017, Daegu (South Korea).
3. **Alfaro, N.**, Díaz, I., Fdz-Polanco, F., Fdz-Polanco, M. Methanogenesis from H₂ and CO₂ in sewage sludge. Kinetic study, hydrogen acclimation and an approach to activity determination. AD15 IWA World Conference on Anaerobic Digestion, 17-20 October 2017, Beijing (China).

STUDENT MENTORING AND CO-SUPERVISION

Master Thesis

Víctor Blanco Guerra. “Estudio de la actividad hidrogenotrófica de un fango granular para el enriquecimiento de un biogás por conversión biológica de CO₂ y H₂ a CH₄”. January 2017 - April 2017, Master in Environmental Engineering of the University of Valladolid (Spain).

Mario Santiago Herrera. “Estudio de la actividad hidrogenotrófica de un fango EDAR para el enriquecimiento de biogás mediante conversión biológica”. January 2017 - April 2017, Master in Environmental Engineering of the University of Valladolid (Spain).

Research Project

Esther del Amo Mateos. "Tests de actividad acetoclástica e hidrogenotrófica para diferentes tipos de fangos". January 2017 - March 2017, Chemical Engineering Degree of the University of Valladolid (Spain).

TEACHING

1. Environmental and Process Technology. Assistant Professor, 3 ECTS. Mechanical Engineering Degree and Industrial Organization Engineering Degree. 1st course, academic year 2017/2018, University of Valladolid (Spain).
2. Environmental and Process Technology. Assistant Professor, 3 ECTS. Industrial Electronics and Automation Engineering Degree. 1st course, academic year 2016/2017, University of Valladolid (Spain).
3. Environmental and Process Technology. Assistant Professor, 3 ECTS. Mechanical Engineering Degree. 1st course, academic year 2015/2016, University of Valladolid (Spain).

RESEARCH STAY ABROAD

Department of Environmental Engineering, Technical University of Denmark: DTU – Environment. 10 months, May 2017 – March 2018. Guest PhD Student. Supervisors: Irini Angelidaki and Panagiotis Kougias.

PATENT

Rogalla, F., Monsalvo, V., Icaran, P., Fdz-Polanco, F., Díaz, I., **Alfaro, N.**, Fdz-Polanco, M., 2017. Method for obtaining methane enriched biogas and an installation for carrying out said method. European patent, application number EP17382699, reference number 2017/71199.

AWARDS

1. Award for the best poster “Methanogenesis from H₂ and CO₂ in sewage sludge” at the 5st Seminar of the Chemical and Environmental Engineering PhD Program. University of Valladolid, 29 November 2017, Valladolid (Spain).
2. Accesit award of the IX Cátedra Ideconsa de Construcción of the University of Zaragoza for the best master thesis project “Hygienization of sewage sludge during Anaerobic Digestion processes”. University of Zaragoza, 30 May 2014, Zaragoza (Spain).
3. Accesit award of the XII National Competition Arquímedes – Introduction to Scientific Research given by the Spanish Government for the research project “Hygienization of sewage sludge during Anaerobic Digestion processes”. Polytechnic University of Madrid, 20 November 2013, Madrid (Spain).
4. Extraordinary End of Degree Award given by the School of Engineering and Architecture of the University of Zaragoza for the best academic scores in Chemical Engineering. University of Zaragoza, 17 April 2012, Zaragoza (Spain).
5. Award for the Best Final Degree Project “Influence of lignosulphonate addition on poplar palletization and combustion” given by the University of Zaragoza and the School of Industrial Engineers of Aragón. University of Zaragoza, 13 May 2011, Zaragoza (Spain).

RESEARCH PROJECTS

Participation in the following Research & Development Projects: CIEN Project “Smart Green Gas” (2014 - 2018) funded by the company FCC Aqualia, Project “Development of processes and anaerobic technology” (2013-2014) and ALLIANCE Project “Evaluation of co-digestion opportunities (SL0801)” (2013).

FELLOWSHIPS

1. Accommodation grant for the research stay abroad in DTU-Environment. Fellowship of the University of Valladolid, 2018.
2. Travel grant for the participation in the international conference AD15 IWA World Conference on Anaerobic Digestion. Fellowship of the University of Valladolid, 2017.
3. Travel grant for the participation in the international conference XII DAAL - XII Latin American Workshop and Symposium on Anaerobic Digestion. Fellowship of the University of Valladolid, 2016.
4. Registration Grant in an English Course – Level B2. Grant of the Regional Government of Castilla y León, 2016.
5. Travel grant for the participation in the international conference AD14 World Congress on Anaerobic Digestion. Fellowship of the University of Valladolid, 2015.
6. Travel, accommodation and registration grant for the participation in the course 3rd Water_2020 Training School “Fate, Treatment, Environmental and Economic Impacts of Micropollutants and Emissions”. Fellowship of COST (European Cooperation in Science and Technology), W₂O₂, Novedar and REGATA (Red Galega de Tratamiento de Aguas), 2015.

7. PhD grant. Grant reference: FPU13/04680. Fellowship of the Spanish Ministry of Education, Culture and Sport, 2014.
8. Travel, accommodation and registration grant for the participation in the course ETeCoS³ Summer School “Biological Treatment of Solid Waste”. Fellowship of COST (European Cooperation in Science and Technology), Erasmus Mundus y EACEA (The Education, Audiovisual and Culture Executive Agency), 2014.
9. Research grant. Fellowship of the Agency of innovation, funding and business internationalization of the Regional Government of Castilla y León, 2012.

Acknowledgements

*Thank
you*



Creo que no hay suficientes páginas ni palabras para que pueda expresar como realmente me gustaría todo lo agradecida que estoy...

En primer lugar, me gustaría agradecer a mis directores, Fernando, María e Israel, por darme la oportunidad de realizar esta tesis, de crecer y desarrollarme personal y profesionalmente durante los años de realización del doctorado. Gracias por vuestro tiempo, esfuerzo y consejos durante estos años.

Fernando, han pasado ya más de 6 años desde que te conocí (nunca olvidaré nuestra primera reunión). Muchas gracias por la confianza que depositaste en mí desde el principio (sin conocerme inicialmente) y en mi forma de trabajar que se ha traducido a lo largo de estos años desde mi inicial colaboración para hacer mi TFM hasta la realización de esta tesis doctoral, pasando por mi periodo de investigadora previo a la tesis con cargo a proyectos. Gracias jefe, ha sido un placer trabajar contigo, he aprendido muchísimo de ti.

María, muchas gracias por tu apoyo, por tu ayuda y confianza en mí y en mi trabajo siempre. Gracias por preocuparte por mí, por escucharme y entenderme, por tu disponibilidad cuando lo he necesitado y por el cariño con el que siempre me has tratado. He aprendido muchas cosas gracias a ti, tanto personal como profesional.

Isra, mis comienzos en el campo de biogas upgrading habrían sido mucho más lentos y costosos sin tu ayuda inicial, gracias.

I would like to thank my supervisors Irini Angelidaki and Panagiotis Kougias for giving me the opportunity to develop my external stay in their research group in Denmark.

Special thanks go to Panagiotis Kougias and Laura Treu, from the Technical University of Denmark, for teaching me (with great patience and professionalism) everything I learned during my external stay in Denmark and for supporting and helping me all the time (there or later by Skype). I learnt a lot with and from you both...not only in the professional way but also in the personal one. Thanks a lot.

Quiero agradecer también al Ministerio de Educación, Cultura y Deporte del Gobierno de España por haberme otorgado la beca FPU para la realización de esta tesis.

Gracias también a todos los profesores del Departamento de Ingeniería Química y Tecnología del Medio Ambiente de la Universidad de Valladolid, en especial a TODOS los del Grupo de Investigación Reconocido Tecnología Ambiental (GIRTA).

Gracias a TODOS y cada uno de mis compañeros del laboratorio de la Universidad de Valladolid, he tenido mucha suerte de compartir con vosotros este tiempo. Es una lista larguísima de nombres, 6 años en total en el GIRTA dan para mucho: los que estabais cuando llegué al departamento y os habéis ido marchando poco a poco, los que habéis aparecido durante estos años por períodos cortos (o no tan cortos) y ya no estáis aquí,

los que seguís estando, las nuevas incorporaciones... gracias a todos por todos los buenos momentos vividos, por las horas de laboratorio pasadas juntos (que han sido un montón), por darme vuestro apoyo y ayuda, por hacer que mi investigación en estos años fuera más fácil, divertida y llevadera.

Gracias a los estudiantes con los que he trabajado estos años, en especial a mi “equipo del 2017”, Víctor, Mario y Esther. Gracias por vuestra ayuda, fue muy motivante y enriquecedor enseñaros lo (mucho o poco) que sabía. Yo también aprendí de vosotros muchas cosas, gracias por todo el tiempo que trabajamos juntos.

Thank you very much to ALL the members of the Bioenergy Research Group of DTU-Environment. I will always remember the period that I worked with you with a big smile and good memories. There is a long list of names of people whom I would like to say thank you very much which can be quickly summarize in all the PhD students, guest PhD students, senior researchers, researchers, the girls of the room 174 (my room, it was great share with you the room) I met there... Thanks for all our days together (in and out the lab), for all the help you provided me, the opportunity to work with you was amazing. Thanks for the conversations, the jokes, the teamwork and the time spent together. Thanks for make me feel a bioenergy member as well. Thanks for sharing with me such a wonderful experience. I really appreciate you, I will never forget you. TAK!

Muchas gracias a los técnicos de laboratorio de la Universidad de Valladolid. En especial a Enrique Marcos y Araceli Crespo. Gracias Enrique por todos los AGVs que has analizado para mí, por todas esas botellas de H₂ que juntos hemos cambiado y purgado y que tanto pánico me daban, por tu disponibilidad y ayuda siempre. Gracias Araceli, por ser mi “madre de laboratorio”, he aprendido muchísimo contigo, gracias no solo por todos esos sólidos (que han sido una barbaridad) y demás análisis f-q de estos años, sino también por toda la relación personal que hemos forjado, me has ayudado y apoyado muchísimo.

Moreover, I want to thank to the technicians of DTU-Environment for the technical support. Help is always welcome even more when somebody is new in a new lab.

Muchas gracias a las chicas del laboratorio de Biología Molecular. En especial, gracias a Patricia y Elisa, por las DGGE y los FISH... gracias por vuestro tiempo, esfuerzo y disponibilidad, me habéis ayudado a enriquecer la tesis con vuestro trabajo... y junto a vosotras he aprendido mucho.

Infinitas gracias a mis amig@s, por vuestra paciencia, cariño, apoyo y ánimo durante estos años. Por vuestras palabras, gestos y acciones que me han ayudado a seguir con ilusión el camino. Gracias por escucharme, entenderme y aconsejarme. En especial, mil gracias a Marisa y a Luis, por hacer que nuestra estancia en Dinamarca fuera maravillosa, por vuestra inestimable y constante ayuda, por todos los momentos

vivididos juntos, por la amistad que nos une, por vuestro cariño y paciencia. Lorena y Javi, son muchísimas las horas que hemos pasado (y pasamos) juntos en Valladolid, gracias mil por inyectarme energía cuando más falta me ha hecho y por estar a mi lado siempre, gracias por vuestro cariño y amistad.

En definitiva... quiero dar las gracias a todas aquellas personas, que, de una manera u otra han formado parte de mi vida en estos últimos años, que se han quedado algo de mí y yo algo de ellos, que han contribuido de una forma u otra, en mayor o menor medida a que este trabajo saliese adelante.

Y aunque les agradezco en último lugar, para mí son los primeros y más importantes:

Muchas gracias a mis padres y hermano. Por vuestro cariño inmensurable, por vuestro apoyo incondicional constante, por confiar en mí y en mis capacidades desde el principio. Por haberme ayudado a llegar a ser lo que soy hoy y sentir lo que siento. Por recordarme que podía sacar todo lo que me propusiera adelante. Por demostrarme lo orgullosos que estáis de mí. Por levantarme el ánimo cuando lo tenía por los suelos, por sacarme mil sonrisas. Por todo lo que me habéis enseñado, por no fallarme nunca, por hacerme tan feliz. Por vuestra implicación a lo largo de esta tesis (incluso habéis venido al laboratorio conmigo). Por perdonarme las ausencias y no haberos dedicado el tiempo que os merecáis o me habría gustado porque estaba muy liada con la tesis. Por enseñarme que en la constancia está la base del éxito. Sois mi ejemplo a seguir.

Me gustaría también dar las gracias a Mariví, Fermín y Julia. Qué suerte que la vida haya hecho que se cruzaran nuestros caminos, gracias familia. Gracias por vuestro apoyo y cariño constante. Sois muy importantes en mi vida.

Mil gracias a Diego, mi media naranja, mi media tableta de chocolate. No tengo suficientes palabras de agradecimiento pero estoy segura de que sabes perfectamente mis sentimientos. Gracias por demostrarme que hay tesis que empiezan y/o terminan por amor. Gracias por caminar de mi mano y no soltarla en este duro camino durante la realización de la tesis, sin tu apoyo diario incondicional no lo habría podido lograr. Gracias por toda tu ayuda, paciencia, cariño y comprensión. Por el sacrificio que has hecho estos años. Por tu amor incondicional y sin límites. Por sostenerme cuando flaqueaba. Gracias por las horas que has pasado en el laboratorio y fuera de él junto a mí trabajando para mi tesis, gran parte de ella es tuya. Por haber compartido conmigo ojeras, sonrisas y lágrimas durante la elaboración de este trabajo. Por tu implicación máxima. Por haber sacado lo mejor de mí. Gracias por esto y por mil cosas más, soy muy afortunada de tenerte en mi vida.

...Where there's a will, there's a way...

NOTHING WORTH HAVING WAS EVER ACHIEVED WITHOUT EFFORT.